

## **TESIS DOCTORAL**

# ***Development of a Bio-based Binder for its Application in the Mineral Wool Insulation Material***

**Autor:**

**María Mercedes Castro Cabado**

**Director:**

**Julio San Román del Barrio**

**Tutor:**

**Belén Levenfeld Laredo**

**DEPARTAMENTO DE CIENCIA E INGENIERÍA DE MATERIALES E INGENIERÍA  
QUÍMICA – INSTITUTO ÁLVARO ALONSO BARBA**

**INSTITUTO DE CIENCIA Y TECNOLOGÍA DE POLÍMEROS**

Leganés, Junio 2016



## TESIS DOCTORAL

# Development of a Bio-based Binder for its Application in the Mineral Wool Insulation Material

**Autor:** María Mercedes Castro Cabado

**Director:** Julio San Román del Barrio

Firma del Tribunal Calificador:

Firma

Presidente:

Vocal:

Secretario:

Calificación:

Leganés/Getafe, de de



*Ami familia*



---

# AGRADECIMIENTOS

---

Como es sabido, el trabajo de una tesis requiere mucha constancia y perseverancia. Es por ello que no puede llevarse a cabo sin el apoyo, recomendaciones y ayuda de las personas que te rodean. En mi caso he podido contar, no con una ni con dos, si no muchas, a las cuales me gustaría mostrar mi agradecimiento.

Empezando por el director de esta tesis, Julio, y mi responsable de departamento en la empresa Ursa Insulation, Arturo. A Julio por sus acertadas directrices a lo largo de este trabajo, siempre dispuesto a pesar de su saturada agenda. Gracias por contagiarme parte de tu pasión por la investigación. A Arturo, ya que con él todo es posible, porque si no lo es, lo hace. Sin él este proyecto no se habría puesto en marcha, y por supuesto no habría visto la luz. Con ambos he pasado no sólo momentos estupendos si no también momentos duros, pero siempre he salido más fortalecida, tanto profesional como personalmente. Muchas gracias.

De la Universidad Carlos III, me gustaría agradecer en particular a Belén su tutoría, y el estar ahí en los momentos que he necesitado, aunque a veces haya resultado de lo más estresante. También a Asun por su buena disposición cuando se han planteado singularidades propias de una tesis en colaboración con una empresa, y al resto de compañeros que se han visto involucrados de alguna manera en la presentación de esta tesis. Muchas gracias.

Quiero hacer mención especial a la empresa Ursa Insulation por su apoyo a este trabajo y haber confiado en mí. También al grupo de biomateriales del ICTP, que son un grupo tan abierto que te permiten trabajar aunque no sea con sus células y biomateriales, siempre en favor de la investigación. Integrarse en un grupo así es infinitamente fácil. Muchas gracias a todos y cada uno de sus integrantes, Blanca, Curra, Mar, Rosana, Raquel, Álvaro, Paco, Luís García, Luís Rojo y Luís Rodríguez.

No podría redactar estos agradecimientos sin referirme a mis compañeros de Ursa que me han apoyado en la iniciativa de realizar este trabajo, y especialmente a Ana por su ayuda con los ensayos de laboratorio siempre que lo he necesitado, a David por su colaboración en la

protección intelectual de este trabajo y consejos técnicos, a Flavia por sus malabarismos ajustando viajes y agenda, y a mis compañeros de Delitzsch, porque sin pruebas industriales no hay desarrollo y sin ellos no hay pruebas. Muchas gracias a todos.

Finalmente, pero tan o más importante si cabe, agradezco a mi familia su eterna comprensión porque a los treinta y tres siga en modo “non paro”. Siempre han creído en mí, a ellos les debo el empezar y terminar con entusiasmo cada una de las etapas de mi vida. A alguien a quien agradezco sin palabras porque todavía no se han creado aquellas que permitan agradecer tal inmensidad de apoyo, comprensión y, paz y amor, él es César. Y a mis amigos, que no son muchos y eso los hace únicos por definición. Muchas gracias.



*El camino del progreso no es ni rápido ni fácil.*

*Marie Curie*



Esta tesis ha dado lugar a las siguientes publicaciones y patente:

### Artículos

I. M. Castro-Cabado, Francisco J. Parra-Ruiz, A.L. Casado, J. San Román

**Thermal crosslinking of maltodextrin and citric acid. Methodology to control the polycondensation reaction under processing conditions.**

*Polymers and Polymer Composites*, 24, (2016)

II. M. Castro-Cabado, A.L. Casado, J. San Román

**Bio-based thermosets: Effect of the structure of polycarboxylic acids on the thermal crosslinking of maltodextrins.**

*European Polymer Journal*, 78, 91-105, (2016)

III. M. Castro-Cabado, A.L. Casado, J. San Román

**Effect of CaO in the thermal crosslinking of maltodextrin and citric acid. A cooperative action of condensation and ionic interactions.**

*Aceptado, Journal of Applied Polymer Science*

### Patente

I. URSA INSULATION, M. Castro-Cabado, A.L. Casado, J. San Román

**Improved curable resin for mineral wool.**

Solicitud de patente europea, no. 16153179.3-1301, presentada el 28/01/2016.



---

# CONTENTS

---

<b>RESUMEN</b> .....	<b>17</b>
<b>ABSTRACT</b> .....	<b>19</b>
<b>ABREVIATIONS</b> .....	<b>21</b>
<b>1 GENERAL INTRODUCTION &amp; OBJECTIVES</b> .....	<b>23</b>
1.1 GENERAL INTRODUCTION.....	25
1.1.1 <i>INSULATION MATERIALS</i> .....	25
1.1.2 <i>MINERAL WOOL</i> .....	28
1.1.3 <i>FORMALDEHYDE EMISSIONS IN MINERAL WOOL</i> .....	33
1.1.4 <i>NEW THERMOSETS IN MINERAL WOOL INDUSTRY</i> .....	34
1.1.5 <i>STARCH DERIVATIVES</i> .....	41
1.1.6 <i>BIO-BASED POLYCARBOXYLIC ACIDS</i> .....	43
1.2 OBJECTIVES.....	44
1.3 REFERENCES .....	46
<b>2 METHODOLOGY TO STUDY THE CROSSLINKING BETWEEN MALTODEXTRIN AND POLYCARBOXYLIC ACIDS UNDER PROCESSING CONDITIONS</b> .....	<b>51</b>
2.1 INTRODUCTION .....	53
2.1.1 <i>POLYCONDENSATION</i> .....	53
2.1.2 <i>POLYCONDENSATION OF POLYSACCHARIDES WITH POLYCARBOXYLIC ACIDS</i> .....	54
2.1.3 <i>PROCESSING CONDITIONS</i> .....	55
2.1.4 <i>CHARACTERIZATION OF POLYCONDENSATION REACTION</i> .....	55
2.2 AIM OF THIS CHAPTER .....	56
2.3 MATERIALS AND METHODS.....	57
2.3.1 <i>MATERIALS</i> .....	57
2.3.2 <i>METHODS</i> .....	57
2.4 CHARACTERIZATION TECHNIQUES .....	58
2.4.1 <i>ATR-FTIR SPECTROSCOPY</i> .....	58
2.4.2 <i>THERMOGRAVIMETRIC ANALYSIS (TGA)</i> .....	58

2.4.3	<i>RHEOLOGICAL MEASUREMENTS</i> .....	59
2.5	RESULTS AND DISCUSSION .....	59
2.5.1	<i>INFRARED ANALYSIS</i> .....	59
2.5.2	<i>TGA</i> .....	65
2.5.3	<i>RHEOLOGICAL CHARACTERIZATION</i> .....	68
2.6	CONCLUSIONS .....	73
2.7	REFERENCES .....	73
<b>3</b>	<b>EFFECT OF THE STRUCTURE OF POLYCARBOXYLIC ACIDS IN THE THERMAL CROSSLINKING OF MALTODEXTRINS</b> .....	<b>77</b>
3.1	INTRODUCTION .....	79
3.1.1	<i>BIO-BASED POLYMERS</i> .....	79
3.1.2	<i>BIO-BASED THERMOSETS</i> .....	79
3.1.3	<i>POLYSACCHARIDE-BASED THERMOSETS</i> .....	80
3.1.4	<i>MALTODEXTRIN</i> .....	81
3.1.5	<i>POLYCARBOXYLIC ACIDS</i> .....	82
3.2	AIM OF THIS CHAPTER .....	82
3.3	MATERIALS AND METHODS .....	83
3.3.1	<i>MATERIALS</i> .....	83
3.3.2	<i>METHODS</i> .....	83
3.4	CHARACTERIZATION TECHNIQUES .....	84
3.5	RESULTS AND DISCUSSION .....	86
3.5.1	<i>TGA STUDY</i> .....	86
3.5.2	<i>INFRARED STUDY</i> .....	91
3.5.3	<i>RHEOLOGICAL STUDY</i> .....	98
3.5.4	<i>MECHANICAL PROPERTIES CHARACTERIZATION</i> .....	102
3.5.5	<i>SCANNING ELECTRON MICROSCOPY (SEM)</i> .....	105
3.6	CONCLUSIONS .....	106
3.7	REFERENCES .....	106
<b>4</b>	<b>EFFECT OF CaO AND ZnO IN THE THERMAL CROSSLINKING OF MALTODEXTRIN AND POLYCARBOXYLIC ACIDS</b> .....	<b>109</b>
4.1	INTRODUCTION .....	111
4.1.1	<i>CROSSLINKING</i> .....	111
4.1.2	<i>CROSSLINKING ENHANCEMENT</i> .....	112

4.1.3	IONIC CROSSLINKING OF POLYSACCHARIDES AND POLYCARBOXYLIC ACIDS WITH METALS	113
4.1.4	CaO AND ZnO.....	113
4.2	AIM OF THIS CHAPTER .....	114
4.3	MATERIALS AND METHODS.....	114
4.3.1	MATERIALS.....	114
4.3.2	METHODS.....	115
4.4	CHARACTERIZATION TECHNIQUES.....	116
4.4.1	RHEOLOGICAL MEASUREMENTS.....	116
4.4.2	MECHANICAL PROPERTIES MEASUREMENTS .....	116
4.4.3	SEM AND ELECTRON DISPERSION X-RAY (EDX).....	117
4.4.4	ATR-FTIR SPECTROSCOPY.....	117
4.4.5	THERMOGRAVIMETRIC ANALYSIS (TGA).....	118
4.5	RESULTS AND DISCUSSION .....	118
4.5.1	METAL OXIDES IN THE SYSTEM CONTAINING MAL AND CA .....	118
4.5.2	CaO IN THE SYSTEM CONTAINING MAL AND TA.....	128
4.5.3	STUDY ON THE INTERACTIONS OF Ca(II) ION WITH CA.....	133
4.6	CONCLUSIONS .....	142
4.7	REFERENCES .....	142
<b>5</b>	<b>EFFECT OF SODIUM HYPOPHOSPHITE IN THE POLYCONDENSATION OF MALTODEXTRIN WITH CITRIC ACID.....</b>	<b>145</b>
5.1	INTRODUCTION .....	147
5.1.1	ESTERIFICATION REACTION.....	147
5.1.2	ESTERIFICATION OF POLYSACCHARIDES .....	148
5.1.3	SODIUM HYPOPHOSPHITE IN THE ESTERIFICATION REACTIONS .....	149
5.2	AIM OF THIS CHAPTER .....	150
5.3	MATERIALS AND METHODS.....	151
5.3.1	MATERIALS.....	151
5.3.2	METHODS.....	151
5.4	CHARACTERIZATION TECHNIQUES.....	152
5.4.1	RHEOLOGICAL MEASUREMENTS.....	152
5.4.2	MECHANICAL PROPERTIES MEASUREMENTS .....	152
5.4.3	ATR-FTIR SPECTROSCOPY.....	153
5.4.4	THERMOGRAVIMETRIC ANALYSIS (TGA).....	153

5.4.5	<i>NMR SPECTROSCOPY</i> .....	154
5.5	RESULTS AND DISCUSSION .....	154
5.5.1	<i>EFFECT OF SHP IN THE ESTERIFICATION REACTION</i> .....	154
5.5.2	<i>EFFECT OF SHP IN THE CROSSLINKING</i> .....	159
5.5.3	<i>EFFECT OF SHP ON THE MECHANICAL PROPERTIES</i> .....	162
5.5.4	<i>ROLE OF SHP IN THE POLYCONDENSATION REACTION OF MAL AND CA</i> .....	166
5.6	CONCLUSIONS .....	179
5.7	REFERENCES .....	180
<b>6</b>	<b>APPLICATION OF BINDER FORMULATION BASED ON MALTODEXTRIN AND CITRIC ACID IN THE MINERAL WOOL INDUSTRY</b> .....	<b>183</b>
6.1	INTRODUCTION .....	185
6.1.1	<i>BINDER IN THE MINERAL WOOL MANUFACTURING PROCESS</i> .....	185
6.1.2	<i>SPECIFICATIONS OF MINERAL WOOL INSULATION MATERIALS</i> .....	187
6.2	AIM OF THIS CHAPTER .....	191
6.3	MATERIALS AND METHODS.....	191
6.3.1	<i>MATERIALS</i> .....	191
6.3.2	<i>METHODS</i> .....	192
6.3.3	<i>CONTROL OF MANUFACTURING PROCESS</i> .....	194
6.3.4	<i>CONTROL OF PRODUCT SPECIFICATIONS</i> .....	194
6.4	RESULTS AND DISCUSSION .....	195
6.4.1	<i>PROCESS PARAMETERS</i> .....	195
6.4.2	<i>PRODUCT PROPERTIES</i> .....	198
6.5	CONCLUSIONS .....	202
6.6	REFERENCES .....	203
	<b>FINAL CONCLUSIONS</b> .....	<b>205</b>
	<b>CONCLUSIONES FINALES</b> .....	<b>209</b>
	<b>ANNEX 1</b> .....	<b>211</b>



---

# RESUMEN

---

Se ha desarrollado una alternativa a las resinas fenólicas tradicionales, basada en fuentes renovables, para su aplicación en la fabricación de material de aislamiento de lana mineral. Para ello se ha utilizado una metodología sistemática a lo largo de todo el trabajo de tesis, para evaluar diferentes composiciones formadas por maltodextrina y ácidos policarboxílicos. Las técnicas analíticas empleadas para este propósito fueron espectroscopia de infrarrojo, TGA, reología y ensayos de propiedades mecánicas.

Se evaluaron dos ácidos policarboxílicos diferentes, de manera que se consiguió un conocimiento sólido para distinguir cuál de ellos se comportaría mejor en cuanto a su reactividad con la maltodextrina. Basándose en los resultados obtenidos, se seleccionó el ácido cítrico como el más apropiado para la aplicación final.

La composición consistente en maltodextrina y ácido cítrico se mejoró, en lo que se refiere a reactividad y propiedades mecánicas del sistema curado, mediante la adición de óxidos de metales y de hipofosfito de sodio. Entre los óxidos de metales estudiados, el óxido de calcio ha proporcionado los mejores resultados.

Ambos compuestos, el óxido calcio y el hipofosfito de sodio, han proporcionado mejoras significativas, aunque el mecanismo de acción de cada uno de ellos es diferente. Esto último se ha podido concluir gracias al análisis hecho por espectroscopía de infrarrojo y resonancia magnética nuclear.

Entre todas las composiciones estudiadas, la que contiene maltodextrina, ácido cítrico e hipofosfito de sodio se propuso para evaluarla en el proceso industrial de fabricación de lana mineral. Mediante la aplicación de esta composición, se ha obtenido un producto de lana mineral bueno, que cumple con las especificaciones requeridas por la norma europea para producto de aislamiento de lana mineral, para equipamiento industrial y aplicaciones industriales.



---

# *ABSTRACT*

---

A bio-based and non-toxic alternative to the phenolic resins traditionally used for the manufacturing of mineral wool insulation material has been developed. A systematic methodology has been applied all the along the thesis work to evaluate different compositions comprising maltodextrin and polycarboxylic acids. The analytical techniques used for that purpose were IR spectrometry, TGA, rheology and mechanical properties testing.

Two different polycarboxylic acids were evaluated, achieving good understanding of their suitability in terms of reactivity with maltodextrin. From this evaluation, one of the polycarboxylic acids, citric acid, was selected as the most appropriate for the final application.

The composition comprising maltodextrin and citric acid was further improved in terms of reactivity and mechanical performance of cured system by the addition of metal oxides, and also by the addition of sodium hypophosphite. Among the metal oxides studied, calcium oxide delivered the best results.

Both compounds, calcium oxide and sodium hypophosphite lead to significant improvements, nevertheless their mechanism of action is different. This was concluded by the analysis done by IR and NMR spectroscopy.

Among all the compositions studied, the one containing maltodextrin, citric acid and sodium hypophosphite was proposed to test in the industrial process of mineral wool manufacturing process. By applying this composition it was obtained successful glass wool product which complies with the specifications stated by the European norm for the mineral wool insulation material for building equipment and industrial applications.



---

# ABBREVIATIONS

---

ATR-FTIR	Attenuated total reflectance Fourier transform infrared
$C_{eq}$	Concentration in the equilibrium
CA	Citric acid
Cit	Citric
DE	Dextrose equivalent
DIM	Dynamic insulation materials
DMA	Dynamic mechanical analysis
DSC	Differential scanning calorimetry
$E_a$	Apparent activation energy
EDX	Energy dispersive x-ray
EPA	Environmental Protection Agency
FTIR	Fourier Transform Infrared
GC	Gas chromatography
GIM	Gas insulation materials
GPC	Gas permeation chromatography
HMBC	Multiple-bond correlation spectroscopy
HPLC	High pressure liquid chromatography
IARC	International Agency for Research on Cancer
IR	Infrared
MAL	Maltodextrin
NIM	Nano-insulation materials
NMR	Nuclear magnetic resonance
SCHER	Scientific Committee on Health and Environmental Risk
SEM	Scanning electron microscopy
SHP	Sodium hypophosphite monohydrate
TA	Tartaric acid
Tar	Tartaric
TGA	Thermogravimetical analysis
VIM	Vacuum insulation materials



---

# *CHAPTER I*

---

## *GENERAL INTRODUCTION & OBJECTIVES*

---





## 1.1 GENERAL INTRODUCTION

---

In the past the demand of synthetic polymers was increasing in order to cover all the necessities of standard living and the growing of population. For instance, most of the houses in developed countries are nowadays insulated by materials which are made of synthetic polymers, as well as the furniture, household, etc. As a consequence in the past few decades more and more concerns have arisen about the impact of these synthetic polymers on the environment, climate change and health. For that reason, intensive research on alternatives to the existing petrol-based polymers has been started in recent years leading to successful solutions, more environmentally friendly and healthy.

An example of research on polymers field which are more environmentally friendly and nontoxic is ongoing in the mineral wool insulation industry. Due to the increased restrictions in the indoor air quality, particularly stricter for formaldehyde emissions for common products used in buildings, this industry has moved to bio-based thermoset systems replacing the traditional phenolic resins. Although some of the alternatives are already partially implemented in the industry, the knowledge of the chemical reactions taking place in these systems is still weak. This makes that its industrial application is not yet well optimized in terms of processability and quality of finished product.

This thesis aims to go deep in the research of the polycondensation reaction of starch derivatives and polycarboxylic acids to get a proper thermoset system for its application in the mineral wool insulation industry.

### 1.1.1 INSULATION MATERIALS

---

Thermal insulation is characterized by the application of a material or a combination of materials which retard the heat flow by conduction, convection and/or radiation; into or out of a cavity due to its high thermal resistance. A building can be understood as a cavity, usually designed to shelter occupants and achieve thermal comfort by means of mechanical heating and air-conditioning systems [1]. Therefore, buildings are high consumers of energy, in fact the energy

use in building sector is a significant part of the world's total energy consumed and a major cause for the greenhouse gas emissions [2]. The amount of energy required to cool/heat a building depends on how well it is insulated. Therefore thermal insulation plays an important role on saving energy. In fact, forty years after the introduction of compulsory thermal insulation for buildings in most of the European countries, thermal insulation materials are still the best mean to improve its energy consumption. As a matter of fact, the use of thermal insulation materials has increased, in terms of type of buildings and minimum values of insulation required by the national regulations [3].

The properties of thermal insulation materials impacting directly the energy efficiency of the building are the thermal conductivity ( $\lambda$ -value) and the thermal resistance (R-value). Both properties define the effectiveness of the material in conducting heat. Thermal conductivity ( $\lambda$ ) is the time rate of steady state heat flow through a unit of area of 1 m thick homogeneous material in a direction perpendicular to isothermal planes, induced by a unit temperature (1 K) difference across the sample [4]. It is expressed in W/m·K and its value depends strongly on the temperature of the material and its humidity content. The thermal resistance (R) measures the resistance to heat flow result of suppressing conduction, convection and radiation. It is a function of the thermal conductivity and thickness, and it is expressed in m<sup>2</sup>·K /W. Each type of insulation material provides different range of thermal resistance which is shown in Figure 1.1.

Additional properties characterize the insulation materials making some of them more suitable than others for the different applications. These properties can be divided in three different categories [3]:

- Physical properties like density, mechanical strength, thermal insulation ability, sound absorption, resistance moisture and fire.
- Environmental impact, defined by the primary embodied energy, the gas emissions released during by the manufacturing of the product, the use of additives against biological impacts, the classification as waste, the re-usability and recyclability and their Life Cycle Analysis.
- Other properties related to the public health, during manufacturing process, the use and the final stage of disposal and fibers emissions, biopersistence, toxicity in case of fire, etc.

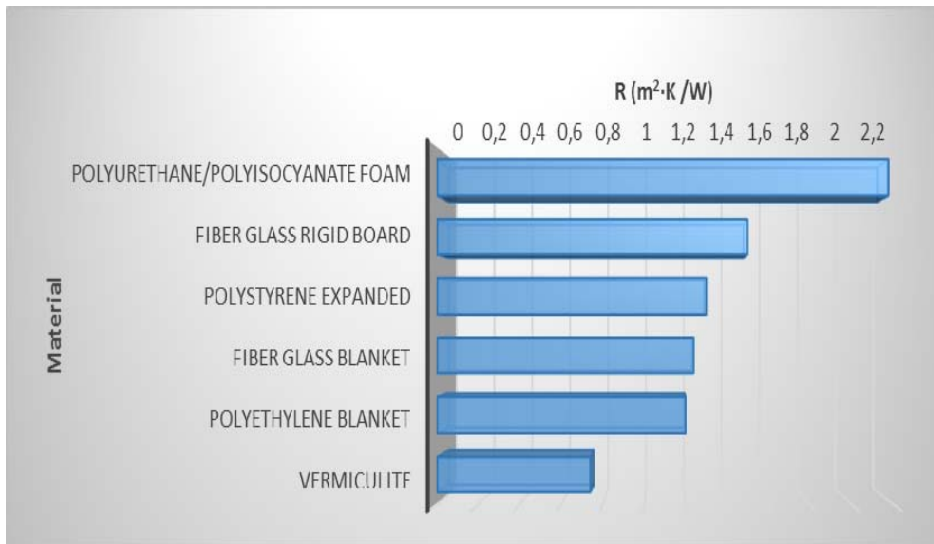


**Figure 1.1– Thermal resistance (per 5 cm thickness) of common building insulation materials [1]**

As shown in Figure 1.2, a first classification of thermal insulation materials can be done based on their raw materials, organic and inorganic materials, or the combination of both. Second classification is based on their structure, either fibrous or cellular. Apart from these classifications, specific class is considered for more recently developed materials. One example of more recently developed products is the dynamic insulation materials (DIM). In this material, the thermal conductivity can be controlled within a desirable range by the inner pore gas content, the emissivity of the inner surfaces of the pores and the solid state thermal conductivity of the lattices. Additionally it is worth to mention other new insulation materials like vacuum insulation materials (VIM), gas insulation materials (GIM) and nano-insulation materials (NIM) [2]. These materials are provided in different forms, loose-fill form, blanket bat or roll form, rigid form, foamed in place, or reflective form.

Among all the insulation materials, the most used are glass and rock wool insulation materials which account for close to 60 % of market share. The organic foamy materials (i.e. polystyrene, polyurethane, polyisocyanurate, etc) are the second most used insulation materials according to the information reported by the market research analyst “Technavio” [5].

The choice of the proper insulation material type and form depends on the type of application and the desired materials physical, thermal and other properties.

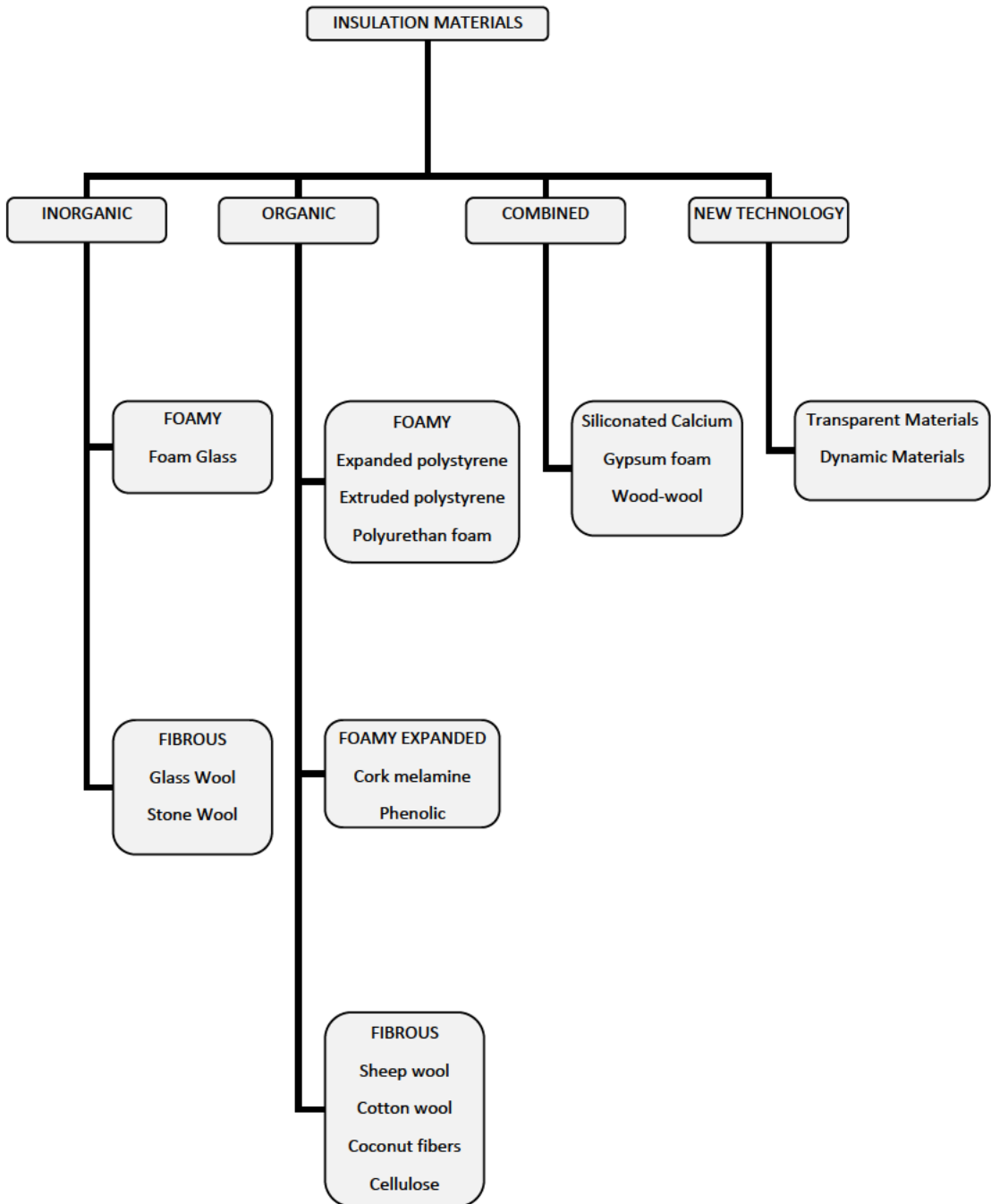


Figure 1.2 – Classification of most used insulation materials [3]

## 1.1.2 MINERAL WOOL

Mineral wool refers to inorganic insulation materials made of fibers, like for instance glass wool and rock wool. These materials are normally produced as mats and boards. They can be

divided as light and soft materials from one side and, heavy and rigid materials from the other side. The light and soft mineral wool is applied in frame houses and other structures with cavities; while the heavier and rigid boards with high densities are used when the thermal insulation is intended for carrying loads, e.g. on floors or roofs [2]. In its final application, the mineral wool may be perforated, and also cut and adjusted, without any loss of thermal resistance. In recent years, mineral wool is also produced as filling material especially for cavity walls in the refurbishment of old houses.

Typical thermal conductivity values for mineral wool are between 0.03 and 0.04 W/m·K, nevertheless glass wool lead to the lower values compared to rock wool. Its thermal conductivity varies with temperature, moisture content and mass density. As an example, the thermal conductivity of mineral wool may increase from 0.037 W/m·K to 0.055 W/m·K with increasing moisture content from 0 vol% to 10 vol%, respectively.

Following are described the main steps in the mineral wool manufacturing process [6]:

i. Supplying the raw materials and energy sources

The raw materials used in mineral wool production are different for glass wool or rock wool. Glass wool material is produced from sand, limestone and soda ash (borosilicate glass) while rock wool is produced from basaltic stone (diabase, dolomite). These raw materials are introduced in a melting furnace.

ii. Melting

The melting process takes place at temperature between 1300 and 1600 °C inside a furnace which can be electric or gas furnace. By melting the chemical substances affecting the material characteristics like viscosity and surface tension are obtained.

iii. Fiberization and collecting

Fiberization of molten rock or glass takes place in the different way, but conceptually similar. For instance, for glass, it takes place in rotating spinning machines (wheels) where the melt is spun into fibers. These machines consist of several cylindrical rotors onto which the melt is directed and fiberized with or without help of stripping air. The fibers coming out of the fiberization process are sprayed with a binder and collected on a conveyor belt.

iv. Primary layer formation

The fibers formed and sprayed with binder are taken by an air flow into interior of the collection chamber, where the primary layer of mineral wool is formed on a perforated conveyor belt.

v. Finishing (curing, cutting, facing, packing, etc.)

The primary layer leaves the collections chamber and passes over an intermediate belt before entering the curing oven. The curing oven squeezes the product at the entrance leading to a redistribution of the mineral wool, therefore a re-formation and re-direction of the fibers. While squeezing the product the polymerization of the binder takes place along the curing oven. Once the product come out of the curing oven it cooled down (in the cooling zone) and latter cut according to the required final dimensions of the product. For some specific applications a facing is glued to the mineral wool after curing oven.

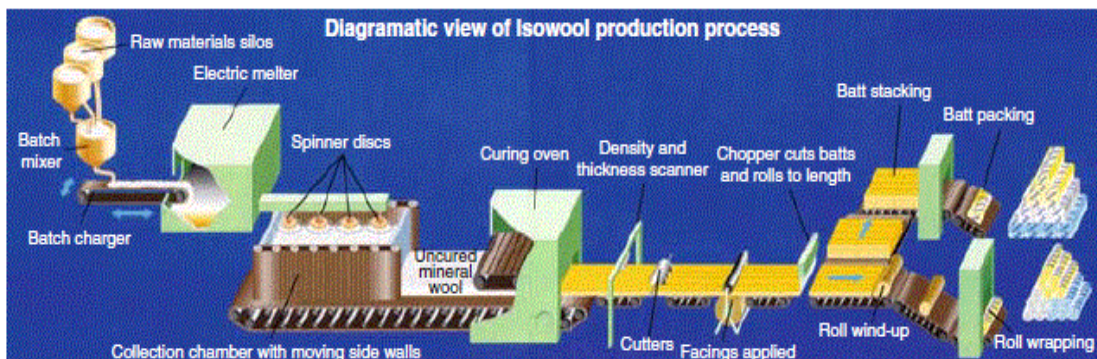


Figure 1.3 – Glass wool manufacturing process [7]

Due to the complexity of manufacturing process, the final properties and quality of the finish product depends on many different factors. The main process steps affecting them are: the structure of fiber and the proportion of solidified shots in the finish products after fiberization step, the geometry of the interlaced fibers as well as the homogeneity of the binder distribution on the fiber surface during the collection of primary layer, and the reformation geometry of the product in the curing oven.

### 1.1.2.1 BINDER SYSTEM

In the mineral wool material, the fibers are bonded together by a binder (Figure 1.4). The effectiveness of this binder has a strong impact in the mechanical properties of the finish product

such as compressive, tensile and bending strengths. The quantity of binder to be applied is adjusted depending on the requirements of the finished product. For instance, flexible glass wool blankets need less binder than rigid slabs.

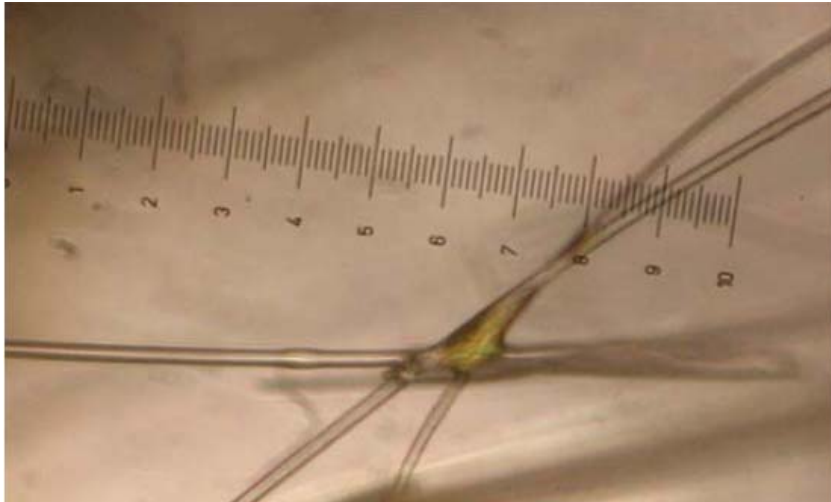


**Figure 1.4 – Mineral fibers bound by binder at their junction points [7]**

The binder is a complex aqueous mixture comprising a reacting thermosetting composition with additives which provides particular additional properties to the finish material apart from the mechanical performance. Among others, polyesters, melamine-urea-formaldehyde, polyamides, furan-based resin, polysiloxane-polyol hybrid organo-inorganic binder, inorganic binder have been reported as suitable thermosetting compositions for mineral wool production. But historically, the most widely used thermoset system for binding mineral wool are phenol-formaldehyde resols. On top of the thermoset system, the binder may contain additives such as de-dusting agents, hydrophobic agents, emulsifiers, dyes, coupling agents and extenders.

### **Phenolic Resins in Mineral Wool**

Within the phenolic resins two different types can be distinguished. First, novolak resins, which are sparingly soluble in water, are rarely used in the binder for mineral wool insulation products. Secondly, resol resins, which are highly water soluble phenolic resins, are the most suitable for mineral wool production. The phenolic resols used for mineral wool are prepared by condensation reaction between phenol and formaldehyde under alkaline conditions at temperature around 60 °C. The ratio phenol/formaldehyde used for condensation reaction is around 3.5 to form mostly monomeric methylolated species, and not oligomeric species [8, 9].

This allows getting a resin fully soluble in water with the composition depicted in Table 1.1. Once the target free phenol is achieved the reaction mixture is cooled to avoid further condensation which would lead to increase the oligomers content and lower the solubility of resin in water.

**Table 1.1 – Typical composition of phenolic resol used for mineral wool production [7]**

Species	Relative GC peak area (%)
Phenol	0.66 (HPLC)
Monomethylol phenol (MMP)	3.93 (GPC)
Dimethylol phenol (DMP)	10.43 (GPC)
Trimethylol phenol (TMP)	57.09 (GPC)
Dimers	25.49 (GPC)
Trimer	2.40 (GPC)
Free phenol <sup>a</sup>	0.37 (GC)

<sup>a</sup>Real content of free unreacted phenol in the final resin based on GC

The obtained phenolic resol is a clear red-colored liquid having a dry content of 45-50 %, pH 8-9, low viscosity ( $\leq 50$  mPas) and water tolerance (i.e. ratio of the weight of resin to the weight of water required to achieve turbidity) 1:50 [7].

The formaldehyde content of phenolic resols, once the condensation reaction is stopped, is 5-15 % depending on the phenol/ formaldehyde ratio. With this content of free formaldehyde high emissions would be generated during the mineral wool manufacturing process. In order to avoid it, formaldehyde scavengers are added to the phenolic resol, which may work also as extenders. These scavengers possess amino groups, able to react with formaldehyde. The most common formaldehyde scavenger used in mineral wool industry is urea, which works also as extender of phenolic resin helping to reduce the cost of the binder.

Other extenders may be used to extend the resin functionality. Some examples of petrol-based extenders used for phenolic resols are polyacrylic acid, melamine, dicyanamide, animal bone glue and polyvinyl alcohol [7].

In the manufacturing process of mineral wool, the phenolic resols mixed with urea are cured under acidic conditions and heating treatment. For that reason it is used a so-called latent catalyst, which is a salt of a strong acid with a weak base. The latent catalyst is able to keep alkaline pH of the resol previous to curing process; but once high temperature is applied it releases the acid, changing the pH of the resin to the acid range. In this way the phenolic resol is able to cure (i.e. crosslink) in the curing oven. The most common used latent catalyst is ammonium sulfate.



### 1.1.3 FORMALDEHYDE EMISSIONS IN MINERAL WOOL

---

The first adverse effects from formaldehyde exposure were reported in the mid 1960's. In 1977, the German Federal Agency of Health proposed the first guideline referring to the limit of exposure for human in dwellings. Later, in Germany and Denmark, in 1981, it was set the first criteria for the limitation and regulation of formaldehyde emissions from wood-based materials. United States followed the trend establishing the first regulation in 1985 [10]. Later, in 1989, the U.S. Environmental Protection Agency (EPA) classified formaldehyde as a probable human carcinogen under conditions of high or prolonged exposure. Different studies suggested that formaldehyde exposure was linked to the nasal cancer and nasopharyngeal cancer, and possibly with leukemia [11]. In 2005, the International Agency for Research on Cancer (IARC) concluded that formaldehyde is a human carcinogen substance [12]. As a consequence the Scientific Committee on Health and Environmental Risks (SCHER) states that formaldehyde is a concerned compound in the indoor environment. Since then, the effects of formaldehyde in human health have been intensively studied, leading to more and more restrictive re-classifications in Europe. In April 2015, the formaldehyde has been classified as carcinogenic category 1B and mutagen category 2.

In general, the exposure to formaldehyde is higher indoors than outdoors; mainly due to the stronger sources and low air exchange rate in the indoor environment. The indoor sources of formaldehyde include furniture and wooden products containing formaldehyde-based resins; insulating material; textiles; do-it-yourself products like paints, wallpapers, glues, adhesives, varnishes and lacquers; household cleaning products such as detergents, disinfectants, softeners, carpet cleaners and shoe products; cosmetics; electronic equipment and other consumers items such as insecticides and paper products [13].

Among the insulation materials, the urea-formaldehyde foam insulation materials are the strongest contributors to the indoor formaldehyde emissions. However the mineral wool insulation materials are also a relevant source of formaldehyde emissions as it is released by the phenol-formaldehyde resols extended with urea used in the binder. According to the study reported by T. Neuhaus et al. the formaldehyde emissions released by a rock wool material containing phenol-urea-formaldehyde resin under real use conditions (covered by wall) are lower than any criteria established up to date in Europe [14]. However the mineral wool industry has

followed the trend to create greener solutions, healthier in terms on indoor air quality and also more environmentally friendly. As a matter of fact, during the last years the manufacturers have been working on alternatives to the phenol-formaldehyde-urea resins with reduced formaldehyde emissions or even not containing formaldehyde, some of them being bio-based alternatives.

## **1.1.4 NEW THERMOSETS IN MINERAL WOOL INDUSTRY**

---

### *1.1.4.1 RENEWABLE RAW MATERIALS IN PHENOLIC RESINS*

---

One of the strategies followed to develop more environmentally friendly phenolic resins consists of replacing its petrol based raw materials by renewable materials. This strategy aims, in general, to the reduction of formaldehyde emission of finish materials. By introduction of the renewable materials in the phenolic resins it is possible to reduce formaldehyde emissions; for instance, in the case of wooden fibers panels, down to the same level as the natural wood [7]. Such approach has been mostly followed by the wooden industry, nevertheless it has been also applied in the mineral wool and composites industries.

One of the most important developments triggered by manufacturers is the use of a protein compound which has the ability to interact chemically with the phenol-formaldehyde network [15, 16]. In fact this development was applied to other formaldehyde based resins such as urea-formaldehyde normally used for wooden fiber panels [17].

Other approaches have focused on the investigation of carbohydrates as co-reactant with phenol leading to carbohydrate-phenol-formaldehyde resins. However it is known that the introduction of sugar and other carbohydrates as replacement of phenol in phenolic resin affects negatively the performance of the material upon exterior weathering conditions [18]. The use of carbohydrate has shown two main advantages for manufacturers, first the decrease of formaldehyde emissions of phenolic resins and second a reduced cost of the resin. Following the same concept, it has been investigated the use of non-reducing sugars or polyols, derived from starch or lactose, as partial replacement of phenol in the phenol-formaldehyde condensation reaction. From these investigations it has been proved these compounds do not deteriorate the performance of materials manufactured with phenolic resins [19].

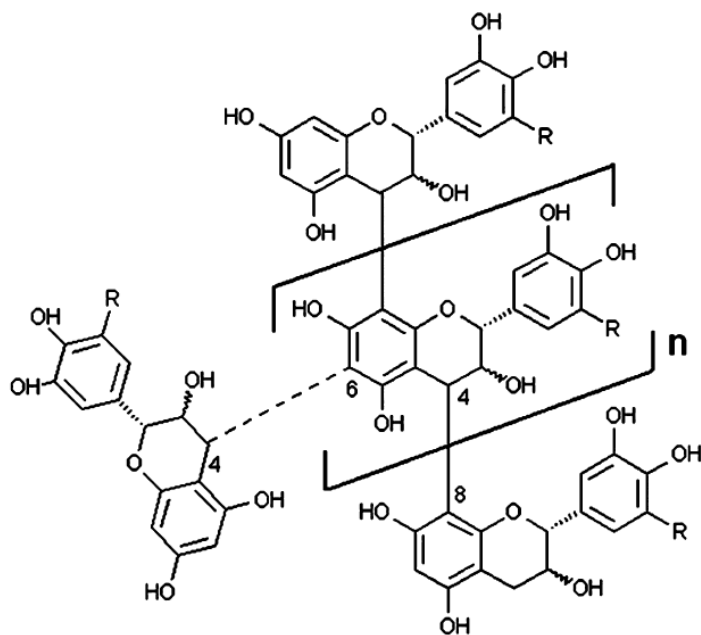


Figure 1.5 – Condensed tannin [20]

Another relevant renewable raw material used in the phenolic resins are tannins. Tannins are natural products obtained from different plants such as Acacia Mimosa tree, characterized by the large amount of phenolic and resorcinol rings in their structure. They can be classified as hydrolysable tannin and condensed tannins (Figure 1.5), which are the most suitable for phenolic resins due to the presence of phenolic rings di-substituted with hydroxyl groups in its structure. This makes them even more reactive than phenol against formaldehyde. The use of tannin-phenol-formaldehyde resins has been considered not only for wooden fiber products but also for composites [20-22].

An additional route in the introduction of renewable materials in phenolic resins has been the use of lignin and lignosulfonates. Lignin is obtained from wood, in fact, after cellulose it is the most abundant renewable carbon source. Its chemical composition consists of a complex polymer of phenylpropane units (Figure 1.6). This makes them particularly suitable to replace partially phenolic resin or the phenol as raw material. Lignosulfonates are sulfur bearing lignins obtained as byproduct of the sulfite method in the paper manufacturing from wood pulp. The use of lignosulfonates has been reported for different products consisting of fiber bonding [20, 23-25].

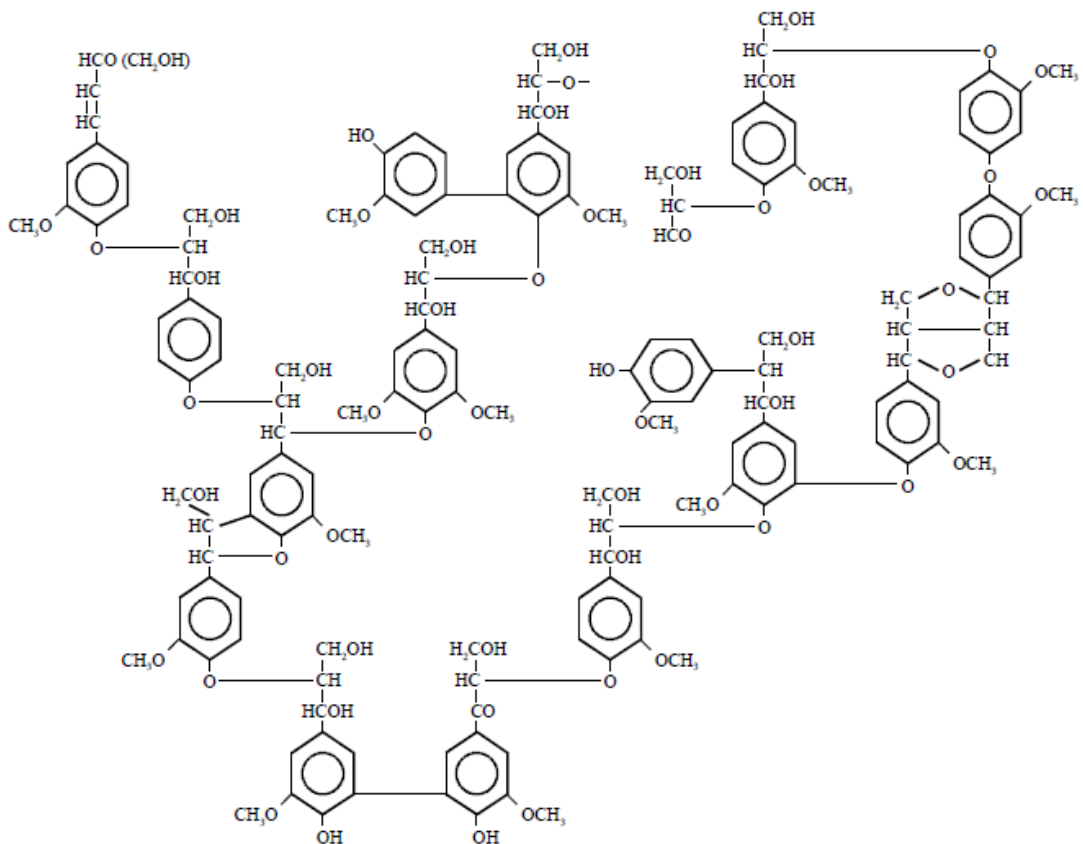


Figure 1.6 – Example of lignin chemical structure [24]

By introduction of the renewable sources in the phenolic resins it is possible to reduce formaldehyde emissions; for instance, in the case of wooden fiber panels the formaldehyde emissions down to the same level as the natural wood [7].

#### 1.1.4.2 FREE-FORMALDEHYDE ALTERNATIVE THERMOSETS

##### Petrol-based Alternatives

The first developments on free-formaldehyde alternatives to phenolic resins were based on esterification reaction between a water-borne polycarboxylic polymer and a polyol working as crosslinker. In 1991, Rohm & Hass (nowadays Dow Chemical) claimed a thermosetting resin, applicable for mineral wool and composites in general [26, 27]. This resin comprises a polyacrylic acid, a polyol and a catalyst (Figure 1.7), all soluble in water. The polyacrylic acid and the polyol goes through polycondensation reaction under thermal treatment (temperature higher than 190 °C) leading to a polyester network.

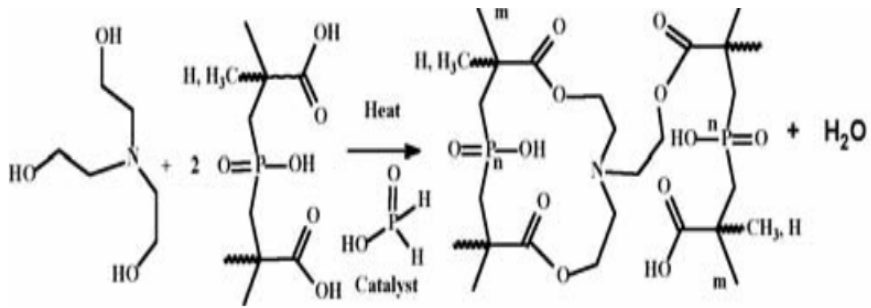


Figure 1.7 – Chemical composition of thermosetting resin developed by Rohm & Haas [28]

After this invention different alternatives based on the same chemistry were proposed by other resin manufacturers and mineral wool manufacturers; by claiming, for instance, different polycarboxylic acids forming the polymer, different molecular weight of polymer, not water-borne system but an emulsion or even by changing the pH of the resulting resin composition [29, 30]. For instance, a resin comprising an unsaturated polyester resulting from the reaction between a polycarboxylic acid and a polyol [31] was claimed by Owens Corning in 1995. Other alternatives followed this trend but comprising additionally extenders such as lignin, starch or soybean oil [32]. Later, in 2007, new alternatives started to be claimed which comprise a polycarboxylic acid and polyol with catalyst [33, 34], but these alternatives do not lead to enough performance in final application. Figure 1.8 shows an example of mineral wool insulation material bound by acrylic resin.



Figure 1.8 – Mineral wool products manufactured with binder system based on acrylic resin

## Bio-based Alternatives

The development of bio-based alternatives to phenolic resin has been approached mainly with two different chemistries: thermosetting systems based on Maillard reaction and those ones based on esterification reaction of a polycarboxylic acid and a polyol.

### Alternatives based on Maillard Reaction

Maillard reaction was first time described by Louis-Camille Maillard in 1912, when he observed that a mixture of sugars and aminoacids in water developed yellow-brown color upon heating. The chemical nature of the reaction is not yet fully defined, however the first stages of the reaction were proposed by Maillard, Amadori et al. In the first stages of the reaction the carbonyl moiety of the sugar molecule forms a Schiff base with an amine (Figure 1.9); then the Schiff base may undergo two sequential rearrangements, yielding a quite stable aminoketose which is so-called Amadori product (Figure 1.10) [35].

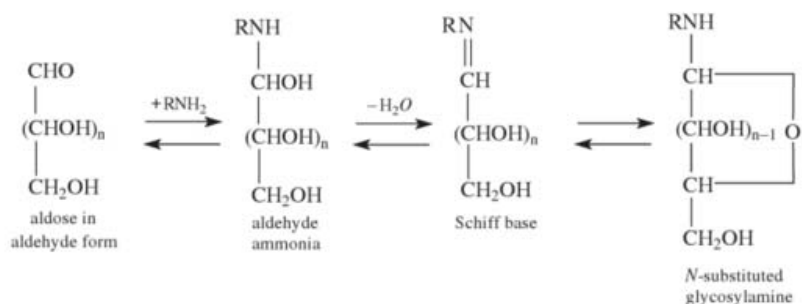


Figure 1.9 – Sugar-amine condensation to form N-substituted glycosylamine (Maillard reaction) [35]

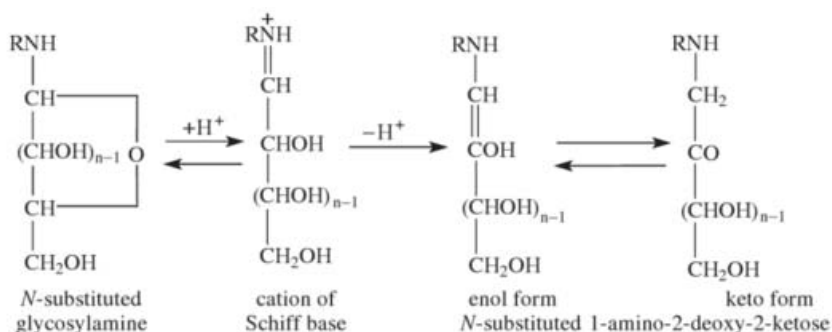


Figure 1.10 – Amadori rearrangement leading to N-substituted 1-amino-2-deoxy-2-ketose [35]

After Amadori product the mechanism of the reaction is more complex leading to a huge variety of products. Each compound at this step is reactive; therefore it can participate in wide

variety of reactions. The ratio of each possible compound at the end of the reaction depends on reaction conditions like pH, temperature, concentrations, etc. [36, 37]. Apart from the low molecular weight compounds, polymeric compounds so-called melanoidins can be formed by Maillard reaction in the last stages (Figure 1.11) [38, 39]. The formation of these polymeric compounds gives the opportunity to use Maillard reaction to create new bio-based polymeric systems.

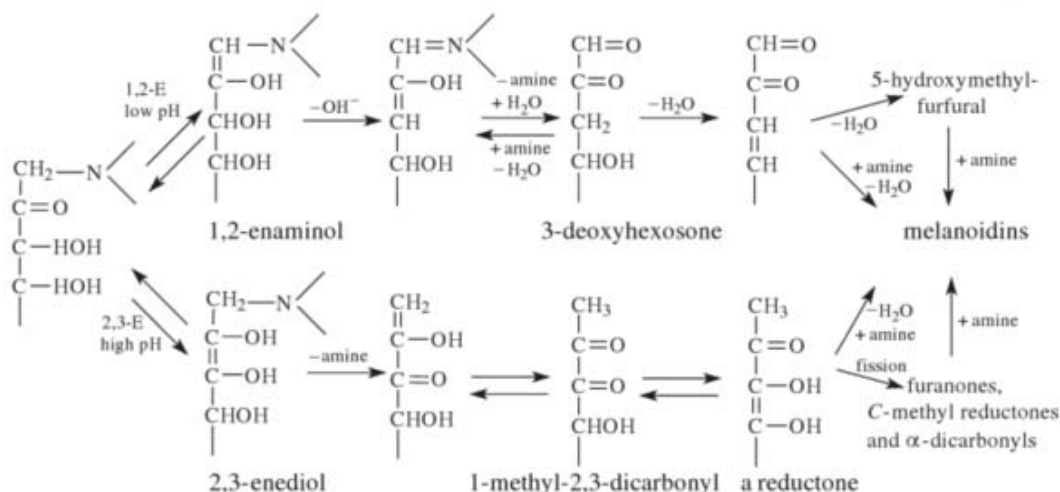


Figure 1.11 – The two major pathways from Amadori compounds to melanoidins [35]

The first reported resin based on Maillard reaction is dated in 1988. This resin used starch mixed with ammonium salt of inorganic acid, which under thermal treatment lead to a crosslinked polymer with low molecular weight. Then, this low molecular weight polymer would react with an anhydride organic acid while all the mixture is applied to manufacturing process of the finish material. The purpose of this development was to apply it to lignocellulosic materials [7, 40], leading to a composite with typical performance as thermoset systems. This chemistry has been re-considered in the last years to develop an alternative system to phenolic resins for mineral wool manufacturing. In 2001, the mineral wool manufacturer Rockwool claimed the use of a water-borne system comprising an amine, an anhydride and a polysaccharide [41]. Later inventions in the same type of chemistry were claimed by different mineral wool manufacturers [42, 43]. An example of mineral wool product produced with binder system based on Maillard reaction is shown in Figure 1.12.



**Figure 1.12 – Mineral wool product manufactured with binder systems based on Maillard reaction**

### *Alternatives based on Esterification Reaction*

In 1998, the producer of polysaccharide derivatives, National Starch, claimed a thermoset system comprising a polycarboxylic polymer and a polysaccharide [44]. This system applied the same rational as acrylic resins; making to react by polycondensation a polycarboxylic polymer with a polyol which is a high molecular weight polyol (i.e. a polysaccharide). However, the polysaccharide might be working more as an extender than crosslinker (i.e. polyol) of the polycarboxylic polymer in this particular system. This could make the system to not properly deliver the requirements of final application (e.g. mineral wool). However this invention could be considered the first one within the strong development of bio-based alternatives to phenolic resin based on polycondensation reaction. In 2007, the phenolic resin producer Dynea (former Bakelite) claimed a binder system comprising a crosslinked carbohydrate with a polycarboxylic acid (e.g. citric acid) [45]. Since then, a variety of inventions based on the same concept of polycondensation with polysaccharides have been applied. The different later inventions although they refers always to polysaccharides, they try to reduce the scope of the invention to a particular polysaccharide. For instance, a binder system comprising a hydrogenated sugar and a polycarboxylic acid [46]; or a binder system comprising a maltodextrin and a polycarboxylic acid [47]; or even the use of native starch with a polyacrylic polymer has been claimed [48].

It is worth to mention that polycondensation reaction by esterification between renewable polycarboxylic acids and polyols has been described as an alternative for thermosetting systems in



general [49]. Also it is known the crosslinking of starch with polycarboxylic acids to form films [50, 51].

## 1.1.5 STARCH DERIVATIVES

Polysaccharides are long chains of monosaccharides linked by glycosidic bonds. Among all polysaccharides available in the nature, starch and cellulose are the most abundant. Both of them are formed by glucose units. In the case of starch glucose units are linked by  $\alpha$ -glycosidic bonds while in cellulose they are bonded by  $\beta$ -glycosidic. Starch is composed by two polysaccharides, amylose and amylopectin, in different ratios depending on the source plant. As shown in Figure 1.13, amylose is a short linear structure with  $\alpha$ -1,4 linked glucose units; whereas amylopectin is a highly branched structure with  $\alpha$ -1,4 and  $\alpha$ -1,6 linked glucose units.

Starch is a semicrystalline polymer where both amylose and amylopectin are well packed in helical structures hold together by hydrogen bond interactions. Starch granules are commonly found in seeds, roots, tubers, stems and leaves. Grain seeds, such as corn kernels, contain up to 75 % of starch. Starch can be easily obtained from their sources industrially, by gravity sedimentation, centrifugation and filtration. The obtained starch can be subjected to different chemical, physical and enzymatic modifications with subsequent washing and processing. As a consequence, starch is one of the most economical commodity products.

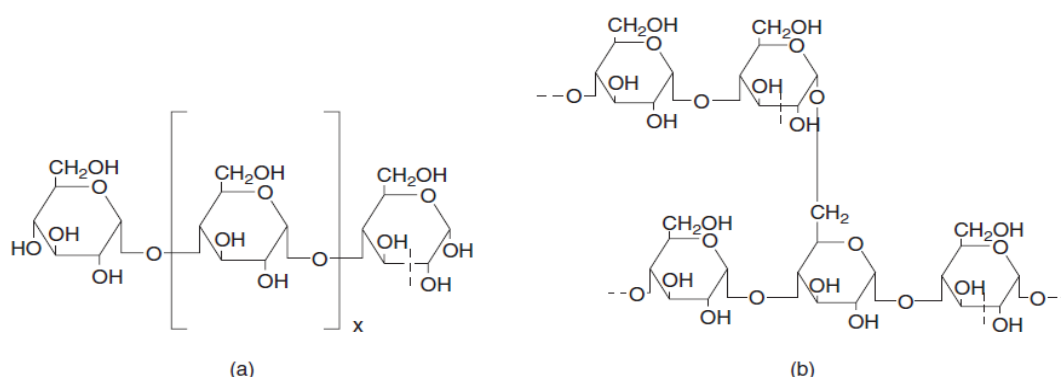


Figure 1.13 – Scheme of (a) amylose and (b) amylopectin [52]

The semicrystalline granule of starch is not soluble in cold water, but it is swelled and even completely solubilized when temperature is increased sufficiently. The temperature at which the

starch starts to swell is known as gelatinization temperature and its value depends on the nature of the starch [53, 54]. Some examples of chemical modifications of starch are esterification [55, 56], etherification [57] or oxidation [58]. For instance, hydroxypropyl-starches are prepared by etherification with propylene oxide and starch acetates prepared by esterification with acetic anhydride, commonly used in food applications [59]. All these possible modifications of starch make it more suitable for numerous applications such as fabric stiffeners, adhesives and binders, sizing agent. Other new applications are steadily emerging such as “biodegradable” packaging materials, thin films, carrier matrices for controlled release of agrochemicals, and thermoplastic materials with improved thermal and mechanical properties [60].

Starch can also be converted into smaller polysaccharide chains by dextrinization or hydrolysis process.

Dextrinization is the breakdown process of starch into dextrans. It can be carried out in two different ways. The first one refers to the partial de-polymerization achieved by roasting the starch either with or without acid in the media. The second one refers to the re-polymerization in a branched way delivering a product so-called dextrin or pyrodextrin [61].

The hydrolysis can be acid hydrolysis or enzymatic hydrolysis. By acid hydrolysis the glycosidic oxygen atom is attacked and hydrolyses the glycosidic bond. In this way the physicochemical properties are changed without destroying its granular structure. However, the enzymatic hydrolysis is able to modify the structure of the starch. A distribution of chain lengths corresponding to glucose (dextrose), maltose, oligosaccharides and polysaccharides are obtained depending on the extent of the hydrolysis and the type of enzyme used. The common enzymes are  $\alpha$ -amylase,  $\beta$ -amylase, glucoamylase, pullulanase and isoamylase. The estimated chain length obtained can be determined by the dextrose equivalent (DE) which is a measure of the degree of starch breakdown. A DE equal to 0 defines native starch. Different starch derivatives are obtained by this process, for instance, glucose syrups and maltodextrins. Maltodextrins are water soluble at room temperature and they are linear chains (i.e. they do not contain  $\alpha$ -1,6 glucosidic bonds but  $\alpha$ -1,4 glucosidic bonds), with chain length 5-10 glucose units/molecule. They are produced industrially starting from starch slurry liquefied by heating at 70-90 °C and at neutral pH in the presence of a bacterial  $\alpha$ -amylase. The liquid hydrolysate is then autoclaved at 110-115 °C to gelatinize completely any remaining insoluble starch and, on cooling, subjected to further enzymatic treatment to reach the desired DE. Once the required DE is achieved the solution is

refined and finally it is concentrated in vacuum evaporators or spray dried to white powder containing 3-5 % humidity [62, 63]. Examples of the final composition of maltodextrin mixtures are shown in Table 1.2.

**Table 1.2 – Composition of two maltodextrin compositions [63]**

DE	% dry weight			
	Glucose	Maltose	Maltotriose	Higher Saccharides
15	0.6	4.0	7.0	88.4
20	0.8	5.5	11.0	82.7

## 1.1.6 BIO-BASED POLYCARBOXYLIC ACIDS

In recent years new technologies have been developed to obtain more and more bio-based polycarboxylic acids. Succinic acid is one of the examples which was traditionally produced from petrol-based compounds and nowadays is commercialized as bio-based material. For that the succinic acid is obtained by fermentation of starch [64]. This opens new opportunities to broaden the field of bio-based polymers comprising succinic acid. Nevertheless these acids are still not economically attractive for some applications due to the larger demand compared to the offer in the market. For that reason, in order to create bio-based polymers the most promising polycarboxylic acids are still some examples like citric and tartaric acid because they are the most economically attractive for the industry and largely available.

Citric acid is a natural compound, synthesized in plant and animal cells during initial transformation in the Krebs cycle. It is a nontoxic compound, used as an antioxidant and preserving agent in the food industry or as stabilizer in the pharmaceutical industry [65].

Tartaric acid is a by-product of wine industry, nontoxic compound also used in the food industry, in medicine and pharmaceutical industry [66].

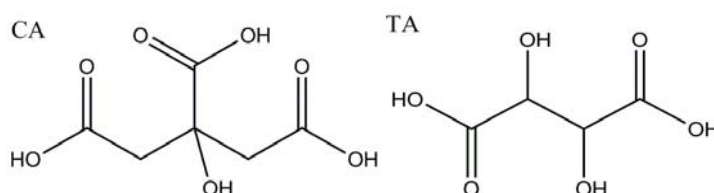


**Figure 1.14 – Scheme of (CA) citric acid and (TA) tartaric acid**

## 1.2 OBJECTIVES

---

As mentioned previously, nowadays the bio-based thermoset systems are strongly interesting for some applications like mineral wool, and glass and wood fiber product in general (i.e. chipboards and non-woven materials). Among them, the thermoset systems based on polycondensation reaction of a polysaccharide and a polycarboxylic acid are one of the most popular. In particular, polysaccharides derived from starch and starch itself seem to be the most promising in terms of cost and availability. Native starch would lead to the most attractive system from economical point of view, however it has some drawbacks regarding to the processability, first due to its insolubility in cold water and second due to its extremely high viscosity when it is heated in water. For some processes, such as spraying application these features might be an important inconvenient. However those starch derivatives from hydrolysis do not present these drawbacks, since they are soluble in cold water with still low viscosity; and they might be still interesting from economical perspective. These makes some starch derivatives such maltodextrin especially suitable for the formation of a crosslinked system with polycarboxylic acids. Regarding to the polycarboxylic acids, as mentioned above, citric and tartaric acids are the best candidates in terms of cost and availability. Furthermore they are water soluble what make them particularly suitable for their application in mineral wool, glass and wood fiber materials, and non-woven. In order to optimize the application of these systems on industrial process, first it is needed a good understanding of the reactions taking place. For this purpose, it has been selected the system comprising maltodextrin and a polycarboxylic acid.

This doctoral thesis is focused on the study of the systems comprising a starch derivative, particularly a maltodextrin derived from corn starch, with DE 12-15, and a polycarboxylic acid, particularly citric and tartaric acid, under simulated processing conditions (thermal treatment), for its application in the production of mineral wool insulation material.

The results of this work have been classified in different chapters where different topics related to the polycondensation of maltodextrin with polycarboxylic acids are described:

- I. First, it has been developed a methodology for the analysis of the polycondensation reaction of both reactants (i.e. maltodextrin and polycarboxylic acid). The methodology was focused on the analysis of the esterification reaction and the analysis of the

crosslinking process. It was developed using a system comprising maltodextrin and citric acid. This methodology was the basis for the characterization of different systems and their optimization all along the thesis work.

- II. By using the methodology previously developed, it was studied the influence of chemical structure of polycarboxylic acid on the reactivity of the system containing maltodextrin. For that, it was compared the reactivity of citric acid and tartaric acid. It was also evaluated the mechanical performance delivered by both systems by tensile-strength test. Furthermore, the distribution of both systems on glass fibers was analyzed by scanning electron microscopy (SEM).
- III. Considering the previous results it has been tried to improve the crosslinking of the system by the addition of divalent metal ions. The candidates selected for that were calcium ion and zinc ion. A comparative study was carried out on systems containing citric acid and tartaric acid. The effect of both ions in the different systems was analyzed by the methods described previously. Furthermore it was analyzed the distribution of the ions in the cured system by energy dispersive x-ray technique (EDX). The addition of calcium in the system containing maltodextrin and citric acid was deeper analyzed. Based on the results obtained it was proposed a mechanism of interaction of calcium ion with the crosslinked system.
- IV. Another feature to improve in the systems under study was its reactivity by the addition of a catalyst. The study was carried out for compositions containing maltodextrin, citric acid and sodium hypophosphite as catalyst. For that, methodology described previously was applied. Additionally, nuclear magnetic resonance (NMR) was used to get better understanding about the mechanisms of reaction involving sodium hypophosphite.
- V. Finally, one of the compositions previously studied was selected to be tested at industrial scale. This composition was integrated as part of the binder system for the production of mineral wool insulation material. Different mineral wool products were produced in industrial facilities and applying real process parameters. The quality of the products was

analyzed according to the standard norms in force in the European market and also it was tested their resistance to accelerated weathering conditions.

### 1.3 REFERENCES

---

1. Al-Homoud DMS. *Building and Environment* 2005;40(3):353-366.
2. Jelle BP. *Energy and Buildings* 2011;43(10):2549-2563.
3. Papadopoulos AM. *Energy and Buildings* 2005;37(1):77-86.
4. ASTM Standard C 168-97. Terminology relating to thermal insulating materials, 1997.
5. Technavio. *Global Cold Insulation Market 2015-2019*. 2015.
6. B. Sirok BB, P. Bullen. *Mineral Wool, Production and Properties*. England: Cambridge International Science Publishing Ltd, Woodhead Publishing Limited and CRC Press LLC, 2008.
7. Pilato L. *Phenolic resins: A century of progress*. New York: Springer Berlin Heidelberg, 2010.
8. A. Gardziella LAP, A. Knop. *Phelic Resins - Chemistry, Applications, Standardization, Safety and Ecology*, 2nd ed. New York: Springer-Verlag Berlin Heidelberg 2000.
9. Kollek H, Brockmann H, and Muller von der Haegen H. *International Journal of Adhesion and Adhesives* 1986;6(1):37-41.
10. Salthammer T, Mentese S, and Marutzky R. *Chemical Reviews* 2010;110(4):2536-2572.
11. IRIS File for Formaldehyde, <http://www.epa.gov>.
12. IARC Monographs on the Evaluation of Carcinogenic Risks to Humans (see <http://monographs.iarc.fr/ENG/Monographs/vol88/index.php> and <http://monographs.iarc.fr/ENG/Meetings/88-formaldehyde.pdf>
13. D.A. Kaden CM, G.D. Nielsen, et al. . Formaldehyde. In: *WHO Guidelines for Indoor Air Quality: Selected Pollutants*. Geneva: World Health Organization, 2010.
14. T. Neuhaus RO, A.U. Clausen. *Formaldehyde emissions from mineral wool in building constructions into indoor air*. Indoor Air 2008. Copennhagen, Denmark, 2008.
15. W. Heep JGB. "AsWood™ Resin System" Protein modified Resol resins for the low formaldehyde emissions panels. 9th Pacific Rim Bio-Based Composites Symposium, 2008. pp. 165-171.
16. Herwijnen Hendrikus W. G. Van WH, Detlef Krug, Andreas Weber, Axel HÖHLING, Maria Schultze. *Liant pour matériaux à base de copeaux et/ou de fibres de bois, procédé de fabrication de ce liant et élément moulé*. WO 2009077571 A1: Dynea Oy, 2008.
17. Nikvash N, Kharazipour A, and Euring M. *Forest Products Journal* 2012;62(1):49-57.
18. Christiansen AW. *Wood adhesives* 1985:211–226.

19. A.H. Conner LFL. *Journal of Wood Chemistry and Technology* 1986; 6(4):59–613.
20. Dotan A. 15 - Biobased Thermosets. In: Dodiuk H and Goodman SH, editors. *Handbook of Thermoset Plastics (Third Edition)*. Boston: William Andrew Publishing, 2014. pp. 577-622.
21. Ramirez EC and Frollini E. *Composites Part B: Engineering* 2012;43(7):2851-2860.
22. Kim S. *Bioresour Technol* 2009;100(2):744-748.
23. Mahendran AR, Wuzella G, Aust N, Müller U, and Kandelbauer A. *Polymers & Polymer Composites* 2013;21(4):199-205.
24. Rubio MVA. *Formulación y curado de resinas fenol-formaldehido tipo "resol" con sustitución parcial de fenol por lignosulfonatos modificados*. Chemical Engineeign Department, vol. PhD. Madrid-Spain: Complutense University, 2002.
25. Engelmann G and Ganster J. 7 - Lignin Reinforcement in Thermosets Composites A2 - Faruk, Omar. In: Sain M, editor. *Lignin in Polymer Composites*: William Andrew Publishing, 2016. pp. 119-151.
26. Charles T. Arkens CEC, Reginald T. Smart. Heat-resistant nonwoven fabric, US5143582A. Rohm & Haas Company, 1991.
27. Charles T. Arkens RDG. Curable aqueous composition and use as fiberglass nonwoven binder, US5661213A. Rohm & Haas Company, 1992.
28. Technical information Aquaset technology Dow Construction Chemicals (see <http://www.dowconstructionchemicals.com/na/en/products/insulation/>).
29. Wilhelm F. Beckerle SD, Bernd Reck, Joachim Roser, Johannes Türk, Eckehardt Wistuba. *Wässrige Zusammensetzungen*, EP1005508A1. BASF Aktiengesellschaft, 1997.
30. Thomas J. Taylor DCB, Paul Nedwick. Polycarboxy/polyol fiberglass binder of low pH, US6331350B1. Johns Manville International, Inc., Rohm & Haas Company, 1998.
31. William K. Cheung PRK, William Barrick, Jeff W. Tigner. Polyester compositions, WO1995016747A1. Owens Corning, 1993.
32. Frank C. O'Brien-Bernini LC, Yadollah Delaviz, Kathleen M. Bullock, William E. Downey. *Extended binder compositions*, US7026390B2. Owens Corning Fiberglass Technology, Inc., 2002.
33. Gudik-Sorensen M. *Binder for mineral fibers*, US20110189492A1. Mads Gudik-Sorensen, 2006.
34. Kevin R. Anderson LTB, Shannon N. Shriver, Shuang Zhou. *Bio-based pre-reacted product of polyol and monomeric or polymeric polycarboxylic acid*, WO2012138718A1. Cargill, Inc., 2011.
35. Baynes JW. *Journal of the American Chemical Society* 2005;127(41):14527-14528.
36. S.E. Fayle JAG. *The Maillard Reaction*. Cambridge: The Royal Society of Chemistry, 2002.
37. Ajandouz EH, Desseaux V, Tazi S, and Puigserver A. *Food Chemistry* 2008;107(3):1244-1252.

38. Wang H-Y, Qian H, and Yao W-R. *Food Chemistry* 2011;128(3):573-584.
39. Yaylayan VA and Kaminsky E. *Food Chemistry* 1998;63(1):25-31.
40. Costa NA, Pereira J, Ferra J, Cruz P, Martins J, Magalhães FD, Mendes A, and Carvalho LH. *Wood Science and Technology* 2013;47(6):1261-1272.
41. Erling Lennart Hansen TH, Povl Nissen. Binder for mineral wool products, EP207523A2. Rockwool International 2000.
42. Philippe Espiard MD, Anne Pagnoux, François Boyer. Mineralfaserplatten schlichtezusammensetzung mit einem poysaure und einer polyamin, verfahren zur herstellung sowie deren produkte, EP1618238B1. Saint-Gobain Isover, 2003.
43. Charles F. Appley RAH, Ronald E. Kissell, Patrick M. Noonan, Brian Lee Swift, Ruijian Xu. Binders and materials therewith, EP2108006A1. Knauf Insulation GmbH, 2007.
44. Sharon P. Lee SPP, Daniel B. Solarek. Thermosetting Polysaccharides, EP0911361B1. National Starch and Chemical Investment Holding Corporation, 1997.
45. HERwijnen Hendrikus W. G. Van EP, Barbara Stefke. Renewable binder for nonwoven materials, EP2077977B1. Dynea Chemicals OY, 2006.
46. Jaffrennou B. Sizing composition for mineral wool based on a hydrogenated sugar and insulating products obtained, EP2324089A1. 2008.
47. Christopher M. Hawkins JMH-T, Liang Chen. Bio-based binders for insulation and non-woven mats. Owens Corning, 2009.
48. M. Castro-Cabado ALCD, et al. Formaldehyde-free binder and use for mineral wool insulation products, US9242899B2. URSA Insulation S.A., 2012.
49. Halpern JM, Urbanski R, Weinstock AK, Iwig DF, Mathers RT, and von Recum HA. *Journal of Biomedical Materials Research Part A* 2014;102(5):1467-1477.
50. Ghosh Dastidar T and Netravali AN. *Carbohydrate Polymers* 2012;90(4):1620-1628.
51. Reddy N and Yang Y. *Food Chemistry* 2010;118(3):702-711.
52. Pérez S, Baldwin PM, and Gallant DJ. Chapter 5 - Structural Features of Starch Granules I. *Starch (Third Edition)*. San Diego: Academic Press, 2009. pp. 149-192.
53. Chen P, Yu L, Simon GP, Liu X, Dean K, and Chen L. *Carbohydrate Polymers* 2011;83(4):1975-1983.
54. G. Gordon Bugg DDG, Robert L. Kearney, Charles P. Klass, Dr. Anthony V. Lyons and Stig V. Renvall. *Starch and Starch Products in Surface Sizing and Paper Coating: Tappi Pr*, 1997.
55. Miao M, Li R, Jiang B, Cui SW, Zhang T, and Jin Z. *Food Chemistry* 2014;151(0):154-160.
56. Han F, Gao C, Liu M, Huang F, and Zhang B. *International Journal of Biological Macromolecules* 2013;59(0):372-376.
57. Bayazeed A, Farag S, Shaarawy S, and Hebeish A. *Starch - Stärke* 1998;50(2-3):89-93.
58. Tolvanen P, Sorokin A, Mäki-Arvela P, Murzin DY, and Salmi T. *Industrial & Engineering Chemistry Research* 2013;52(27):9351-9358.



59. Chiu C-w and Solarek D. Chapter 17 - Modification of Starches. Starch (Third Edition). San Diego: Academic Press, 2009. pp. 629-655.
60. Schwartz D and Whistler RL. Chapter 1 - History and Future of Starch. Starch (Third Edition). San Diego: Academic Press, 2009. pp. 1-10.
61. Jane J. Journal of Macromolecular Science, Part A 1995;32(4):751-757.
62. Robyt JF. Chapter 7 - Enzymes and Their Action on Starch. Starch (Third Edition). San Diego: Academic Press, 2009. pp. 237-292.
63. M. W. Kearsley SZD. Handbook of Starch Hydrolysis Products and their Derivatives: Springer US, 1995.
64. Bechthold I, Bretz K, Kabasci S, Kopitzky R, and Springer A. Chemical Engineering & Technology 2008;31(5):647-654.
65. Apelblat A. Citric Acid: Springer International Publishing, 2014.
66. Jacek Gawroński KG. Tartaric and Malic Acids in Synthesis. A source book of building blocks, ligands, auxiliaries and resolving agents: John Wiley and Sons, 1999.



---

## *CHAPTER II*

---

# *METHODOLOGY TO STUDY THE CROSSLINKING BETWEEN MALTODEXTRIN AND POLYCARBOXYLIC ACIDS UNDER PROCESSING CONDITIONS*

---

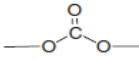
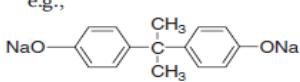
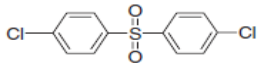
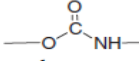
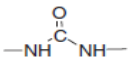
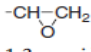
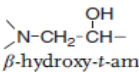
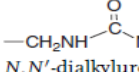


## 2.1 INTRODUCTION

### 2.1.1 POLYCONDENSATION

The polycondensation reaction refers to the formation of large molecules starting from smaller ones containing suitable groups (e.g. carboxyls and hydroxyls) to react and to create a bond by splitting off a small molecule (e.g. water). This concept was introduced in the middle of nineteenth century [1]. The first commercial product synthesized by this technique was phenol-formaldehyde resins. Later, in 1930's it appeared the polyesters discovered by Carothers [2, 3]. The most relevant examples of polycondensation reactions are shown in Table 2.1.

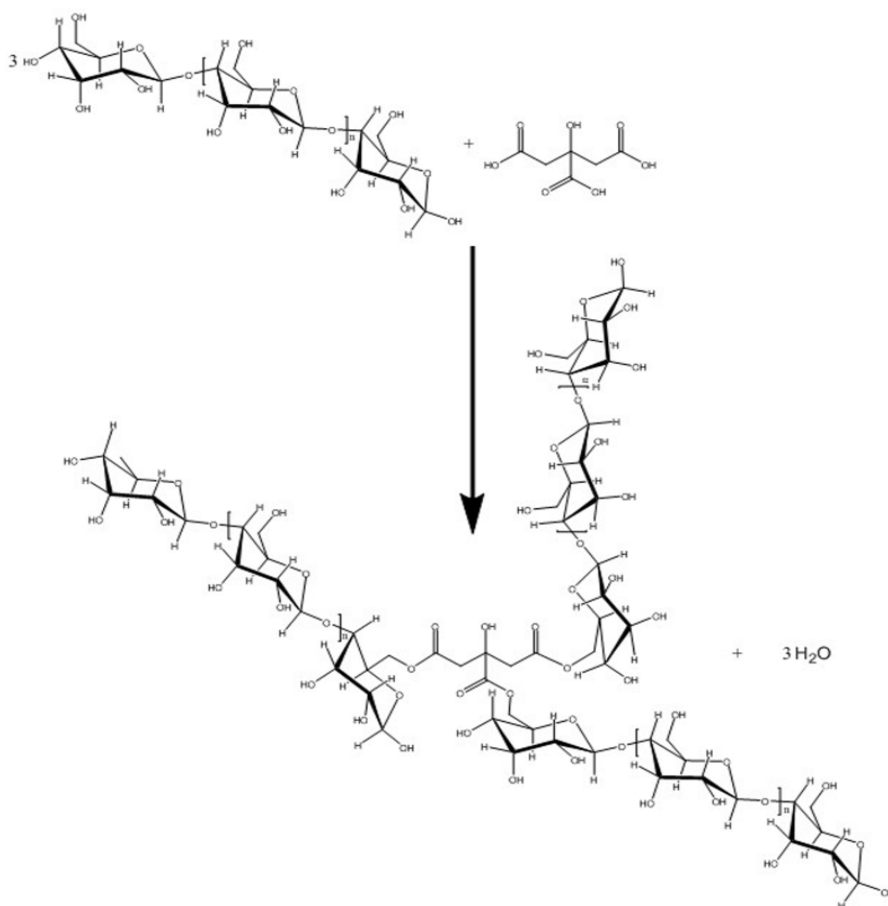
Table 2.1 – Most relevant polycondensation reactions [1]

Functional groups or monomers		Connecting group	By-product
–COOH Carboxylic acid	–OH hydroxyl	–COO– ester	H <sub>2</sub> O
–COOR Ester	–OH hydroxyl	–COO– ester	R–OH
–COOH Carboxylic acid	–NH <sub>2</sub> primary amine	–CONH– amide	H <sub>2</sub> O
ClCOCl/–COCl Phosgene/chloroformate	–OH hydroxyl	 carbonate	HCl
Na <sub>2</sub> S/–SNa Di-sodium sulfide monomer/sodium sulfide end group	–Cl chloro end group (as in ClC <sub>6</sub> H <sub>4</sub> Cl)	–S– sulfide	NaCl
NaO– Sodium alkoxide/phenoxide, e.g., 	–Cl chloro end group, e.g., 	–O– ether	NaCl
–N=C=O Isocyanate	–OH hydroxyl	 urethane	none
–N=C=O Isocyanate	–NH <sub>2</sub> primary amine	 urea	none
 1,2-epoxide	–NH– secondary amine	 <i>β</i> -hydroxy- <i>t</i> -amine	none
–CH <sub>2</sub> OH Methylol	(NH <sub>2</sub> ) <sub>2</sub> CO/NH <sub>2</sub> CONH– urea/ <i>N</i> -alkylurea	 <i>N,N'</i> -dialkylurea	H <sub>2</sub> O
Ar–CH <sub>2</sub> OH Aromatic methylol	Ar'–CH <sub>2</sub> OH aromatic methylol	Ar–CH <sub>2</sub> –Ar'	HCHO

Polycondensation takes place either between monomers having two unlike groups suitable for reaction like, for instance hydroxycarboxylic acids (AB-AB type); or between two different monomers, each possessing two identical reactive groups like, for instance, polycondensation of diols with dicarboxylic acids (AA-BB type) [4-6].

## 2.1.2 POLYCONDENSATION OF POLYSACCHARIDES WITH POLYCARBOXYLIC ACIDS

Polycondensation reaction of polysaccharides with polycarboxylic acids belongs to the type AA-BB described above, reacting the hydroxyl groups of polysaccharide (AA monomer) with the carboxyl groups of polycarboxylic acid (BB monomer). The polycondensation reaction in this case might follow the reaction shown in Scheme 2.1.



Scheme 2.1 – Possible polycondensation reaction between maltodextrin and citric acid

In 1988, Welch reported that polycarboxylic acids could be efficient crosslinking agents of cellulose, therefore they were used in the durable press finishing of cotton [7]. Later in 2005, Martel et al. studied the same reaction but replacing the cellulose by cyclodextrin [8]. Nowadays, the crosslinked systems, result of the polycondensation reaction between starch based polysaccharides and polycarboxylic acids, are being of great interest as replacement of the petrol based thermoset systems in non-woven, glass and wood fiber industries [9, 10]. In this context, the multifunctional carboxylic acids such as citric acid are reported as suitable candidates for crosslinking reactions with the polysaccharides by esterification (Scheme 2.1), in addition to their secondary interactions through hydrogen bonds [11-13].

### **2.1.3 PROCESSING CONDITIONS**

---

Bonding of wood and glass fibers and non-woven fibers takes place by coating the fibers with the corresponding binder and followed by a heating treatment. The heating treatment is applied, on the fiber mat coated with the binder, by different technologies like, for instance, hot air, pressing, calendering, etc. The temperature applied is higher than 100 °C, for some seconds or even up to around 5 min [14-16]. These processing conditions are difficult to be fully reproduced in lab, however some techniques might allow to predict the crosslinking behavior of systems based on polysaccharides and polycarboxylic acids later in the industrial process.

### **2.1.4 CHARACTERIZATION OF POLYCONDENSATION REACTION**

---

Citric acid is a non-toxic and inexpensive weak organic acid from natural origin, known to react with polysaccharides in a variety of industries [13, 17, 18]. Maltodextrin is a starch-based polysaccharide produced by hydrolysis of starch down to glucose polymers with an average chain length of 5-10 glucose units/molecule [19]. Maltodextrin is soluble in water what makes it more attractive for the industry compared to insoluble starch, and it can be used as model molecule of high molecular weight starch to study its modification by condensation reactions with polycarboxylic acids [20]. The results can be easily extrapolated to specific industrial processes and applications already mentioned above.

Different techniques like titration, NMR, optical spectroscopy and chromatography [21] have been reported in the literature to study the condensation reaction between polysaccharides and polycarboxylic acids. Nevertheless, some of these techniques present important drawbacks for the industry. For instance, titration allows determining the degree of esterification but it would be difficult to use when the resulting polycondensate is applied over a substrate like a non-woven glass fiber. NMR and chromatography are very expensive techniques which cannot be afforded normally by the industry. In the field of optical spectroscopy, FTIR has been previously reported for the analysis of the polycondensation reaction in polyesters, based on the evolution of C=O stretching band [22, 23]. This technique would allow the analysis of the polycondensation over any substrate and could be easily afforded by the industry. Other techniques, like differential scanning calorimetry (DSC) are usually applied to evaluate the reaction kinetics. However, it has been found that DSC does not give accurate information about the kinetics of the esterification reaction due to the overlapping of the heat related to the esterification reaction and the heat related to the evaporation of the water released by the esterification. TGA has been previously reported to evaluate the esterification reaction kinetics between glycerol and citric acid, based on the measurement of the water lost during the heating process [12]. Therefore, TGA could be a useful technique providing information about the progress of the polycondensation reaction between maltodextrin and citric acid. Dynamic mechanical analysis (DMA) and rheology are well-known techniques to study polymeric systems [24]. Among them, rheology seems to be the most appropriate to study crosslinking systems in water solution [25, 26]. This technique could provide information about the crosslinking capacity of the water-based systems containing maltodextrin and citric acid.

## 2.2 AIM OF THIS CHAPTER

---

The aim of this chapter was to study the suitability of IR, TGA and rheology as complementary techniques to come across with a reliable protocol to characterize polycondensation reactions between starch-based polysaccharides and polycarboxylic acids under thermal processing conditions interesting for the industry. The information obtained allowed well understanding not only the polycondensation reaction taking place but also the formation of crosslinked systems



under thermal treatment for their application as binding systems in glass and wood fiber as well as non-woven materials.

## 2.3 MATERIALS AND METHODS

---

### 2.3.1 MATERIALS

---

Powdered maltodextrin Maldex 120 (dextrose equivalent (DE) 11 to 15), manufactured by spray-drying of liquid maltodextrin derived from edible corn starch hydrolysis, was provided by Tereos Syral. Citric acid reagent was purchased from Sigma-Aldrich. The products were used without additional purification.

### 2.3.2 METHODS

---

Solutions of maltodextrin (MAL) and citric acid (CA) were prepared in water at different ratios (Table 2.2). Maltodextrin was dissolved in distilled water under mechanical stirring and then citric acid was added to the solution under the same stirring. Unless otherwise stated, solutions in water were prepared with 50 % dry content. Polycondensation reaction was carried out on 20 g of water solution in a ventilated oven at 140 °C, simulating the thermal treatment of the potential industrial applications. Freeze-dried samples of the different water solutions were also prepared to avoid the influence of the water in their later analysis (i.e. TGA) [27].

**Table 2.2 – Compositions MAL/CA**

Composition	MAL/CA (dry w/w)
M20C80	20/80
M40C60	40/60
M60C40	60/40
M80C20	80/20

## 2.4 CHARACTERIZATION TECHNIQUES

---

### 2.4.1 ATR-FTIR SPECTROSCOPY

---

ATR-FTIR spectra were measured in a Spectrum One FT-IR Spectrometer (Perkin Elmer) with a split peak accessory for ATR. Absorbance spectra were acquired in ATR mode, at  $4\text{ cm}^{-1}$  resolution and signal-averaged over 10 scans recorded from  $4000\text{ cm}^{-1}$  to  $650\text{ cm}^{-1}$ . Spectra were baseline corrected and normalized to the most intense absorbance peak. FTIR spectra were measured for MAL and CA, as well as for the freeze-dried samples of the compositions in Table 2.2, and the corresponding water solutions upon thermal treatment at  $140\text{ }^{\circ}\text{C}$ . In order to assure the interpretation of the spectra of the compositions after thermal treatment, spectra were measured for the resulting polycondensate samples before and after purification. The polycondensate samples were purified by membrane dialysis, placing approximately 2 g of sample in a 1000 Da membrane, in 2 L of water for 20 hours, renovating the water after 10 hours. The purified product was dried under vacuum at  $40\text{ }^{\circ}\text{C}$  for 24 hours. The thermal treatment and corresponding spectra measurement was done by duplicate, and all samples were powdered previously to their analysis. In order to follow the progress of the polycondensation reaction, the peak assigned to the ester carbonyl (C=O) stretching vibrations and the peak due to hydroxyl (OH) stretching were selected as analyte peaks.

### 2.4.2 THERMOGRAVIMETRIC ANALYSIS (TGA)

---

TGA was performed using a TGA Q500 (TA Instruments). The CA, MAL and the different freeze-dried samples of the compositions in Table 2.2 were heated in a platinum pan from  $25$  to  $600\text{ }^{\circ}\text{C}$ , under a nitrogen atmosphere at a heating rate of  $10\text{ }^{\circ}\text{C}/\text{min}$ . The derivative thermogram (wt %/ $^{\circ}\text{C}$ ) of each sample was obtained from the software TA Universal Analysis. The composition M60C40 was found to be the most interesting from application point of view. Therefore, isothermal treatment at temperature of  $140\text{ }^{\circ}\text{C}$  was also followed for the freeze-dried sample of this composition at different heating times; for that, previously heating up to  $140\text{ }^{\circ}\text{C}$  was carried out at a heating rate of  $10\text{ }^{\circ}\text{C}/\text{min}$ . The isothermal analyses were done by duplicate.

### 2.4.3 RHEOLOGICAL MEASUREMENTS

---

The rheological measurements were carried out with an AR1000 rheometer (TA Instruments). Disposable plate-plate geometry with diameter 25 mm was used. Dynamic measurements in oscillatory mode were performed at frequency 1 Hz, with a fixed torque value (tests were performed previously to ensure that the response was in the viscoelastic region) and a gap of 1000  $\mu\text{m}$ . First, rheological behavior of the freeze-dried samples of the compositions in Table 2.2 was monitored for temperature range between 50  $^{\circ}\text{C}$  and 200  $^{\circ}\text{C}$  (typical range of the working temperature in real industrial applications) with a ramp rate of 5  $^{\circ}\text{C}/\text{min}$ . Second, isothermal monitoring was carried out at 140  $^{\circ}\text{C}$  during maximum 100 min, previously heating up to 140  $^{\circ}\text{C}$  with a ramp rate of 10  $^{\circ}\text{C}/\text{min}$ . All the rheological measurements were done by duplicate.

## 2.5 RESULTS AND DISCUSSION

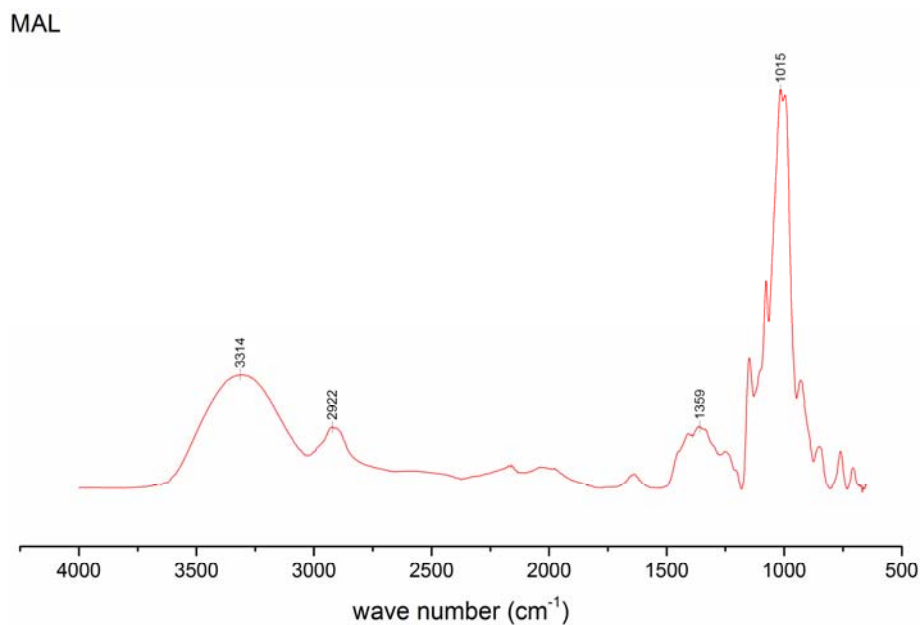
---

The behavior of the compositions in Table 2.2 under thermal treatment was systematically evaluated by three techniques, namely FTIR, TGA and rheology.

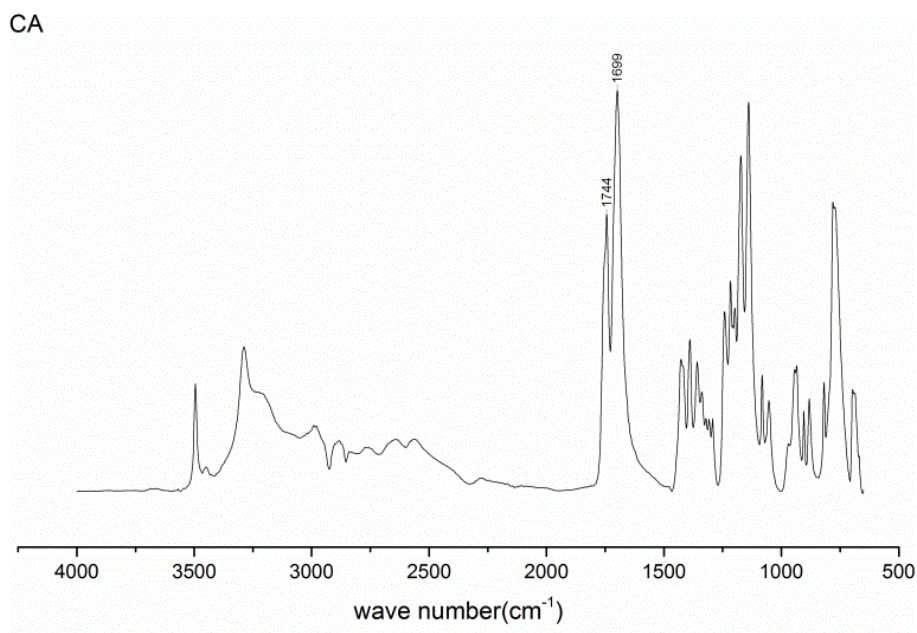
### 2.5.1 INFRARED ANALYSIS

---

The evolution of the esterification reaction between CA and MAL was analyzed comparing the FTIR spectra of water solutions of different compositions described in Table 2.2, under treatment at 140  $^{\circ}\text{C}$ . As a reference, Figure 2.1 and Figure 2.2 show the FTIR spectra of MAL and CA respectively. The main IR regions of MAL are below 1000  $\text{cm}^{-1}$ , which characterizes the anhydroglucose ring stretching vibrations; between 800-1500  $\text{cm}^{-1}$  assigned to C-O bond stretching; the region between 2800 and 3000  $\text{cm}^{-1}$  attributed to C-H deformation; and finally the region between 3000 and 3600  $\text{cm}^{-1}$  assigned to OH stretching [28, 29]. In the spectrum of CA, the absorptions at 1699 and 1745  $\text{cm}^{-1}$  are assigned to the C=O stretching vibration of the carboxylic acid groups, which are the most relevant bands regarding the esterification reaction.

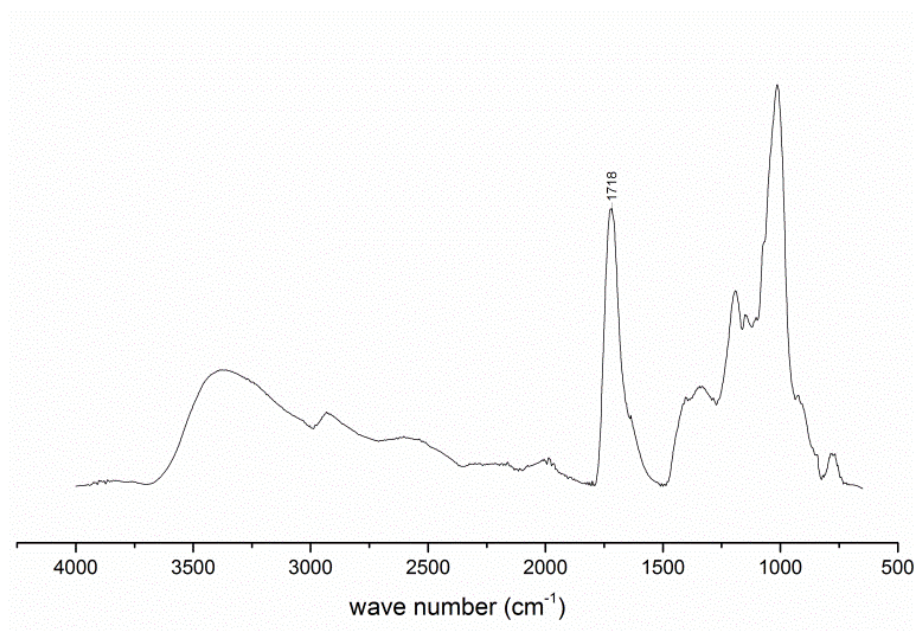


**Figure 2.1 – FTIR spectra of (MAL) maltodextrin**



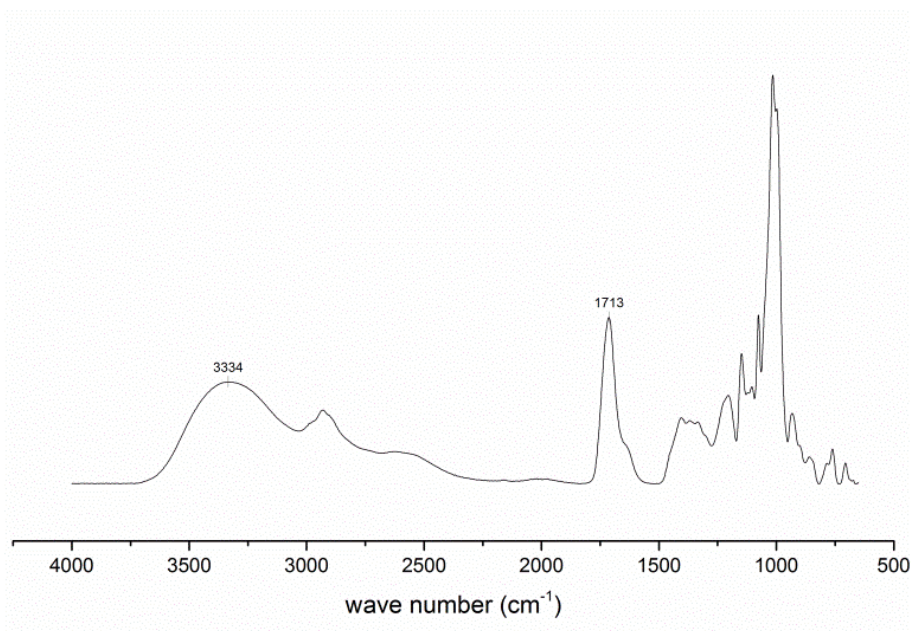
**Figure 2.2 – FTIR spectra of (CA) citric acid**

Figure 2.3 shows the spectrum of water solution of the composition M60C40 after thermal treatment at 140 °C for 4 hours. This spectrum shows clear differences with respect to the initial reactants (MAL and CA). The two characteristic C=O stretching bands in free CA at 1699 and 1745  $\text{cm}^{-1}$  convert to one single signal at 1718  $\text{cm}^{-1}$  in the reaction product, which corresponds to the coalescence of the new ester carbonyl bond and remaining free carboxyl groups of CA [12, 30].



**Figure 2.3 – FTIR spectrum of the composition M60C40 after thermal treatment at 140 °C during 4 hours**

It is well known that not all the carboxyl groups of CA have the same reactivity, therefore, it is expected that not all the carboxyl groups participate in the esterification reaction [17]. Alternatively, unreacted carboxyl groups in CA could interact by hydrogen bond with the hydroxyl groups of MAL. This hypothesis is supported when comparing the spectrum of the freeze-dried sample of the composition M60C40, without thermal treatment (Figure 2.4), with the spectrum of CA (Figure 2.2). It can be observed that the C=O stretching bands of carboxyl groups in CA shift to one single band at  $1713\text{ cm}^{-1}$ . Simultaneously, the peak due to OH stretching it makes broader with maximum absorbance at  $3334\text{ cm}^{-1}$ . This indicates the existence of interactions between carboxyl groups of CA and hydroxyl groups of MAL although no thermal treatment was applied. These interactions could be assigned to hydrogen bond interactions [13]. This result is relevant because non-reacted carboxyl groups in the CA moieties (i.e. with no participation in the esterification reaction) would still contribute to improve the properties of the polymer network by the additional hydrogen bond interactions with the polysaccharide chains. A similar behavior is observed in the rest of the compositions from Table 2.2.



**Figure 2.4 – FTIR spectrum of freeze-dried sample of composition M60C40**

The FTIR spectra of the compositions in Table 2.2 after 4 hours thermal treatment at 140 °C are shown in Figure 2.5. The absorption peaks at 1709, 1713, 1718 and 1725  $\text{cm}^{-1}$  are ascribed to the C=O stretching vibration corresponding to the coalescence of the ester carbonyl bond and free carboxyl groups of CA [30]. These signals confirm that the esterification of MAL has taken place with relatively good extension [31, 32]. However, the shift of the C=O stretching band towards higher wave number depends on the composition of the system, being more accentuated the greater the ratio of MAL. This may suggest that reactivity of the polycondensation system strongly depends on its composition.

The composition M60C40 has been identified to be the most interesting from application point of view. As an example, the progress of the esterification reaction of this composition was studied by following the evolution of IR signals at 140 °C, during different reaction times, as shown in Figure 2.6. It is observed that the original C=O stretching bands in free citric acid change their wave number and intensity as the esterification progresses. The signal at 1699  $\text{cm}^{-1}$  disappears in no more than 1 hour while the resulting band shifts wave number until reaching maximum value in more than 4 hours. The characteristic bands corresponding to the C-O stretching of MAL, from 1000 to 1500  $\text{cm}^{-1}$ , appear broader with the time of treatment due to the condensation with the carboxyl groups of the polycarboxylic acid, and simultaneously the band in range 3000-3600  $\text{cm}^{-1}$  corresponding to OH stretching becomes less intense.

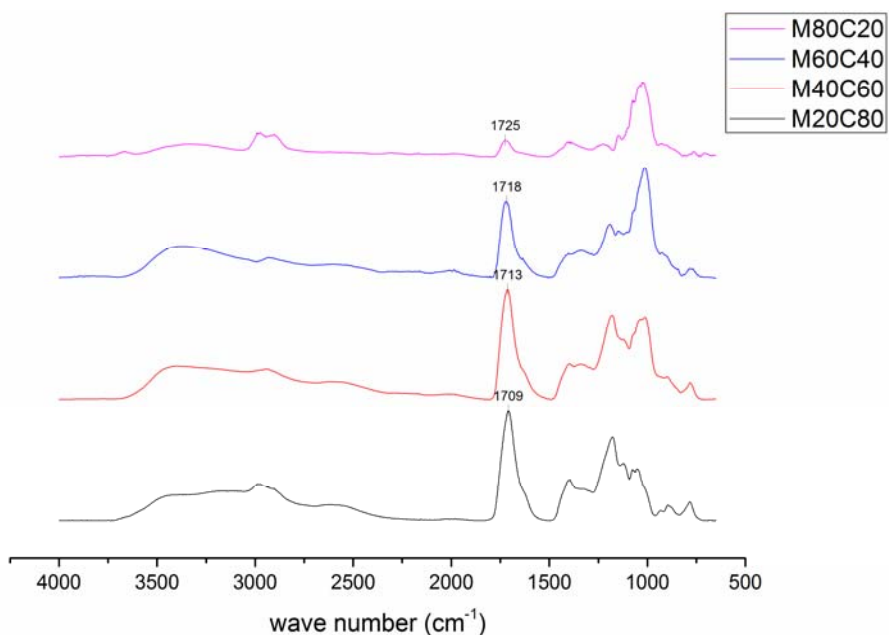


Figure 2.5 – FTIR spectra of compositions M20C80, M40C60, M60C40 and M80C20. All the spectra correspond to the polycondensation products after a thermal treatment at 140 °C during 4 hours

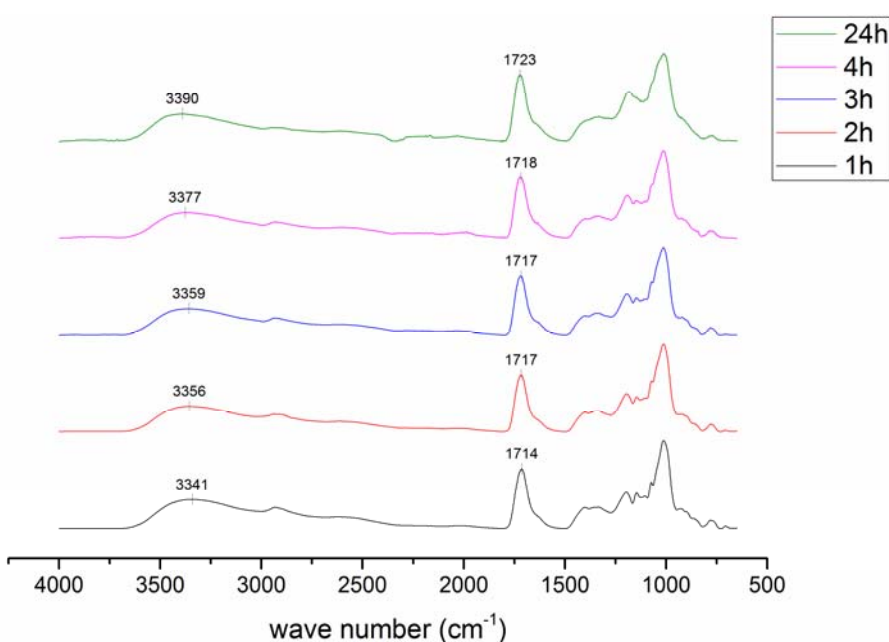


Figure 2.6 – FTIR spectra of composition M60C40 at different times under thermal treatment at 140 °C

According to the FTIR spectra in Figure 2.6, the absorbance of C=O stretching band is increasing while the absorbance of OH stretching band is decreasing as esterification reaction progresses. Therefore, the progress of the polycondensation reaction could be quantified by the ratio between the absorbance of C=O stretching band and OH stretching band. The data obtained for the composition M60C40 are quoted in Table 2.3. Overall, it can be seen that the greatest

increase of the ratio, between the absorbance of C=O stretching band and OH stretching band, is taking place during the first 2 hours of treatment. Afterwards, the reaction progresses smoothly until 4 hours heating. After 24 hours heating, the ratio, between the absorbance of C=O stretching band and OH stretching band, is not increasing but keeping in the same level or even it could decrease due to the partial decomposition of the different compounds [33].

**Table 2.3 – Ratio between absorbance of C=O band and OH band**

Heating Time (h)	Ratio Absorbance CO/OH
1	2,06 ± 0,02
2	2,22 ± 0,01
3	2,21 ± 0,05
4	2,36 ± 0,02
24	2,31 ± 0,22

The presence of unreacted polycarboxylic acid after thermal treatment was proven by comparing the FTIR spectrum of the polycondensation product after dialysis purification with the spectra of the supernatant dialysis water. As an example, Figure 2.7 shows these two spectra for the polycondensation product of composition M60C40 after 24 hours heating at 140 °C. The C=O stretching band ascribed to carboxyl ester can be clearly seen in the spectrum of the dialyzed polycondensation product, at 1723 cm<sup>-1</sup>; yet, a typical band of free carboxyl group can be observed in the spectrum of the supernatant dialysis water at 1638 cm<sup>-1</sup>.

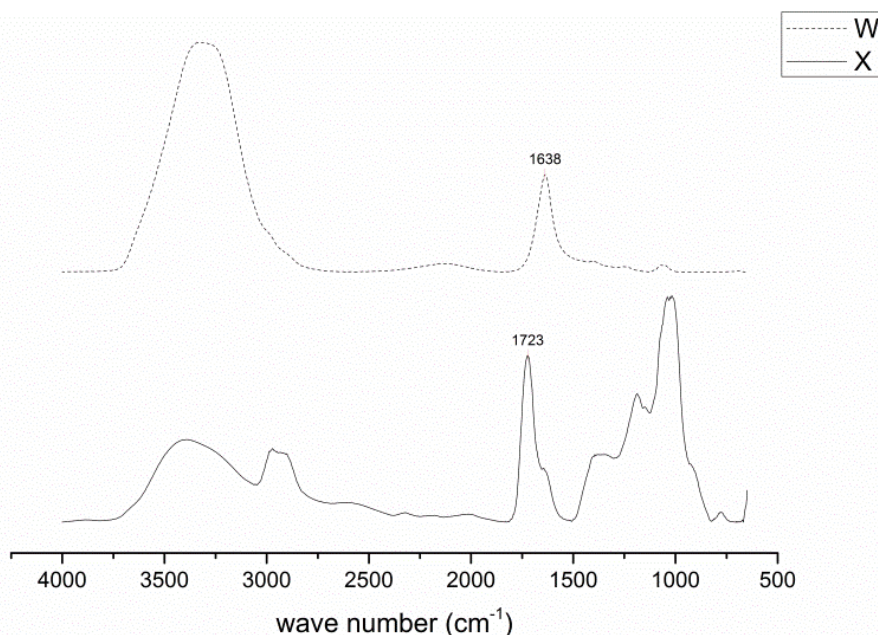


**Figure 2.7 – FTIR spectra of (X) composition M60C40 after the polycondensation reaction at 140 °C during 24 hours, and later dialysis and (W) supernatant dialysis water**



By IR it is proved the esterification taking place between MAL and CA; but also the polycondensation by esterification is demonstrated by the persistence of ester groups in the cured material after leaching treatment.

## 2.5.2 TGA

The TGA weight loss curves of MAL and CA are shown in Figure 2.8, which serve as references to later study the systems in Table 2.2. The differences suggest different mechanism of degradation. The thermogram of MAL exhibits a small weight loss at around 100 °C assigned to desorption of water (i.e. humidity). The onset degradation temperature can be identified at around 208 °C and, maximum decomposition rate at around 308 °C, which is the typical thermal degradation profile of polysaccharides [34, 35]. This corresponds to a depolymerization of the macromolecules with the formation of a range of lower molecular-weight volatile and gaseous fragmentation products [36, 37]. The small amount of non-volatilized residue at 600 °C (13 % weight of sample) is assigned to a final carbon residue. This residue is oxidized to carbon dioxide when the experiment is carried out in oxygen atmosphere [34]. The thermogram of CA shows a degradation onset around 150 °C and a maximum decomposition rate around 205 °C as early described [38]. This corresponds to the thermal degradation of the acid to give carbon dioxide and water as well as intermediate cyclic acids [39].

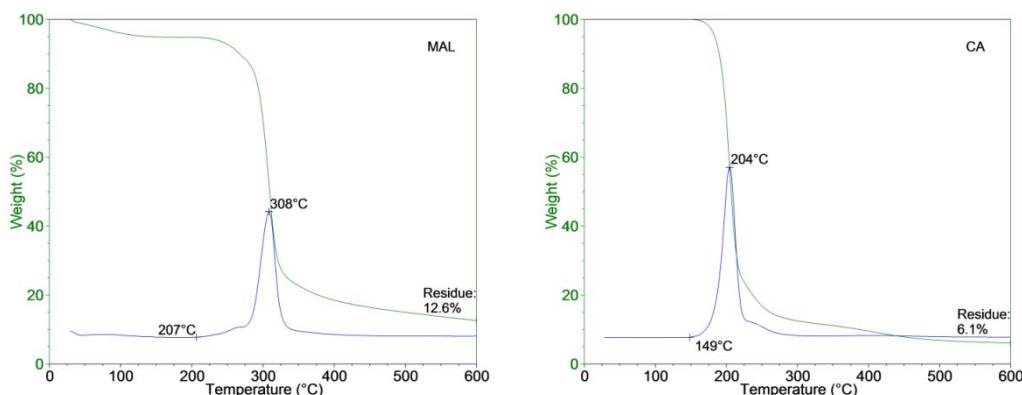
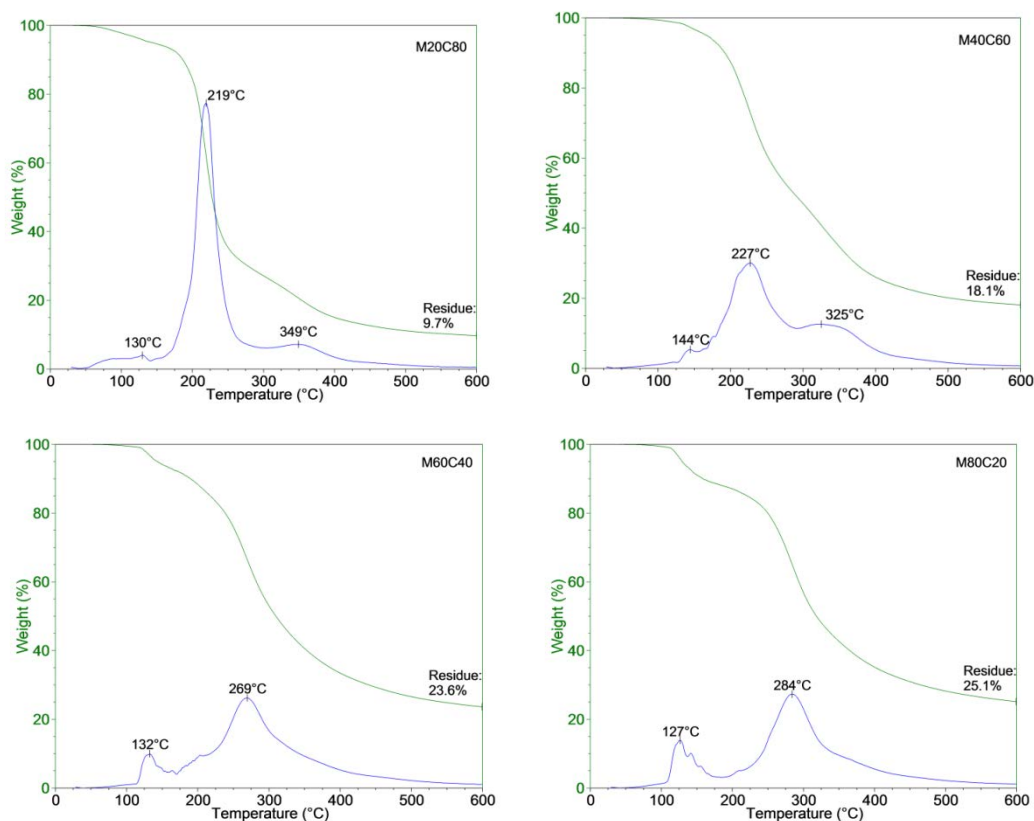


Figure 2.8 – TGA and corresponding derivative of (MAL) maltodextrin and (CA) citric acid

The TGA curves for freeze-dried samples of compositions in Table 2.2 are shown in Figure 2.9.



**Figure 2.9 – TGA and corresponding derivative of freeze-dried sample of compositions in Table 2.2**

The most remarkable feature is the mass loss at 130-140 °C, which is not present in either MAL or in CA. This weight loss has been assigned to the release of water following the esterification reaction between hydroxyl groups of maltodextrin and the carboxyl groups of citric acid [12]. Note that this weight loss cannot be assigned to desorption of water from maltodextrin because the samples have been previously freeze-dried, and because if there would be a residual amount of humidity, it would be released at temperatures around 100 °C, as seen in the thermogram of MAL (Figure 2.8). Similarly, the mass loss at 130-140 °C cannot be assigned to the degradation of CA, as this would start at 149 °C (Figure 2.8). Two additional weight losses can be identified for compositions rich in CA. The first weight loss starts at around 180 °C and the second one starts at around 280 °C, both of them assigned to the thermal degradation of polycondensate products. These two weight losses merge to one single weight loss process starting at around 180 °C when compositions are rich in MAL. In any case, the maximum weight loss rate shifts to higher temperatures as mixtures are richer in MAL. The thermodegradation behavior of the

polycondensate products is intermediate between that of MAL and CA. It is important to stress that it is not observed independent thermal degradation to be assigned to free CA or MAL. The residual weight left at 600 °C also varies depending on the composition. It shifts to greater values as maltodextrin content is increasing in the composition (from 10 % to 25 %). In all cases, this value is greater than the residue left by CA (6 %) and, greater than MAL (13 %) residue except for composition containing mostly citric acid. This could be a consequence of the thermal stability of the compounds formed by the polycondensation reaction. All these results together prove the polycondensation reaction between MAL and CA.

The TGA was used to quantify the progress of the esterification reaction of the composition M60C40, following the weight loss under isothermal heating at 140 °C with the time. Considering the above mentioned results, the weight loss occurring at this temperature is due to the water released by reacting the carboxyl groups from citric acid and the hydroxyl groups from maltodextrin (Scheme 2.1) [12]. In this context, the number of carboxyl and hydroxyl equivalents reacted under the isothermal heating are equal to the consequent number of equivalents of the water released. According to this interpretation, the number of carboxyl and hydroxyl equivalents reacted for different heating times were calculated; and, the ratio between the number of reacted equivalents and the number of equivalents in the original composition was considered as signal to quantify the progress of polycondensation reaction of the composition M60C40. Table 2.4 shows this ratio for carboxyl equivalents ( $\alpha_{COOH}$ ) and hydroxyl equivalents ( $\alpha_{OH}$ ) reacted at a given heating time according to the Equation 2.1 and 2.2 respectively. Where “*eq. COOH<sub>r</sub>*” and “*eq. OH<sub>r</sub>*” are the number of carboxyl and hydroxyl equivalents reacted respectively; and “*eq. COOH<sub>0</sub>*” and “*eq. OH<sub>0</sub>*” are the number of carboxyl and hydroxyl equivalents in the original composition respectively.

$$\alpha_{COOH} = \frac{eq. COOH_r}{eq. COOH_0}$$

Equation 2.1 – Ratio of COOH equivalents reacted

$$\alpha_{OH} = \frac{eq. OH_r}{eq. OH_0}$$

Equation 2.2 – Ratio of OH equivalents reacted

After 4 hours heating at 140 °C, nearly 60 % of carboxyl groups and around 30 % of hydroxyl groups have reacted. As it has been observed by FTIR analysis, polycondensation reaction between maltodextrin and citric acid is slow. Both compounds could still further react after 4 hours heating.

Although it is not common to follow the progress of reactions by TGA, this work demonstrates that this can be an accurate and fast technique to prove the advance of the polycondensation reaction under thermal processing conditions.

**Table 2.4 – Ratio of active groups reacted ( $\alpha$ ) based on TGA results at different times at 140 °C**

Heating Time (h)	$\alpha_{\text{COOH}}$	$\alpha_{\text{OH}}$
0,5	0,19 ± 0,02	0,11 ± 0,01
1	0,28 ± 0,05	0,16 ± 0,03
2	0,41 ± 0,06	0,23 ± 0,04
4	0,59 ± 0,09	0,33 ± 0,05

### 2.5.3 RHEOLOGICAL CHARACTERIZATION

---

The evolution of storage modulus ( $G'$ ) and loss modulus ( $G''$ ) with temperature, for freeze-dried samples of compositions M60C40 and M40C60, is shown in Figure 2.10. At temperature of 50 °C,  $G''$  is higher than  $G'$ , which corresponds to liquid-like behavior. From that temperature on, both  $G'$  and  $G''$  diminish as temperature increases according to the thermoplastic character of the original mixture. This thermoplastic character is assigned to hydrogen bond interactions between hydroxyl groups of maltodextrin and carboxyl groups of citric acid, which has been previously proved by FTIR analysis. The minimum of  $G'$  and  $G''$  is reached at 140 °C, followed by a raise of both moduli. This is assigned to the molecular weight increase due to polycondensation reaction and the subsequent crosslinking process, fully consistent with the TGA results [40]. However,  $G''$  remains higher than  $G'$  until approximately 192 °C, temperature where  $G'$  and  $G''$  intercept, which indicates the formation of a crosslinked polymer. Nevertheless, at 192 °C should be expected partial decomposition of the material as indicated by TGA.

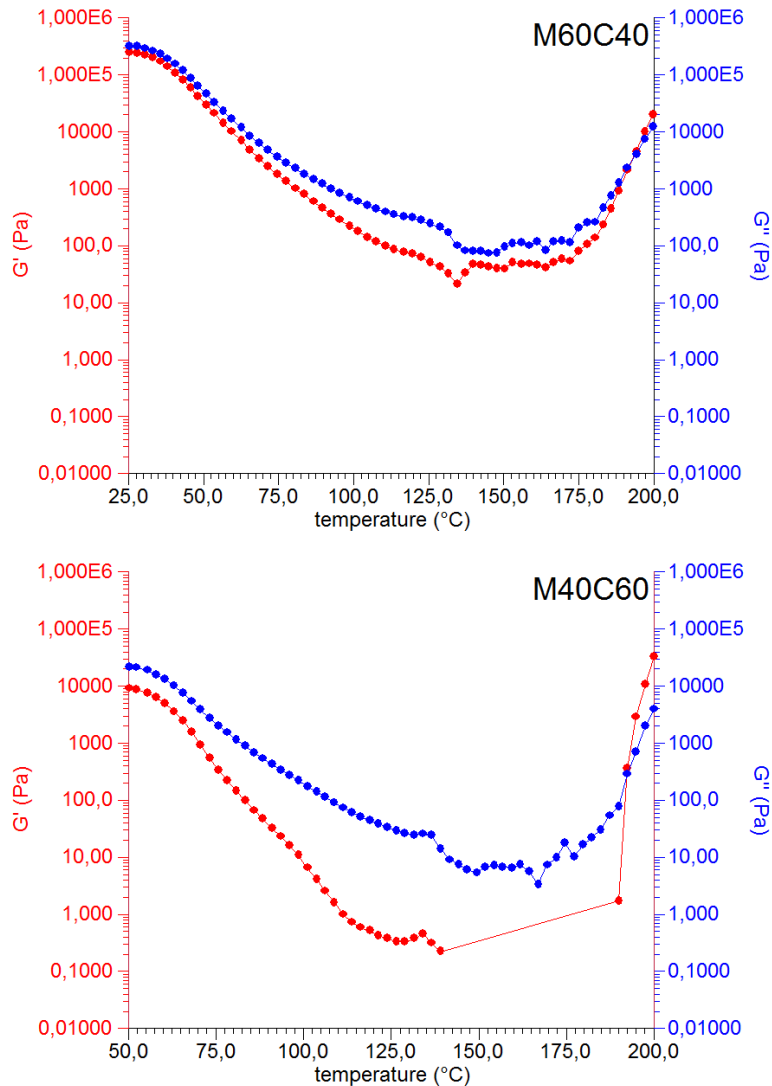


**Figure 2.10 – Rheology plot of  $\log G'$  and  $\log G''$  against temperature of compositions M60C40 and M40C60**

The evolution of  $G'$  and  $G''$  with temperature, for freeze-dried samples of compositions M80C20 and M20C80, is shown in Figure 2.11. For maltodextrin-rich composition (M80C20),  $G'$  is higher than  $G''$  at 50 °C, which is typical for solid-like behavior materials. This is probably due to the higher contribution of hydrogen bond interactions compared to the compositions with lower content of maltodextrin; contributing not only hydrogen bonds between hydroxyl groups of maltodextrin and carboxyl groups of citric acid but also the hydrogen bonds between hydroxyl groups of different maltodextrin molecules [41]. Both modulus,  $G'$  and  $G''$  diminish when temperature increases up to around 125 °C. From 125 °C on,  $G'$  and  $G''$  increase as result of the polycondensation. Curves of  $G'$  and  $G''$  cross-over at around 145 °C; from 145 °C on,  $G''$  becomes greater than  $G'$ , what is typical for liquid-like behavior. This suggests that, although the

polycondensation reaction starts at 125 °C, under these conditions no extensive crosslinking has been formed. In the case of citric-rich composition (M20C80),  $G'$  is higher than  $G''$  at 50 °C, and the value of both modulus is higher than for the rest of the compositions. This seems dominated by the contribution of solid citric acid in the freeze-dried sample.  $G'$  and  $G''$  suddenly decrease in the range of 135-150 °C, corresponding to melting point of citric acid [42]. From that temperature on,  $G''$  keeps greater than  $G'$ , so no starting point of polycondensation or crosslinking could be identified. Net, the high amount of citric acid seems to prevent extensive polycondensation reaction.

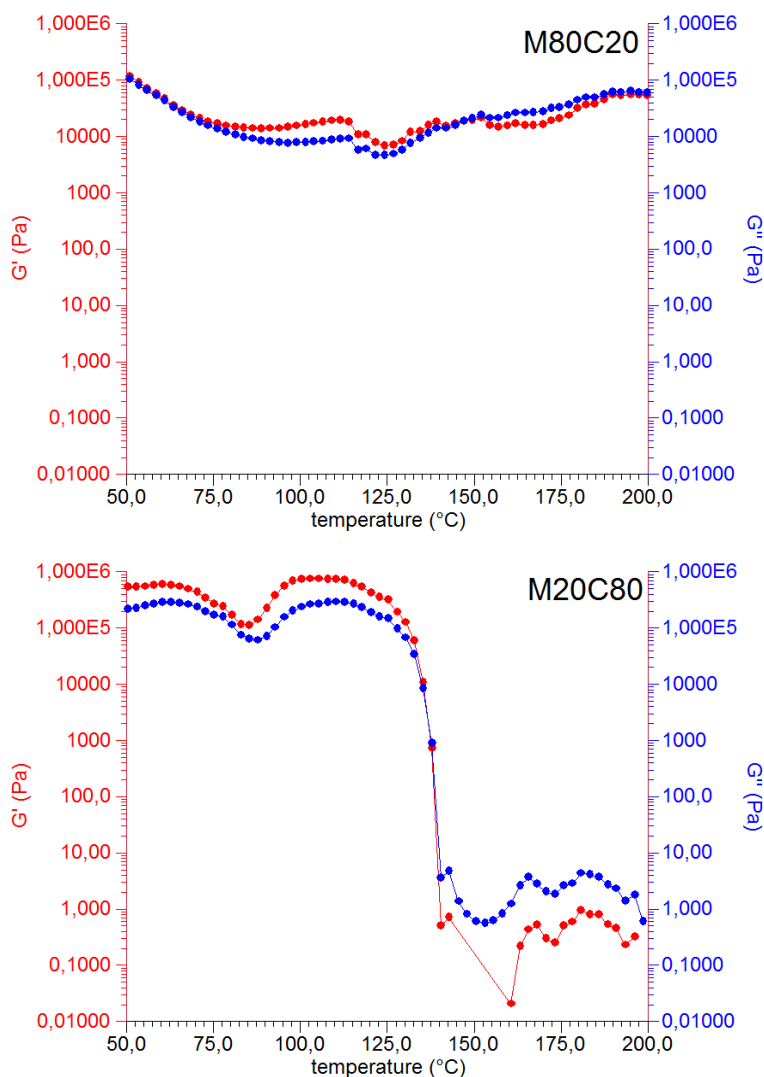


Figure 2.11 – Rheology plot of  $\log G'$  and  $\log G''$  against temperature of compositions M80C20 and M20C80

The different behavior found for the compositions in Table 2.2 points out that the ratio between MAL and CA has a big impact in the crosslinking capacity of the system. Compositions containing balanced amounts of CA (in the range 40-60 %) seem to be the most appropriate ones.

The polycondensation process of freeze-dried samples of the compositions in Table 2.2 was also evaluated under isothermal conditions at 140 °C (Figure 2.12 and Figure 2.13).

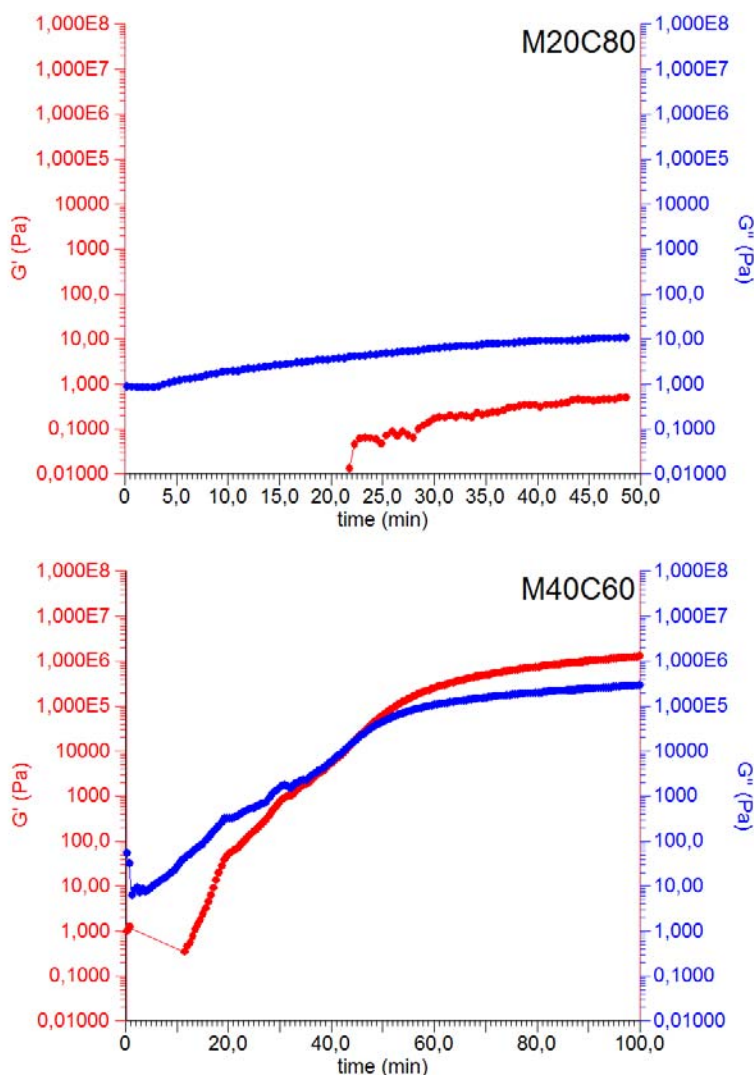


Figure 2.12 – Plot of  $\log G'$  and  $\log G''$  against time of compositions M20C80 and M40C60 at 140 °C

Graphs for compositions M40C60 and M60C40 clearly show the cross-over between  $G'$  and  $G''$  curves, which is an indication that the system changes from non-crosslinked to crosslinked gel. This cross-over point is normally considered as the gel time of the polymer [43, 44]. Based on this criterion, gel time for composition M40C60 would be 44 min while for composition M60C40 the

gel time would be 38 min. The graphs for compositions M20C80 and M80C20 are very different, as no cross-over between  $G'$  and  $G''$  could be identified. For citric-rich composition (M20C80) a slight raise of  $G''$  is found as from 5 min.  $G''$  is higher than  $G'$  which is characteristic of liquid-like behavior, and both modulus present very low values, this means that no polymer network is taking place for this period of time heating at 140 °C. This result is assigned to the melting of citric acid. For maltodextrin-rich composition (M80C20), both modulus increase since the beginning of isotherm, always keeping  $G'$  higher than  $G''$  which is characteristic of solid-like behavior. The starting point of polycondensation could not be detected at 140 °C isotherm in Figure 2.13, probably because it is too high temperature, as indicated by the result from the thermal monitoring shown previously.

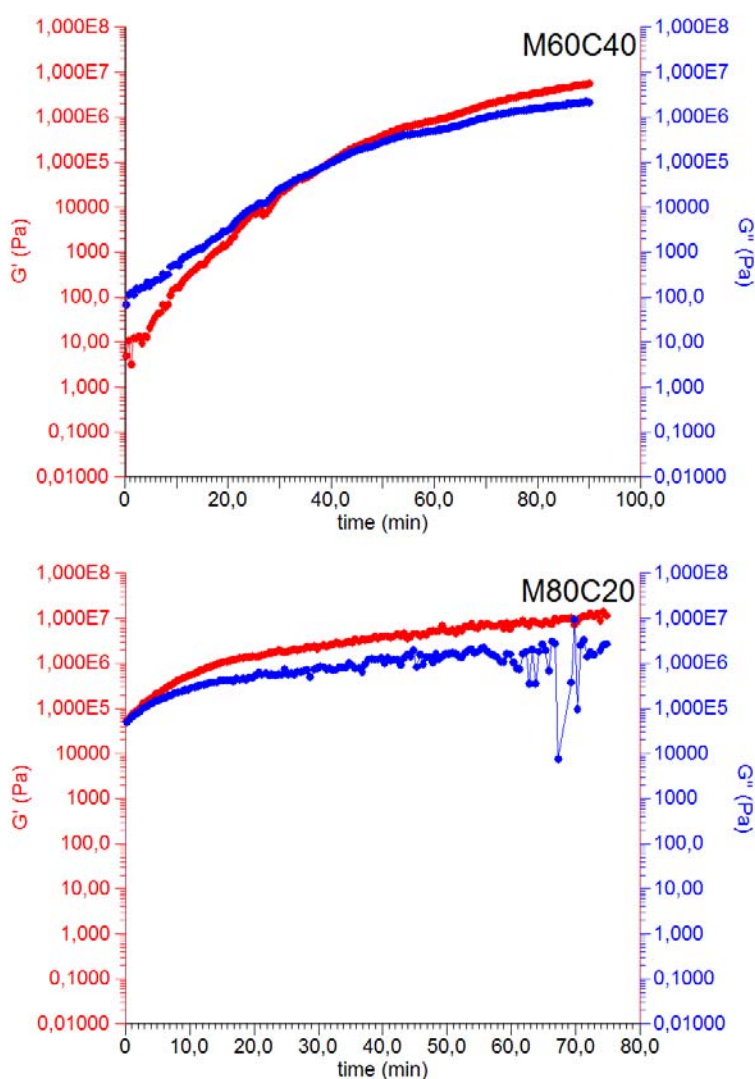


Figure 2.13 – Plot of log  $G'$  and log  $G''$  against time of compositions M60C40 and M80C20 at 140 °C



The rheological results under isothermal conditions confirm that compositions containing balanced amount of citric acid (40-60 %) can be crosslinked by thermal processing at 140 °C.

## 2.6 CONCLUSIONS

---

The methodology presented in this chapter allows concluding that the crosslinking by polycondensation reaction of systems containing maltodextrin and citric acid is effectively produced by thermal treatment. Also, by this methodology it could be concluded that the composition of the system has a big impact in the polycondensation behavior as well as on the resulting crosslinked product, being the best systems those containing 40-60 % of citric acid. FTIR has shown the formation of ester covalent bonding upon thermal treatment, well evidenced by the shift of the C=O stretching band. It has also proven the existence of strong hydrogen bond interactions between maltodextrin and citric acid in the solid phase. The reaction progress could be estimated by FTIR, as from the ratio of absorption bands associated to C=O and OH groups. TGA allowed the detection of the esterification reaction at about 140 °C. The progress of the reaction could be quantified as from the weight loss associated to the release of water due to the esterification. Overall, the reaction at 140 °C is slow, with conversion of 60 % of carboxyl groups after 4 hours. The formation of crosslinked polymer upon thermal treatment could be studied by rheology. The evolution and cross-over of the curves for moduli  $G'$  and  $G''$  allowed to determine the gel time of about 40 minutes for composition with 40-60 % of citric acid at 140 °C. Overall, this study showed that the combination of FTIR, TGA and rheology techniques is very useful for the characterization and quantification of the polycondensation reaction between starch-based polysaccharides and polycarboxylic acids under thermal conditions.

## 2.7 REFERENCES

---

1. Costa MRPFN and Bachmann R. Polycondensation. Handbook of Polymer Reaction Engineering: Wiley-VCH Verlag GmbH, 2008. pp. 57-151.
2. Carothers WH. Journal of the American Chemical Society 1929;51(8):2548-2559.
3. Carothers WH and Arvin JA. Journal of the American Chemical Society 1929;51(8):2560-2570.

4. Kricheldorf HR. Polycondensation: History and New Results. Berlin: Springer-Verlag Berlin Heidelberg, 2014.
5. Zhang J, Krishnamachari P, Lou J, and Shahbazi A. Synthesis of Poly(L+) Lactic Acid) by Polycondensation Method in Solution. In: Nzewi E, Reddy G, Luster-Teasley S, Kabadi V, Chang S-Y, Schimmel K, and Uzochukwu G, editors. Proceedings of the 2007 National Conference on Environmental Science and Technology: Springer New York, 2009. pp. 3-8.
6. Edlund U and Albertsson AC. *Advanced Drug Delivery Reviews* 2003;55(4):585-609.
7. Welch CM. *Textile Research Journal* 1988;58(8):480-486.
8. Martel B, Ruffin D, Weltrowski M, Lekchiri Y, and Morcellet M. *Journal of Applied Polymer Science* 2005;97(2):433-442.
9. M. Castro-Cabado ALCD, et al. Formaldehyde-free binder and use for mineral wool insulation products, US9242899B2. URSA Insulation S.A., 2012.
10. B. Jaffrennou DS, J. Douce. Sizing composition for mineral wool comprising a monosaccharide and/or a polysaccharide and an organic polycarboxylic acid, and insulating products obtained, US8951341B2. US: Saint-Gobain Isover, 2008.
11. Tisserat B, O'Kuru RH, Hwang H, Mohamed AA, and Holser R. *Journal of Applied Polymer Science* 2012;125(5):3429-3437.
12. Halpern JM, Urbanski R, Weinstock AK, Iwig DF, Mathers RT, and von Recum HA. *Journal of Biomedical Materials Research Part A* 2014;102(5):1467-1477.
13. Jiugao Y, Ning W, and Xiaofei M. *Starch - Stärke* 2005;57(10):494-504.
14. B. Sirok BBaPB. *Mineral Wool: Production and Properties*. Cambridge - England: Cambridge International Science Publishing Limited in association with Woodhead Publishing Limited, 2008.
15. *Nonwoven Fabrics: Raw Materials, Manufacture, Applications, Characteristics, Testing Processes*. Weinheim: Wiley-VCH, 2003.
16. Ansell MP. *Wood Composites*. Cambridge: Elsevier, 2015.
17. Reddy N and Yang Y. *Food Chemistry* 2010;118(3):702-711.
18. Yoon S-D, Chough S-H, and Park H-R. *Journal of Applied Polymer Science* 2007;106(4):2485-2493.
19. Dziejczak S.Z. KMW. *Handbook of Starch Hydrolysis Products and their Derivatives*. London: Springer, 1995.
20. Ghosh Dastidar T and Netravali AN. *Carbohydrate Polymers* 2012;90(4):1620-1628.
21. T. Heinze TL, A. Koschella. *Esterification of Polysaccharides*. Berlin: Springer, 2006.
22. Umare SS, Chandure AS, and Pandey RA. *Polymer Degradation and Stability* 2007;92(3):464-479.
23. Dhamaniya S and Jacob J. *Polymer* 2010;51(23):5392-5399.

24. Webb AR, Yang J, and Ameer GA. *Journal of Polymer Science Part A: Polymer Chemistry* 2008;46(4):1318-1328.
25. Núñez-Regueira L, Gracia-Fernández CA, and Gómez-Barreiro S. *Polymer* 2005;46(16):5979-5985.
26. Auad ML, Nutt SR, Stefani PM, and Aranguren MI. *Journal of Applied Polymer Science* 2006;102(5):4430-4439.
27. Kawai K and Hagura Y. *Carbohydrate Polymers* 2012;89(3):836-841.
28. Galat A. *Acta Biochim Pol* 1980;27(2):135-142.
29. Kizil R, Irudayaraj J, and Seetharaman K. *Journal of Agricultural and Food Chemistry* 2002;50(14):3912-3918.
30. Shi R, Zhang Z, Liu Q, Han Y, Zhang L, Chen D, and Tian W. *Carbohydrate Polymers* 2007;69(4):748-755.
31. Han F, Liu M, Gong H, Lü S, Ni B, and Zhang B. *International Journal of Biological Macromolecules* 2012;50(4):1026-1034.
32. Xu J, Zhou C-w, Wang R-z, Yang L, Du S-s, Wang F-p, Ruan H, and He G-q. *Carbohydrate Polymers* 2012;87(3):2137-2144.
33. Claude J and Ubbink J. *Food Chemistry* 2006;96(3):402-410.
34. Danilovas PP, Rutkaite R, and Zemaitaitis A. *Carbohydrate Polymers* 2014;112(0):721-728.
35. Shen DK, Gu S, and Bridgwater AV. *Carbohydrate Polymers* 2010;82(1):39-45.
36. Aggarwal P, Dollimore D, and Heon K. *Journal of thermal analysis* 1997;50(1-2):7-17.
37. Aggarwal P and Dollimore D. *Thermochimica Acta* 1998;319(1-2):17-25.
38. Dollimore D and O'Connell C. *Thermochimica Acta* 1998;324(1-2):33-48.
39. Wyrzykowski D, Hebanowska E, Nowak-Wicz G, Makowski M, and Chmurzyński L. *Journal of Thermal Analysis and Calorimetry* 2011;104(2):731-735.
40. Papadopoulos E, Ginic-Markovic M, and Clarke S. *Journal of Applied Polymer Science* 2009;114(6):3802-3810.
41. Loret C, Meunier V, Frith WJ, and Fryer PJ. *Carbohydrate Polymers* 2004;57(2):153-163.
42. Poerwono H, Higashiyama K, Kubo H, Poernomo AT, Suharjo, Suidiana IK, Indrayanto G, and Brittain HG. Citric Acid. In: Harry GB, editor. *Analytical Profiles of Drug Substances and Excipients*, vol. Volume 28: Academic Press, 2001. pp. 1-76.
43. Tung C-YM and Dynes PJ. *Journal of Applied Polymer Science* 1982;27(2):569-574.
44. Jin-Tae K, Martin D, Halley P, and Dae Su K. *Composite Interfaces* 2007;14(5/6):449-465.



---

## *CHAPTER III*

---

# *EFFECT OF THE STRUCTURE OF POLYCARBOXYLIC ACIDS IN THE THERMAL CROSSLINKING OF MALTODEXTRINS*

---



## 3.1 INTRODUCTION

---

### 3.1.1 BIO-BASED POLYMERS

---

Synthetic polymers have been used in every field of human activity for years. They are based on petroleum, and characterized by their non-degradability [1]. Furthermore, a lot of synthetic polymers are known to release toxic compounds which are unhealthy and environmentally unfriendly [2]. For that reason, strong development has been done on eco-friendly bio-based polymers during the last years [3, 4]. Bio-based polymers can be obtained mainly from two different sources: by bacterial fermentation processes by synthesizing the monomers from renewable resources, including lignocellulosic biomass (e.g. starch and cellulose), fatty acids and organic waste. Natural bio-based polymers are the other class of bio-based polymers which are found naturally, such as proteins, nucleic acids, and polysaccharides (e.g. collagen, chitosan, etc.). This last source of bio-based polymers have been the one showing more growth in recent years in terms of technological developments and their industrial applications. Considering this, three main ways to produce bio-based polymers can be distinguished [5]:

- 1) Using natural bio-based polymers with partial modification to meet the requirements (e.g. starch)
- 2) Producing bio-based monomers by fermentation/conventional chemistry followed by polymerization (e.g. polylactic acid, polybutylene succinate, and polyethylene glycol)
- 3) Producing bio-based polymers directly by bacteria (e.g. polyhydroxyalkanoates).

In the field of bio-based polymers, the thermosets are one of the most challenging due to the required properties for different applications; e.g. chemical resistance, humidity resistance, structural integrity [6].

### 3.1.2 BIO-BASED THERMOSETS

---

Thermoset polymer systems undergo a transformation, often referred to as “curing”, from liquid or soft solid where the molecules can move freely to a material where the molecules are

interconnected to form a strong network. Therefore, the curing process of a thermoset involves the formation of new chemical bonds between molecules in the thermoset, resulting in most molecules being linked in continuous network. This network is able to resist a change in shape, with certain degree of resistance depending on the properties of the linked molecules.

The recent explosion of interest and research in chemicals and polymers from renewable raw materials has led to many new approaches to renewable thermoset technology. Some of them are based on the direct utilization of renewable raw materials, such as unsaturated fats and oils in thermosets; others require the fermentation and/or chemical conversion of renewable raw materials such as sugars to get monomers, crosslinking agents and polymers thermosets. For some traditional thermosets like epoxy, unsaturated polyester, polyurethanes, alkyd resins and phenolic resins, renewable raw materials are already in use. Wide range of bio-sources like polysaccharides, lignins, natural oils, proteins, pine resin derivatives and furans have been used for the development of the corresponding bio-based thermosets [3]. For instance, phenolic resins, used in plywood, oriented strand boards, glass and carbon composites, etc., are produced by reacting phenol and formaldehyde, which are petroleum-based raw materials. Their replacement by bio-based, non-toxic substituents has become a necessity. In this context lignin, cardanol and tannins have been proposed as candidates to substitute the phenol; while formaldehyde has been replaced by glyoxal, obtained by the oxidation of lipids [7]. Alkyd resins typically produced by reacting a polyol, dicarboxylic acids and fatty acids are already synthesized with nearly 100 % bio-based raw materials (e.g. glycerol, fatty acids, maleic acid). Other bio-based raw materials like natural oils and polysaccharides have been proposed for the synthesis of epoxy and polyurethane thermosets [8-10].

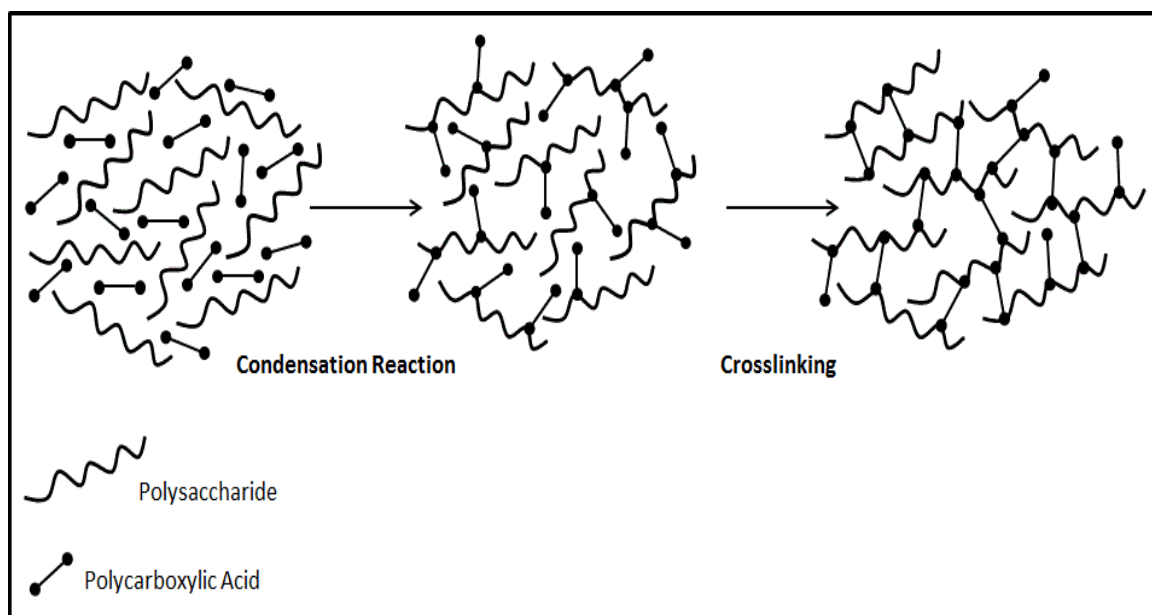
### **3.1.3 POLYSACCHARIDE-BASED THERMOSETS**

---

Saccharides are considered a very important renewable source of monomer for the preparation of a variety of polymers since they are the most abundant class of organic compounds found in living organisms. Saccharides can be introduced into the polymer architecture in three different ways: by addition reaction involving vinyl-type saccharides; functionalization based on appending the carbohydrate to a reactive backbone; and polycondensation reactions of saccharide-based monomers and polymers. It is well described in



different works crosslinkable systems based on polysaccharides and polycarboxylic acids for their application in packaging and paper industry [7, 11-14]. From the other side a thermoset system based on the polycondensation reaction between glycerol and the polycarboxylic acids, citric acid and lactic acid, has been also reported [6, 15]. Following the rationale of these recent developments, a fully bio-based thermoset is intended to be created from bio-based polyols, like a polysaccharide, and bio-based polycarboxylic acids, like citric acid or tartaric acid. The resulting crosslinked system due to the polycondensation reaction between the polysaccharide and the polycarboxylic acid (Scheme 3.1) would deliver a thermoset suitable for some applications like, for instance, fiber wood and fiber glass binding.



**Scheme 3.1 – Model of reaction steps between polysaccharide chains and polycarboxylic acid molecules leading to a crosslinked system**

### 3.1.4 MALTODEXTRIN

The vast majority of saccharides present in nature are polysaccharides, being starch and its derivatives one of the most abundant in nature, very attractive for the industry due to its low market price [16]. Maltodextrin is a starch-based polysaccharide produced by hydrolysis of starch down to glucose polymers with an average chain length of 5-10 glucose units/molecule.

Maltodextrin is soluble in water, what makes it more attractive for industrial applications compared to insoluble starch.

### 3.1.5 POLYCARBOXYLIC ACIDS

---

Citric acid is a polycarboxylic acid, extensively reported to crosslink with different polysaccharides [14, 17]. However, alternative polycarboxylic acid, easily affordable, is tartaric acid which has not been deeply discussed in the literature working as crosslinker [18]. Both acids are non-toxic and inexpensive organic acids, from natural origin. They are polyfunctional carboxylic acids; but, their reactivity might be different due the different molecular structure (Figure 3.1) [19], thus leading to different binding performance. For instance, citric acid molecule has three carboxyl groups while tartaric acid molecule has two carboxyl groups. This could make citric acid to crosslink better than tartaric acid. On the other side, citric acid has one hydroxyl group while tartaric acid has two hydroxyl groups. This could lead to a different degree of interactions by hydrogen bond depending on the polycarboxylic acid.

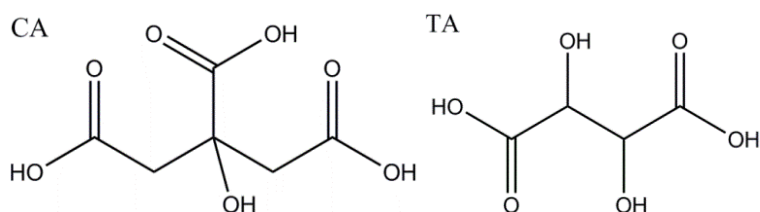


Figure 3.1 – Molecular structure of citric acid (CA) and L-tartaric acid (TA)

## 3.2 AIM OF THIS CHAPTER

---

The aim of this chapter was to study the reactivity and final properties of crosslinked systems consisting of maltodextrin and citric acid compared to the systems consisting of maltodextrin and tartaric acid. Therefore elucidate which system would perform better for its application as part of the binder for bonded wood and glass fiber materials.

### 3.3 MATERIALS AND METHODS

---

#### 3.3.1 MATERIALS

---

Powdered maltodextrin (MAL) Maldex 120 (dextrose equivalent (DE) 11 to 15), manufactured by spray-drying of liquid maltodextrin, derived from edible corn starch hydrolysis was provided by Tereos Syral. Citric acid (CA) and L-tartaric acid (TA) reagents were purchased from Sigma-Aldrich. The products were used without additional purification.

#### 3.3.2 METHODS

---

Different systems containing MAL and CA, or MAL and TA were prepared by mixing MAL and the corresponding carboxylic acid (CA or TA) at different ratios in water (Table 3.1). MAL was dissolved in distilled water at room temperature under mechanical stirring. Then the polycarboxylic acid was added to the solution keeping the stirring until obtaining a homogenous solution. Unless otherwise stated, the solutions in water were prepared with 50% dry content.

**Table 3.1 – Compositions of maltodextrin (MAL) and carboxylic acid (CA or TA)**

Composition	MAL (% dry weight)	CA (% dry weight)	TA (% dry weight)
MAL20CA	20	80	-
MAL40CA	40	60	-
MAL60CA	60	40	-
MAL80CA	80	20	-
MAL20TA	20	-	80
MAL40TA	40	-	60
MAL60TA	60	-	40
MAL80TA	80	-	20

## 3.4 CHARACTERIZATION TECHNIQUES

---

### 3.4.1.1 THERMOGRAVIMETRIC ANALYSIS (TGA)

---

TGA was performed using a TGA Q500 (TA Instruments). Samples of CA, TA and MAL, and the different freeze-dried samples of the compositions in Table 3.1 were heated in a platinum pan from 25 to 600 °C, under a nitrogen atmosphere at a heating rate of 10 °C/min. The derivative TGA (wt %/°C) of each sample was obtained from the software TA Universal Analysis. Isothermal treatment at temperature of 140 °C and different heating times was followed for the freeze-dried samples of the compositions MAL60CA and MAL60TA; for that, previous heating up to 140 °C was carried out at a heating rate of 10°C/min. The isothermal analysis was done by duplicate.

### 3.4.1.2 ATR-FTIR SPECTROSCOPY

---

ATR-FTIR spectra were measured in a Spectrum One FT-IR Spectrometer (Perkin Elmer) with a split pea accessory for ATR. Absorbance spectra were acquired at 4 cm<sup>-1</sup> resolution and signal-averaged over 10 scans recorded from 4000 cm<sup>-1</sup> to 650 cm<sup>-1</sup>. The spectra were baseline corrected and normalized to the most intense absorbance peak. FTIR spectra were measured for MAL, CA and TA, as well as for the water solutions of the compositions in Table 3.1 upon heating treatment at 140 °C. In order to make the follow-up of the polycondensation reaction, the peak assigned to the ester carbonyl (C=O) stretching vibrations and the peak due to hydroxyl (OH) stretching were selected as the analyte peaks. In order to assure the interpretation of the spectra of the compositions after thermal treatment spectra were measured for the resulting polycondensate samples before and after purification. The polycondensate compositions were purified by membrane dialysis, placing approximately 2 g of composition in a 1000 Da membrane, in 2 L of water for 20 hours, renovating the water after 10 hours. The purified polymer was freeze-dried for 24 hours. The data were taken from the average of three measurements.

### 3.4.1.3 RHEOLOGICAL MEASUREMENTS

---

Rheological measurements were carried out with an AR1000 rheometer (TA Instruments). Disposable plate-plate geometry with diameter 25 mm was used. Dynamic measurements in

oscillatory mode were performed for approximately 1 mL sample in 2000  $\mu\text{m}$  gap, applying multiple frequency mode ranging from 1 Hz to 25 Hz and a fixed torque value (tests were performed previously to ensure that the response was in the viscoelastic region). Rheological behavior of water solutions of the compositions in Table 3.1 was monitored for temperature range between 25  $^{\circ}\text{C}$  and 200  $^{\circ}\text{C}$ , with ramp rate of 3  $^{\circ}\text{C}/\text{min}$ . Isothermal monitoring was carried out at 140  $^{\circ}\text{C}$  during maximum 160 min, previously heating up to 140  $^{\circ}\text{C}$  with ramp rate of 10  $^{\circ}\text{C}/\text{min}$ . The measurements were done by duplicate.

#### *3.4.1.4 MECHANICAL PROPERTIES MEASUREMENTS*

---

Mechanical properties measurements were carried out on glass paper “Whatman GF/A 8x10 ins” impregnated with the corresponding composition and cured by heating treatment. A glass paper sheet was soaked in a water solution of the different compositions in Table 3.1 diluted with distilled water down to 20% solid content. The soaked sheet was pressed between the squeezing rolls of a laboratory padder (Mathis) at 3 mm/min speed of the rolls and pressure between the rolls at 2.5 bars. Heating treatment on the impregnated glass paper was applied in a Labdryer oven (Mathis) at 140  $^{\circ}\text{C}$ . Specimens were cut from the cured glass paper sheet with size 75x25 mm. Cured specimens were treated with accelerated weathering conditions in a climate chamber (Ineltec) at 50  $^{\circ}\text{C}$  and 95 % humidity for 24 hours. Tensile strain measurements were carried out for the specimens previous to the treatment with accelerated weathering conditions and after the application of accelerated weathering conditions. The tensile strain measurements were carried out on a Universal Testing Machine (Instron) equipped with a 500 N load cell. The cross-head speed applied was 2.3 m/min and the gauge length was 50 mm. The data was taken from the average of at least six specimens.

#### *3.4.1.5 SCANNING ELECTRON MICROSCOPY (SEM)*

---

Morphology of the surface and the cross-section after tensile strain test of the glass paper specimens impregnated and cured with the compositions in Table 3.1 was observed by SEM. For that an US8000 (Hitachi) was used.

## 3.5 RESULTS AND DISCUSSION

### 3.5.1 TGA STUDY

The thermogravimetical scans for the starting materials and for the compositions in Table 3.1 are shown in Figure 3.2 and Figure 3.3 respectively.

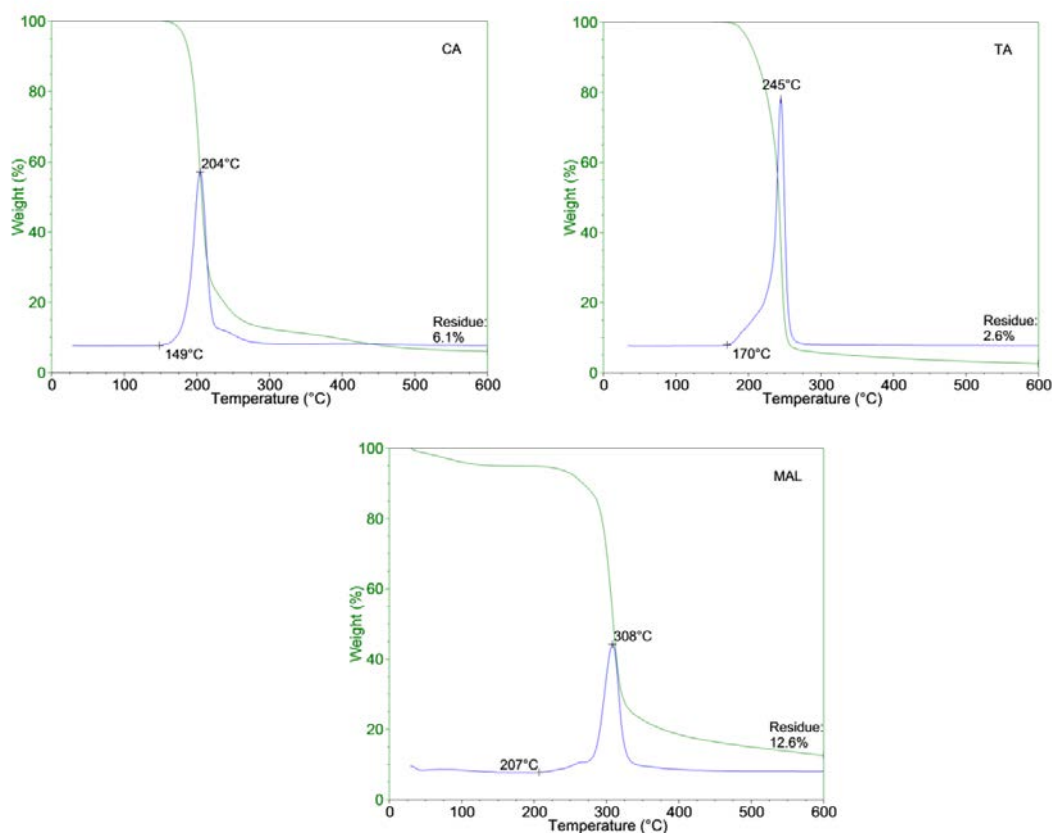


Figure 3.2 – TGA and the corresponding derivative for (CA) citric acid, (TA) tartaric acid and (MAL) maltodextrin

Compositions containing MAL and CA, and MAL and TA show, at least, two different steps of weight loss. The first one (Step 1), which takes place at 130-140 °C for the systems containing CA and at 140-160 °C for the systems containing TA is assigned to the water released due to the esterification reaction [15, 20]. This mass loss cannot be alternatively assigned to the decomposition of MAL nor polycarboxylic acids because, as seen in Figure 3.2, their decomposition take place at higher temperatures [20].

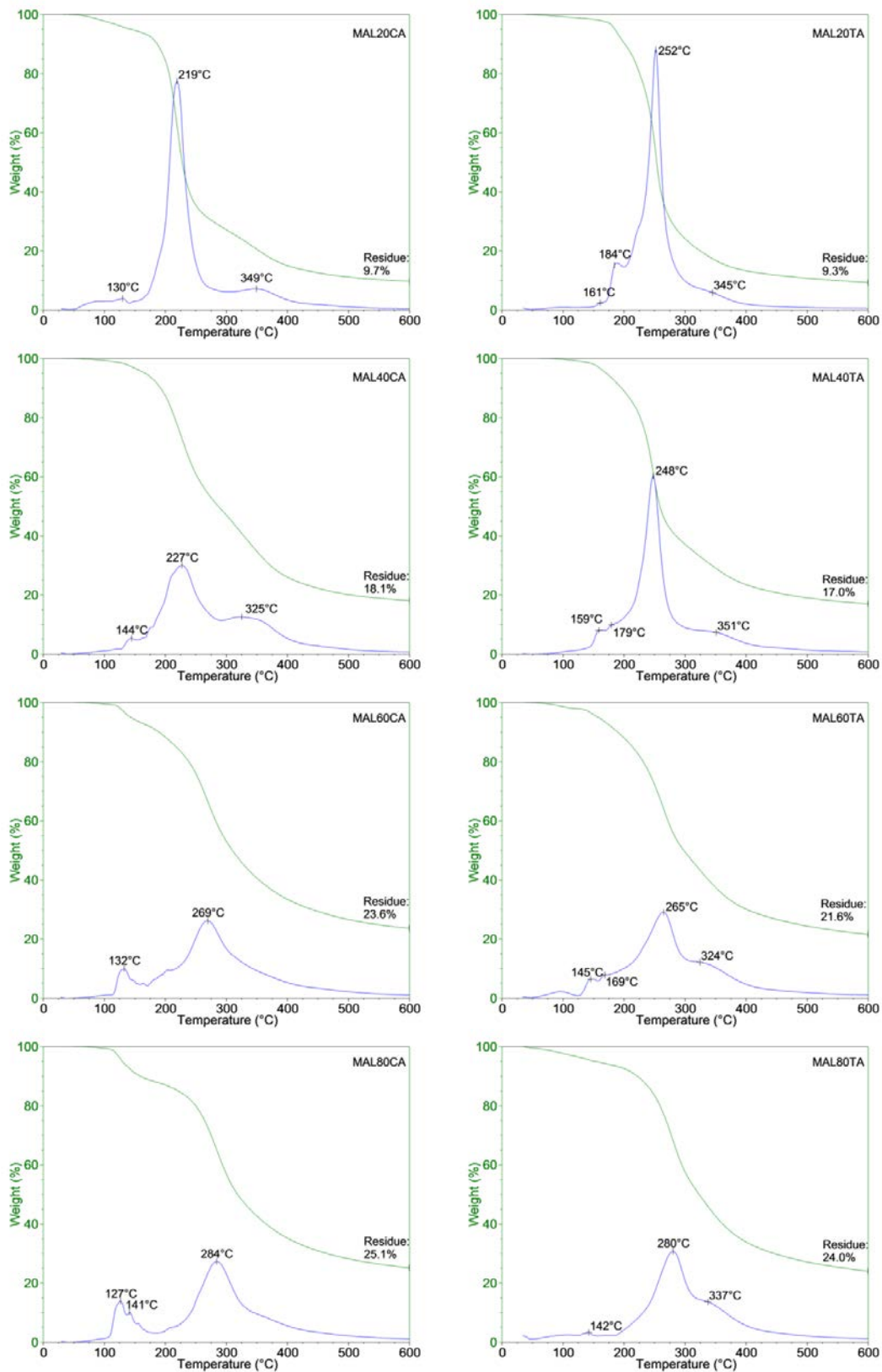
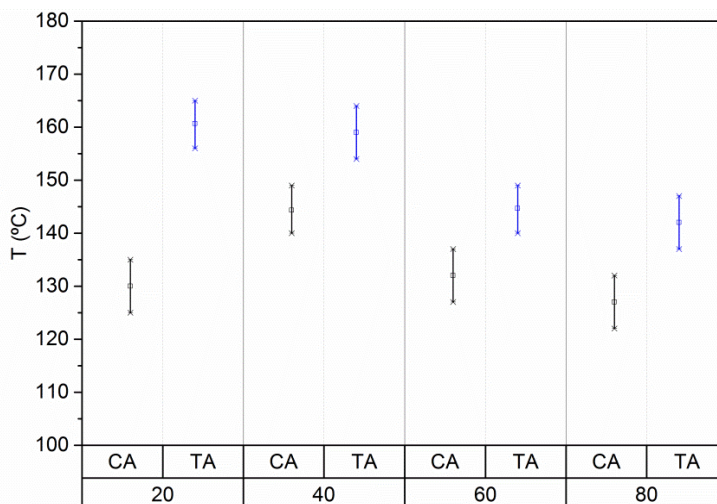


Figure 3.3 – TGA and corresponding derivative for all the compositions in Table 3.1

The second weight loss (Step 2), which shows maximum rate in the range 219-284 °C, is ascribed to the decomposition of the polycarboxylic acids and their condensation derivatives with MAL. Still a third weight loss (Step 3) can be identified in the thermogravimetical scans in Figure 3.3, with maximum rate at about 325-350 °C, significantly higher than the decomposition temperature of MAL, which maximum rate is at about 308 °C (Figure 3.2) [21]. This Step 3 might be assigned to the decomposition of products result of the polycondensation reaction between MAL and the polycarboxylic acids, which are more stable than the starting MAL [15]. Finally, it is also noteworthy that the residue left at 600 °C increases with the content of MAL, from about 9 % residue for the systems with 20 % content of MAL, to proximately 25 % for the systems containing 80% MAL. Furthermore, these values are, in most of the systems, much higher than the residue of the MAL alone. This would be a consequence of the polycondensation reaction between MAL and the polycarboxylic acids (CA or TA).



**Figure 3.4 – Temperature (°C) of the esterification reaction determined by TGA for the systems containing citric acid (CA) and the systems containing tartaric acid (TA) with different content of MAL (20, 40, 60 and 80 %)**

The Step 1 in thermogravimetical scans in Figure 3.3, assigned to the esterification reaction, has been analyzed in more detail to understand the difference across the compositions. Figure 3.4 shows the temperature of maximum rate of the Step 1 for all the compositions in Table 3.1. It can be noted that the temperature of maximum esterification rate is lower for those systems containing CA, demonstrating higher reactivity of the systems containing CA compared to the systems containing TA.



Figure 3.5 shows the weight loss during the Step 1, which is assigned to the loss of water due to the esterification reaction. This weight loss is higher for compositions with 40 - 60% MAL, depending on the carboxylic acid type. This might reflect the stoichiometry of the reaction between the polycarboxylic acids and the MAL; i.e. excess of any starting material would not contribute positively to the esterification.

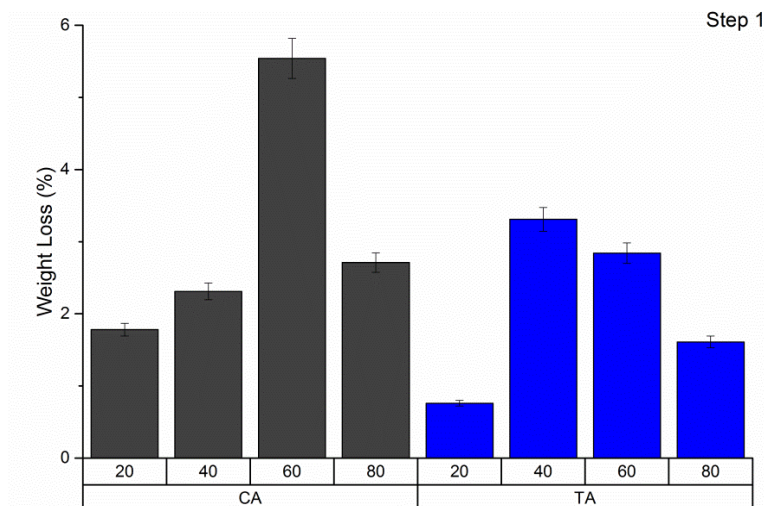


**Figure 3.5 - Weight loss (%) related to the esterification reaction (Step 1), for the compositions containing citric acid (CA) and the ones containing tartaric acid (TA) with different percentage of MAL (20, 40, 60 and 80 %)**

In Figure 3.5, it is also noticeable that the weight loss is, in general, higher for systems containing CA. This indicates that the reactivity of CA is higher than the reactivity of TA. This is consistent to the lower esterification temperatures shown in Figure 3.4.

The weight loss associated to the steps 2 and 3 in thermogravimetical scans in Figure 3.3 has been also analyzed (Figure 3.6). The Step 2 is assigned to thermal decomposition of the carboxylic acids and their corresponding condensation products. This weight loss is higher for the compositions containing TA. According to the data from Step 1, which shows that TA is less reactive than CA, it is assumed that more free molecules of TA remains after Step 1 so that it would decompose more later on in Step 2. The Step 3 is assigned to the decomposition of compounds result of the polycondensation reaction (this step could not be identified for compositions MAL60CA and MAL80CA). In this Step 3, the compositions containing TA lose less weight than compositions containing CA, what may indicate that compositions containing TA generates less polycondensation products. All these findings are consistent with the higher reactivity of the compositions containing CA.

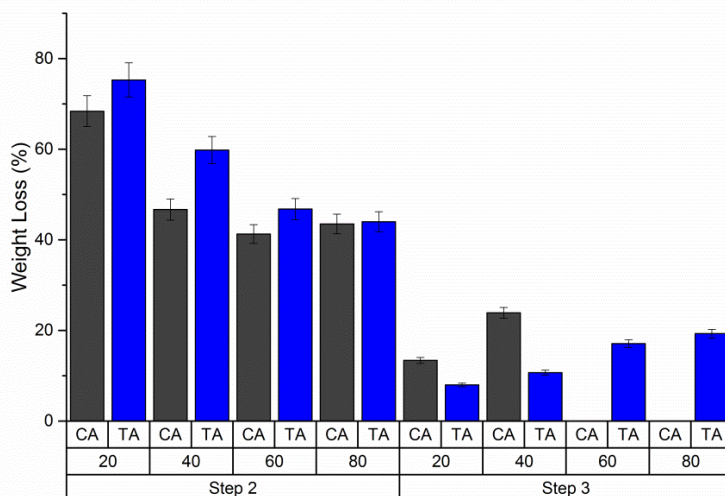


**Figure 3.6 – Weight loss (%) associated to the TGA Step 2 and Step 3, for the compositions containing citric acid (CA) and the compositions containing tartaric acid (TA) with different percentage of MAL (20, 40, 60 and 80 %)**

The quantification of the esterification reaction progress between polyols and polycarboxylic acids by TGA, based on the determination of the weight loss due to the water released by the esterification, has been previously reported [15, 22]. This methodology has been applied here to follow the reaction progress of the compositions containing 60 % MAL under isothermal treatment at 140°C. Two different steps (Step A and Step B) have been identified when running the experiment. Step A is considered from the esterification starting temperature (example shown in Annex 1) until 140 °C, and Step B corresponds to the isothermal treatment at 140°C for different periods of time, 0.5, 1, 2 and 4 hours. The progress of the reaction expressed as the ratio of carboxyl groups reacted ( $\alpha_{\text{COOH}}$ ) has been calculated according to J. Kapusniak [20] and it is shown in Figure 3.7. In the Step A, 40 % of carboxyl groups have reacted in the system containing CA, while around 35 % of carboxyl groups have reacted in the system containing TA. This is due to the ability of CA to react at lower temperature than TA as proved previously in this work. In the Step B the ratio of carboxyl groups reacted is lower in the system containing CA than in the system containing TA. This may indicate that CA is mainly reacting in the Step A while TA is reacting mainly in the Step B. At the end of the heating treatment (considering Step A and Step B), after 4 hours heating treatment the ratio of carboxyl groups reacted is around 100 % for both systems independently of the carboxylic acid nature. This means that, although the systems containing CA can react at lower temperatures, both CA and TA are able to reach full conversion after 4 hours thermal treatment at 140 °C.

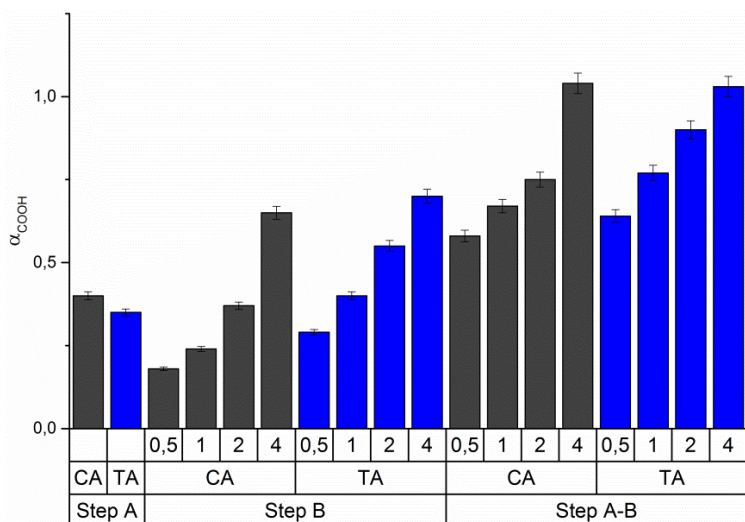


**Figure 3.7 – Ratio of COOH groups reacted ( $\alpha_{\text{COOH}}$ ) associated to each weight loss step due to esterification reaction, Step A (heating up to 140 °C), Step B (isotherm at 140 °C) and both steps together (Step A-B), at the different isotherm times (0.5, 1, 2 and 4 hours) for the system containing citric acid (CA) and the system containing tartaric acid (TA), containing 60 % of MAL**

The higher reactivity of CA compared to TA could be explained by the different mechanism they follow during the esterification reaction. For instance, CA is able to form a five member cyclic anhydride as reaction intermediate making it more reactive in two of the three carboxylic acid groups available while TA does not have this possibility [23, 24].

### 3.5.2 INFRARED STUDY

The esterification reaction between MAL and the carboxylic acids, CA and TA, has been studied by ATR-FTIR. As reference, the spectra of starting materials, MAL and the carboxylic acids CA and TA are shown in Figure 3.8 and Figure 3.9. The most interesting IR region of MAL is between 800 and 1200  $\text{cm}^{-1}$ , assigned to C-O bond stretching, which characterizes the anhydroglucose ring vibrations, and finally the band at 3314  $\text{cm}^{-1}$  which corresponds to OH stretching. Other bands appear at 1636  $\text{cm}^{-1}$ , assigned to the water absorbed, and the bands at 1359 and 2922  $\text{cm}^{-1}$  attributed to C-H bond bending and stretching respectively [25, 26]. Regarding to the carboxylic acids, CA and TA, the most interesting IR signals are the ones related to the carboxyl groups. The main difference between CA acid and TA acid spectra are the signals assigned to C=O stretching. For CA two bands can be identified, at 1699 and 1744  $\text{cm}^{-1}$ , while for

TA one broader single band appears at  $1716\text{ cm}^{-1}$ . The fact of having two different bands assigned to the C=O stretching in case of CA is due to the intramolecular interactions of the carboxyl groups [27, 28]. This does not happen in the case of TA due to its different geometry [29, 30]. Apart from the C=O stretching bands other characteristic bands can be identified in both acids. For instance, the bands corresponding to C-H bond bending in the range from  $1300$  to  $1400\text{ cm}^{-1}$ ; C-O vibration due to hydroxyl and carboxyl groups in the range from  $1050$  to  $1350\text{ cm}^{-1}$  which are difficult to differentiate; and the region from  $3000$  to  $3600\text{ cm}^{-1}$ , assigned to OH stretching of the hydroxyl groups and carboxyl groups.

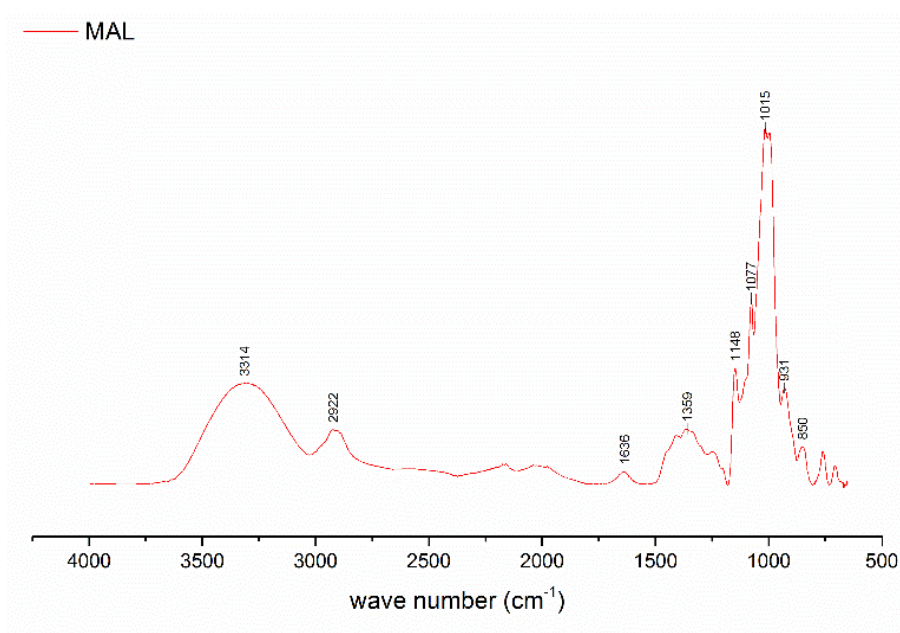
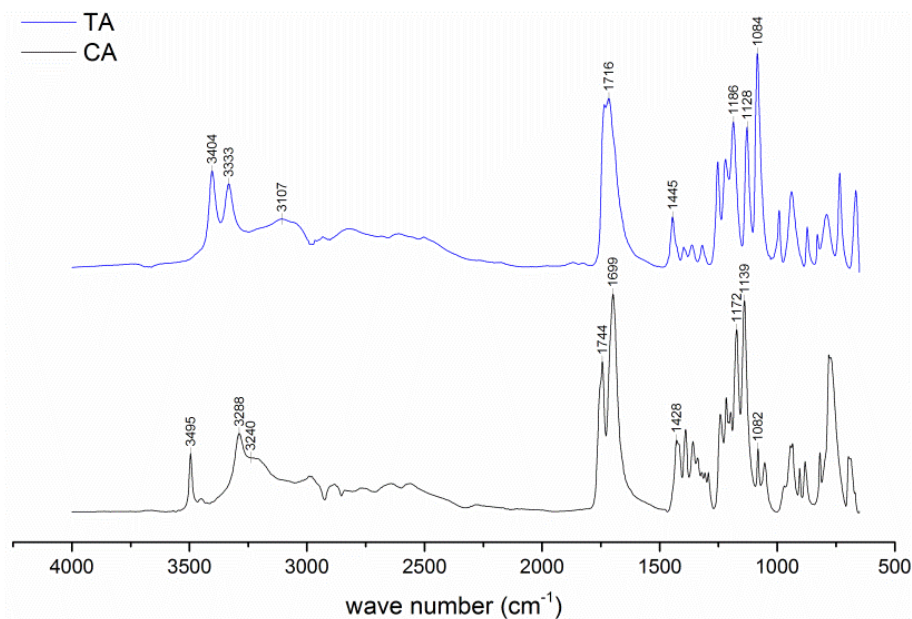


Figure 3.8 – IR spectra of (MAL) maltodextrin



**Figure 3.9. IR spectra of (CA) citric acid and (TA) tartaric acid**

All the compositions in Table 3.1 have been analyzed by ATR-FTIR after thermal treatment at 140 °C for different times. The selected temperature of 140 °C avoid the thermal decomposition affecting the starting materials, MAL, CA and TA, as observed in the TGA measurements (Figure 3.2). The IR spectra of the compositions in Table 3.1 after 4 hours thermal treatment are shown in Figure 3.10 and Figure 3.11.

The most remarkable feature of their spectra is the shift of the C=O stretching band towards higher wave number as well as a residual shoulder at lower wave number. For the CA containing systems the main peak is in the range of 1709-1723  $\text{cm}^{-1}$  and the shoulder is in the range 1637-1649  $\text{cm}^{-1}$ ; the later seen mostly when ratio of CA is lower (e.g. MAL60CA, MAL80CA). According to previous works [31] the single peak observed at 1709-1725  $\text{cm}^{-1}$  is assigned to the carbonyl of ester bonds whereas the shoulder would correspond to the free carboxyl groups. For the TA containing systems, the C=O stretching band is in the range of 1723-1740  $\text{cm}^{-1}$  and the shoulder in the range of 1629-1652  $\text{cm}^{-1}$ ; both are clearly visible independently on the TA content in the mixture. The first peak is assigned to the carboxyl ester bond result of the esterification reaction between MAL and TA, whereas the shoulder would correspond to free, unreacted carboxyl groups [20]. Therefore by ATR-FTIR analysis the esterification reaction between MAL and both carboxylic acids, CA and TA, can be identified.

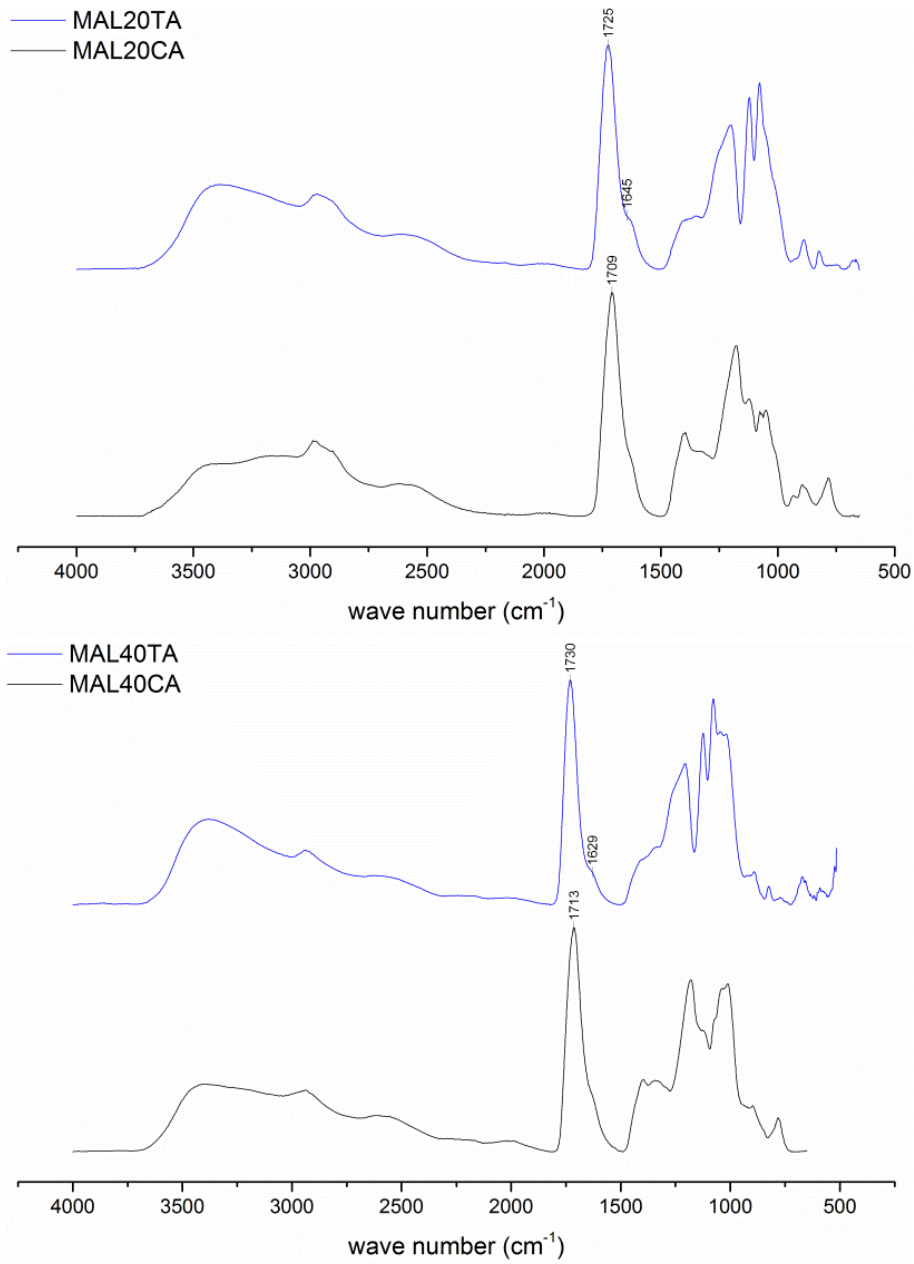


**Figure 3.10 – ATR-FTIR spectra of the compositions MAL20CA, MAL20TA, MAL40CA and MAL40TA, after 4 hours thermal treatment at 140 °C**

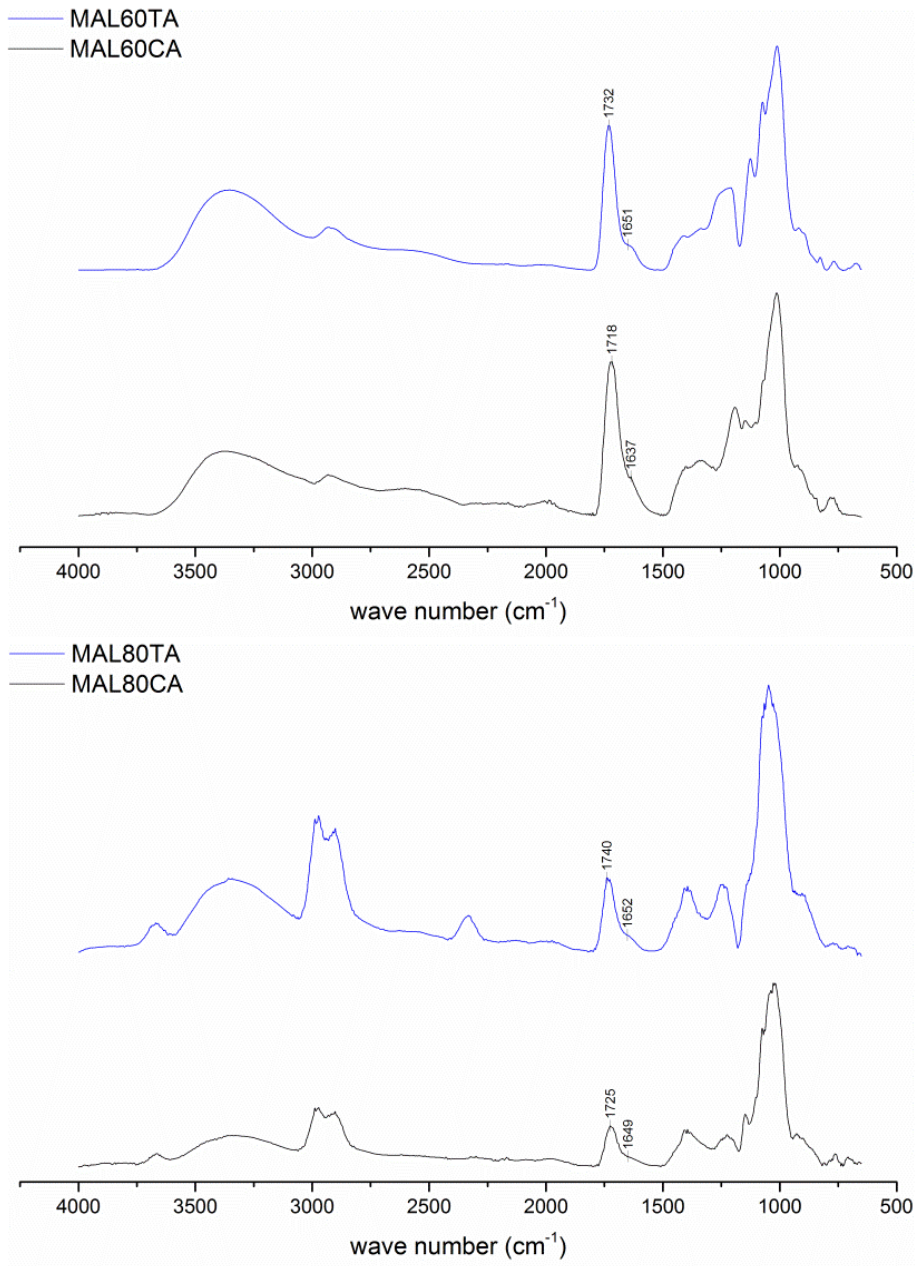


**Figure 3.11 – ATR-FTIR spectra of the compositions MAL60CA, MAL60TA, MAL80CA and MAL80TA after 4 hours thermal treatment at 140 °C**

The progress of the esterification reaction for the compositions in Table 3.1 has been studied by IR at 140 °C, recording the spectra at 1, 2, 3 and 4 hours (see Annex 1). The sequence of IR spectra shows that the absorbance of the C=O stretching band (1709-1740  $\text{cm}^{-1}$ ) increases while the intensity of OH stretching band decreases (3300-3500  $\text{cm}^{-1}$ ) when heating time increases [32].

Thus the progress of the esterification reaction has been followed by the evolution of the ratio between the absorbance of C=O stretching band ( $A_{CO}$ ) and the absorbance of OH stretching band ( $A_{OH}$ ). Figure 3.12 and Figure 3.13 shows the evolution of the  $A_{CO}/A_{OH}$  ratio with the heating time for the compositions in Table 3.1.

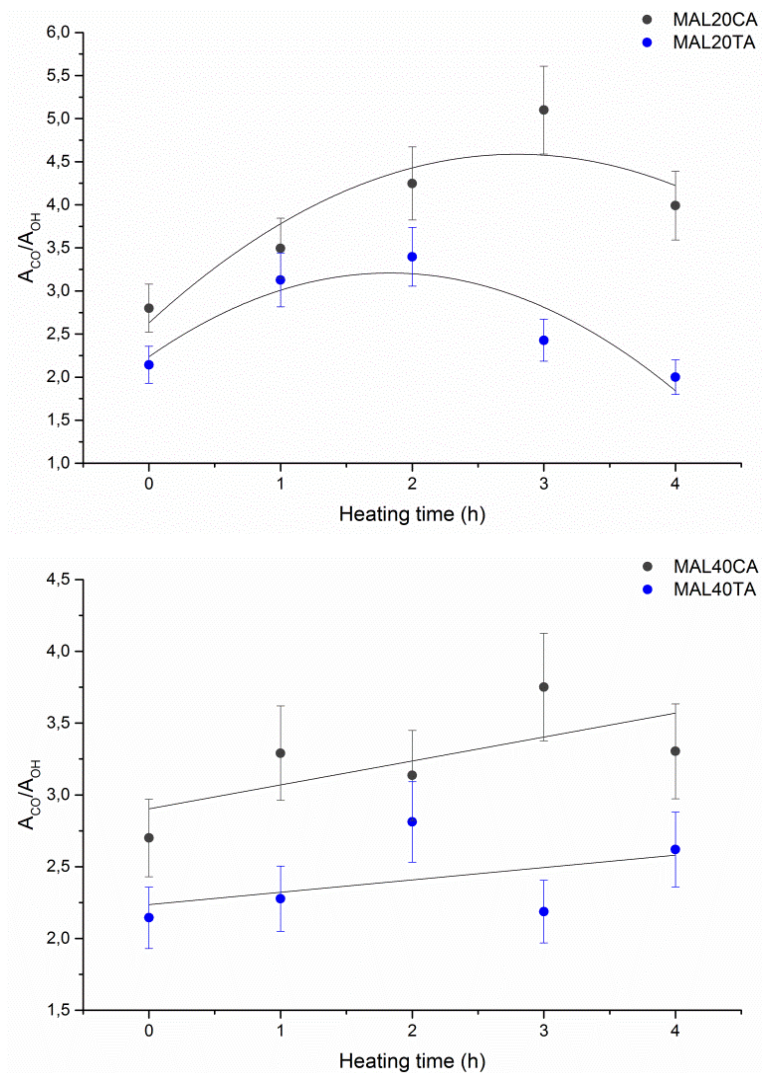


**Figure 3.12 – Ratio of  $A_{CO}/A_{OH}$  of the compositions MAL20CA, MAL20TA, MAL40CA and MAL40TA under thermal treatment at 140 °C as function of heating time**

It can be observed that the systems with 20% MAL follow a non-linear trend. The ratio  $A_{CO}/A_{OH}$  increases until 2-3 hours heating as consequence of esterification reaction, decreasing afterwards most likely as consequence of partial thermal decomposition of the system [33, 34]. The systems with intermediate content of MAL (i.e. 40% to 60 %) follow a linear trend up to 4 hours heating. This allows a quick comparison between the CA containing systems and the TA containing systems. Based on the slope of the lineal model it can be noted that in the systems



containing CA the esterification reaction progresses faster. For the systems with 80% MAL, the ratio  $A_{CO}/A_{OH}$  follows a linear trend until 3 hours heating when the system is containing CA. But, for the system containing TA the ratio  $A_{CO}/A_{OH}$  starts its linear trend after 1 hour heating. This may indicate that the esterification reaction goes smoothly for the system containing TA.

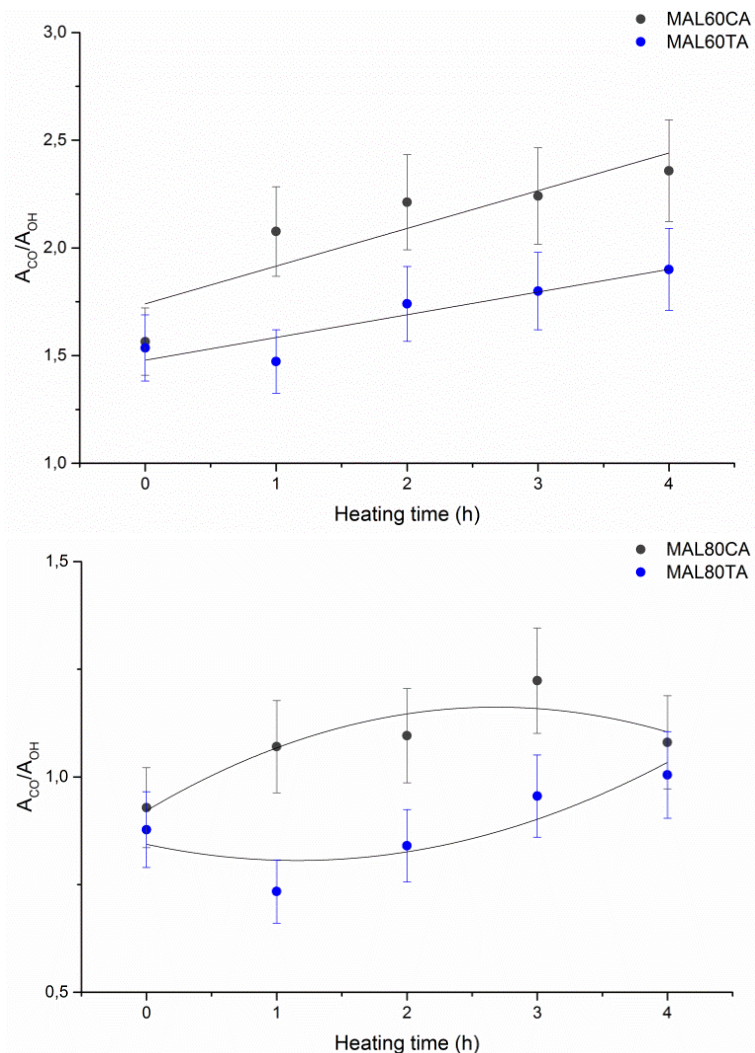


**Figure 3.13 – Ratio of  $A_{CO}/A_{OH}$  of the compositions MAL60CA, MAL60TA, MAL80CA and MAL80TA under thermal treatment at 140 °C as function of heating time**

This IR study proves that the progress of the esterification reaction is strongly dependent on the carboxylic acid nature, CA being more reactive than TA. For the other side it is also proved that the content of carboxylic acid could affect to earlier thermal decomposition of the system, being more stable those systems with intermediate content of MAL. Therefore the prediction of reaction progress by IR technique might be done accurately for the systems containing 40-60 % of MAL.

### 3.5.3 RHEOLOGICAL STUDY

The rheological behavior against temperature was compared for the systems containing CA and TA. The evolution of the storage modulus ( $G'$ ) for all the compositions in Table 3.1 is shown in Figure 3.14 and Figure 3.15.

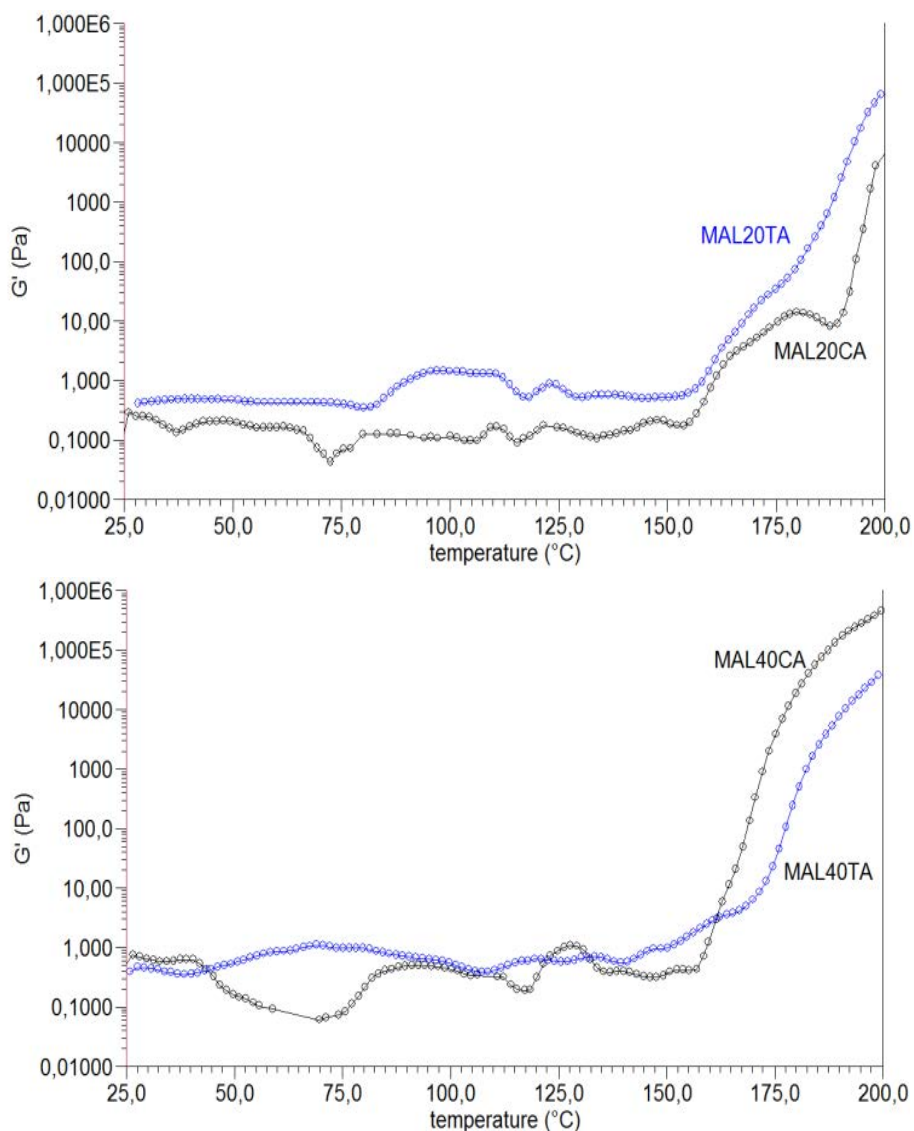
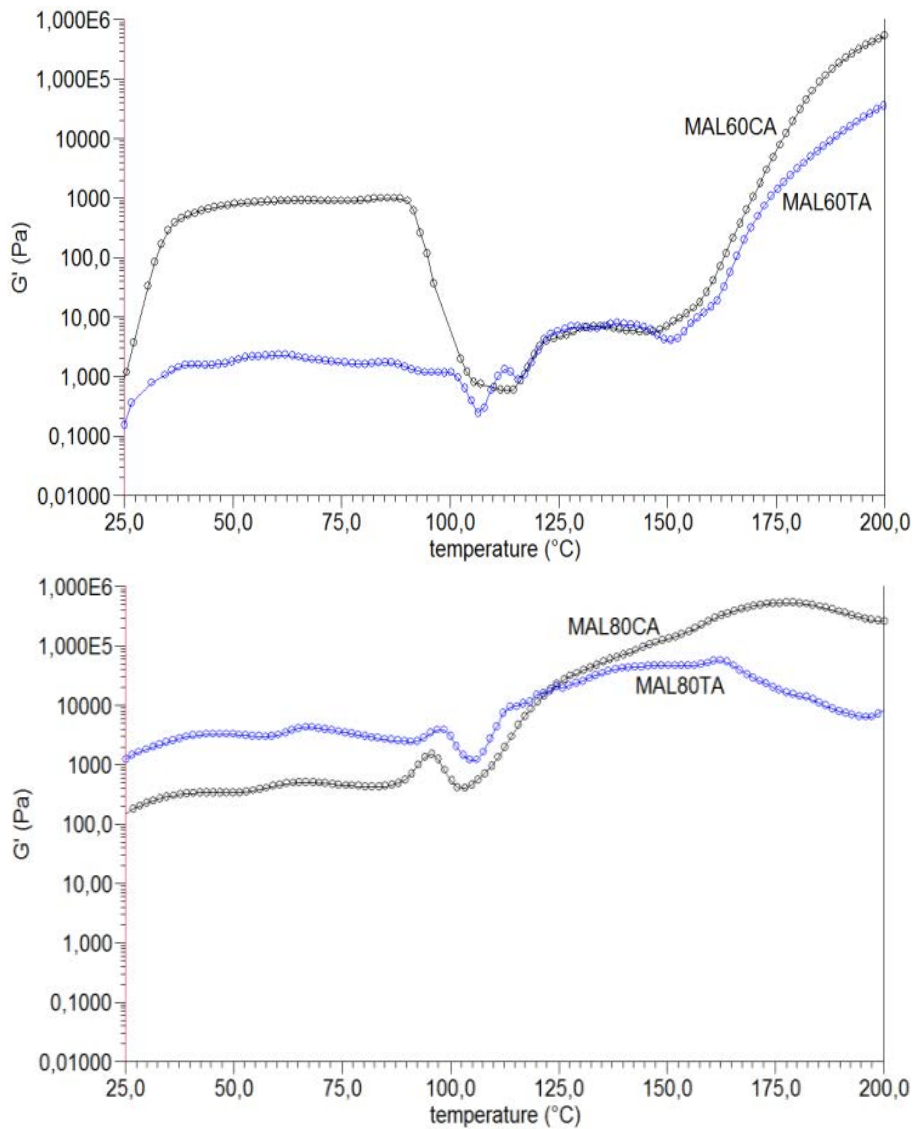


Figure 3.14 – Log  $G'$  against temperature for compositions MAL20CA, MAL20TA, MAL40CA and MAL40TA



**Figure 3.15 – Log  $G'$  against temperature for compositions MAL60CA, MAL60TA, MAL80CA and MAL80TA**

The temperature at which continuous increase of  $G'$  starts, as consequence of the polymer chains growing [35, 36], has been assigned to the starting temperature of the crosslinking reaction. In the compositions containing 20% MAL,  $G'$  follows a similar evolution for CA and TA systems, being both flat until around 153 °C, then the modulus starts to increase strongly due to the crosslinking reaction. For the compositions containing 40 % MAL, a sharp raise of the modulus is detected at 156 °C for the system containing CA and at 167 °C for the systems containing TA. For the compositions containing 60 % of MAL, a remarkable higher value of  $G'$  is found for the system containing CA in the range temperature between 25 and 90 °C. This could be an effect of the physical interactions (e.g. hydrogen bond) between different molecules of MAL [37] and

between MAL and CA, present at low temperature but disappearing at temperature above 90 °C. Then,  $G'$  increases strongly as from 146 °C for the system containing CA and as from 150 °C for the systems containing TA. The effect of physical interactions between different molecules of MAL is even more noticeable for the compositions with 80% MAL. As a consequence,  $G'$ , at low temperature, is higher for the systems with 80 % content of MAL than for the rest of the systems. For these compositions,  $G'$  increases from around 100 °C, when water starts to evaporate [38, 39]. In this case, the starting temperature of the crosslinking reaction cannot be easily identified. In general, these results show that the crosslinking depicted in Scheme 3.1, measured by a dynamic rheological experiment is detected at slightly higher temperature (146-167 °C) than the condensation reaction observed by TGA (130-160 °C). But, in any case it has been proved that the crosslinking temperature is higher for the systems containing TA as predicted by the higher condensation temperature seen at the TGA results.

Rheological measurements were also carried out for all the compositions in Table 3.1 under isothermal conditions at 140 °C. The measurement was stop when the modulus was independent of frequency. The isothermal scanning for the compositions containing CA is shown in Figure 3.16 and, for the compositions containing TA it is shown in Figure 3.17.

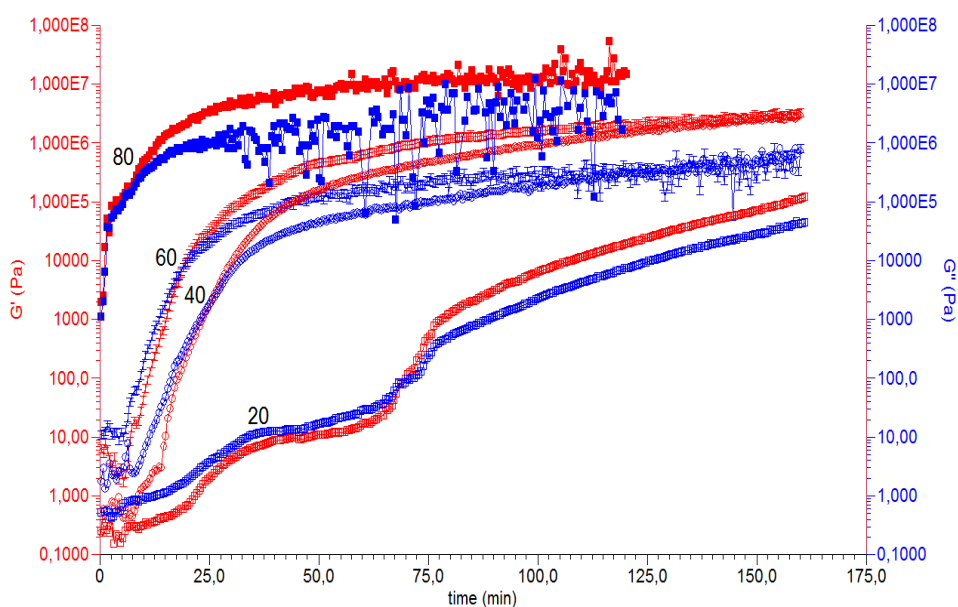


**Figure 3.16 – Plot of log  $G'$  and log  $G''$  against time of composition (20) MAL20CA, (40) MAL40CA, (60) MAL60CA and (80) MAL80CA**

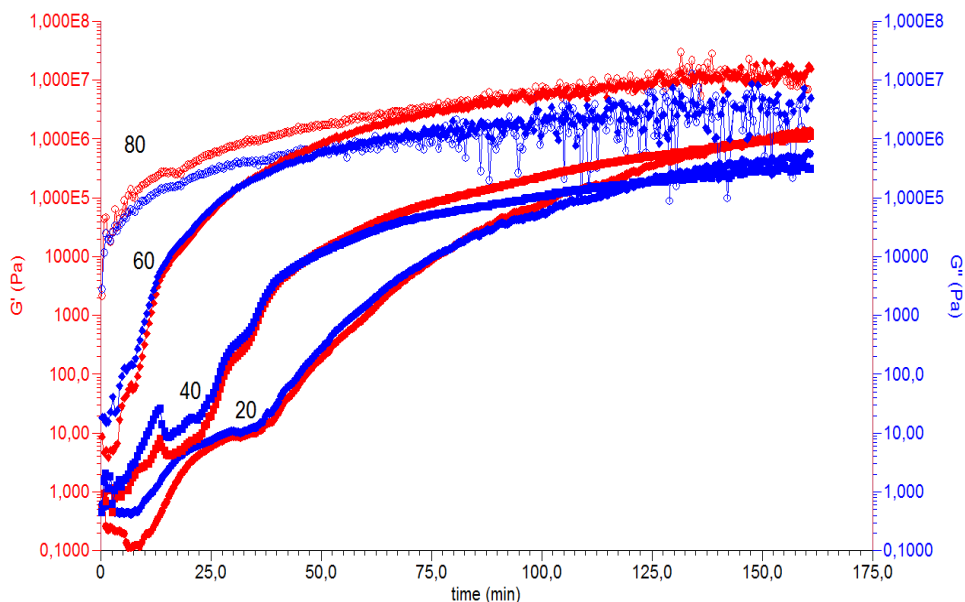


**Figure 3.17 – Plot of log  $G'$  and log  $G''$  against time of composition (20) MAL20TA, (40) MAL40TA, (60) MAL60TA and (80) MAL80TA**

The gel time for each composition, i.e. the time at which the system goes from non-crosslinked to crosslinked gel has been identified by the cross-over between storage modulus ( $G'$ ) and loss modulus ( $G''$ ) [40]. At this stage material changes from liquid-like to solid-like behavior as consequence of the crosslinking. The resulting gel time for each composition is quoted in Figure 3.18. The gel time is lower for the systems containing CA, except for the compositions containing 80 % MAL. For these compositions it has not been possible to detect the gel time difference at 140 °C between the CA and TA systems. These results are aligned with the results from the IR and TGA before, from where it has been concluded that the systems containing CA are more reactive than the systems containing TA, not only regarding to the esterification (condensation) reaction but also regarding to the crosslinking process.

The isothermal measurements demonstrate that the composition is not only having influence on gel time but also on the modulus evolution under heating. In general, the value of  $G'$  increases faster in compositions containing CA, suggesting a faster cross-linking process. A maximum value of  $G'$ , from 5-10 MPa, is achieved for those compositions with 40 – 80 % of MAL in case of the systems containing CA, while for the systems containing TA, this maximum value of  $G'$  is achieved with 60 – 80 % of MAL. Overall the compositions with 40 – 80 % MAL are able to achieve typical values of  $G'$  for thermoset resins depending on the type of polycarboxylic acid [41, 42].

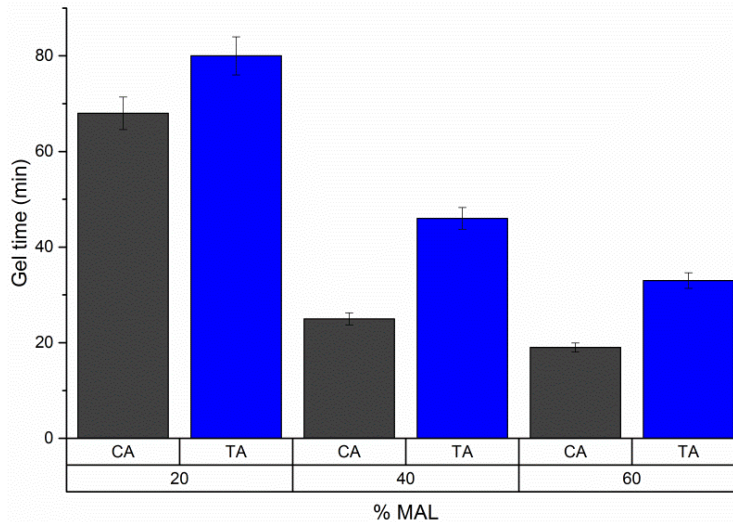


**Figure 3.18.** Gel time of for the systems containing citric acid (CA) and the systems containing tartaric acid (TA) with different content of MAL (20, 40, 60 and 80 %)

### 3.5.4 MECHANICAL PROPERTIES CHARACTERIZATION

The effect of the curing time at 140 °C for the compositions MAL60CA and MAL60TA on mechanical performance has been analyzed. Figure 3.19 shows the tensile strain at maximum load of specimens bonded with the systems containing CA and the systems containing TA, against curing time. Tensile strain decreases as curing time is increasing, reaching minimum value after 15 and 30 min for the system containing CA and TA respectively. This result indicates that the network rigidity increases with the curing time, leading to a stiffer material [43] after 15 or 30 min depending on the carboxylic acid nature. The curing time also has a strong effect on the retention of tensile strain measured upon accelerated weathering conditions. The retention of tensile strain is higher as curing time is increased. This might be due to the higher crosslinking density when curing longer. The system containing CA reaches retention values close to 100% earlier (after 15 min) than the system containing TA (which required 30 min). These two facts prove the thermoset character of both systems, being the CA one faster to crosslink than the TA one.

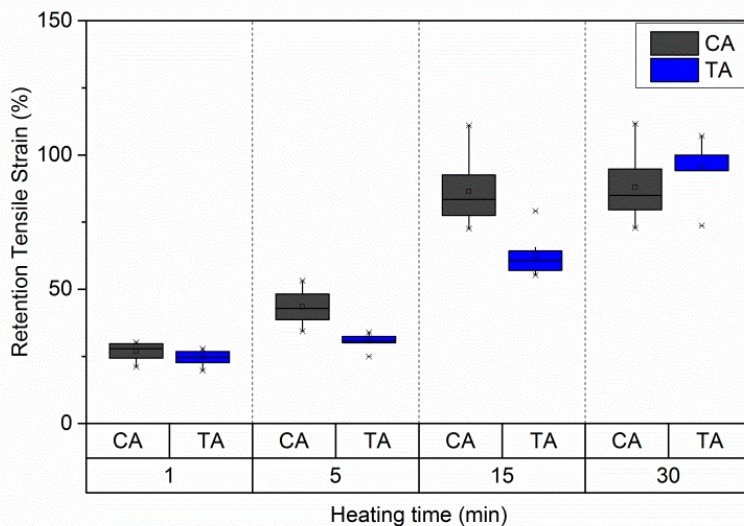
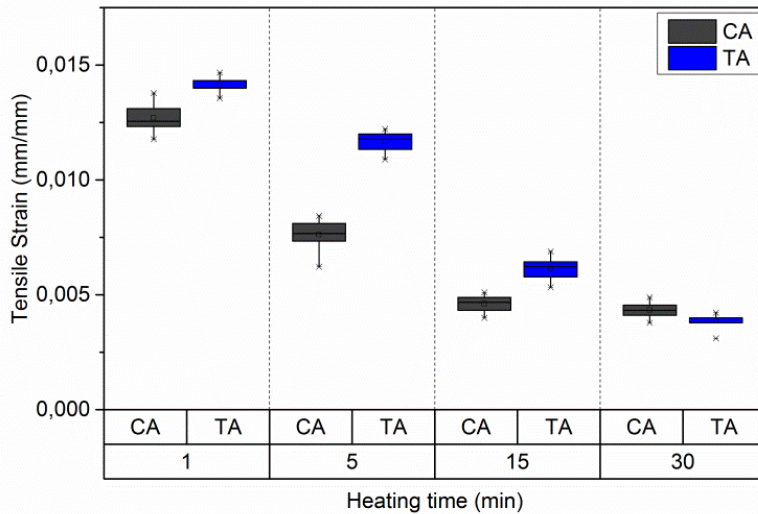
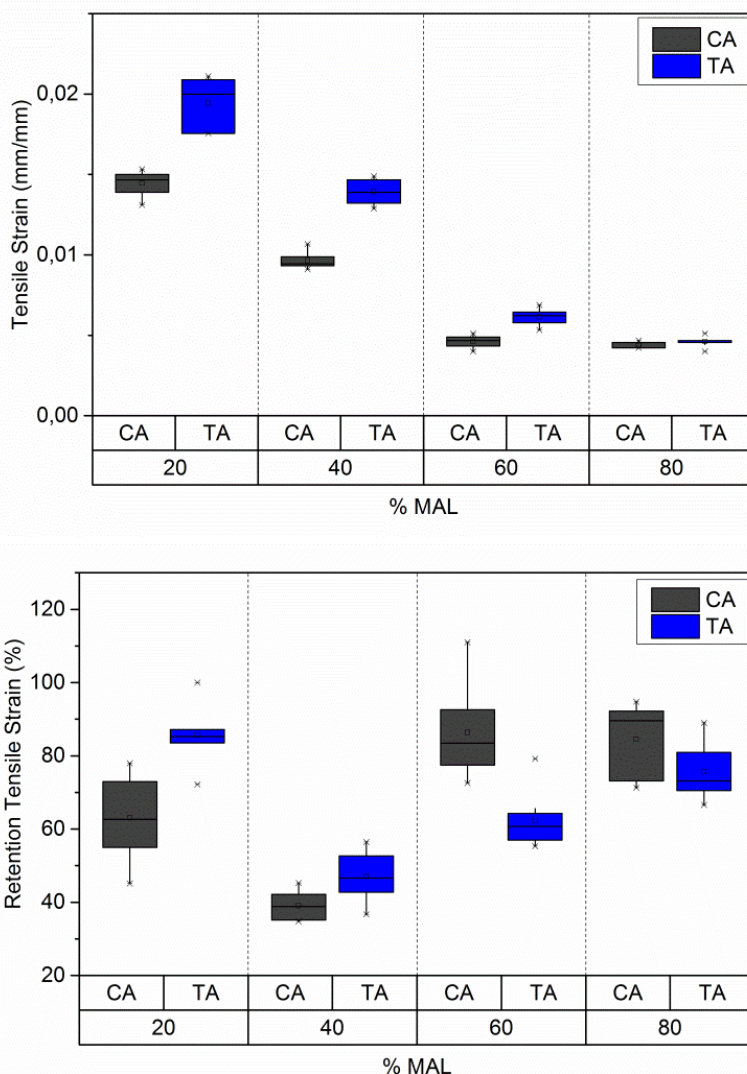


Figure 3.19 – Tensile strain against curing time at 140 °C for composition (CA) MAL60CA and (TA) MAL60TA

The comparison of the tensile strain of the compositions in Table 3.1 cured at 140 °C for 15 min is shown in Figure 3.20. Tensile strain decreases with the content of MAL, reaching the minimum value at 60 % of MAL in the systems with CA, and at 80 % of MAL in the systems with TA. This indicates that stiffer material is obtained with compositions rich in MAL, most likely due to its higher crosslinking density. The tensile strain retention upon accelerated weathering conditions is above 50 % when the content of MAL is 20 %, dropping below 50 % at 40 % MAL, to increase again in compositions with content of MAL  $\geq$  60 %.



**Figure 3.20 – Tensile strain against % of MAL (20, 40, 60 and 80) for the system containing (CA) CA and the system containing (TA) TA after curing at 140 °C for 15 min**

In general, the compositions containing 60-80 % of MAL would give the best mechanical performance, depending on the carboxylic acid type, due to the lower mechanical strain and higher retention capacity. In particular, the system containing CA leads to the lowest tensile strain and the highest retention. This might be due to the higher crosslinking ability of the CA compared to the TA. Overall the thermoset character is more remarkable in the systems containing CA. From TGA has been demonstrated that both, CA and TA can fully react. But, as shown in Figure 3.1, CA has three carboxyl equivalents while TA has two carboxyl equivalents. This could explain that the crosslinking capacity of CA is higher, leading to stronger thermoset character, therefore better



mechanical properties. For those systems with high content of MAL even TA is able to deliver proper performance.

### 3.5.5 SCANNING ELECTRON MICROSCOPY (SEM)

Scanning electron microscopy (SEM) micrographs of the glass-paper impregnated with composition MAL60CA after mechanical characterization are shown in Figure 3.21. The surface of the glass fiber paper is homogeneously impregnated. In the cross-section pictures it can be observed that the composition is partially covering the fibers and gluing different fibers together. This indicates the good adhesion of the crosslinked system to the glass fibers. The compositions MAL60TA shows very similar results (see Annex 1). Based on SEM analysis no difference can be identified between the systems containing CA and the systems containing TA. Nevertheless this is a qualitative analysis which may only help to assure that the different systems are glued to the fibers.

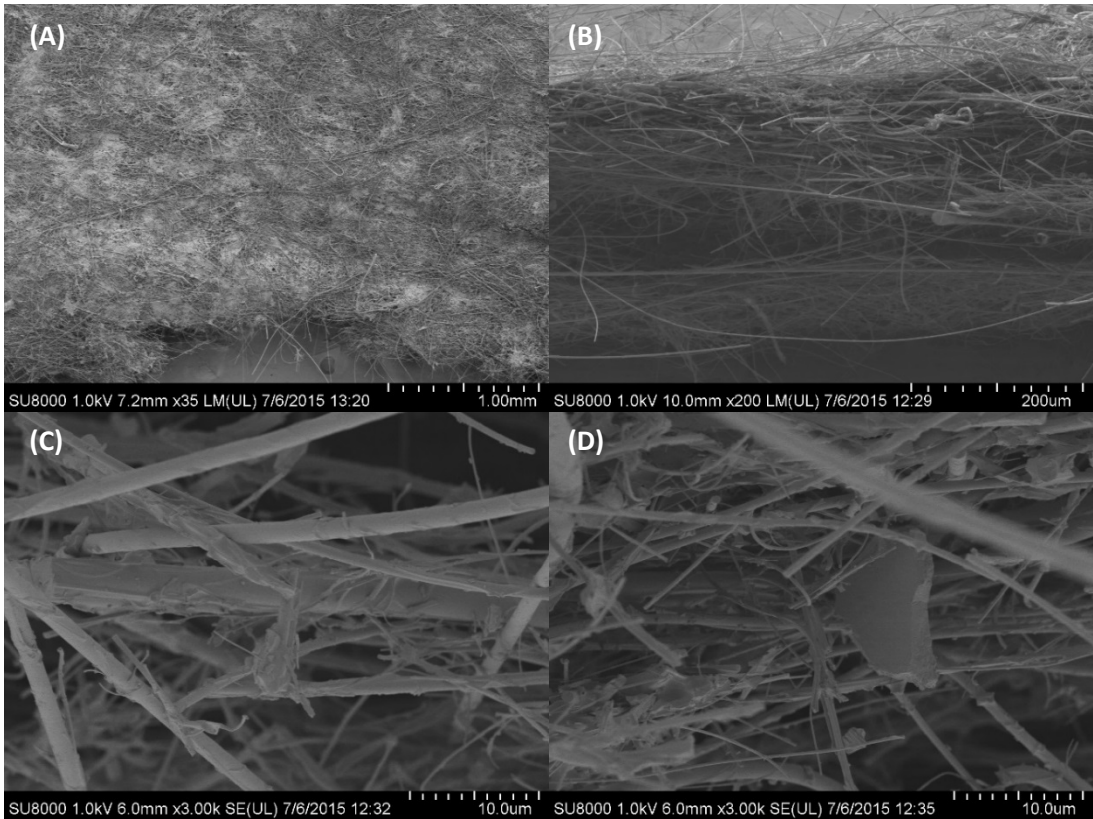


Figure 3.21 – SEM micrographs of glass paper impregnated with composition MAL60CA upon heating treatment for 15 min, on the surface (A), cross-section (B) and the glass fibers in the cross-section (C and D)

## 3.6 CONCLUSIONS

---

The results presented in this chapter show that the crosslinking by polycondensation reaction of compositions containing maltodextrin and citric or tartaric acids takes effectively place at moderate temperatures (i.e. 140 °C). These systems can lead to thermoset materials upon thermal treatment on substrates like, for instance, fiber glass. This means they could be used as thermoset resins in the binder for the mineral wool production. However, the nature of the polycarboxylic acid has an important impact on the performance of the material. This makes that one system is more attractive than the other for final application. First, the reactivity of the systems containing citric acid is higher than those containing tartaric. Second, the systems containing citric acid show better crosslinking capacity than the systems containing tartaric acid. Both features, reactivity and crosslinking ability are key for the final application. On the one hand, the reactivity of the system would have an impact on the energy and time needed to cure it in a real industrial process. The higher the reactivity, the less energy and time will be required. On the other hand, the crosslinking capacity of the system is directly related to performance of the finish product. For instance, in the case of mineral wool material, glass fibers will be stronger bonded when the crosslinking capacity is greater. This would lead to better mechanical performance of the product obtained, what eventually could allow to decrease the quantity of binder system needed. Considering both aspects, the system containing citric acid would be recommended as the most suitable compared to the one containing tartaric acid for its application in industrial process. The system comprising maltodextrin and citric acid could provide a fairly good eco-friendly alternative to replace the traditional petrol-based systems.

## 3.7 REFERENCES

---

1. Vert M, Santos ID, Ponsart S, Alauzet N, Morgat J-L, Coudane J, and Garreau H. *Polymer International* 2002;51(10):840-844.
2. Wu G-m, Chen J, Huo S-p, Liu G-f, and Kong Z-w. *Carbohydrate Polymers* 2014;105:207-213.
3. Preface. In: Wool RP and Sun XS, editors. *Bio-Based Polymers and Composites*. Burlington: Academic Press, 2005. pp. XIII-XVI.

4. Gandini A and Belgacem MN. Chapter 1 - The State of the Art. In: Gandini MNB, editor. *Monomers, Polymers and Composites from Renewable Resources*. Amsterdam: Elsevier, 2008. pp. 1-16.
5. Babu RP, O'Connor K, and Seeram R. *Progress in Biomaterials* 2013;2(1):1-16.
6. Esmaeili N, Bakare F, Skrifvars M, Javanshir Afshar S, and Åkesson D. *Cellulose* 2015;22(1):603-613.
7. Dotan A. 15 - Biobased Thermosets. In: Dodiuk H and Goodman SH, editors. *Handbook of Thermoset Plastics (Third Edition)*. Boston: William Andrew Publishing, 2014. pp. 577-622.
8. Can E, Küsefoğlu S, and Wool RP. *Journal of Applied Polymer Science* 2001;81(1):69-77.
9. Liu X, Xu K, Liu H, Cai H, Su J, Fu Z, Guo Y, and Chen M. *Progress in Organic Coatings* 2011;72(4):612-620.
10. Polyakov AI and Bitenbayev MI. *Solid State Sciences* 2009;11(5):945-947.
11. Liu K, Madbouly SA, and Kessler MR. *European Polymer Journal* 2015;69:16-28.
12. Reddy N and Yang Y. *Food Chemistry* 2010;118(3):702-711.
13. Ghanbarzadeh B, Almasi H, and Entezami AA. *Industrial Crops and Products* 2011;33(1):229-235.
14. Widsten P, Dooley N, Parr R, Capricho J, and Suckling I. *Carbohydrate Polymers* 2014;101:998-1004.
15. Halpern JM, Urbanski R, Weinstock AK, Iwig DF, Mathers RT, and von Recum HA. *Journal of Biomedical Materials Research Part A* 2014;102(5):1467-1477.
16. Davies JA, Dutremez S, and Pinkerton AA. *Inorganic Chemistry* 1991;30(10):2380-2387.
17. Olsson E, Menzel C, Johansson C, Andersson R, Koch K, and Järnström L. *Carbohydrate Polymers* 2013;98(2):1505-1513.
18. Olivato JB, Müller CMO, Carvalho GM, Yamashita F, and Grossmann MVE. *Materials Science and Engineering: C* 2014;39(0):35-39.
19. Coma V, Sebti I, Pardon P, Pichavant FH, and Deschamps A. *Carbohydrate Polymers* 2003;51(3):265-271.
20. Kapuśniak J. *Journal of Polymers and the Environment* 2005;13(4):307-318.
21. Danilovas PP, Rutkaite R, and Zemaitaitis A. *Carbohydrate Polymers* 2014;112(0):721-728.
22. Xu F, Weng B, Gilkerson R, Materon LA, and Lozano K. *Carbohydrate Polymers* 2015;115(0):16-24.
23. Yang CQ and Wang X. *Journal of Applied Polymer Science* 1998;70(13):2711-2718.
24. Mao Z and Yang CQ. *Journal of Applied Polymer Science* 2001;81(9):2142-2150.
25. Kizil R, Irudayaraj J, and Seetharaman K. *Journal of Agricultural and Food Chemistry* 2002;50(14):3912-3918.
26. Galat A. *Acta Biochim Pol* 1980;27(2):135-142.

27. Tisserat B, O'Kuru RH, Hwang H, Mohamed AA, and Holser R. *Journal of Applied Polymer Science* 2012;125(5):3429-3437.
28. Lin-Vien D, Colthup NB, Fateley WG, and Grasselli JG. CHAPTER 9 - Compounds Containing the Carbonyl Group. In: Grasselli DL-VBCGFG, editor. *The Handbook of Infrared and Raman Characteristic Frequencies of Organic Molecules*. San Diego: Academic Press, 1991. pp. 117-154.
29. Kozhevina LI, Skryabina LG, and Tselinskii YK. *Journal of Applied Spectroscopy* 1980;33(6):1347-1351.
30. Sasikala V, Sajan D, Vijayan N, Chaitanya K, Babu Raj MS, and Selin Joy BH. *Spectrochimica Acta Part A: Molecular and Biomolecular Spectroscopy* 2014;123(0):127-141.
31. Shi R, Zhang Z, Liu Q, Han Y, Zhang L, Chen D, and Tian W. *Carbohydrate Polymers* 2007;69(4):748-755.
32. Han F, Liu M, Gong H, Lü S, Ni B, and Zhang B. *International Journal of Biological Macromolecules* 2012;50(4):1026-1034.
33. Claude J and Ubbink J. *Food Chemistry* 2006;96(3):402-410.
34. Menzel C, Olsson E, Plivelic TS, Andersson R, Johansson C, Kuktaite R, Järnström L, and Koch K. *Carbohydrate Polymers* 2013;96(1):270-276.
35. Vlassopoulos D, Chira I, Loppinet B, and McGrail PT. *Rheologica Acta* 1998;37(6):614-623.
36. Tribut L, Fenouillot F, Carrot C, and Pascault JP. *Polymer* 2007;48(22):6639-6647.
37. Chronakis IS. *Critical Reviews in Food Science and Nutrition* 1998;38(7):599-637.
38. Loret C, Meunier V, Frith WJ, and Fryer PJ. *Carbohydrate Polymers* 2004;57(2):153-163.
39. Dokic P, Jakovljevic J, and Dokic-Baucal L. *Colloids and Surfaces A: Physicochemical and Engineering Aspects* 1998;141(3):435-440.
40. Martin JS, Laza JM, Morrás ML, Rodríguez M, and León LM. *Polymer* 2000;41(11):4203-4211.
41. Rusli A, Cook WD, and Schiller TL. *Polymer International* 2014;63(8):1414-1426.
42. Block C, Van Mele B, Van Puyvelde P, and Van Assche G. *Reactive and Functional Polymers* 2013;73(2):332-339.
43. Ma Q, Liu X, Zhang R, Zhu J, and Jiang Y. *Green Chemistry* 2013;15(5):1300-1310.

---

# *CHAPTER IV*

---

## *EFFECT OF CaO AND ZnO IN THE THERMAL CROSSLINKING OF MALTODEXTRIN AND POLYCARBOXYLIC ACIDS*

---



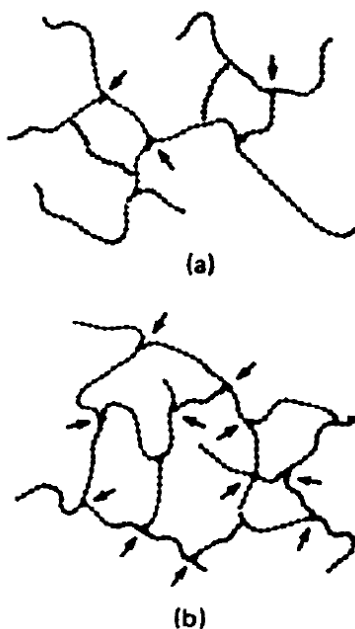
## 4.1 INTRODUCTION

---

### 4.1.1 CROSSLINKING

---

By crosslinking terminology we may refer to polymer network formation. A polymer network is formed as a result of the chemical interaction between linear polymer chains or the build-up of a three-dimensional fish-net configuration from monomeric reactants [1]. According to this, any type of chemical reaction of functional groups may be used for the purpose of polymer network formation allowing nearly quantitative conversion of these functionalities. Crosslinking can be formed whenever there are two branches that have different functional groups at their end, one has an A group and the other one has a B group.



**Scheme 4.1 – Lightly crosslinked polymer network (a) and highly crosslinked polymer network (b) [1]**

Crosslinking is the main characteristic of a thermosetting material. The polymer network formed has an “infinite” molecular weight with chemical interactions which restricts the movement of long chains. The chemical and physical properties of the polymer network strongly depend on the chemical nature of the monomers involved and on the crosslinking density. Therefore a wide variety of physical properties of crosslinked polymeric materials is available and

considerable technological input is made to design the network in order to match the demands [2].

Traditional crosslinking chemistry for step-growth polymers involves polycondensation with multifunctional monomers, leading in parallel to chain growth and network formation. An example of crosslinking systems involving polycondensation reaction are those based on polysaccharides and polycarboxylic acids. These systems have been developed in recent years for their application in the wood and glass fiber industry [3-5]. One of the weak points of these binder systems is their slow crosslinking poor polymer network and reversibility of ester bond upon humidity [6]. This makes these systems to easily lose their mechanical performance upon weathering conditions (temperature, humidity). The systems containing the polysaccharide maltodextrin and polycarboxylic acids, citric and tartaric acid have been deeply studied in previous chapters. It was proved the ability of these systems to behave as a thermoset. However improvement of the polymer network of these systems may be required in order to get proper mechanical performance in their final application.

#### **4.1.2 CROSSLINKING ENHANCEMENT**

---

The prime techniques to modify polymers properties are grafting, crosslinking, blending and composite formation. In particular, crosslinking technique is applied whenever the polymer need to be more resistant to heat, light and other physical agents, giving it a high degree of dimensional stability, mechanical strength and chemical and solvent resistance [7]. The effect of crosslinking on the physical properties of the polymer is mainly influenced by the degree of crosslinking. Therefore, in order to improve the mechanical performance of the system based on maltodextrin and polycarboxylic acids, an increase of the crosslinking density would be required. It is known that the crosslinking process takes place by covalent bond in most of the polymer networks, for instance like sulfur vulcanization, peroxide curing, radiation curing, or by amine, ether and ester bonds. However, the application of this kind of crosslinking to enhance that of the system based on maltodextrin and polycarboxylic acids would require the modification of the polysaccharide. For instance, by appending the corresponding reactive groups to the polysaccharide [8, 9]. This approach would imply too complex steps of reaction in order to increase the crosslinking degree of the final system. Another alternative is the ionic crosslinking [10, 11]. This strategy has been



used to enhance the ester crosslinking of cotton fabrics by cationization of cotton fabric and later interaction with carboxylic acids leading to an improvement of the mechanical properties [12, 13]. Ionic crosslinking could be achieved in the system containing the polysaccharide and carboxylic acid by adding suitable ionic compounds, as the ionic compounds would enhance the crosslinking by interacting with the moieties in the polymer network.

### **4.1.3 IONIC      CROSSLINKING      OF      POLYSACCHARIDES      AND POLYCARBOXYLIC ACIDS WITH METALS**

---

Interaction of starch with metal ions have been reported [14, 15], particularly the formation of complexes of metals with starch and maltodextrin [16-20]. Interaction on metal ions with carboxylic acids is well described and applied in different fields. For instance, it has been reported the use of metal ions as crosslinkers in polymer compositions containing poly(acrylic acid) [21, 22] by the interaction between the metal ions and the carboxyl groups of the poly(acrylic acid) [23, 24]. It is also well known the interaction of citric and tartaric acid with metal ions [25-27], in water treatments and wine industry. Crosslinking of ionic polysaccharides has also been reported in previous works by the introduction of Ca(II) ion [28]. Typical ions reported as strongly interacting with polysaccharides and polycarboxylic acids are: Mg(II), Ca(II), Zn(II), Cu(II), Fe(III), Mn(II). Whenever metal ions are introduced as crosslinkers, they are introduced as salts, like for instance calcium chloride. However the counterion of the salt could generate some drawbacks in final application like for instance corrosion in the steel facilities due to chloride ion [29]. For that reason metal oxides, and not metal salts, are proposed in this work.

### **4.1.4 CaO AND ZnO**

---

Calcium oxide (CaO) is high volume alkaline earth metal oxide used in many applications as catalyst, toxic-water remediation agent, additive in refractory, doped material to modify electrical and optical properties, crucial factor for CO<sub>2</sub> capture, flue gas desulfurization, food pH control and pollutant emission control. Many of the applications are successful due to the high ability of Ca(II)

ion to interact with other counterions. It is inexpensive and easy to produce by heating calcium carbonate.

Zinc oxide (ZnO) is a multifunctional material due its unique physical and chemical properties, such as high chemical stability, high electrochemical coupling coefficient, broad range of radiation absorption and high photostability. Because of its diverse properties, ZnO is widely used in many areas. It can be produced by different methods, metallurgical and chemical. Some of the applications are tyres, ceramics, pharmaceuticals, agriculture, paints and chemicals. The major portion of its global production is used in crosslinked rubber products as crosslinker of carboxylates [30].

## **4.2 AIM OF THIS CHAPTER**

---

Considering the previous works, it has been investigated the introduction of calcium and zinc ions in the systems containing maltodextrin and a polycarboxylic acid in order to enhance the polymer network. From one side interactions between maltodextrin and the ion could take place. But, from the other side additional interactions between citric acid and tartaric acid with ion could also help to increase the crosslinking density in the system.

The aim of this work is to study the crosslinking capacity of Ca and Zn(II) ions in those systems containing maltodextrin and citric acid or tartaric acid by means of the addition of CaO and ZnO respectively. It has been also evaluated the impact of the additional crosslinking in the mechanical properties of finish material. Finally a crosslinking mechanism has been proposed for Ca ion in the system containing maltodextrin and citric acid.

## **4.3 MATERIALS AND METHODS**

---

### **4.3.1 MATERIALS**

---

Powdered maltodextrin (MAL) Maldex 120 (dextrose equivalent (DE) 11 to 15), manufactured by spray-drying of liquid maltodextrin, derived from edible corn starch hydrolysis was provided by

Tereos Syral. Citric acid (CA) reagent, CaO and ZnO were purchased from Sigma-Aldrich. The products were used without additional purification.

## 4.3.2 METHODS

Different systems containing MAL and CA, or MAL and TA with CaO or ZnO were prepared. For that, the three compounds, MAL, the carboxylic acid and the metal oxide were mixed in water at different ratios. The compositions containing CA are quoted in Table 4.1, and the compositions containing TA are in Table 4.2. MAL was dissolved in distilled water under mechanical stirring and then the polycarboxylic acid was added keeping the stirring until the solution was homogeneous. Finally the metal oxide was added keeping the same stirring conditions until it was completely dissolved.

**Table 4.1 – Compositions containing maltodextrin (MAL) and citric acid (CA) with CaO or ZnO**

Composition	MAL (% dry weight)	CA (% dry weight)	CaO (% dry weight)	ZnO (% dry weight)
M60C	60	40	-	-
M60C1Ca	59.4	39.6	1.0	-
M60C3Ca	58.3	38.8	2.9	-
M60C1Zn	59.4	39.6	-	1.0
M60C3Zn	58.3	38.8	-	2.9

**Table 4.2 – Compositions containing maltodextrin (MAL) and tartaric acid (TA) with CaO**

Composition	MAL (% dry weight)	TA (% dry weight)	CaO (% dry weight)
M60T	60	40	-
M60T1Ca	59.4	39.6	1.0
M60T3Ca	58.3	38.8	2.9

Additional mixtures were prepared containing only CA and CaO in the same proportion as in the compositions containing MAL (Table 4.3). Unless otherwise stated, all the mixtures were prepared with 50% dry content. Freeze-dried samples were prepared to avoid the influence of water in the thermogravimetical analysis.

**Table 4.3 – Compositions containing citric acid (CA) and CaO**

Composition	CA (% dry weight)	CaO (% dry weight)
C1Ca	97.6	2.4
C3Ca	93.0	7.0

## 4.4 CHARACTERIZATION TECHNIQUES

---

### 4.4.1 RHEOLOGICAL MEASUREMENTS

---

Rheological measurements were carried out with an AR1000 rheometer (TA Instruments). Disposable plate-plate geometry with diameter 25 mm was used. Dynamic measurements in oscillatory mode were performed for approximately 1 mL sample in 2000  $\mu\text{m}$  gap, applying multiple frequency mode ranging from 1 Hz to 25 Hz and a fixed torque value (tests were performed previously to ensure that the response was in the viscoelastic region). Rheological behavior of water solutions of the different compositions was monitored at isothermal conditions at 140  $^{\circ}\text{C}$  and 130  $^{\circ}\text{C}$  until maximum modulus plateau was achieved, previously heating to the isothermal temperature with ramp rate of 3  $^{\circ}\text{C}/\text{min}$ . The measurements were done by duplicate.

### 4.4.2 MECHANICAL PROPERTIES MEASUREMENTS

---

Mechanical properties measurements were carried out on glass paper “Whatman GF/A 8x10 ins” impregnated with the corresponding composition and cured by thermal treatment. A glass paper sheet was soaked in a water solution with 20% solid content of the different compositions.

The treated sheet was pressed between the squeezing rolls of a laboratory padder (Mathis) at 3 mm/min speed of the rolls and pressure between the rolls at 2.5 bars. Thermal treatment on the impregnated glass paper was applied in a Labdryer oven (Mathis) at 140 °C. Specimens were cut from the cured glass paper sheet with size 75x25 mm. Cured specimens were treated with accelerated weathering conditions in a climate chamber (Ineltec) at 50 °C and 95 % humidity for 24 hours. Tensile strain measurements were done for the specimens previous to the treatment with accelerated weathering conditions and after the application of accelerated weathering conditions. The tensile strain measurements were carried out in an Instron Universal Testing Machine equipped with a 500 N load cell. The cross-head speed applied was 2.3 m/min and the gauge length was 50 mm. The data were taken from the average of at least six specimens.

#### **4.4.3 SEM AND ELECTRON DISPERSION X-RAY (EDX)**

---

A microscope US8000 (Hitachi) with EDX system was used for SEM/EDX analysis of different compositions after the curing process. An accelerated voltage of 1 and 5 kV was applied to carry out the SEM analysis and 15 kV for the EDX analysis.

#### **4.4.4 ATR-FTIR SPECTROSCOPY**

---

ATR-FTIR spectra were measured in a Spectrum One FT-IR Spectrometer (Perkin Elmer) with a split peak accessory for ATR. Absorbance spectra were acquired at 4 cm<sup>-1</sup> resolution and signal-averaged over 10 scans recorded from 4000 cm<sup>-1</sup> to 650 cm<sup>-1</sup>. The spectra were baseline corrected and normalized to the most intense absorbance peak. FTIR spectra were measured for the different compositions upon thermal treatment at 140 °C. In order to assure the interpretation of the spectra of the compositions after the thermal treatment spectra were recorded before and after the purification of the corresponding samples. The cured compositions were purified by membrane dialysis, placing approximately 2 g of composition in a 1000 Da membrane, in 2 L of water for 20 hours, renovating the water after 10 hours. The purified polymer was dried under vacuum at 40 °C for 24 hours.

#### 4.4.5 THERMOGRAVIMETRIC ANALYSIS (TGA)

---

TGA was performed using a TGA Q500 (TA Instruments). Different freeze-dried samples of the compositions were heated in a platinum pan from 25 to 600 °C, under a nitrogen atmosphere at a heating rate of 10 °C/min. The derivative TGA (wt %/°C) of each sample was obtained from the software TA Universal Analysis.

### 4.5 RESULTS AND DISCUSSION

---

#### 4.5.1 METAL OXIDES IN THE SYSTEM CONTAINING MAL AND CA

---

##### 4.5.1.1 EFFECT OF CaO AND ZnO IN THE CROSSLINKING

---

The impact of CaO and ZnO on the crosslinking formation in the system containing MAL and CA (M60C) has been studied by rheology. Figure 4.1 shows the evolution of storage modulus ( $G'$ ) and loss modulus ( $G''$ ) against time, under isothermal treatment at 140 °C, for the compositions in Table 4.1. Both moduli increase since the beginning of isothermal treatment for all the compositions as a consequence of the crosslinking reaction [31]. This increase is stronger when CaO or ZnO is added in the composition containing MAL and CA [32]. Particularly, the increase of the moduli is much more important when CaO is added. A maximum storage modulus of around 10 MPa and loss modulus close to 1 MPa are achieved in any composition, but this is faster achieved when CaO or ZnO is added; and especially much faster in case of CaO addition. This indicates that CaO and ZnO contribute positively to the crosslinking formation.

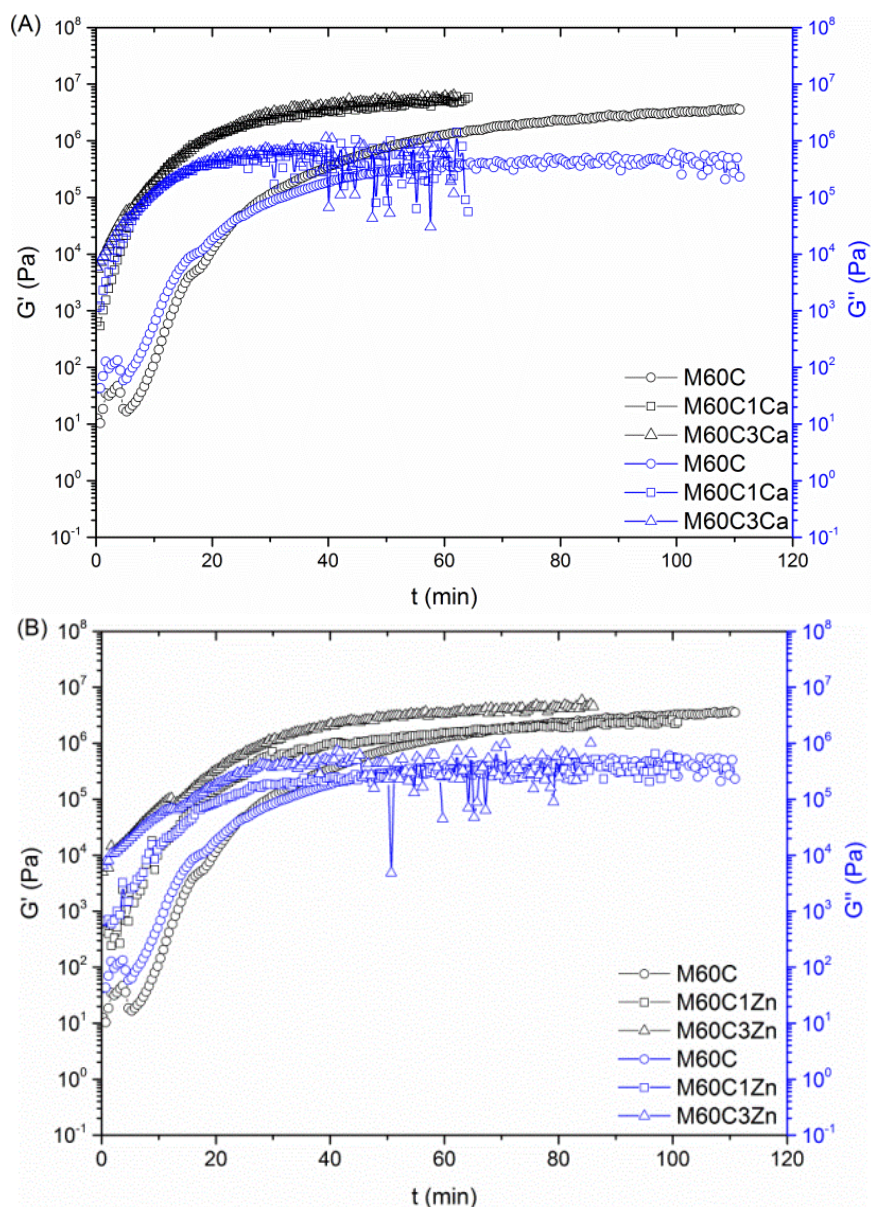


**Figure 4.1 – Log G and log G'' against time upon isothermal treatment at 140 °C for the systems containing MAL, CA and (A) CaO and (B) ZnO**

The addition of CaO and ZnO to the system containing MAL and CA has been also analyzed at 130 °C (Figure 4.2). Comparing the experiment curing at 140 °C with the experiment at 130 °C it can be observed that the maximum modulus achieved for the system M60C at 130 °C is much lower than at 140 °C (i.e. lower than 10 MPa). When CaO and ZnO is added the maximum modulus around 10 MPa can be achieved at 130 °C. This indicates that the similar level of crosslinking as in the systems containing MAL and CA can be achieved with 10 °C lower

temperature when CaO or ZnO is added. This would mean a clear advantage in the processability of the system based on MAL and CA in terms of energy consumption.

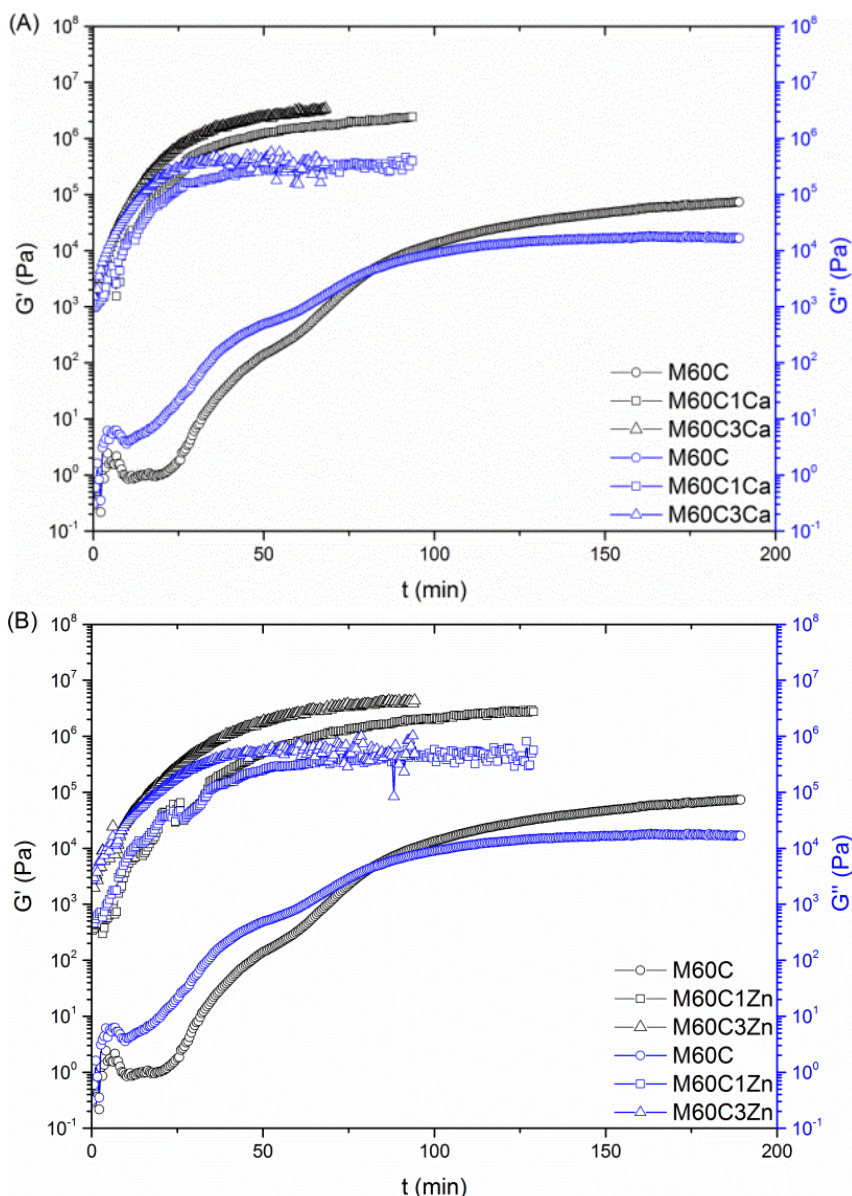


**Figure 4.2 – Log  $G'$  and log  $G''$  against time upon isothermal treatment at 130 °C for the systems containing MAL, CA and (A) CaO and (B) ZnO**

From the rheological experiments it has been also determined the gel time. Considering that the gel time is the time at which storage modulus and loss modulus cross-over [33, 34]. The gel time for the different compositions in Table 4.1 is shown in Figure 4.3. Both metal oxides, CaO and ZnO decrease strongly the gel time of the system containing MAL and CA. But the addition of CaO has stronger impact than the addition of ZnO. The gel time for the composition M60C at 130 °C is approximately 4 fold the gel time at 140 °C. When ZnO is added the gel time is still strongly



depending on the curing temperature. However, by adding CaO the gel time is nearly the same independently of the temperature. This means that CaO contributes on the crosslinking formation more, independently of the temperature.

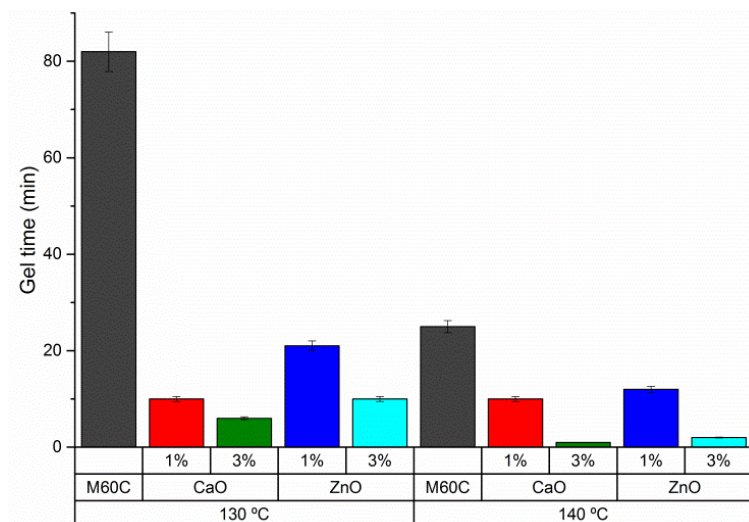
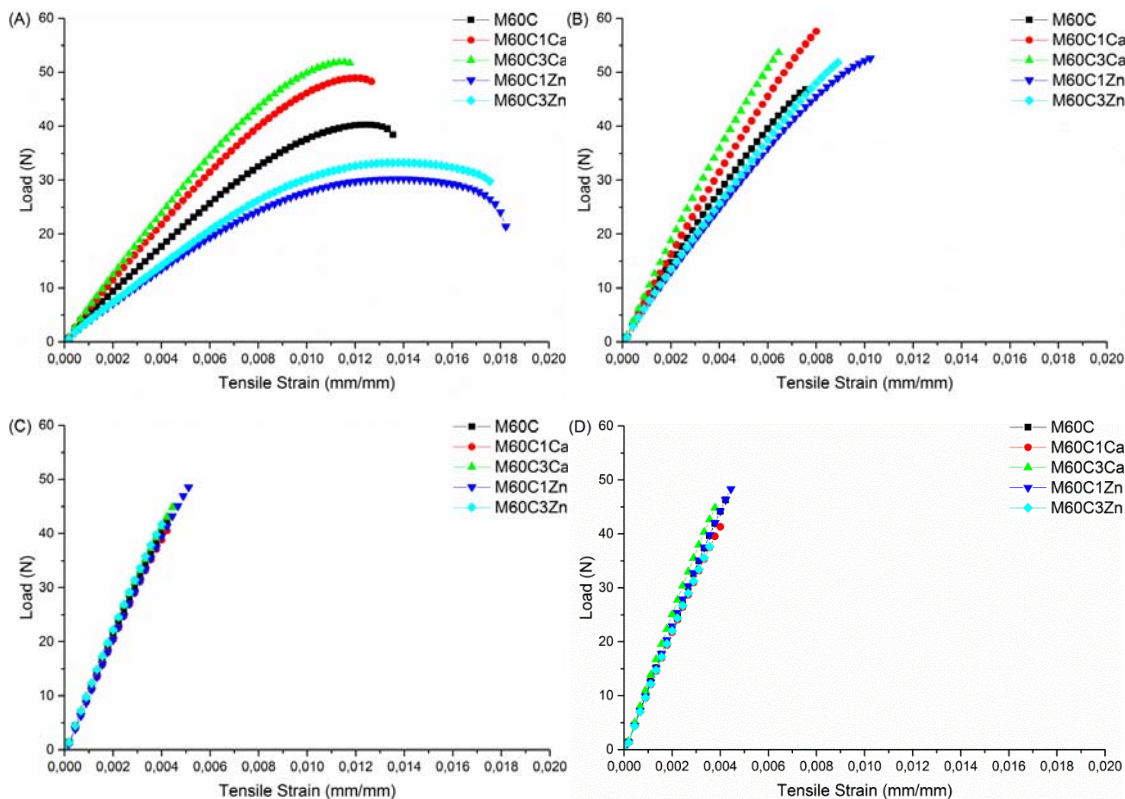


Figure 4.3 – Gel time of the system M60C with different ratios of CaO and ZnO under different isothermal conditions, 140 °C and 130 °C

#### 4.5.1.2 EFFECT OF CaO AND ZnO IN THE MECHANICAL PROPERTIES

The mechanical performance of the system M60C is improved by adding CaO. As representative examples, Figure 4.4 shows the stress-strain curves of glass paper impregnated with the different compositions in Table 4.1 and cured at 140 °C for different curing times, 1, 5, 15 and 30 min. In all the cases the material behaves as a stiff thermoset because it breaks, but the deformation is elastic [35, 36]. Flexible behavior is perceived when short curing time (i.e. 1 min) is applied. In this case the yield point is well-defined after elastic region and the material breaks in the plastic deformation. This flexible behavior is reduced when curing time is 5 min, and completely disappears after 15 min curing. The addition of CaO helps to make the material stiffer especially at shorter curing times (1 and 5 min). However the addition of ZnO makes the material to be even more flexible, particularly observed at shorter curing times (1 and 5 min). Deeper analysis on the mechanical characterization has been made based on the tensile strain and young's modulus data.



**Figure 4.4 – Stress-strain curves of glass paper impregnated with the compositions in Table 4.1, cured at 140 °C and different times, (A) 1 min, (B) 5 min, (C) 15 min and (D) 30 min**

The data on tensile strain at maximum load is shown in Figure 4.5. In general, the tensile strain decreases strongly when curing time increases, reaching a minimum plateau after 15 min curing. This might be a consequence of increasing crosslinking density [27, 37]. When CaO is added to the system containing MAL and CA, tensile strain is lower, particularly detected at short curing times and 3 % CaO ( $p < 0.05$ ). The effect is the opposite when ZnO is added; making the tensile strain to increase as more ZnO is added. This indicates that CaO contributes positively to the network rigidity, therefore to the stiff behavior of the material while ZnO contributes into the elastic behavior [38, 39].

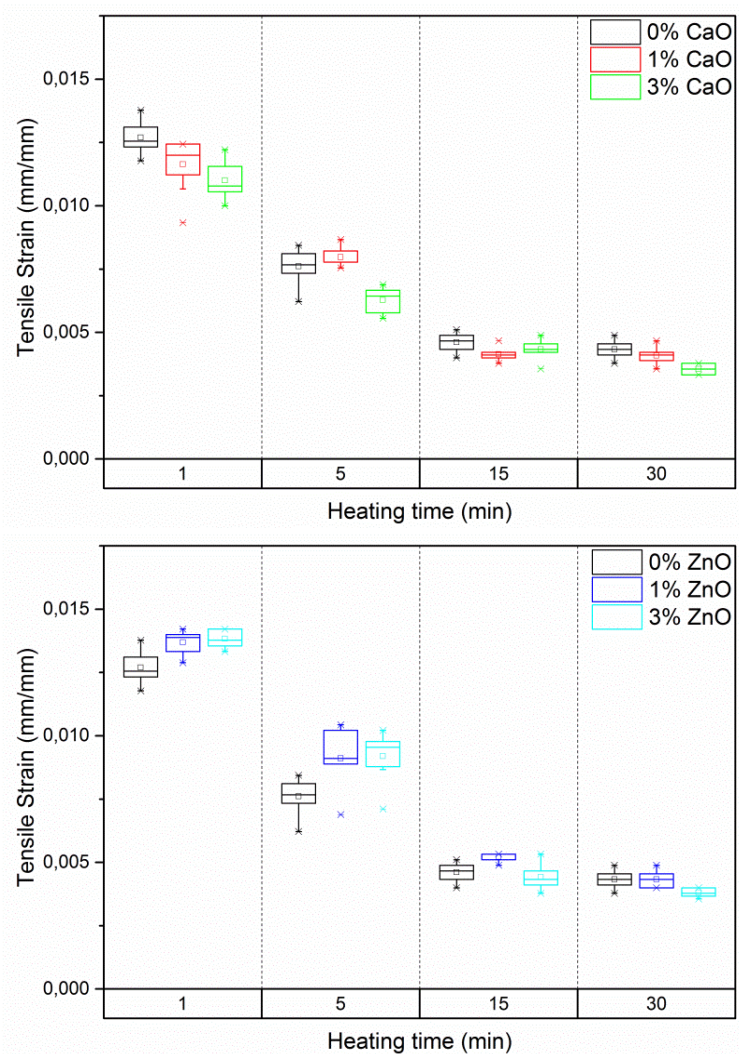


**Figure 4.5 – Tensile strain and its retention upon accelerated weathering conditions of glass paper impregnated with the compositions in Table 4.1 cured at 140 °C and different curing times (1, 5, 15 and 30 min)**

The stiffening effect of CaO on the crosslinking is also noticeable when evaluated upon accelerated weathering conditions. Figure 4.6 shows that the addition of CaO has a positive effect on the retention of the tensile strain to a different extent, depending on the amount of CaO and the curing time. For short curing (1 or 5 min) the effect is more remarkable, and even more in the system containing 1 % of CaO.

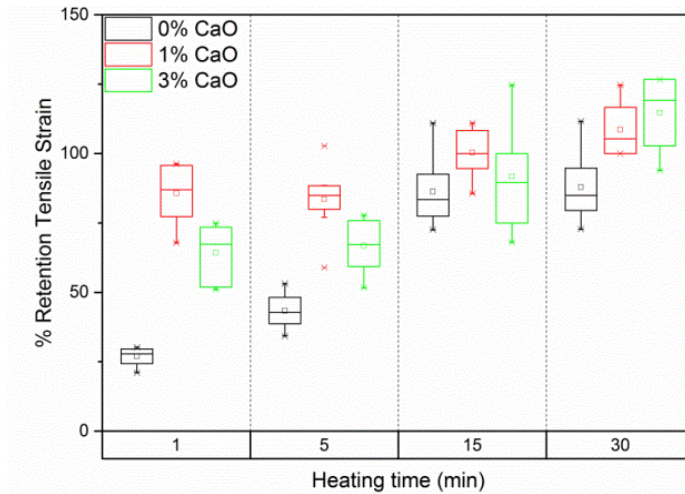


Figure 4.6 – Retention of tensile strain upon accelerated weathering conditions of glass paper impregnated with the systems M60C, M60C1Ca and M60C3Ca, cured at 140 °C and different curing times (1, 5, 15 and 30 min)

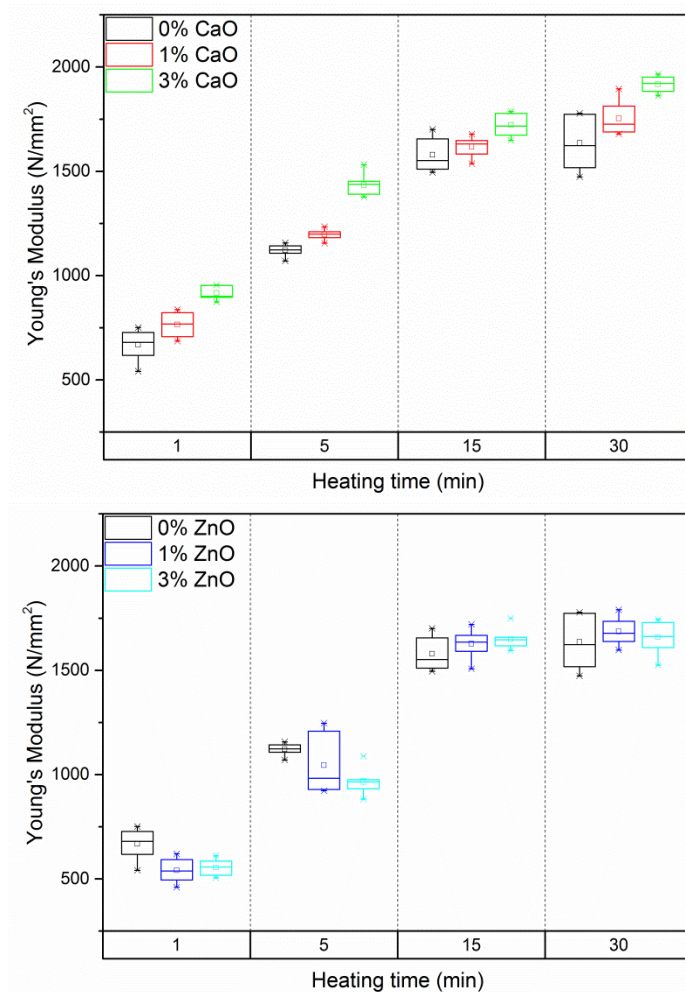
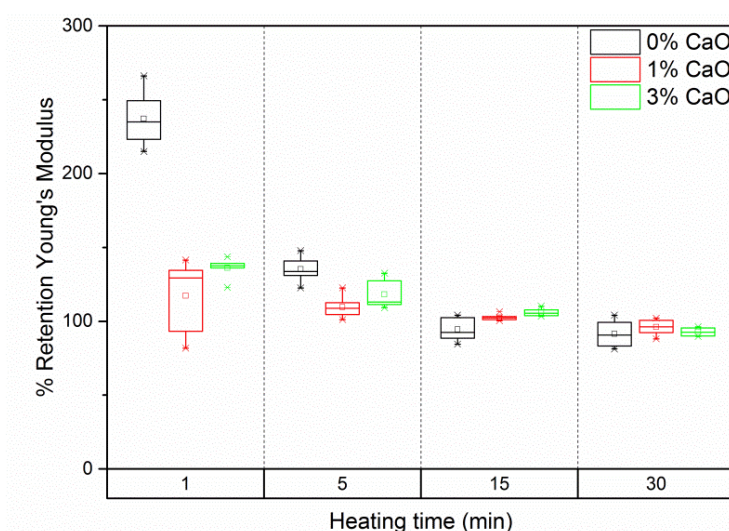


Figure 4.7 – Young's modulus of glass paper impregnated with the compositions in Table 4.1, cured at 140 °C and different times (1, 5, 15 and 30 min)

Figure 4.7 shows the data of young's modulus. In general, it can be observed that it increases with longer curing time. Further increase of the young's modulus is achieved when CaO is added. In the contrary, the addition of ZnO makes the young's modulus to decrease, particularly at short curing times. This means that CaO contributes to make a more rigid network while ZnO lead to a more elastic network [27, 40].

As it is shown in Figure 4.8, the retention of the young's modulus is around 100 % when CaO is added. When the system does not contain CaO the young's modulus is strongly modified particularly at short curing times (1 and 5 min), indicating not enough curing (i.e. crosslinking).



**Figure 4.8 – Retention of young's modulus upon accelerated weathering conditions of glass paper impregnated with the systems M60C, M60C1Ca and M60C3Ca, cured at 140 °C and different times (1, 5, 15 and 30 min)**

All the results point out that the addition of CaO boosts the stiffness of the cured system containing MAL and CA, especially at shorter curing times. Furthermore, CaO helps to preserve the mechanical properties upon weathering conditions.

The stronger contribution of CaO to the crosslinking formation and mechanical properties of the systems containing MAL and CA in comparison to ZnO can be explained by previous results in the literature. Both metal ions, Ca(II) and Zn(II) would be able to interact with CA [25, 26, 41]; however, the strength of interaction is different [42]. It is reported that Ca(II) ion has more affinity to the carboxyl groups of ionic polysaccharides than Zn ion, ionic bond being weaker in the later [10].

### 4.5.1.3 EFFECT OF CaO AND ZnO ANALYZED BY SEM/EDX

CaO or ZnO lead to Ca and Zn(II) ions respectively when dissolved in the system containing MAL and CA. The distribution of Ca and Zn(II) ions in the compositions after curing was studied by EDX. As representative examples, in Figure 4.9 are shown the SEM/EDX micrographs of films obtained after curing the compositions M60C3Ca and M60C3Zn. The corresponding SEM micrograph shows that the surface of the cured composition M60C3Zn is smoother than the surface of M60C3Ca. In EDX micrograph it can be observed that Ca and Zn(II) ions are homogeneously distributed all over the cured composition.

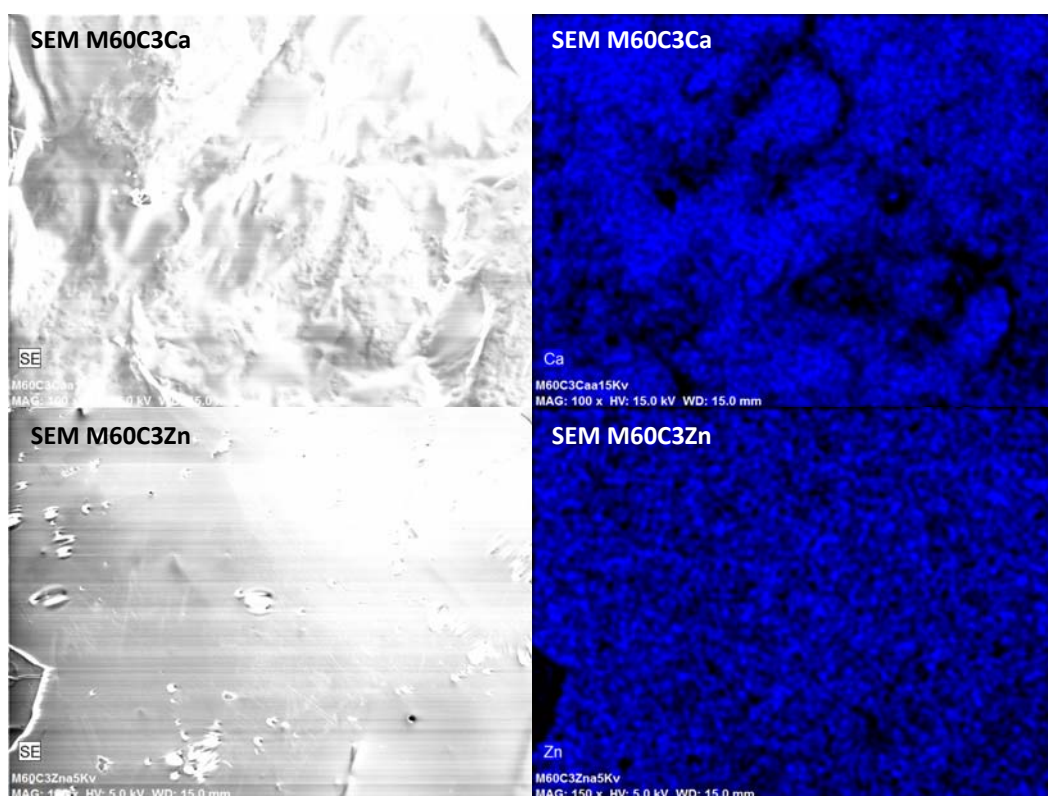


Figure 4.9 – SEM/EDX micrograph of the system M60C3Ca and M60C3Zn, cured at 140 °C for 4 hours

Scanning electron microscopy (SEM) micrographs of the glass-paper impregnated with the compositions in Table 4.1 used for the mechanical characterization are shown in Figure 4.10. The surface of the glass fiber paper is homogeneously impregnated independently of the composition. In the cross-section pictures it can be observed that the composition is partially covering the

fibers and gluing different fibers together. This indicates the good adhesion of the crosslinked system to the glass fibers.

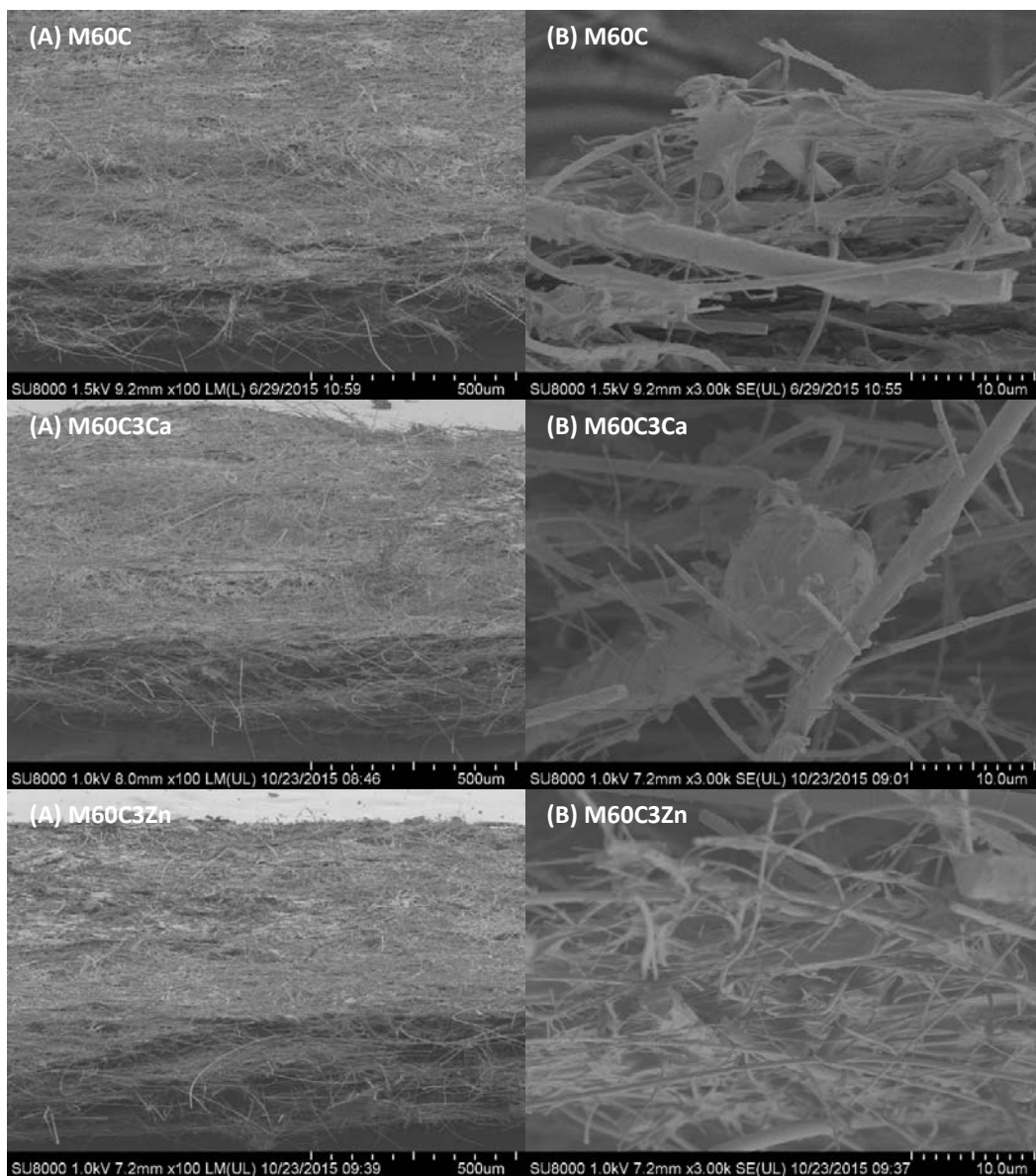


Figure 4.10 – SEM micrographs of glass paper impregnated with system M60C, M60C3Ca and M60C3Zn, cured 15 min, after tensile strength test, on the (A) surface and (B) cross-section fibers

## 4.5.2 CaO IN THE SYSTEM CONTAINING MAL AND TA

Based on results from Chapter III, the systems containing MAL and CA lead to better performance than the systems containing MAL and TA; in terms on reactivity, crosslinking and consequent mechanical properties. In order to check whether the performance of these last could be improved by the addition of ions, the effect of CaO was also studied for the systems containing MAL and TA.

### 4.5.2.1 EFFECT OF CaO IN THE CROSSLINKING

In Figure 4.11 is shown the evolution of  $G'$  and  $G''$  against time under isothermal treatment at 140 °C for the compositions quoted in Table 4.2. The maximum value of  $G'$ , around 10 MPa, is faster achieved when CaO is added in the system containing MAL and TA but the maximum value of  $G''$  achieved when CaO is added is lower. This could lead to a different mechanical behavior of the crosslinked system.

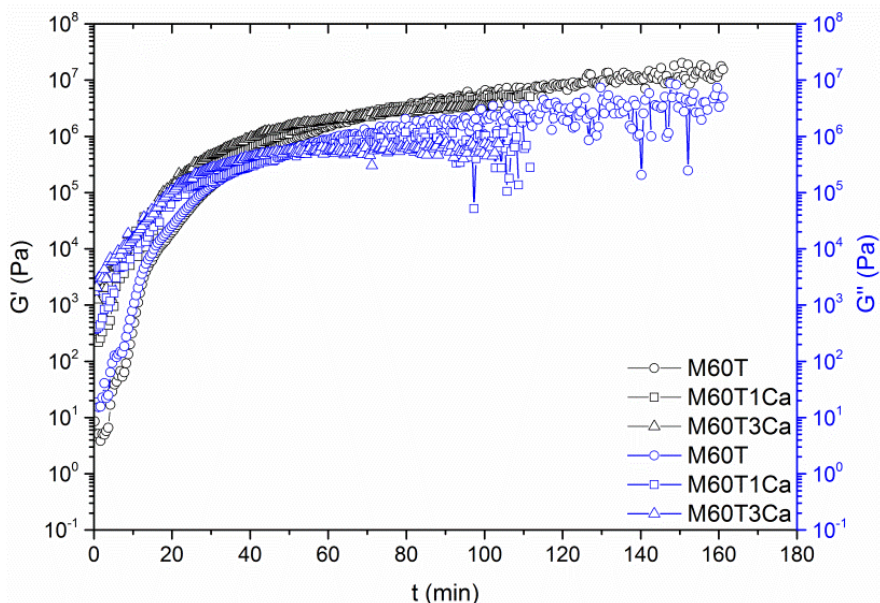
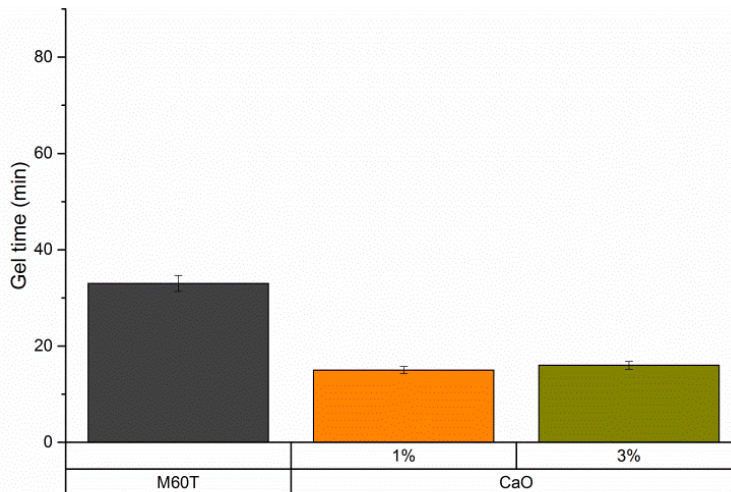


Figure 4.11 – Log  $G'$  and log  $G''$  against time upon isothermal treatment at 140 °C for the compositions in Table 4.2

The effect of CaO on the gel time is shown in Figure 4.12. When CaO is added the gel time is approximately 50 % reduced. Comparing the addition of 1 % of CaO with 3 % it can be observed that the minimum gel time is already achieved with 1 % of CaO.





**Figure 4.12 – Gel time of the compositions in Table 4.2 under isothermal treatment at 140 °C**

Based on these results the addition of CaO promotes the crosslinking formation in the system containing MAL and TA.

#### *4.5.2.2 EFFECT OF CaO IN THE MECHANICAL PROPERTIES*

Figure 4.13 shows the tensile strain curves of the glass paper impregnated with the different compositions in Table 4.2 and cured at 140 °C for different times (1, 5, 15 and 30 min). The material shows flexible behavior when it is cured for 1 min [27]. The addition of CaO in this case could even promote the elastic behavior. The elastic behavior is disappearing when the material is cured for 5 min. Then it shows a stiff behavior because it breaks, but with elastic deformation [27]. The addition of 3 % of CaO in this case promotes the stiffness of the material. The contribution of CaO on the stiffness is also perceived when curing for 15 and 30 min. Nevertheless there is no correlation between the ratio of CaO added and the mechanical behavior of the network.

The tensile strain and young's modulus of the stiff material (i.e. 5 min curing or higher) is shown in Figure 4.14 and Figure 4.15 respectively. Tensile strain for the glass paper cured for 5 min is increased when adding 1 % of CaO, but it is reduced when 3 %. The young's modulus evolves in the opposite direction, it decreases when 1 % of CaO is added, but it increases with 3 % of CaO. This indicates a stiffening effect of CaO at 3 %; which is less relevant when the system is cured 15 min or longer.

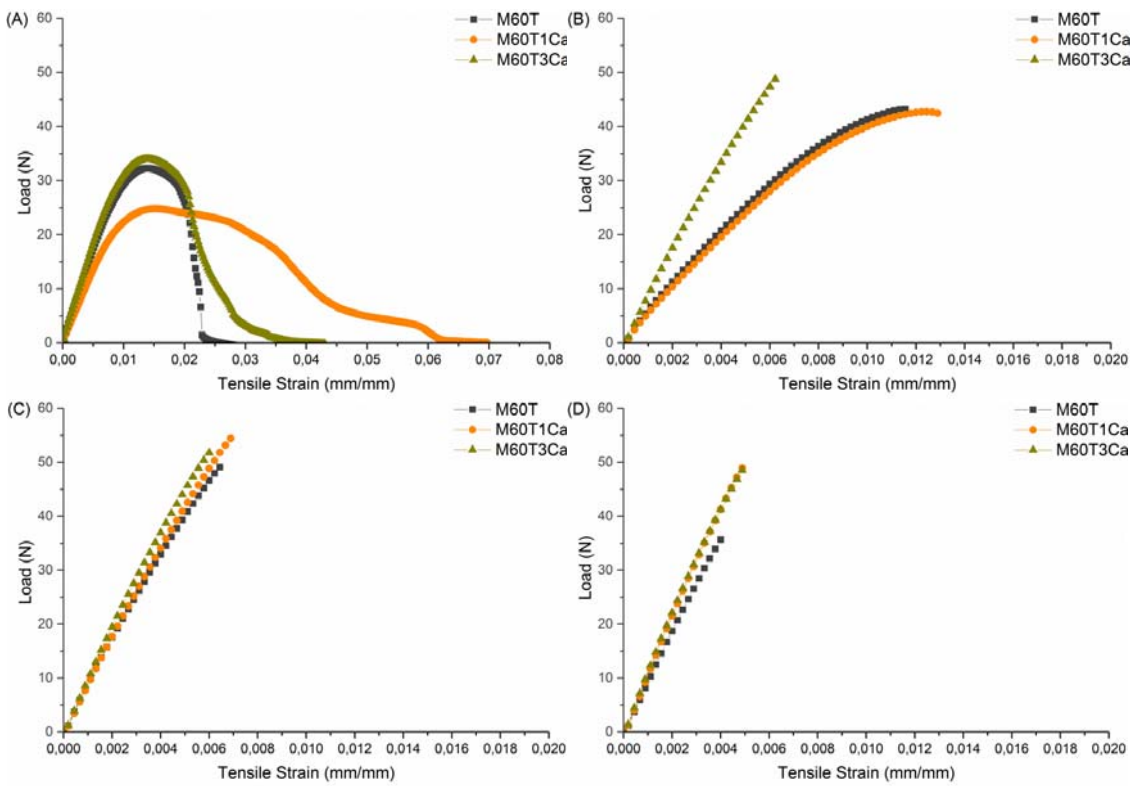


Figure 4.13 – Stress-strain curves of glass paper impregnated with the compositions in Table 4.2, cured at 140 °C and different times, (A) 1 min, (B) 5 min, (C) 15 min and (D) 30 min

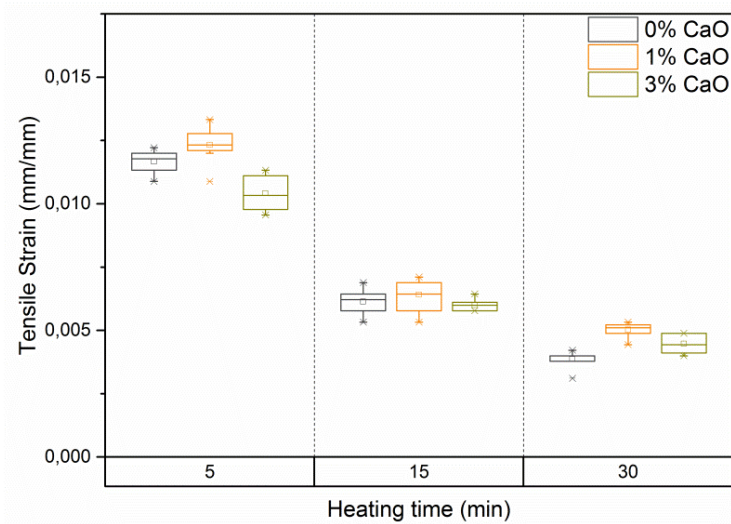


Figure 4.14 – Tensile strain of glass paper impregnated with the compositions in Table 4.2, cured at 140 °C and different times (5, 15 and 30 min)

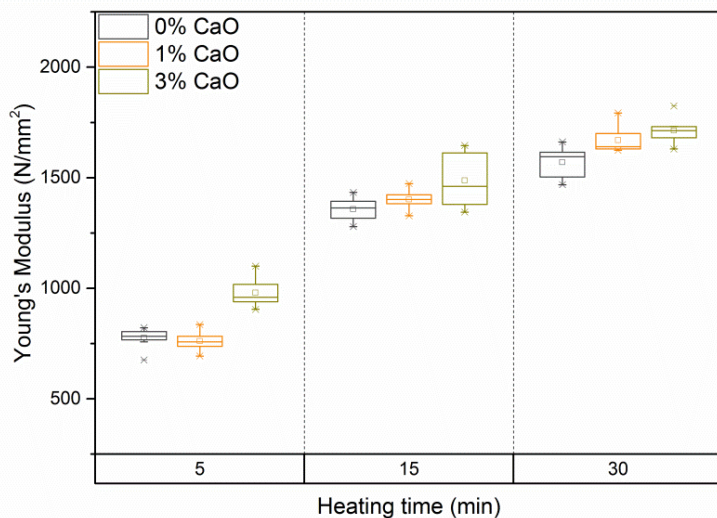


Figure 4.15 –Young’s modulus of glass paper impregnated with the compositions in Table 4.2, cured at 140 °C and different times (5, 15 and 30 min)

#### 4.5.2.3 EFFECT OF CaO ANALYZED BY SEM/EDX

The distribution of Ca(II) ion once the composition was cured has been analyzed by EDX micrographs, shown in Figure 4.16. It can be observed that Ca(II) ions are significantly concentrated in some parts of the surface of cured composition, and not homogeneously distributed. In the corresponding SEM micrograph some cracks are observed in those areas where the Ca(II) ions are allocated. This may explain that there is no perfect correlation of mechanical properties against content of CaO, although slight positive effect could be found with 3 % addition of CaO.

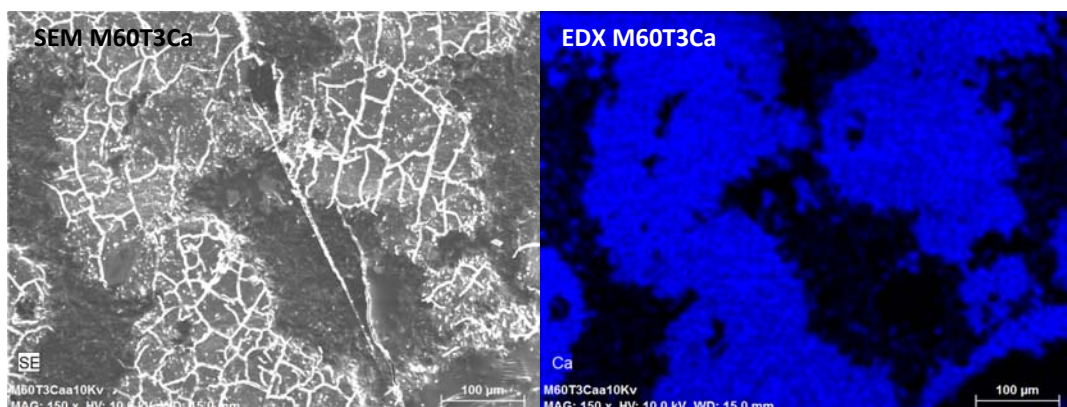
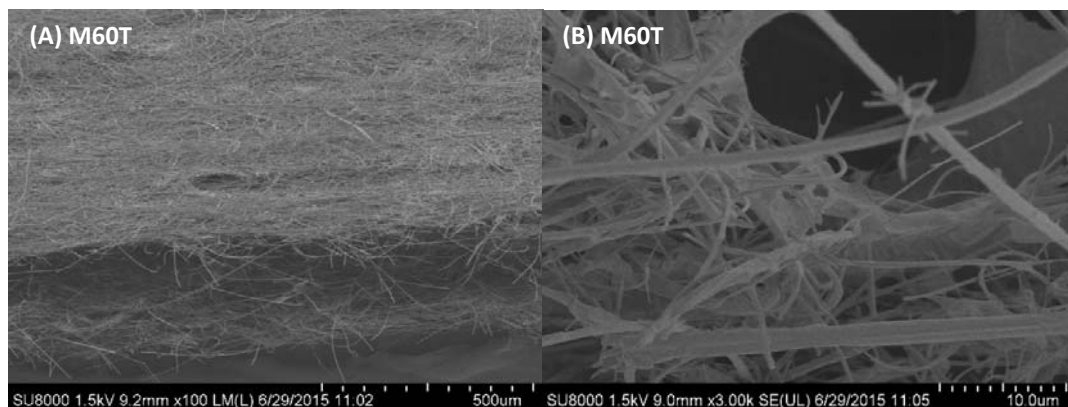
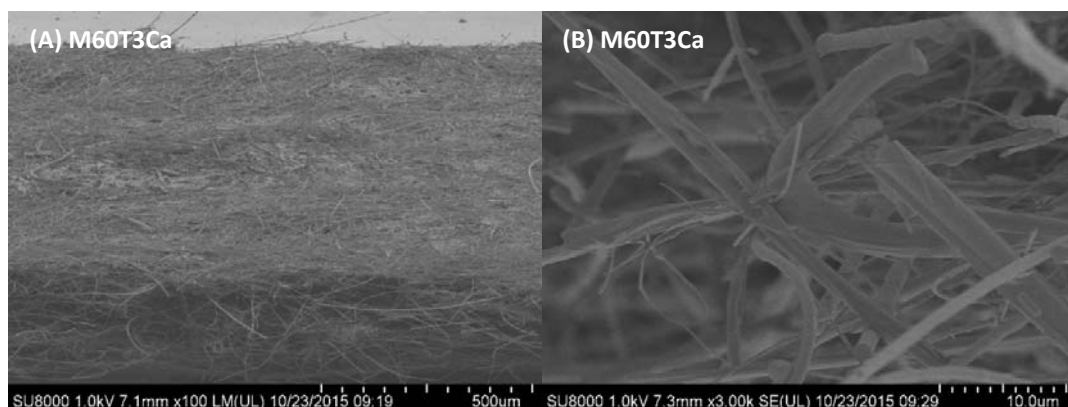


Figure 4.16 – SEM/EDX micrograph of the composition M60T3Ca after curing at 140 °C for 4 hours

Scanning electron microscopy (SEM) micrographs of the glass-paper impregnated with the compositions in Table 4.2 used for the mechanical characterization are shown in Figure 4.17 and Figure 4.18. The glass fiber paper sheet is homogeneously impregnated independently of the composition. In the cross-section pictures it can be observed that the composition is partially covering the fibers and gluing different fibers together. This indicates the good adhesion of the crosslinked system to the glass fibers.



**Figure 4.17 – SEM micrographs of glass paper impregnated with composition M60T cured for 15 min, after tensile strength test on the (A) surface and (B) cross-section**



**Figure 4.18 – SEM micrographs of glass paper impregnated with composition M60T3Ca cured for 15 min, after tensile strength test on the (A) surface and (B) cross-section**

The addition of Ca(II) ions in the system containing MAL and TA improves the mechanical properties under some curing conditions, although not as remarkable as in the case of the systems containing MAL and CA. As mentioned in the introduction of this work, Ca(II) ion has the ability to interact with both carboxylic acids; but the number of carboxyl groups available to interact makes a difference: CA could interact by means of three carboxyl groups while TA has only two available, in either case depending on the pH (Figure 4.19 shows the concentration of

species of TA in equilibrium against the pH). This would explain the weaker contribution of Ca(II) ion to the crosslinking and mechanical performance of the systems containing MAL and TA [26, 43].

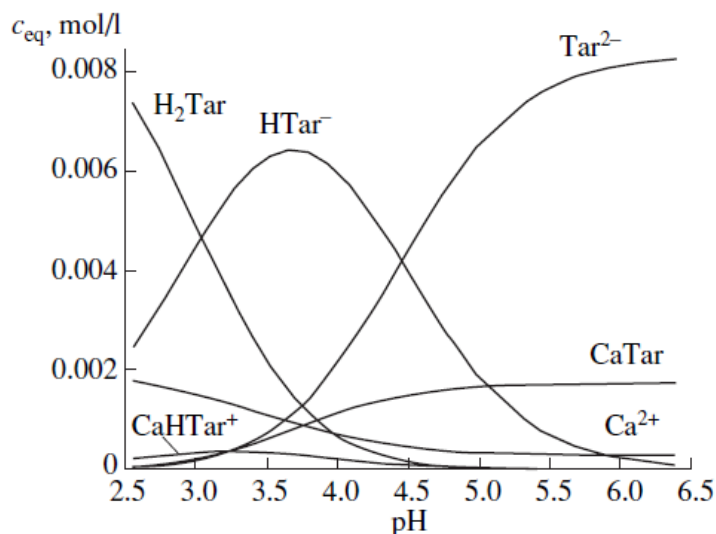


Figure 4.19 – Equilibrium Ca-TA interactions [43]

### 4.5.3 STUDY ON THE INTERACTIONS OF Ca(II) ION WITH CA

#### 4.5.3.1 INFRARED STUDY

According to previous work (Chapter II and III) the evolution of the polycondensation reaction between MAL and CA can be followed by IR. The C=O stretching band assigned to the ester bond between the hydroxyl groups of MAL and the carboxyl group of CA, and the OH stretching band evolve as the esterification reaction is progressing. In Figure 4.20, Figure 4.21 and Figure 4.22 are shown the IR spectra of the different systems containing MAL and CA, and with Ca(II), after curing treatment for different periods of time at 140 °C. The C=O stretching band evolves similarly in all the compositions. The OH band moves to different wave numbers when CaO is added to the composition M60C. This may be assigned to the different evolution of the hydrogen bond interactions of the MAL and CA with the Ca(II) ion present in the media [14, 18, 20]. Furthermore, new bands in the range of 1630-1637 and 1546-1547  $\text{cm}^{-1}$  can be identified in the system containing 3 % of CaO (M60C3Ca). These bands have been further investigated.

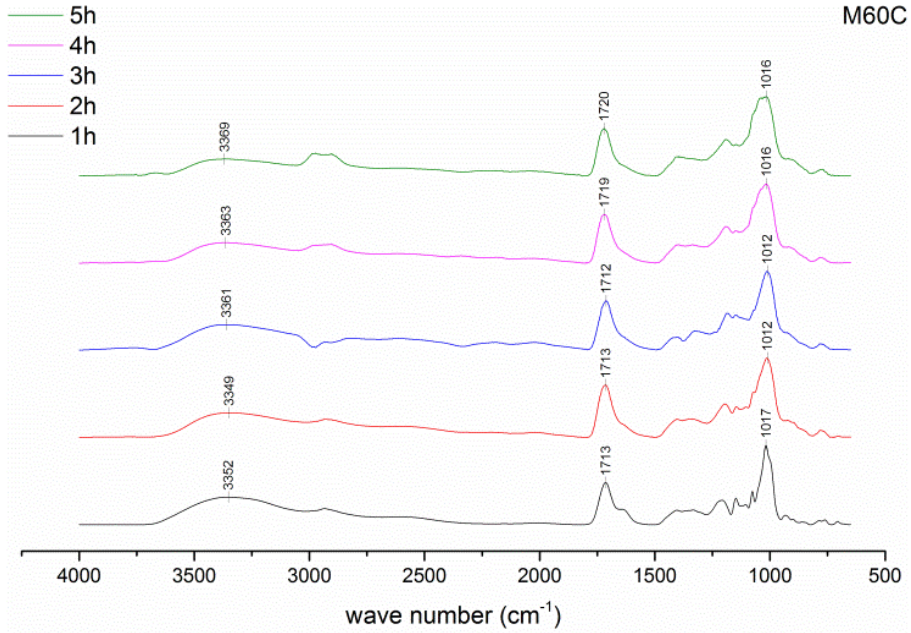


Figure 4.20 – IR spectra of the composition M60C upon thermal treatment at 140 °C for different times

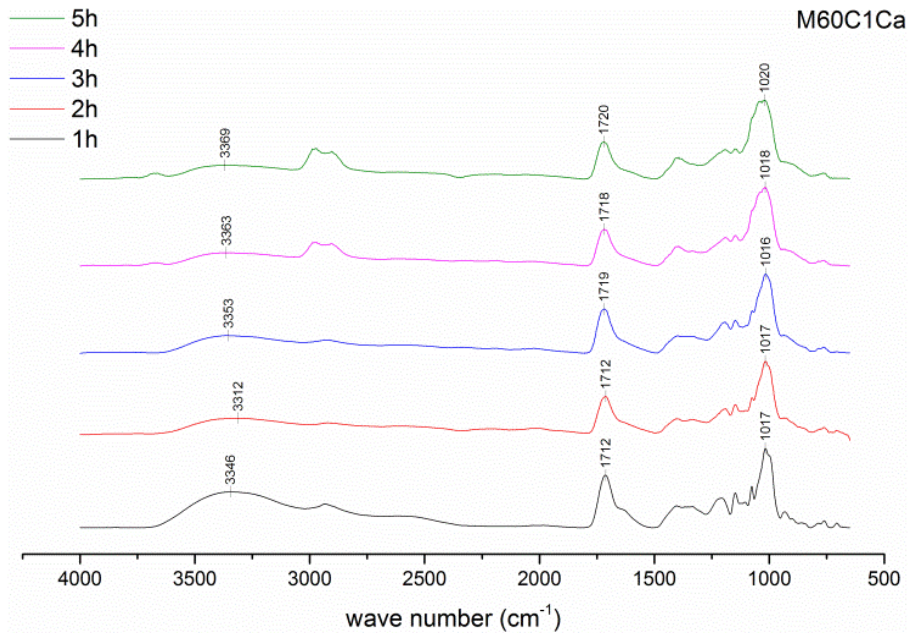
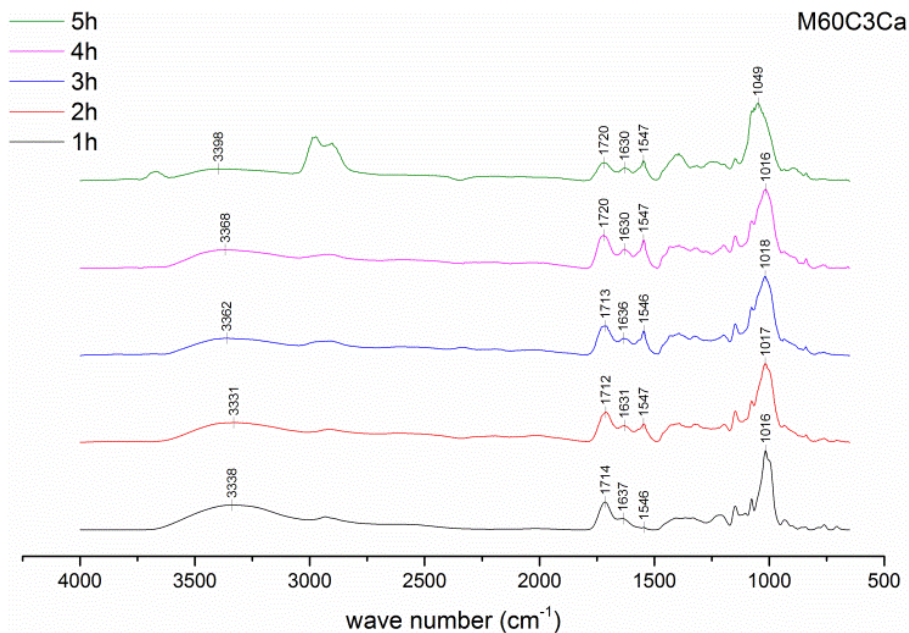


Figure 4.21 – IR spectra of the composition M60C1Ca upon thermal treatment at 140 °C for different times



**Figure 4.22 – IR spectra of the composition M60C3Ca upon thermal treatment at 140 °C for different times**

As representative example, in Figure 4.23 can be observed the C=O stretching band assigned to the ester bond at 1721-1728  $\text{cm}^{-1}$ , after 4 hours thermal treatment at 140 °C and later purification, for the compositions M60C, M60C1Ca and M60C3Ca. This result proves that the esterification reaction between the hydroxyl groups of MAL and the carboxyl groups of CA takes place independently of adding CaO.

Quantitative comparison of the intensity of C=O stretching band due to ester bond for the different compositions containing CA is shown in Figure 4.24. The intensity of the band decrease when CaO is added to the system containing MAL and CA (M60C). This may be consequence of the ionic interactions between the Ca(II) ions and the carboxyl groups of CA not involved in the ester formation with MAL [26, 44].

Apart from the C=O stretching band, a new band at 1590  $\text{cm}^{-1}$  assigned to a carboxylate [41] can be clearly identified for the composition in the composition containing 3 % of CaO. This band may be assigned to the interaction of carboxyl groups of CA with Ca(II) ion, still remaining after purification. To further understand the interactions leading to these results, mixtures without MAL were studied.

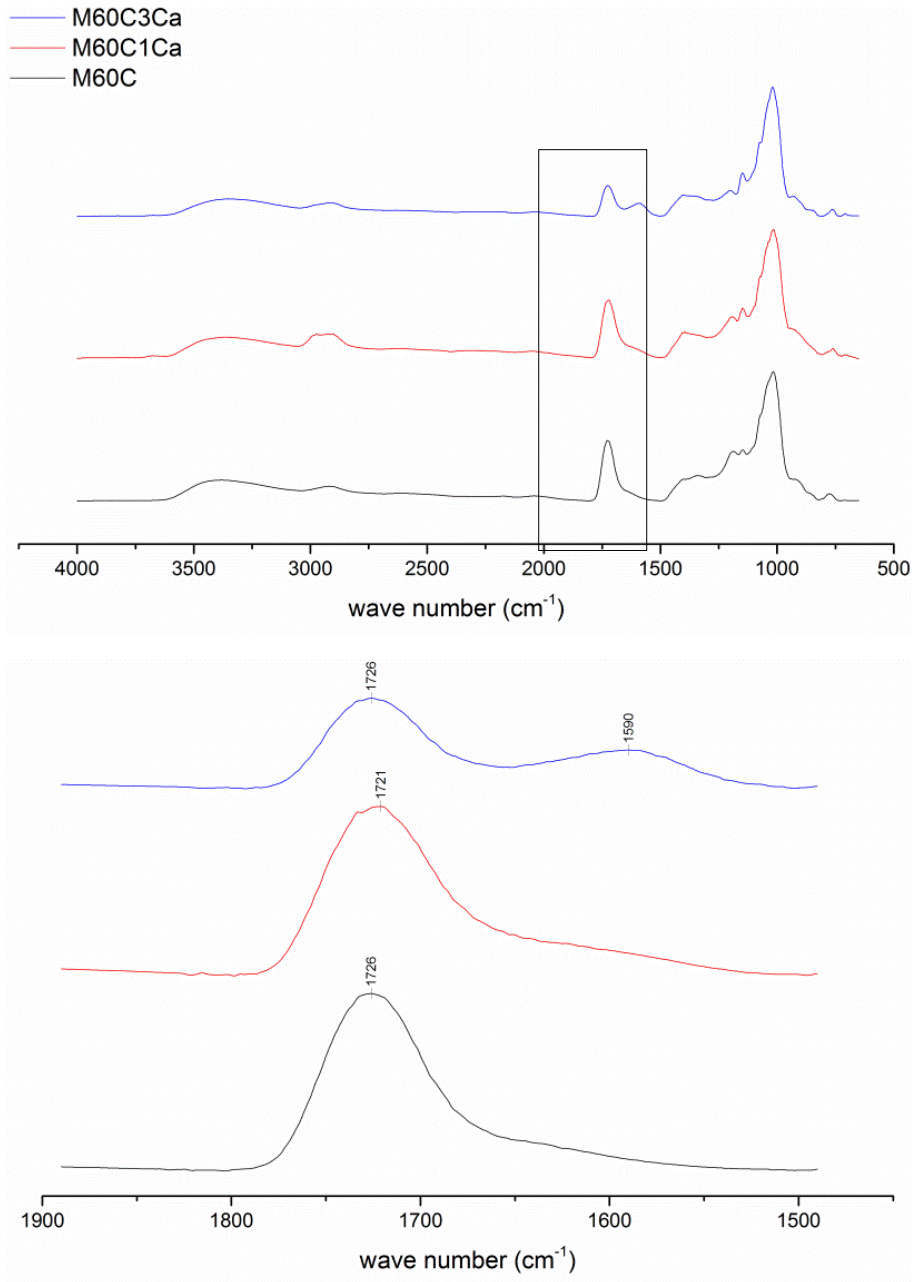
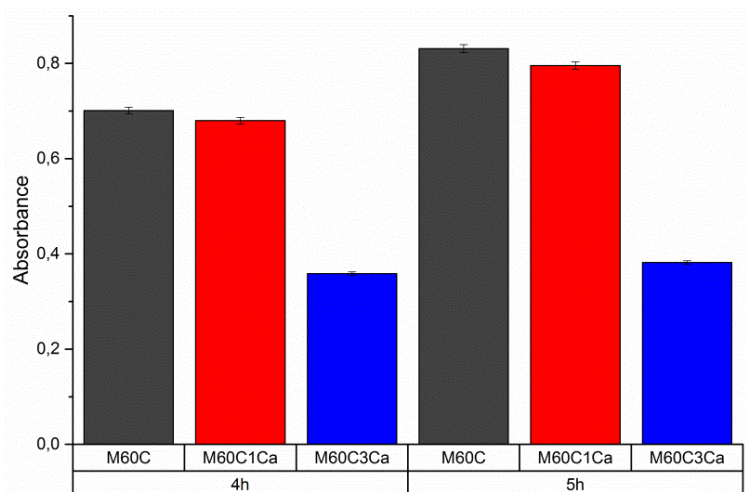


Figure 4.23 – IR spectra of the binder systems M60C, M60C1Ca and M60C3Ca after 4 hours thermal treatment at 140 °C and later purification





**Figure 4.24 – Intensity of C=O stretching band due to ester bond in the compositions M60C, M60C1Ca and M60C3Ca after 4 hours curing at 140 °C and later purification**

In Figure 4.25, the spectra of the systems containing MAL and CA with CaO are compared with the mixtures containing only CA and CaO, both after 4 hours thermal treatment. It can be observed that the bands at around 1550 and 1630  $\text{cm}^{-1}$  identified in the spectra of the cured mixtures containing only CA and Ca(II) can be also identified in the spectra of the composition M60C3Ca. These bands are assigned to antisymmetric stretching vibrations of the carboxylate groups [41]. This proves that the interactions between CA and Ca(II) can take place in those systems containing MAL, CA and Ca(II) leading, for instance, to the formation of complexes CA-Ca [45, 46].

The IR study demonstrates the existence of ionic interactions between Ca(II) ion and CA, which are resistant to water. These ionic interactions seem to compete with the esterification between MAL and CA; however, in the final cured systems the contribution of ionic interactions overcomes the lack of covalent bonds, leading to a net improvement of the mechanical performance. The resistance to water of the additional crosslinking generated by ionic interactions might be explained by an embedded effect (i.e. protection) of the polycondensate network formed by the reaction between the hydroxyl groups of MAL and the carboxyl groups of CA. Altogether would lead to a synergetic effect of the two types of crosslinking, covalent and ionic.

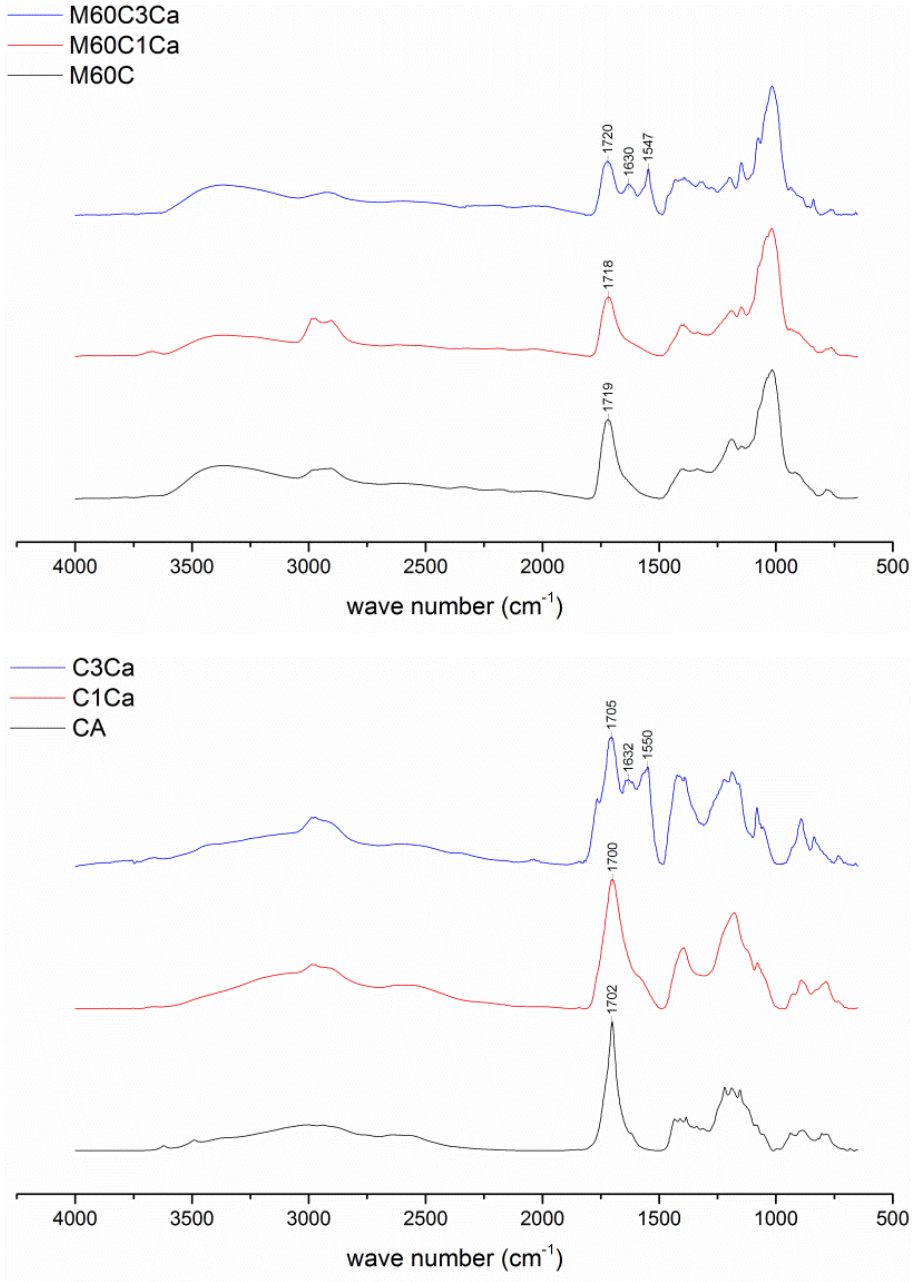


Figure 4.25 – IR spectra of the compositions in Table 1 and the cured mixtures containing CA and Ca after 4 hours thermal treatment at 140 °C

### 4.5.3.2 TGA STUDY

The esterification reaction between carboxyl groups of CA and hydroxyl groups of MAL has been analyzed by TGA according to the methodology described in previous chapters. In Figure 4.26 are compared the TGA and corresponding derivative for the compositions containing MAL and CA, and Ca(II).

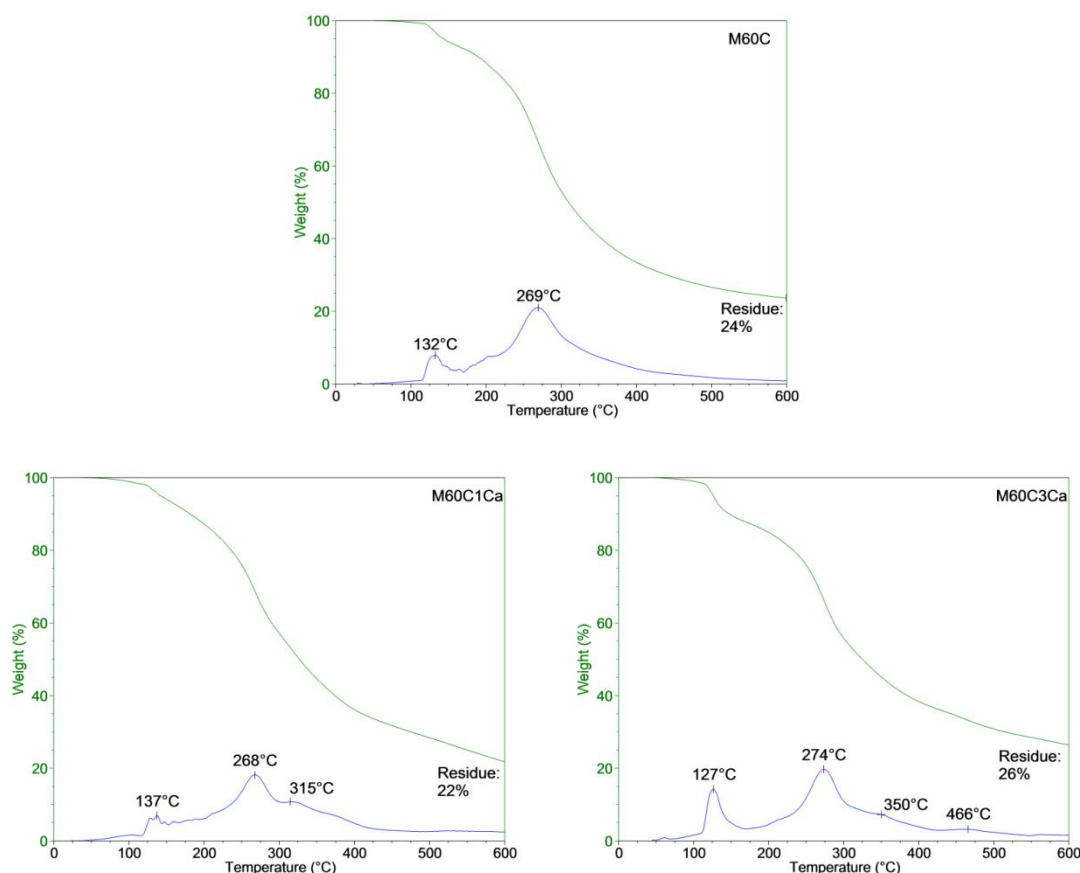


Figure 4.26 – TGA and its first derivative for the compositions M60C, M60C1Ca and M60C3Ca

The weight loss due to the water released by the esterification reaction around 130 °C can be identified in all the compositions [47]. The second weight loss step at around 270 °C, related to decomposition of esterification derivatives can be also identified in all the compositions. Still, a third weight loss step is found at 315 °C and 350 °C for the compositions M60C1Ca and M60C3Ca respectively, which is assigned to the decomposition of the polycondensation derivatives. And even a fourth weight loss at 466 °C can be detected for the composition M60C3Ca, which is due to the decomposition of compounds result of the interaction of CA with Ca(II) ion. The assignment

of this weight loss has been proved by the analysis of the mixtures containing only CA and CaO quoted in Table 4.3.

In Figure 4.27 is shown the TGA and corresponding derivative curve for the mixtures containing only CA and CaO. In the mixture C3Ca several weight loss steps are identified which most of them are related to the decomposition of calcium citrate tetrahydrated as reported previously by Seham A.A. Mansour [48]; result of the complexes formation between CA and Ca(II) ion. These weight loss steps are: the first one at 86 °C assigned to the water retained by the calcium citrate; the one at 487 °C assigned to the formation of calcium carbonate and corresponding water released; and the one at 654-686 °C due to the formation of CaO and corresponding water and CO released. The additional weight loss steps at 182-184 °C and 231-233 °C appear in both mixtures, C1Ca and C3Ca; however the relation between their decomposition rates is different depending on the percentage of CaO in the mixture. This suggests that the compounds related to these decompositions are due to the interaction of CA with Ca(II); maybe not generating complexes which lead to calcium citrate tetrahydrate, but just interacting, for instance, one single carboxyl group of CA with Ca(II) ion.

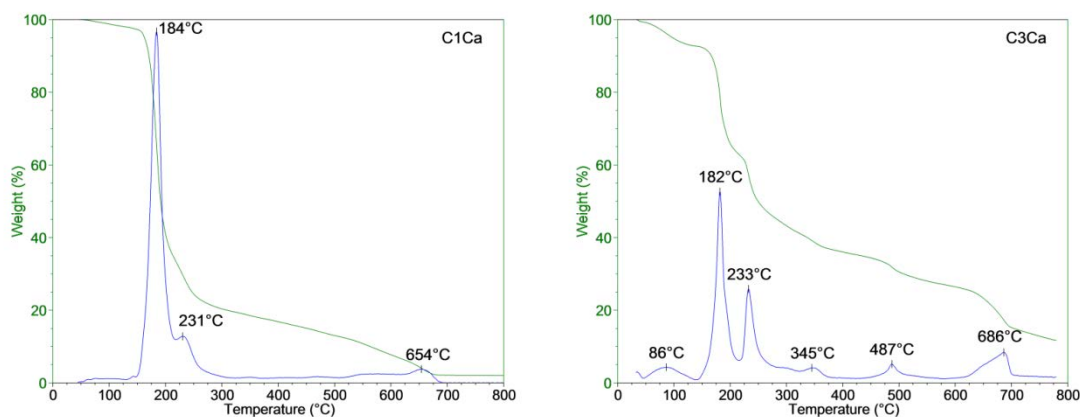


Figure 4.27 – TGA and its first derivative for the mixtures C1Ca and C3Ca

Based on the IR and TGA results it is proposed that the crosslinking enhancement of the system containing MAL and CA by the addition of CaO is due to the Ca(II) ion interacting in different ways with CA and MAL-CA polycondensates. According to the chelation activity of CA reported by Welling et al. (Figure 4.28), a portion of Ca(II) ions would form  $\text{Ca-Cit}^{3-}$  complexes which later become calcium citrate tetrahydrated [26, 44]. The rest of Ca would interact with CA

in the form of  $\text{HCit}^{2-}$  and  $\text{H}_2\text{Cit}^-$ . The formation of these complexes would contribute not directly to the polymer network but as reinforcement [32].

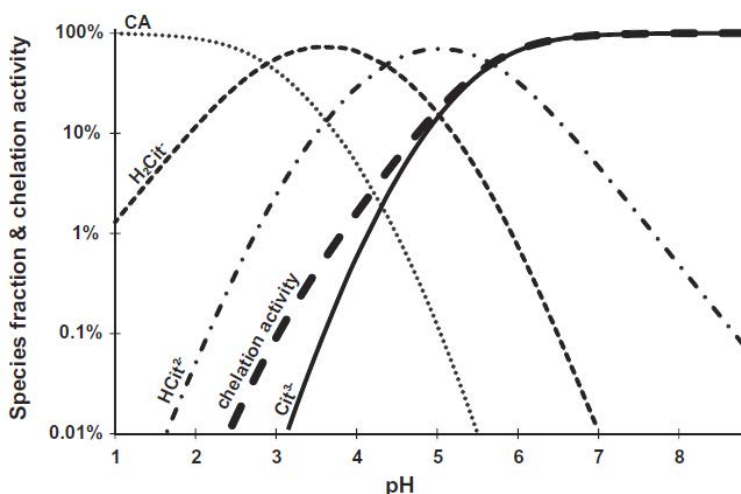
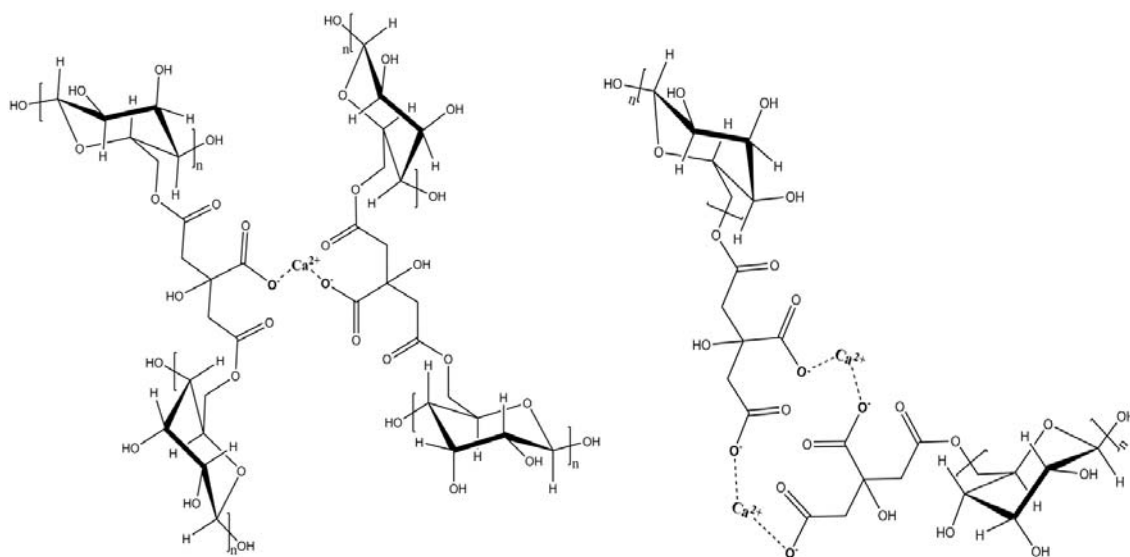


Figure 4.28 – Relationship between each form of CA ( $\text{H}_2\text{Cit}^-$ ,  $\text{HCit}^{2-}$ ,  $\text{Cit}^{3-}$ ) and their calcium chelation activity [44]

Furthermore, although it was not possible to prove, it is proposed that, as shown in Scheme 4.2, other interactions of  $\text{Ca}(\text{II})$  takes place with the free carboxyl groups of CA molecules with are attached to MAL chains by the other carboxyl group. These kind of interactions have been described for some natural ionic polysaccharides like alginate and pectin [28, 49]. In this way  $\text{Ca}(\text{II})$  ions would contribute directly to the polymer network by additional crosslinking formation.



Scheme 4.2 – Possible interactions of  $\text{Ca}$  ions with CA attached to MAL chains

## 4.6 CONCLUSIONS

---

The addition of metal oxides to the systems containing maltodextrin and polycarboxylic acids modifies the crosslinking rate and the mechanical properties of crosslinked system, depending on the metal oxide and polycarboxylic acid. In the system containing citric acid, both, CaO and ZnO, accelerate the crosslinking. Remarkably, the crosslinking reaction in the system containing maltodextrin and citric acid could be carried out at 10 °C lower when Ca(II) ion is in the media. Moreover CaO contributes to stiffness in the final material whereas ZnO does the opposite. This behavior has been explained by the different interaction mechanism of Ca(II) ion compared to Zn(II) ion with polycarboxylic acids. The improvement of the mechanical properties by addition of CaO is even clearly perceived upon weathering conditions. Furthermore, the addition of CaO promotes the crosslinking of the system containing maltodextrin and tartaric acid. Nevertheless, it does not increase significantly the stiffness of the crosslinked system. Altogether suggests that CaO is the most suitable candidate to improve the mechanical performance of binders based on maltodextrin and citric acid.

From the other side, it has been demonstrated the existence of interactions between citric acid and Ca(II) ion. These interactions would be the reason for the enhancement of the crosslinking formation. Based on the results obtained, a mechanism of interaction of Ca(II) ion with citric acid has been proposed. The interactions between both would take place not only with single citric acid molecules but also with the citric moieties of the polycondensate derivatives from maltodextrin and citric acid. This would help to the reinforcement of the original polymer network formed between maltodextrin and citric acid.

## 4.7 REFERENCES

---

1. Goodman SH. 1 - Introduction. Handbook of Thermoset Plastics (Second Edition). Westwood, NJ: William Andrew Publishing, 1999. pp. 1-22.
2. Hernández-Ortiz JC and Vivaldo-Lima E. Crosslinking. Handbook of Polymer Synthesis, Characterization, and Processing: John Wiley & Sons, Inc., 2013. pp. 187-204.
3. Hawkins CM, Hernandez-Torres JM, and Chen L. Bio-based binders for insulation and non-woven mats. Google Patents, 2014.

4. Jaffrennou B and Obert E. Sizing composition for mineral wool based on maltitol and insulating products obtained. Google Patents, 2015.
5. Jaffrennou B, Serughetti D, and Douce J. Mineral wool sizing composition comprising a monosaccharide and/or a polysaccharide and an organic polycarboxylic acid, and insulating products obtained. Google Patents, 2009.
6. Kim H-S and Kim H-J. *Polymer Degradation and Stability* 2008;93(8):1544-1553.
7. Bhattacharya A and Ray P. *Basic Features and Techniques. Polymer Grafting and Crosslinking: John Wiley & Sons, Inc., 2008. pp. 7-64.*
8. J. Brandrup EHI, E.A. Grulke. *Polymer Handbook*, 4 ed. New York: John Wiley & Sons, Ltd., 2003.
9. Akihiro Abe KDe, Shiro Kobayashi. *Crosslinking in Materials Science*, 1 ed.: Springer Berlin Heidelberg, 2005.
10. Liling G, Di Z, Jiachao X, Xin G, Xiaoting F, and Qing Z. *Carbohydrate Polymers* 2016;136:259-265.
11. Xu ZJ, Tian YL, Liu HL, and Du ZQ. *Applied Surface Science* 2015;324:68-75.
12. Hashem M, Elshakankery MH, El-Aziz SMA, Fouda MMG, and Fahmy HM. *Carbohydrate Polymers* 2011;86(4):1692-1698.
13. Harifi T and Montazer M. *Carbohydrate Polymers* 2012;88(4):1125-1140.
14. Ciesielski W, Lii C-y, Yen M-T, and Tomasik P. *Carbohydrate Polymers* 2003;51(1):47-56.
15. Baran W, Sikora M, Tomasik P, and Anderegg JW. *Carbohydrate Polymers* 1997;32(3-4):209-212.
16. Tyrlik SK, Tomasik P, Anderegg JW, Baczkowicz Mx, and Igorzata. *Carbohydrate Polymers* 1997;34(1-2):1-7.
17. Tomasik P, Schilling C, Anderegg J, and Refvik M. *Carbohydrate Polymers* 2000;41(1):61-68.
18. Bączkowicz M, Wójtowicz D, Anderegg JW, Schilling CH, and Tomasik P. *Carbohydrate Polymers* 2003;52(3):263-268.
19. Ciesielski W and Tomasik P. *Journal of Inorganic Biochemistry* 2004;98(12):2039-2051.
20. Tomasik P, Anderegg J, and Schilling C. *Molecules* 2004;9(7):583.
21. Gustafson RL and Lirio JA. *The Journal of Physical Chemistry* 1968;72(5):1502-1505.
22. Czech Z and Wojciechowicz M. *European Polymer Journal* 2006;42(9):2153-2160.
23. Hu H, Saniger J, Garcia-Alejandre J, and Castaño VM. *Materials Letters* 1991;12(4):281-285.
24. Kriwet B and Kissel T. *International Journal of Pharmaceutics* 1996;127(2):135-145.
25. Bertoli AC, Carvalho R, Freitas MP, Ramalho TC, Mancini DT, Oliveira MC, de Varennes A, and Dias A. *Inorganica Chimica Acta* 2015;425:164-168.

26. Karar A, Naamoune F, and Kahoul A. *Desalination and Water Treatment* 2015;1-10.
27. Ventruti G, Scordari F, Bellatreccia F, Della Ventura G, and Sodo A. *Acta Crystallogr B Struct Sci Cryst Eng Mater* 2015;71(Pt 1):68-73.
28. Silva MAd, Bierhalz ACK, and Kieckbusch TG. *Carbohydrate Polymers* 2009;77(4):736-742.
29. Höpfner W. *Materials and Corrosion* 1996;47(1):53-54.
30. Kołodziejczak-Radzimska A and Jesionowski T. *Materials* 2014;7(4):2833.
31. Mussatti FG and Macosko CW. *Rheologica Acta* 1973;12(2):189-193.
32. Jin-Tae K, Martin D, Halley P, and Dae Su K. *Composite Interfaces* 2007;14(5/6):449-465.
33. Tung C-YM and Dynes PJ. *Journal of Applied Polymer Science* 1982;27(2):569-574.
34. Martin JS, Laza JM, Morrás ML, Rodríguez M, and León LM. *Polymer* 2000;41(11):4203-4211.
35. Pan X, Sengupta P, and Webster DC. *Biomacromolecules* 2011;12(6):2416-2428.
36. Buchdahl R. *Journal of Polymer Science: Polymer Letters Edition* 1975;13(2):120-121.
37. Ma Q, Liu X, Zhang R, Zhu J, and Jiang Y. *Green Chemistry* 2013;15(5):1300-1310.
38. Wu G-m, Chen J, Huo S-p, Liu G-f, and Kong Z-w. *Carbohydrate Polymers* 2014;105:207-213.
39. Ma S, Liu X, Jiang Y, Tang Z, Zhang C, and Zhu J. *Green Chemistry* 2013;15(1):245-254.
40. Cheng Q, Jiang L, and Tang Z. *Accounts of Chemical Research* 2014;47(4):1256-1266.
41. Tritt TM. *Thermal Conductivity. Theory, Properties and Applications.*: Springer US, 2004.
42. Renuka R, Ramamurthy S, and Muralidharan K. *Journal of Power Sources* 1998;76(2):197-209.
43. Zelenina TE and Zelenin OY. *Russian Journal of Coordination Chemistry*;31(9):623-626.
44. Welling SH, Hubálek F, Jacobsen J, Brayden DJ, Rahbek UL, and Buckley ST. *European Journal of Pharmaceutics and Biopharmaceutics* 2014;86(3):544-551.
45. Grabowska B, Sitarz M, Olejnik E, and Kaczmarska K. *Spectrochim Acta A Mol Biomol Spectrosc* 2015;135:529-535.
46. Grabowska B, Sitarz M, Olejnik E, Kaczmarska K, and Tyliszczak B. *Spectrochim Acta A Mol Biomol Spectrosc* 2015;151:27-33.
47. Halpern JM, Urbanski R, Weinstock AK, Iwig DF, Mathers RT, and von Recum HA. *Journal of Biomedical Materials Research Part A* 2014;102(5):1467-1477.
48. Mansour SAA. *Thermochimica Acta* 1994;233(2):243-256.
49. Benavides S, Villalobos-Carvajal R, and Reyes JE. *Journal of Food Engineering* 2012;110(2):232-239.



---

*CHAPTER V*

---

*EFFECT OF SODIUM  
HYPOPHOSPHITE IN THE  
POLYCONDENSATION OF  
MALTODEXTRIN WITH  
CITRIC ACID*

---



## 5.1 INTRODUCTION

---

### 5.1.1 ESTERIFICATION REACTION

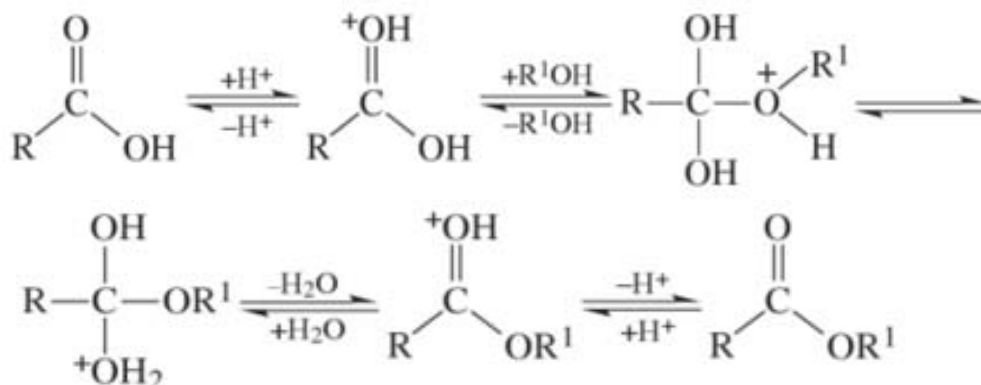
---

Esterification is the transformation of a carboxylic acid into an ester by reacting with an alcohol. Normally the reaction between carboxylic acids and alcohols takes place under acid or base catalysis conditions. However it is possible that the esterification reaction takes place without catalyst when high temperatures are applied. For instance, the reaction between hexanol and an aliphatic carboxylic acid can be conducted successfully in an autoclave at 150 °C. In case of using an acids as catalyst several options exists. One of the most used acids are Bronsted acids like HCl, HBr, H<sub>2</sub>SO<sub>4</sub>, AcOH, etc. Another important option with increased importance is Lewis acids such as ZnO, ZnCl<sub>2</sub>, BCl<sub>3</sub>, etc. Solid acids are also use for esterification, the great advantage of these acids is that they can be removed once the esterification is finished, however they are quite limited due to their strong acidity. An example of solid acids is the Amberlyst 15. On the contrary, basic catalysts are not suitable for esterification since esters can be hydrolyzed when the reaction mixture is subjected to aqueous workup. Nevertheless, a few nonaqueous methods are used, like for instance, the lactonization of  $\omega$ -hydroxy acids upon KOH/KOMe/glycerin. Other methods used for esterification reaction are the following: by carbodiimide activators, Mitsunobu reaction, and activation of carboxylic acids, enzymes and  $\pi$ -acids [1].

Among the most used methods for esterification reaction one of them need special attention. This is the so-called Fischer esterification. This esterification refers to the direct conversion of a carboxylic acid and an alcohol into an ester, catalyzed by a mineral acid according to the Scheme 5.1. As it can be seen in the Scheme 5.1, the esterification reaction in this case is an equilibrium. Therefore different strategies need to be followed in order to obtain the ester with a good yield. One of the strategies is consists of using a large excess of one of the reactants or removing one of the products, or both [2]. This type of esterification is used at industrial scale to synthesize some of the most relevant

esters like, for instance, ethyl acetate by esterification of acetic acid with ethanol. Also alkyl acrylates, monomers of polymers used in paints, adhesives, rubbers, etc., are produced by this

method; they are produced by esterification between acrylic acid and methanol, ethanol, butanol, etc. [1].



Scheme 5.1 – Reaction mechanism of Fischer esterification [2]

Esterification reaction is also used to synthesize a group of polymers which are named polyesters. Among polyesters, one of the most popular polymers are the polycondensates formed by esterification reaction of alcohols and polycarboxylic acids. This kind of polymers is broadly used in medical field due to their biocompatibility and their biodegradability [3, 4]. Apart from this application their use in disposable plastics is of great interest as well as for eco-materials under development. However, their physical and mechanical properties need still to be improved to achieve the requirements of the finish goods [5].

## 5.1.2 ESTERIFICATION OF POLYSACCHARIDES

Esterification of polysaccharides with carboxylic acids and their derivatives is one of the most versatile transformations of these compounds. This reaction allows making the polysaccharides, for instance, less or more soluble depending on the requirement; but also this reaction has open new alternatives to create bio-based functional polymers [6, 7]. Some of the esterification reactions involving polysaccharides take place in heterogeneous phase with carboxylic anhydrides or chlorides. However in order to

control better the polymerization degree of polysaccharide, homogenous phase reactions are recommended. For that reason variety of solvents have been investigated. Nevertheless the use of organic solvents shows important limitations due to their high toxicity, and high reactivity

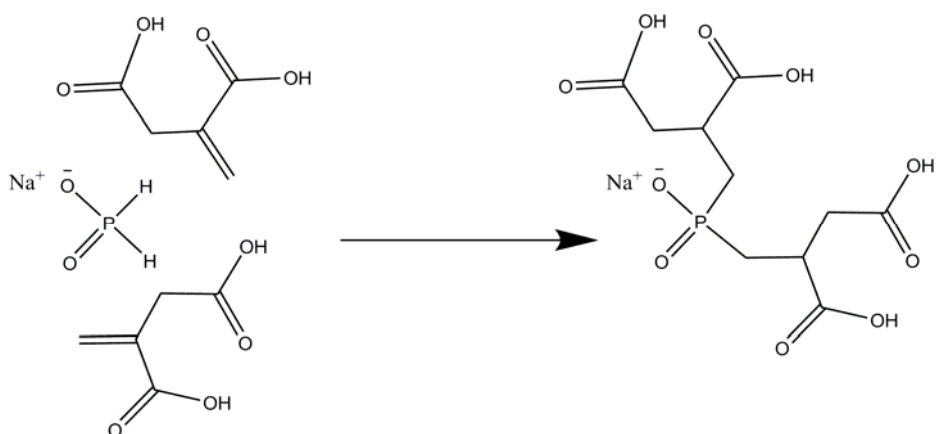
leading to undesired side reactions and the loss of solubility during the reactions [8]. Among the different methods known for esterification reaction, Fischer esterification has been developed as an appropriate alternative for polysaccharides in solid state or in water solution. For example, in case of using starch and their derivatives water is the most suitable solvent since it helps to solubilize the starch via gelatinization process; in this way starch is more reactive, making the hydroxyl moieties more available to react with carboxylic moieties. Regarding the acid, it is described the esterification reaction of starch with, for instance, citric acid, tartaric acid or octenyl succinic acid which apart from providing the carboxylic moieties for the esterification to take place, it also provides the acid pH required to promote the reaction [9, 10]. By these reactions crosslinked network containing starch are obtained leading to a polyester. The esterification reaction studied in this work (described in previous chapters), consisting of maltodextrin and polycarboxylic acids follows the Fischer mechanism to obtain a polyester network.

### 5.1.3 SODIUM HYPOPHOSPHITE IN THE ESTERIFICATION REACTIONS

---

Sodium hypophosphite has been intensively investigated in the last years as catalyst of esterification reaction involving polycarboxylic acids like 1,2,3,4-butanetetracarboxylic acid (BTCA) and citric acid (CA) although in esterification reactions it was first reported in 1980's [11]. These reactions are mainly applied in the finishing of cotton cellulose fabrics substituting the traditional formaldehyde containing finishing [12, 13]. The esterification reaction between the cellulose and the carboxylic acid is conducted by Fischer esterification method. This means that the polycarboxylic acids provide the acid pH needed to catalyze the reaction. However, it has been recently found out that sodium salts are able to promote the esterification reaction in this kind of systems as well, working as a side catalyst. According to the works carried out by Gang Sun et al. the phosphorous anion existing in the acid media may assist the removal of the proton in the Fischer mechanism (Scheme 5.1) promoting the formation of the ester bond [14, 15]. Furthermore, it is known that esterification reaction is enhanced for those polycarboxylic acids which are able to form an intermediate five membered ring by dehydration upon thermal treatment [16-18]. In this context, it has been proposed that sodium hypophosphite promotes the dehydration of these acids enhancing the formation of the five membered ring intermediate,

therefore the esterification reaction [15, 19]. From the other side it has been also reported the ability of sodium hypophosphite to form P-C bonds by reacting the phosphorous compound with olefinic carboxylic acids like maleic acid [20-22]. The use of sodium hypophosphite as esterification catalyst of the reaction between itaconic acid and cellulose is an example of this last approach (Scheme 5.2) [23]. Itaconic acid is a derivative formed by citric acid dehydration or decarboxylation. This suggests that sodium hypophosphite could catalyze not only the esterification reaction of a polyol with citric acid but also with its reactive derivatives upon thermal treatment.



**Scheme 5.2 – Reaction of sodium hypophosphite with itaconic acid**

## 5.2 AIM OF THIS CHAPTER

---

Taking into account the previous works describing the use of sodium hypophosphite as a catalyst of the esterification reaction between cellulose and polycarboxylic acids; it has been considered as an alternative to catalyze the polycondensation of maltodextrin and citric acid.

The aim of the work in this chapter is to prove the ability of sodium hypophosphite as catalyst of the esterification reaction between maltodextrin and citric acid; and as a consequence to study its effect on the mechanical properties of the crosslinked system. Furthermore it has been investigated the mechanism of action for the sodium hypophosphite during the polycondensation reaction.

## 5.3 MATERIALS AND METHODS

---

### 5.3.1 MATERIALS

---

Powdered maltodextrin (MAL) Maldex 120 (dextrose equivalent (DE) 11 to 15), manufactured by spray-drying of liquid maltodextrin, derived from edible corn starch hydrolysis was provided by Tereos Syral. Citric acid (CA) reagent and sodium hypophosphite monohydrate (SHP) were purchased from Sigma-Aldrich. The products were used without additional purification.

### 5.3.2 METHODS

---

Different systems containing MAL and CA with SHP were prepared. For that, the three compounds, MAL, CA and SHP were mixed in water at different ratios. The compositions studied are quoted in Table 5.1. MAL was dissolved in distilled water under mechanical stirring and then CA was added keeping the stirring until the solution was homogeneous. Finally SHP was added keeping the same stirring conditions until it was completely dissolved. Unless otherwise stated, all the mixtures in water were prepared with 50% dry content. Freeze-dried samples were prepared to avoid the influence of water in the thermogravimetric analysis.

**Table 5.1 – Compositions containing maltodextrin (MAL) and citric acid (CA) with sodium hypophosphite (SHP)**

Composition	MAL (% dry weight)	CA (%dry weight)	SHP (% dry weight)
M60C	60	40	-
M60C1SHP	59.4	39.6	1.0
M60C3SHP	58.3	38.8	2,9

Additional mixtures were prepared containing only CA and SHP in the same proportion as in the compositions containing MAL (Table 5.1). Unless otherwise stated, all the mixtures were prepared with 50% dry content. Freeze-dried samples were prepared to avoid the influence of water in the thermogravimetric analysis.

**Table 5.2 – Compositions containing citric acid (CA) and CaO**

Composition	CA (% dry weight)	SHP (% dry weight)
C1SHP	97.6	2.4
C3SHP	93.0	7.0

## 5.4 CHARACTERIZATION TECHNIQUES

---

### 5.4.1 RHEOLOGICAL MEASUREMENTS

---

Rheological measurements were carried out with an AR1000 rheometer (TA Instruments). Disposable plate-plate geometry with diameter 25 mm was used. Dynamic measurements in oscillatory mode were performed for approximately 1 mL sample in 2000  $\mu\text{m}$  gap, applying multiple frequency mode ranging from 1 Hz to 25 Hz and a fixed torque value (tests were performed previously to ensure that the response was in the viscoelastic region). Rheological behavior of water solutions of the different compositions was monitored at isothermal conditions between 130  $^{\circ}\text{C}$  and 140  $^{\circ}\text{C}$  until maximum modulus plateau was achieved, previously heating to reach the isothermal temperature with ramp rate of 3  $^{\circ}\text{C}/\text{min}$ . The measurements were done by duplicate.

### 5.4.2 MECHANICAL PROPERTIES MEASUREMENTS

---

Mechanical properties measurements were carried out on glass paper “Whatman GF/A 8x10 ins” impregnated with the corresponding composition and cured by heating treatment. A glass paper sheet was soaked in a water solution with 20% solid content of the different compositions. The treated sheet was pressed between the squeezing rolls of a laboratory padder (Mathis) at 3 mm/min speed of the rolls and pressure between the rolls at 2.5 bars. Heating treatment on the impregnated glass paper was applied in a Labdryer oven (Mathis) at 140  $^{\circ}\text{C}$ . Specimens were cut from the cured glass paper sheet with size 75x25 mm. Cured specimens were treated with



accelerated weathering conditions in a climate chamber (Ineltec) at 50 °C and 95 % humidity for 24 hours. Tensile strain measurements were done for the specimens previous to the treatment with accelerated weathering conditions and after the application of accelerated weathering conditions. The tensile strain measurements were carried out in an Instron Universal Testing Machine equipped with a 500 N load cell. The cross-head speed applied was 2.3 m/min and the gauge length was 50 mm. The results were taken from the average of at least six specimens.

### 5.4.3 ATR-FTIR SPECTROSCOPY

---

ATR-FTIR spectra were measured in a Spectrum One FT-IR Spectrometer (Perkin Elmer) with a split pea accessory for ATR. Absorbance spectra were acquired at 4 cm<sup>-1</sup> resolution and signal-averaged over 10 scans recorded from 4000 cm<sup>-1</sup> to 650 cm<sup>-1</sup>. The spectra were baseline corrected and normalized to the most intense absorbance peak. FTIR spectra were measured for the different compositions in Table 5.1 upon heating treatment at 140 °C. In order to assure the interpretation of the spectra of the compositions after the thermal treatment spectra were recorded before and after the purification of the corresponding samples. The cured compositions were purified by membrane dialysis, placing approximately 2 g of composition in a 1000 Da membrane, in 2 L of water for 20 hours, renovating the water after 10 hours. The purified polymer was dried under vacuum at 40 °C for 24 hours.

### 5.4.4 THERMOGRAVIMETRIC ANALYSIS (TGA)

---

TGA was performed using a TGA Q500 (TA Instruments). Different freeze-dried samples of the compositions were heated in a platinum pan from 25 to 600 °C, under a nitrogen atmosphere at a heating rate of 10 °C/min. The derivative TGA (wt %/°C) curve of each sample was obtained from the software TA Universal Analysis.

## 5.4.5 NMR SPECTROSCOPY

---

$^{31}\text{P}$ ,  $^1\text{H}$ ,  $^{13}\text{C}$  and Heteronuclear Multiple-Bond Correlation spectroscopy (HMBC) NMR analysis was performed using a spectrometer Avance TM 400 WB from Bruker. Spectra were recorded at room temperature from deuterium oxide solutions. Sample concentration was  $\sim 20$  mg/mL for  $^1\text{H}$ , and  $\sim 50$  mg/mL for  $^{13}\text{C}$  and HMBC spectra. Spectra were analyzed with the MestreNova v 6.1 software.

## 5.5 RESULTS AND DISCUSSION

---

### 5.5.1 EFFECT OF SHP IN THE ESTERIFICATION REACTION

---

#### 5.5.1.1 INFRARED ANALYSIS

---

The effect of the SHP on the polycondensation reaction has been analyzed by IR. Figure 5.1, Figure 5.2 and Figure 5.3 show the evolution of IR spectra for the compositions in Table 5.1. The C=O stretching band, the characteristic band assigned to ester bond between the hydroxyl groups of MAL and the carboxylic groups of CA [24], evolves to  $1720\text{ cm}^{-1}$  after 5 hours thermal treatment in the composition with no SHP. In the compositions containing 1 % SHP this evolution is already reached after 3 hours, while with 3 % this shift is achieved after 2 hours thermal treatment.

By this first analysis it is demonstrated that the addition of SHP to the system containing MAL and CA has positive effect on the esterification reaction by promoting the formation of the ester bond in shorter thermal treatment.

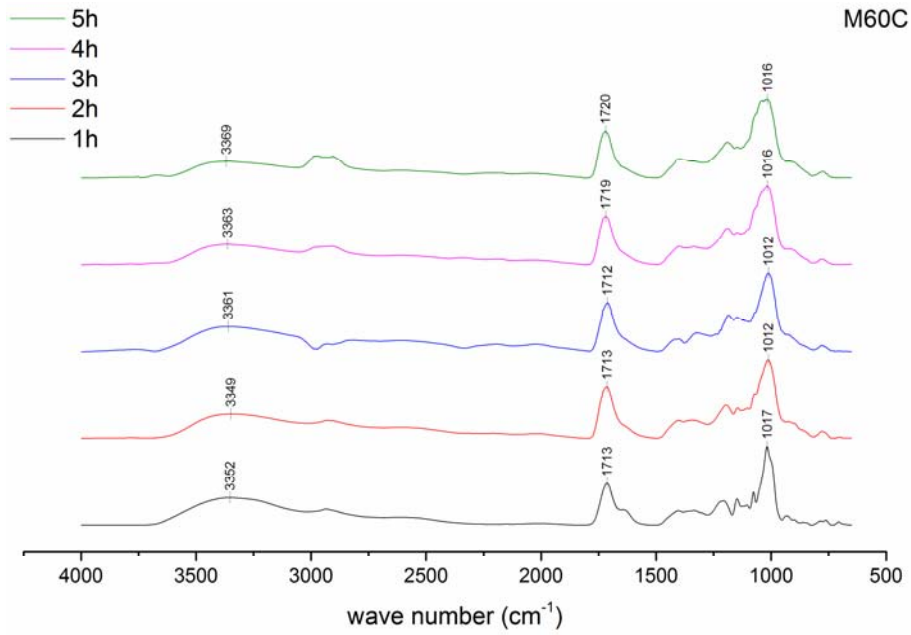


Figure 5.1 – IR spectra of the composition M60C under thermal treatment at 140 °C for different times

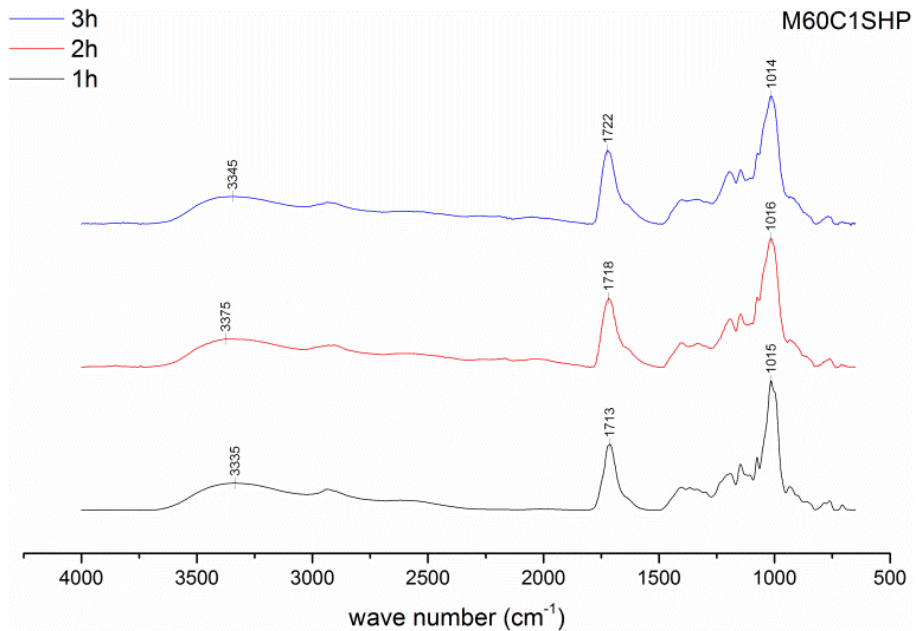


Figure 5.2– IR spectra of the composition M60C1SHP under thermal treatment at 140 °C for different times

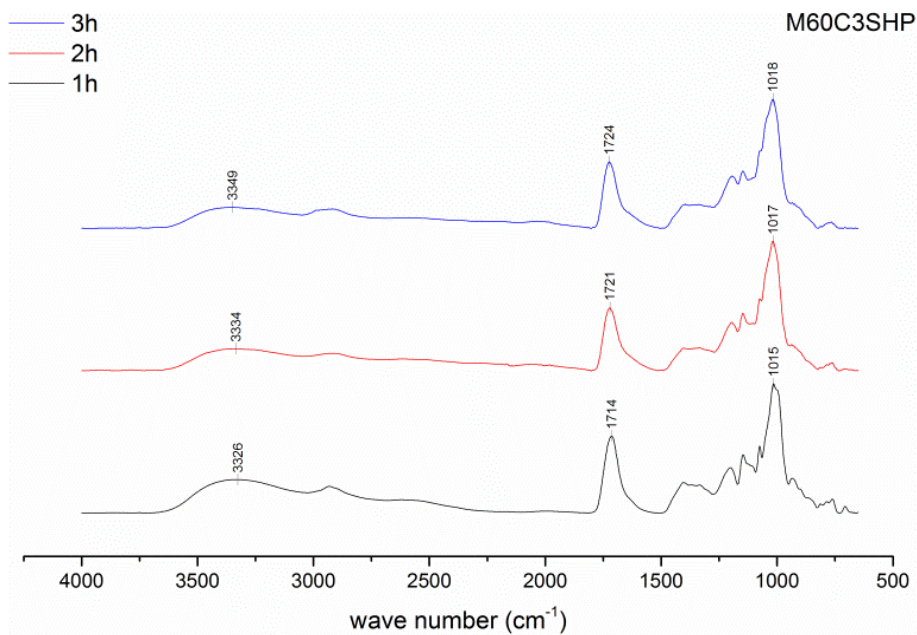


Figure 5.3 - IR spectra of the composition M60C3SHP under thermal treatment at 140 °C for different times

As seen in previous chapters, the progress of the polycondensation reaction between MAL and CA can be followed based on the evolution of the ratio between the intensity of the C=O stretching band and intensity of OH stretching band ( $A_{CO}/A_{OH}$ ) [25].

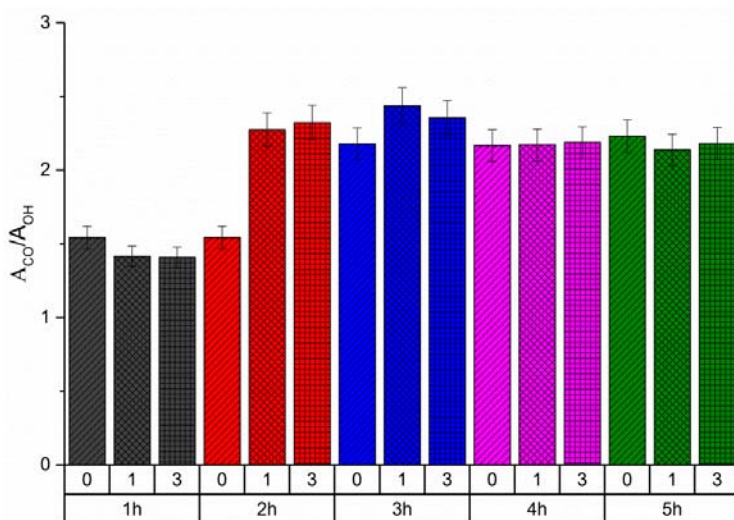


Figure 5.4 – Evolution of ratio  $A_{CO}/A_{OH}$  for the composition (0) M60C, (1) M60C1SHP and (3) M60C3SHP under thermal treatment at 140 °C and different times (1h, 2h, 3h, 4h and 5h)

Figure 5.4 shows this evolution for the compositions in Table 5.1 according to the spectra shown above. The strongest effect of SHP addition is detected after 2 hours treatment, leading to a much higher increase of the ratio  $A_{CO}/A_{OH}$ . However this effect vanishes after 4 hours treatment.

This indicates that the esterification reaction is more advanced in 2 hours when SHP is added to the system; and might enhance thermal decomposition of CA and its derivatives when heating longer.

### 5.5.1.2 TGA

The compositions in Table 5.1 were studied by TGA. Figure 5.5 shows the TGA curves and the corresponding first derivative curves.

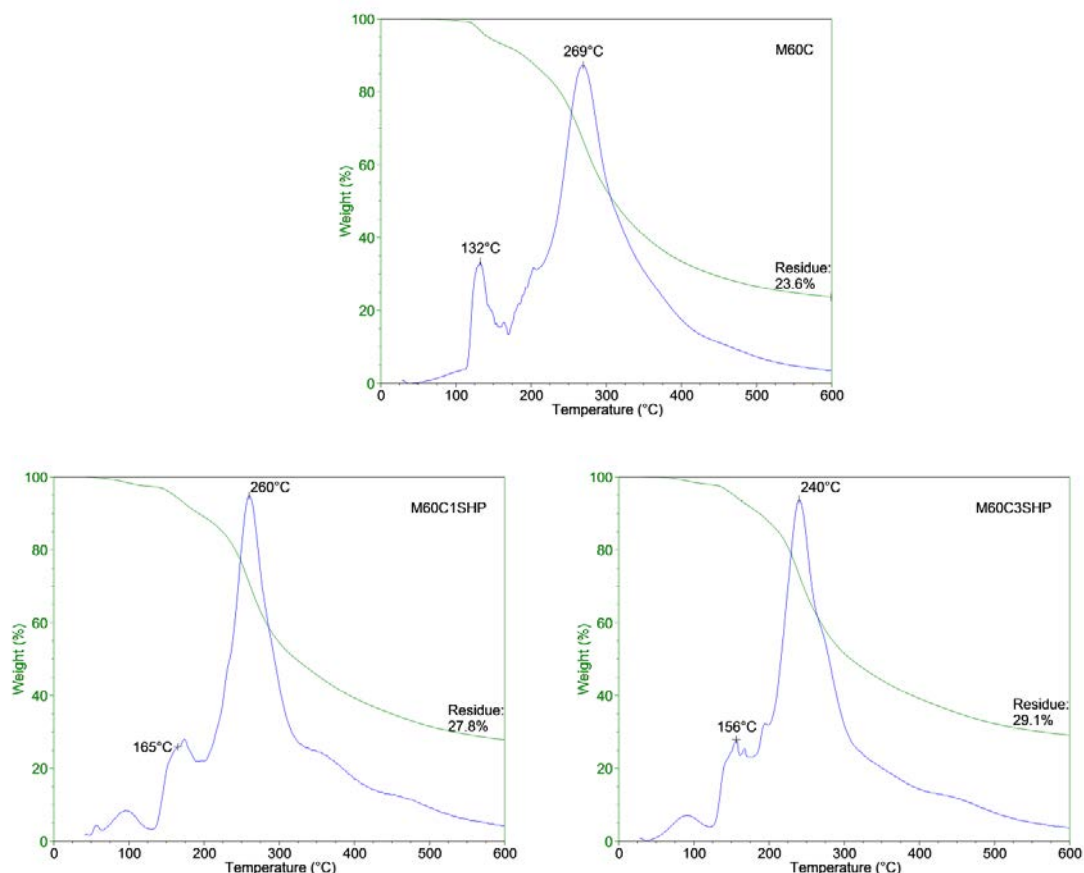
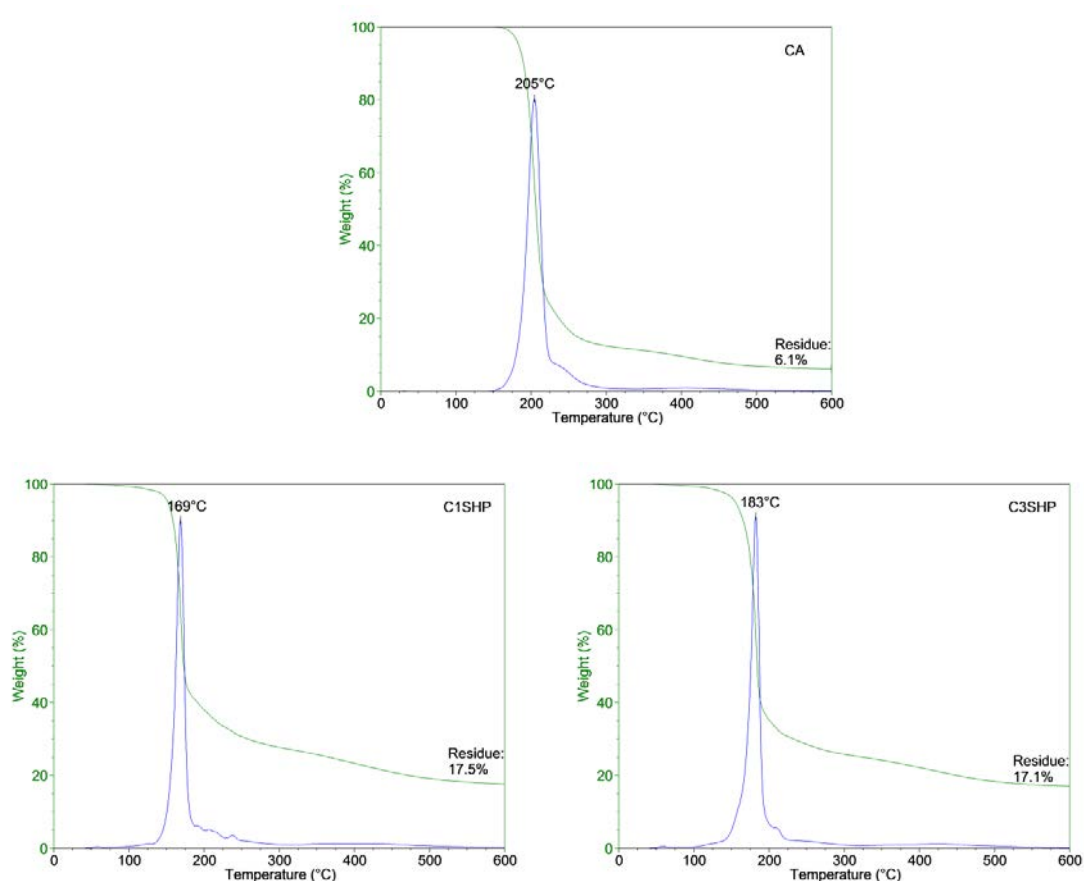


Figure 5.5 – TGA and its first derivative of the compositions M60C, M60C1SHP and M60C3SHP

In general, the addition of SHP to the system containing MAL and CA modifies its thermal response. First, the temperature of the maximum decomposition rate decreases as the ratio of SHP is increased in the system containing MAL and CA, going from 269 °C to 240 °C. This proves that accelerated decomposition of the system containing MAL and CA can take place by the addition of SHP as suggested in the IR study. Second, the maximum rate of the step assigned to esterification reaction according to previous works [9, 25] can be identified at around 160 °C

when SHP is added to the system containing MAL and CA while it is at 130 °C when there is no addition of SHP. In either case, the starting temperature of this step is 120-130 °C independently of the SHP ratio. Third, apart from the two main weight loss steps, other weight losses can be slightly detected at around 350 °C and 450 °C when SHP is used. The first is ascribed to the decomposition of the polycondensate products formed between MAL and CA; and the second is related to the decomposition of the phosphorus compounds. Furthermore, the residue remaining at 600 °C is higher for those compositions containing SHP. This is typical result found when SHP is used as, for instance, flame retardant in materials such as cotton fabrics, due to the increase of the amount of char formed [26, 27].



**Figure 5.6 – TGA and its first derivative for (CA) CA and the mixtures C1SHP and C3SHP**

The effect of SHP on CA has been deeper analyzed in the mixtures containing only CA and SHP (i.e. compositions in Table 5.2). It can be observed in Figure 5.6 that the addition of SHP decreases the temperature of the maximum rate decomposition of CA from ar. 205 °C to 170-180 °C. But, in the other side, the residue amount at 600 °C is doubled with the addition of SHP. This evidences

clearly the effect of SHP on the thermal behavior of CA. As mentioned above this behavior is well known in those applications where SHP is used as flame retardant.

Overall, the TGA analysis shows that SHP modifies the thermal behavior of the system based on MAL and CA; nevertheless its contribution to the esterification reaction cannot be clearly studied.

## 5.5.2 EFFECT OF SHP IN THE CROSSLINKING

The effect of SHP on the crosslinking of the system based on MAL and CA has been evaluated by rheology. Figure 5.7 and Figure 5.8 show the evolution of moduli,  $G'$  and  $G''$ , under the isothermal treatment at 130 °C and 140 °C respectively for the compositions in Table 5.1. It can be observed that SHP has a remarkable acceleration effect making moduli ( $G'$  and  $G''$ ) to increase much faster. The maximum  $G'$  close to 10 MPa is reached much earlier, being the composition with 3 % SHP the fastest one. The same maximum value of  $G'$  close to 10 MPa can be achieved even with 10 °C lower temperature (i.e. 130 °C).

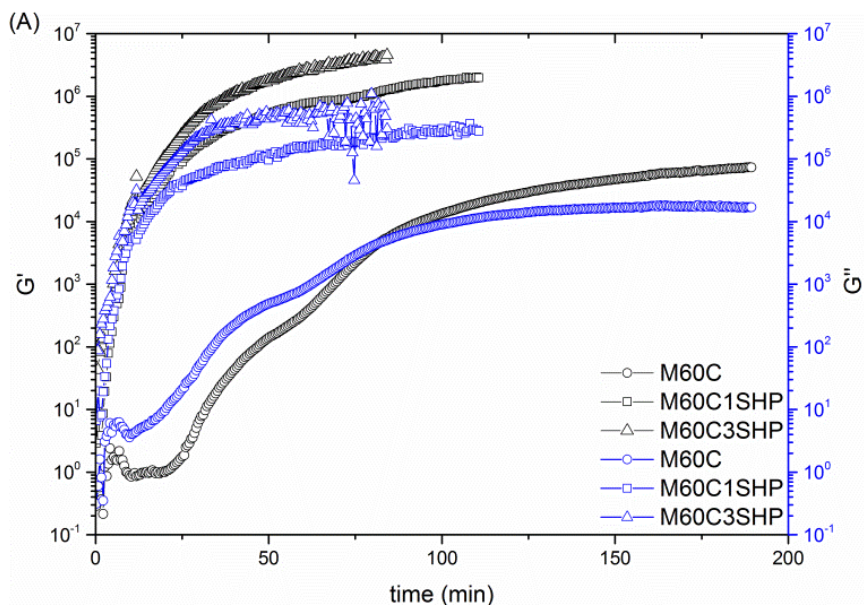


Figure 5.7 – Plot of  $\log G'$  and  $\log G''$  against time of composition M60C, M60C1SHP and M60C3SHP at 130 °C

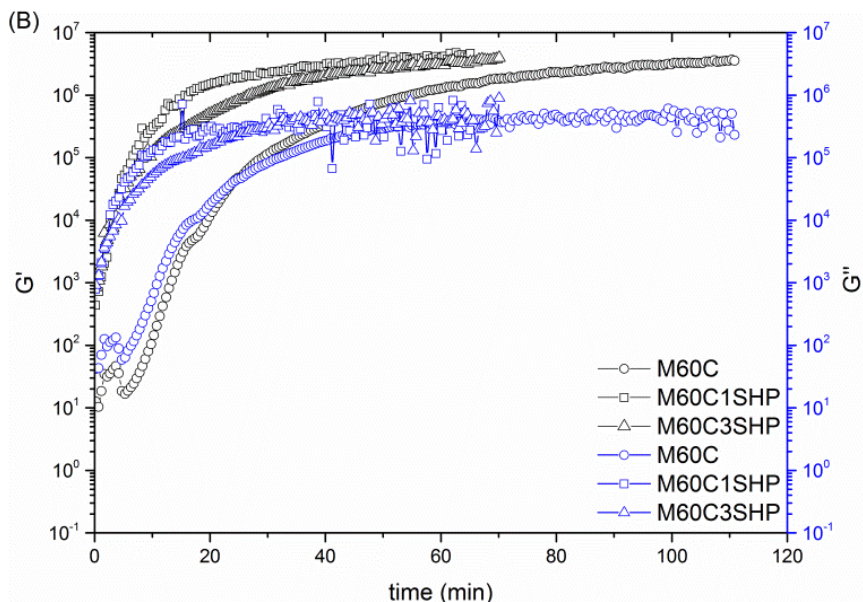


Figure 5.8 – Plot of log  $G'$  and log  $G''$  against time of composition M60C, M60C1SHP and M60C3SHP at 140 °C

By the rheological experiments it has been determined the gel time. The gel time has been considered as the time point at which the  $G'$  and  $G''$  the cross-over [28, 29]. In Figure 5.9 is shown the gel time for the different compositions studied. The addition of SHP makes gel time to shorten strongly. Even applying lower temperature during the thermal treatment the gel time clearly decreases when adding SHP; being this decrease more noticeable when SHP ratio is higher (i.e. 3 %).

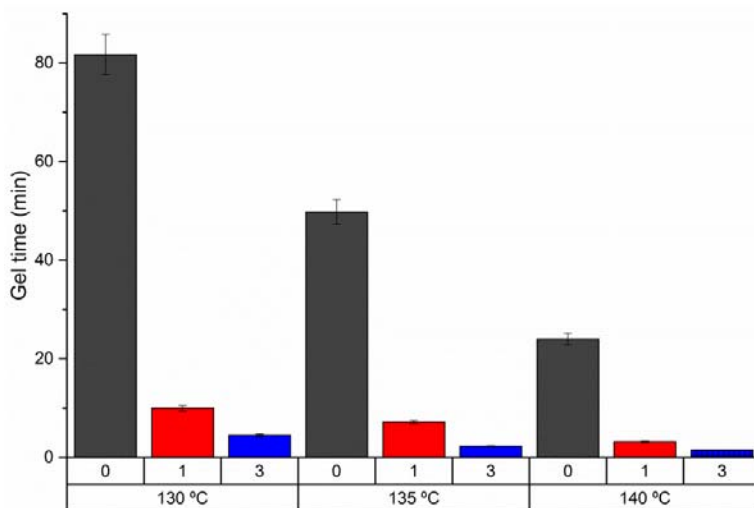


Figure 5.9– Gel time of the composition (0) M60C, (1) M60C1SHP and (3) M60C3SHP under isothermal treatment at 130, 135 and 140 °C



Experimental calculation of apparent activation energy ( $E_a$ ) has been done in order to evaluate the effect of the SHP addition on the kinetic of the system containing MAL and CA. For its calculation the Arrhenius law (Equation 5.1) has been applied. Assuming that the chemical conversion of the system at the gel time is constant [29], apparent kinetic constant ( $k'$ ) would be related to the gel time ( $t_g$ ) according to the Equation 5.2. By replacing Equation 5.2 in Equation 5.1 it can be obtained the Equation 5.3. By plotting  $\ln(t_g)$  against the inverse of the temperature corresponding slope is obtained (Figure 5.10), and from the slope the apparent activation energy ( $E_a$ ) can be calculated.

$$\ln k' = \ln A - \frac{E_a}{R \cdot T}$$

Equation 5.1 – Arrhenius law

$$t_g = \frac{C}{k'}$$

Equation 5.2 – Relation between apparent kinetic constant and gel time

$$\ln t_g = \ln C - \frac{E_a}{R \cdot T}$$

Equation 5.3 – Relationship between gel time and inverse of temperature

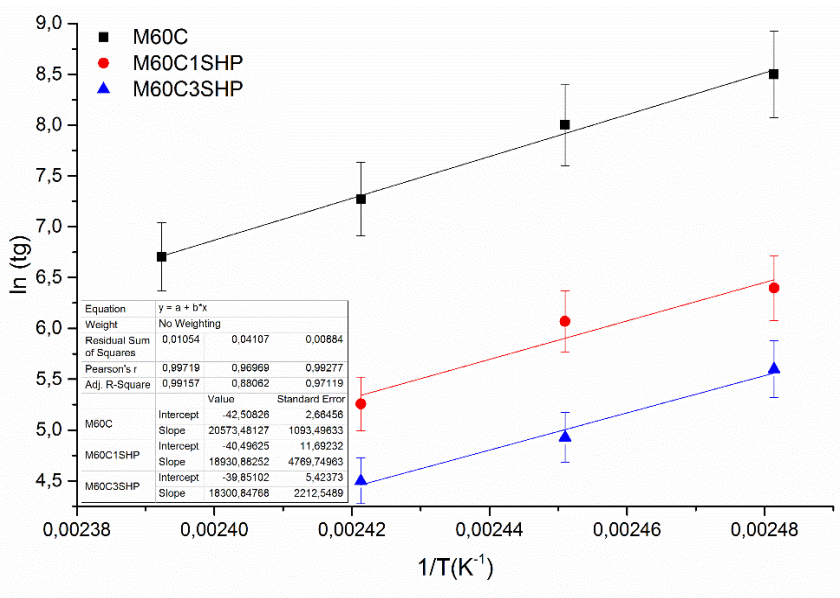


Figure 5.10 – Plot of  $\ln(t_g)$  against the inverse of corresponding temperature

In Table 5.3 is collected the resulting  $E_a$  for the different compositions in Table 5.1. The results show that activation energy of the system containing MAL and CA decreases when SHP is present. In other words, SHP helps to accelerate the crosslinking reaction between MAL and CA.

Table 5.3 – Activation energy of composition M60C, M60C1SHP and M60C3SHP

Composition	$E_a$ (kJ/mol)
M60C	171.0
M60C1SHP	157.3
M60C3SHP	152.1

In general, the rheology results demonstrate that SHP accelerates the crosslinking of the system based on MAL and CA, decreasing its apparent activation energy.

### 5.5.3 EFFECT OF SHP ON THE MECHANICAL PROPERTIES

---

The effect of SHP on the mechanical properties of crosslinked system has been analyzed. The compositions in Table 5.1 impregnated in glass paper were cured during different times and later evaluated. In Figure 5.11 is shown the evolution of stress strain curve for the different compositions cured at 140 °C and different curing times. In all the cases the material reaches a breaking point but showing previously elastic deformation [30]. The glass paper impregnated with the composition M60C and cured for 1 min shows more elastic behavior where clear yield point can be identified [31]. The elastic behavior decreases when SHP is added. The effect of SHP is also detected when curing longer, 5, 15 and 30 min, always leading to stiffer material. This may be explained by the increase of crosslinking density of the polymer network [32].

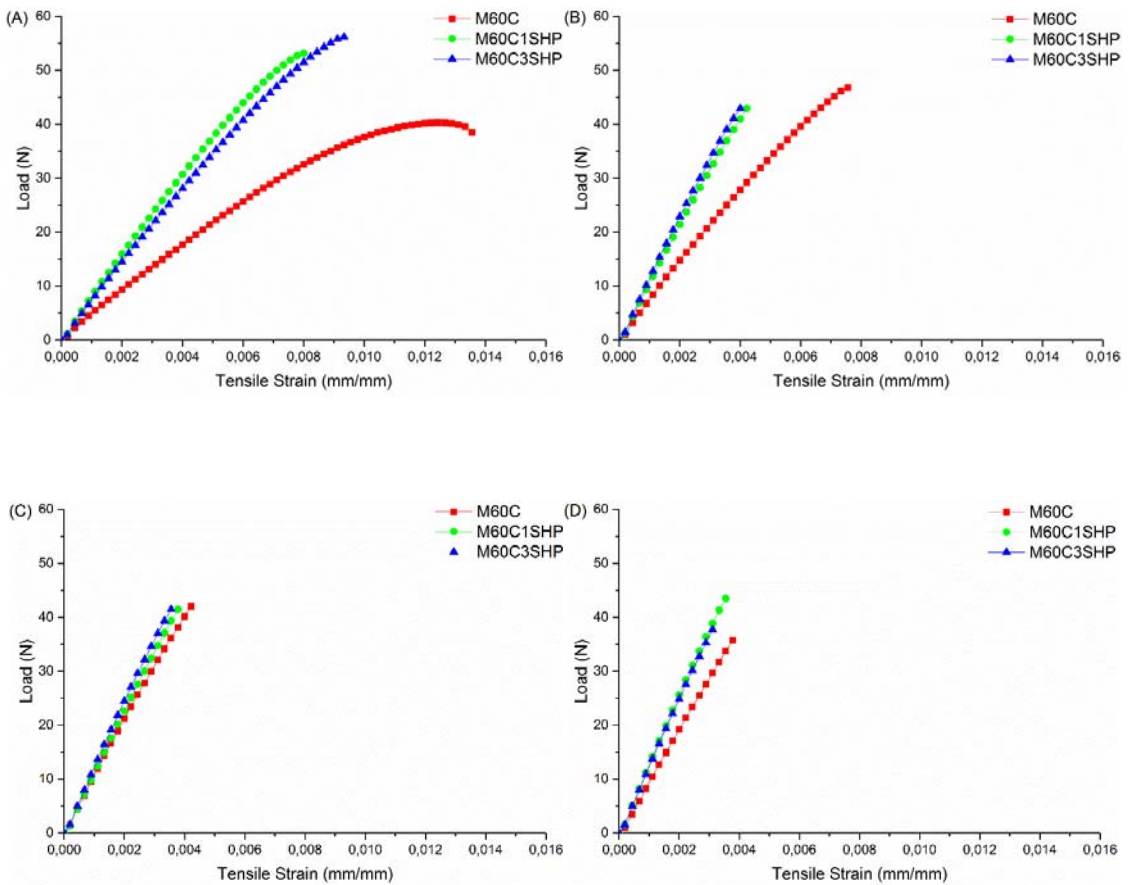


**Figure 5.11 – Stress-strain curves of glass paper impregnated with the compositions in Table 5.1, cured at 140 °C and different times, (A) 1 min, (B) 5 min, (C) 15 min and (D) 30 min**

The corresponding tensile strain data and its retention after accelerated weathering conditions treatment are shown in Figure 5.12. The addition of SHP makes to decrease the tensile strain at maximum load of glass paper. However there is no statistic difference ( $p > 0.05$ ) between 1 % and 3 % SHP. It is also relevant that the minimum tensile strain value is achieved after 5 min heating treatment when SHP is added. However this minimum value is achieved after 15 min when no SHP is in the system. This suggests that SHP helps to increase the crosslinking density of polymer network, allowing shorter curing times to achieve similar stiffness. The retention of the tensile strain seems to be improved in general when SHP is added to the system. Yet, its retention in some cases is higher than 100 %, what would mean that tensile strain increases after accelerated weathering. The only explanation possible to this stage (without any further study on that) would be that the material become more flexible after accelerated weathering.

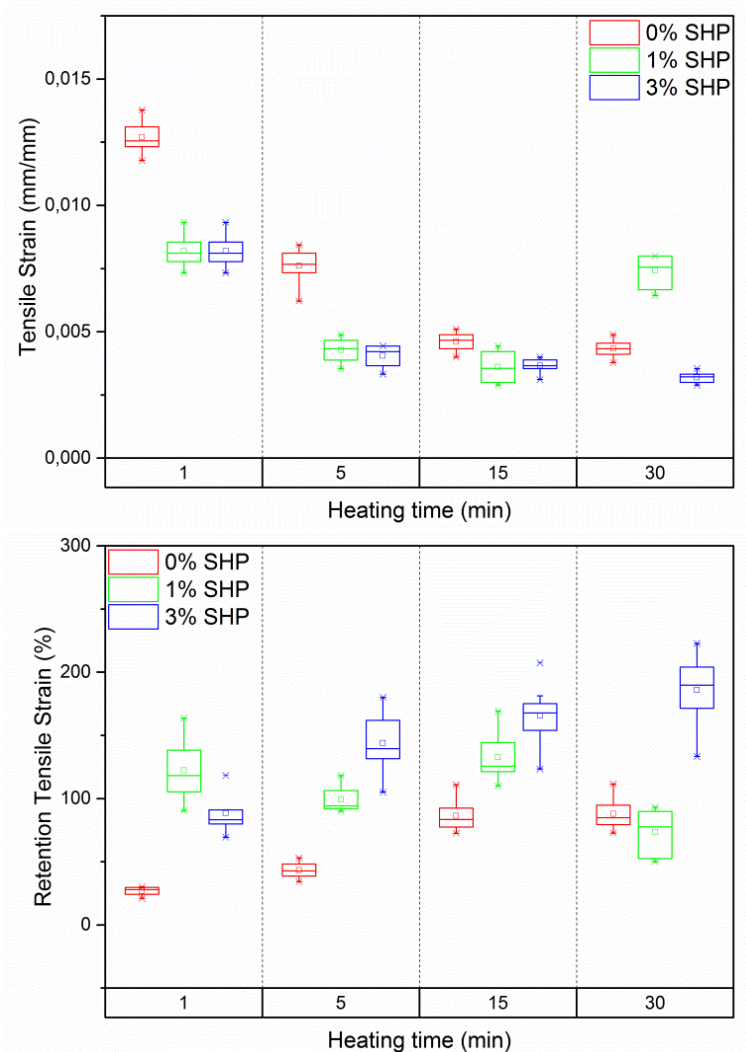


**Figure 5.12 – Tensile strain and its retention upon accelerated weathering conditions of glass paper impregnated with the compositions in Table 5.1 cured at 140 °C and different heating times (1, 5, 15 and 30 min)**

Data on the young's modulus and its retention after accelerated weathering conditions are shown in Figure 5.13. The young's modulus strongly increases with SHP. The maximum value of young's modulus is already achieved after 5 min. The young's modulus is better preserved when SHP is added, being close to 100 % retention independently of the curing time.

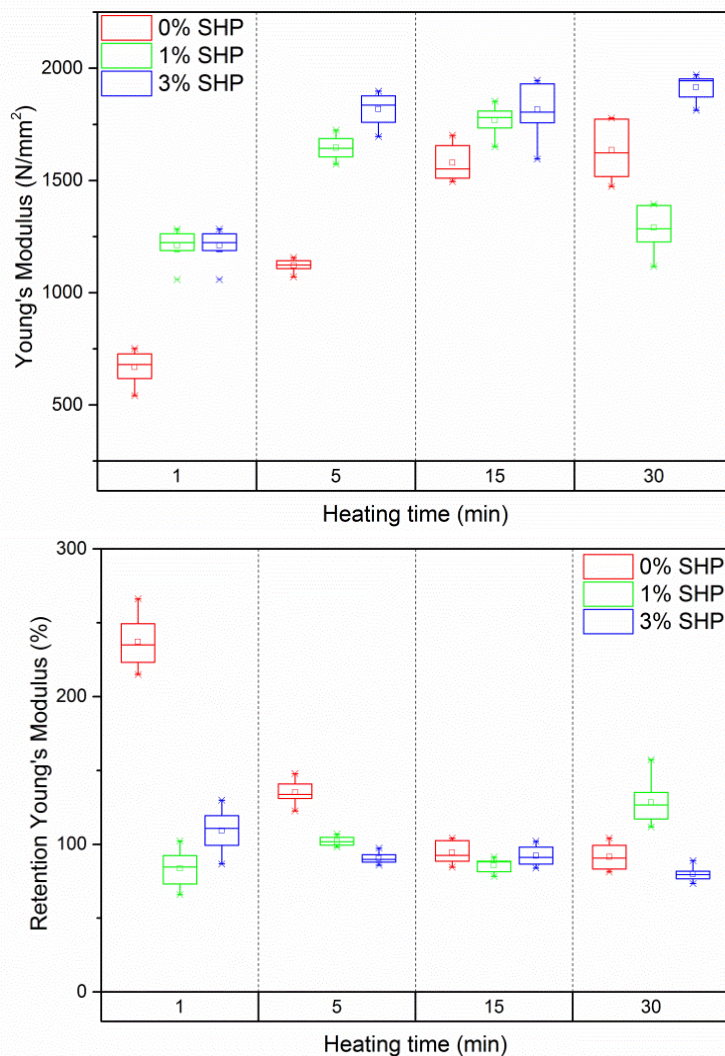


**Figure 5.13 – Young's Modulus and its retention upon accelerated weathering conditions of glass paper impregnated with the compositions in Table 5.1 cured at 140 °C and different heating times (1, 5, 15 and 30 min)**

The mechanical characterization of the crosslinked system proves that the addition of SHP to the system containing MAL and CA improves the stiffness of the material, particularly in short curing process. These results suggest that SHP remarkably promotes the crosslinking of the system containing MAL and CA.

## 5.5.4 ROLE OF SHP IN THE POLYCONDENSATION REACTION OF MAL AND CA

### 5.5.4.1 NMR STUDY

The evolution of MAL, CA, SHP and the composition M60C3SHP under thermal treatment at 140 °C has been studied by NMR spectroscopy.  $^{13}\text{C}$  NMR spectra were done for MAL and CA before thermal treatment and, after 3h thermal treatment, without SHP in the media and with SHP added in same proportion as in the composition M60C3SHP. Figure 5.14 shows the  $^{13}\text{C}$  NMR spectra of MAL under the different conditions.

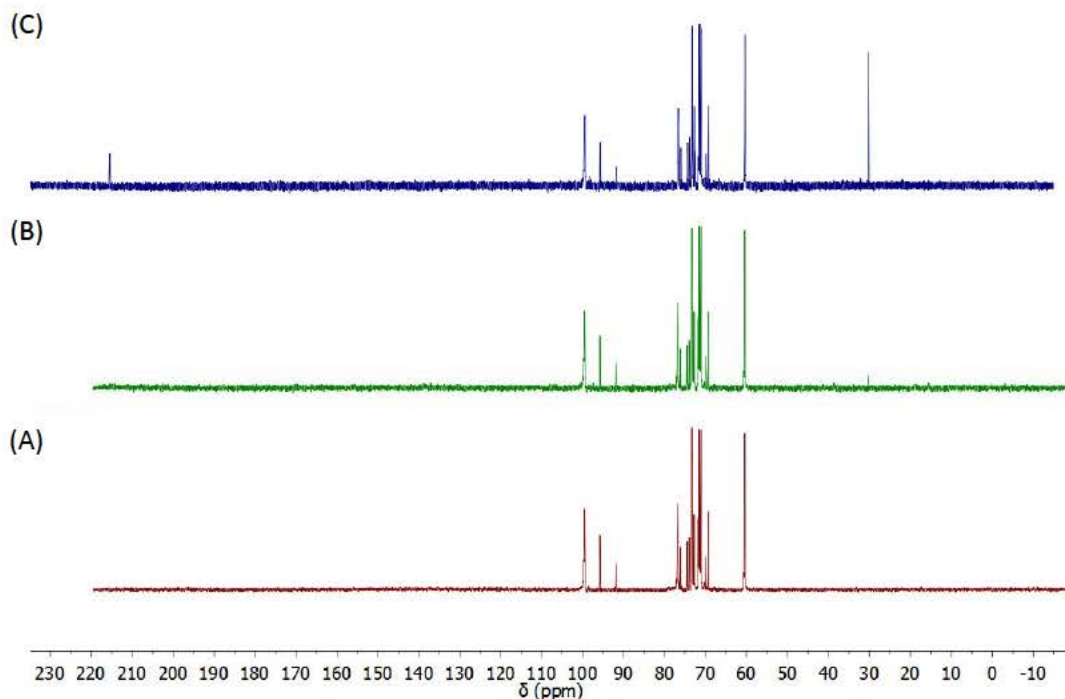


Figure 5.14 -  $^{13}\text{C}$  NMR spectra of (A) original MAL, (B) MAL after 3 hours thermal treatment at 140 °C and (C) mixture of MAL with SHP after 3 hours thermal treatment at 140 °C

It can be observed that MAL  $^{13}\text{C}$  NMR shows slight changes upon thermal treatment at 140 °C. The typical  $^{13}\text{C}$  NMR signals of MAL [33] can be distinguished in both cases, with and without SHP. Only a new peak at 30.07 ppm can be identified after thermal treatment of MAL without SHP. This peak is assigned to an aliphatic carbon. When SHP is added over MAL the same peaks appear, but additionally a new peak at 215.42 ascribed to a ketone moiety is found. In particular this new

peak at 215.42 ppm may indicate the presence of new compounds containing ketone groups which are characteristic polysaccharides derivatives produced by the caramelization process [34, 35]. Nevertheless it might be that this process is also slightly taking place without SHP in the media as indicated by the peak at 30.07 ppm. Therefore, the caramelization process over MAL may take place, with and without SHP, but it seems to be more important when SHP is present.

Figure 5.15 shows the  $^{13}\text{C}$  NMR of CA under thermal treatment, with and without SHP, as well as CA starting material.

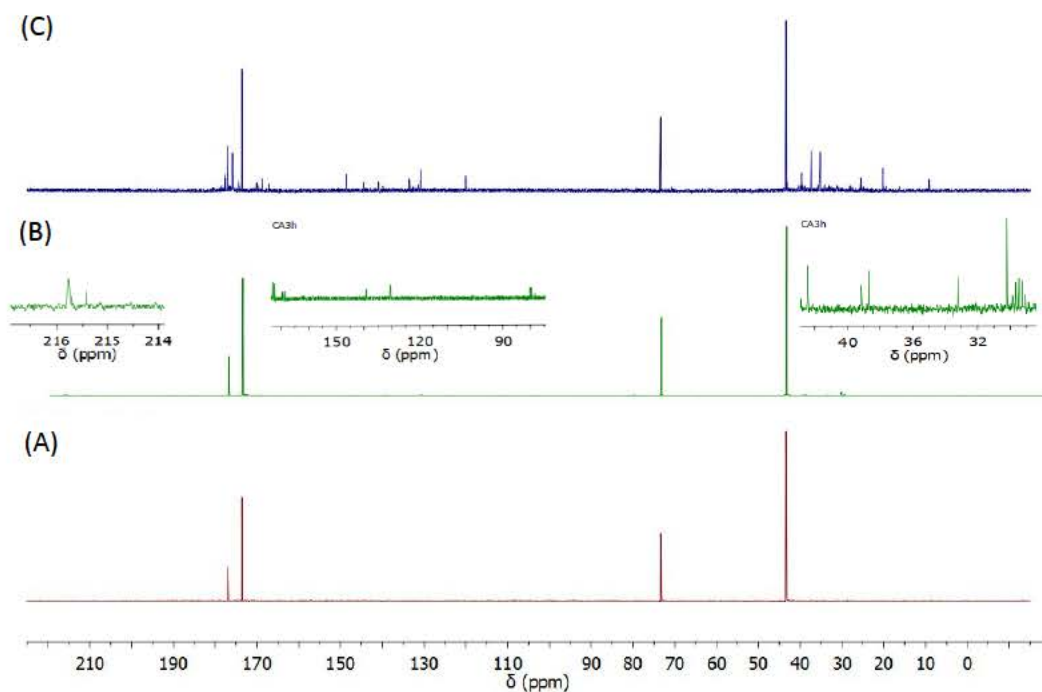
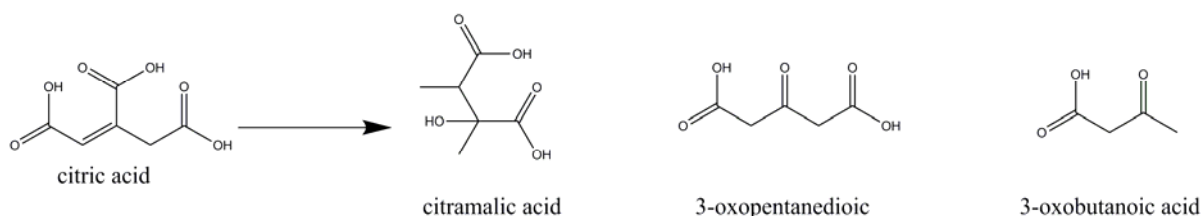


Figure 5.15 –  $^{13}\text{C}$  NMR spectra of (A) original CA, (B) CA and (C) mixture of CA with SHP, after 3 hours thermal treatment at 140 °C after 3 hours thermal treatment at 140 °C

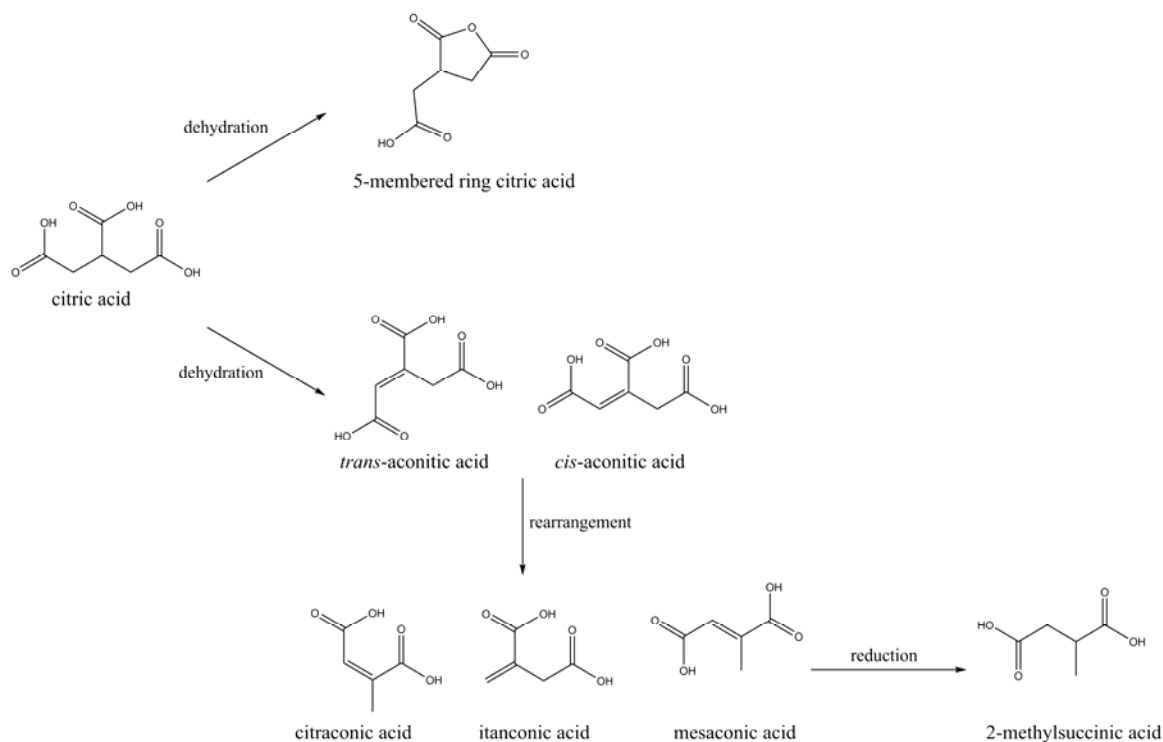
The typical peaks related to carboxyl and methylene groups of CA can be identified in the three spectra in Figure 5.15 [36]. The spectrum of CA after thermal treatment shows minor new peaks: around 215 ppm assigned to ketone moieties, around 170 ppm assigned to new carboxylic acid groups, 120-140 ppm assigned to alkene moieties, around 78 ppm assigned to CH moieties bonded to an OH group and 29-40 ppm assigned to new  $\text{CH}_2$  moieties. All these new peaks indicate that CA evolves under thermal treatment. According to the peaks at around 215 and 170 ppm compounds containing a ketone group and a carboxyl group are produced by the thermal treatment, which might be, for instance 3-oxopentanedioic acids and 3-oxobutanoic acid,

generated by the decarboxylation process of CA (Scheme 5.3) [37]. Other non ketonic compounds like citramalic acid (Scheme 5.3), which are intermediates of the decarboxylation process of CA [37, 38] are related to the new peaks found at around 78 ppm. The alkene moieties identified at this stage are assigned to the aconitic acid produced by dehydration process of CA (Scheme 5.4) [36]. In the spectrum of the mixture of CA with SHP upon thermal treatment the previous signals related to ketonic groups and the signal at around 78 ppm assigned to CH moieties bonded to an OH group cannot be found anymore. This indicates that the decarboxylation of CA does not take place when SHP is present. However, additional signals assigned to alkene and CH<sub>2</sub> moieties can be identified, apart from a new signal at 9.10 ppm assigned to a CH<sub>3</sub> group. All these signals are the result of further dehydration process of CA, leading to new acids apart from the aconitic acid, such as citraconic, mesaconic and itaconic acid (Scheme 5.4). The weak signal at 71.01 ppm, assigned to a CH moiety, is related to the five-membered ring (Scheme 5.4) formed also by dehydration of CA under thermal treatment. This has been reported as a relevant intermediate compound enhancing the esterification reaction between polycarboxylic acids and hydroxyl containing compounds like, for instance, cotton and cellulose [16]. According to the signals at 16.37, 35.28, 37.43, 174.41 and 175.92 ppm the 2-methylsuccinic acid could also be present, as a consequence of the reducing activity from the SHP over mesaconic acid (Scheme 5.4) [37].



**Scheme 5.3 – Possible compounds obtained by decarboxylation of CA**





**Scheme 5.4 – Citric acid major derivatives from dehydration process due to the presence of SHP**

When comparing the spectra of the mixture containing CA and SHP after 3 hours thermal treatment with the 4 and 5 hours thermal treatment (Figure 5.16) it can be noted that the same main peaks identified after 3 hours can also be found after 4 and 5 hours. Some of the peaks described above are more pronounced in the spectra after 4 hours; for instance the peak at 70.80 ppm which is ascribed to the intermediate five-membered ring of CA. Other signals like the one at 61.81 identified after 4 hours thermal treatment may indicate the presence of C-P bonds [39].

Figure 5.17 compares the spectra of the mixture containing CA and SHP with the soluble material (after purification) of the cured composition M60C3SHP, both after 3 hours thermal treatment. It can be observed that most of peaks identified in the mixture containing CA and SHP can be found in the compositions M60C3SHP. But it can be also noted that the peak at 70.80 ppm ascribed to the five-membered ring intermediate compound derivative from CA cannot be identified in the cured composition M60C3SHP. This means that the well-known five-membered ring intermediate of esterification of polycarboxylic acids (i.e. CA) is not present in the soluble part of the cured composition M60C3SHP. This may indicate that it has fully reacted with MAL.

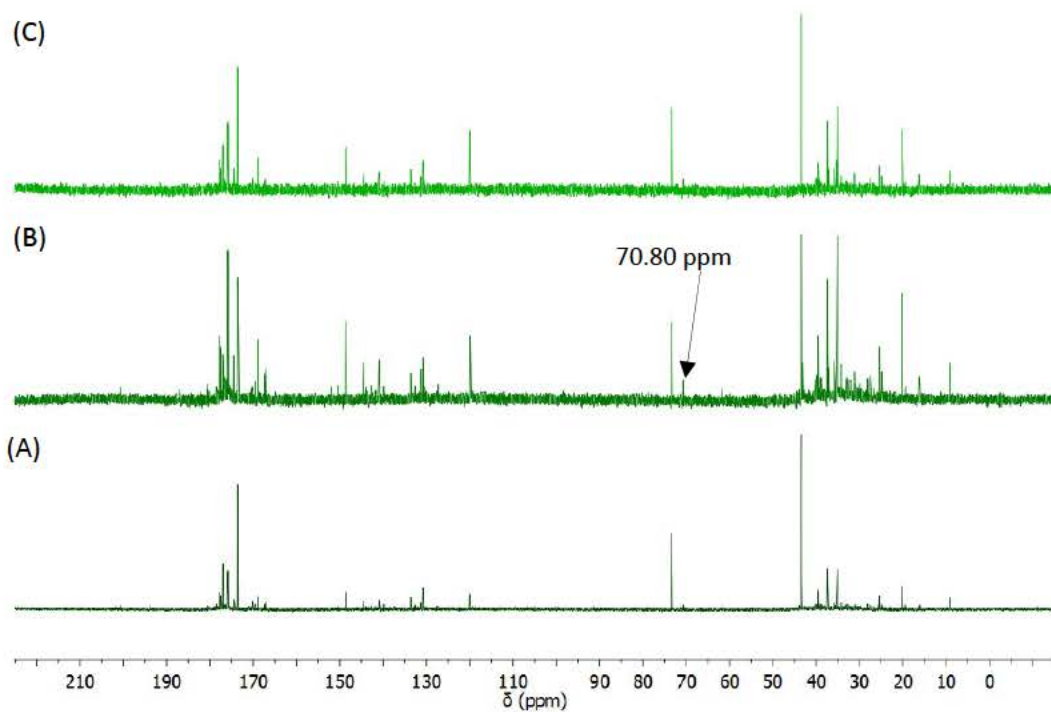


Figure 5.16 –  $^{13}\text{C}$  NMR spectra of mixture of CA with SHP, after thermal treatment at for (A) 3 hours, (B) 4 hours and (C) 5 hours

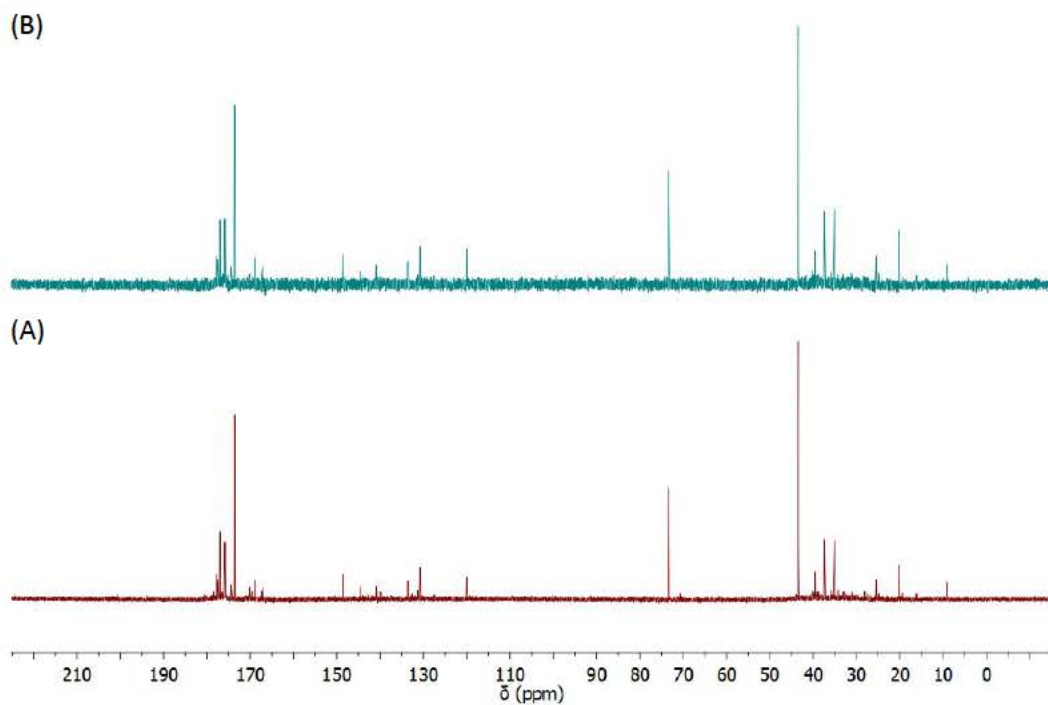


Figure 5.17 –  $^{13}\text{C}$  NMR spectra of the mixtures (A) CA with SHP and (B) soluble part of composition M60C3SHP, after 3 hours thermal treatment at 140 °C

The comparison of the spectra of the soluble material for composition M60C3SHP after 3 hours and 4 hours thermal treatment is shown in Figure 5.18. It can be observed that all the peaks assigned to the alkene compounds and 2-methylsuccinic acid found in the spectrum after 3 hours treatment cannot be identified in the spectrum after 4 hours treatment. In this last, only CA peaks are found. This proves that alkene compounds and 2-methylsuccinic acid are taking part of the insoluble polymer network formed between MAL and CA, while still part of CA remains unreacted.

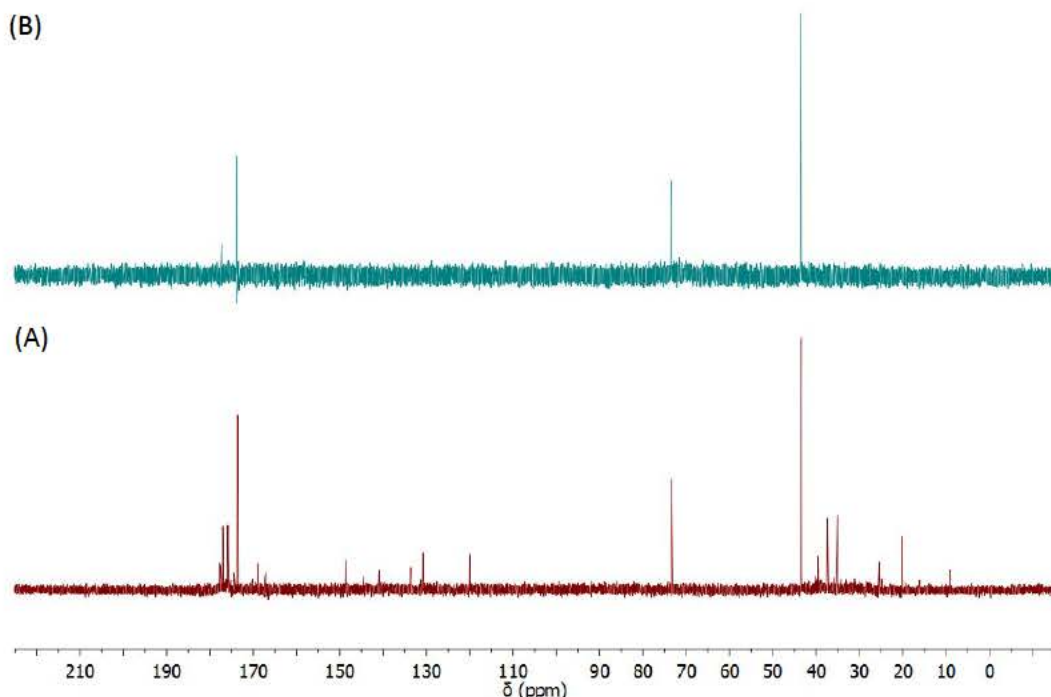


Figure 5.18 –  $^{13}\text{C}$  NMR spectra of the mixtures CA with SHP after (A) 3 hours and (B) 4 hours at 140 °C

The identification of the different compounds done by  $^{13}\text{C}$  NMR has been confirmed by  $^1\text{H}$  NMR. For that the same approach as for  $^{13}\text{C}$  NMR analysis has been followed. In Figure 5.19 is shown the evolution of MAL under thermal treatment with and without SHP in the media. It can be observed that the peaks identified in the starting material can be also identified after thermal treatment. In addition to this, a new peak at 2.16 ppm with weak intensity can be found after thermal treatment of MAL without SHP, assigned to the proton of CH moiety bonded to a carbonyl group such as ketone; the corresponding carbon has been identified by  $^{13}\text{C}$  NMR at 30.07 ppm. When SHP is in the media, additional new peaks at 6.24 and 7.56 ppm appear which are assigned to protons belonging to alkene moieties. Considering these signals together with the peaks identified by  $^{13}\text{C}$  NMR, it is proven that the caramelization process over MAL upon thermal

treatment takes place with and without SHP, but maybe at different speed. The mechanism of caramelization process is highly complex, making it hard to recognize which compounds are the most abundant in each of the different conditions (i.e. with and without SHP).

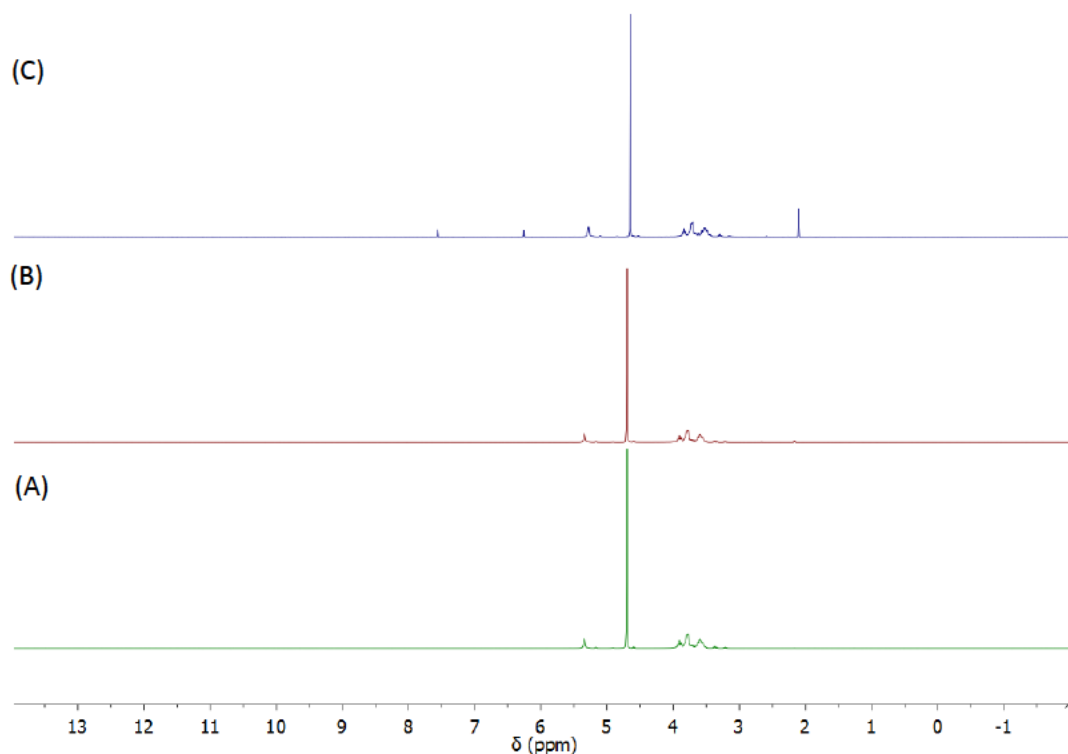


Figure 5.19 –  $^1\text{H}$  NMR spectra of (A) original MAL, (B) MAL after 3 hours thermal treatment at  $140\text{ }^\circ\text{C}$  and (C) mixture of MAL with SHP after 3 hours thermal treatment at  $140\text{ }^\circ\text{C}$

Following, in Figure 5.20 shows the  $^1\text{H}$  NMR spectra of CA upon thermal treatment, with and without SHP, as well as the starting material. The spectrum of CA after treatment without SHP does not give additional information to  $^{13}\text{C}$  NMR, this is the presence of the different ketonic compounds derived from decarboxylation of CA (i.e. 3-oxopentanedioic acids and 3-oxobutanoic acid). Also, as proved by  $^{13}\text{C}$  NMR, the evolution of CA is different when SHP is added. By  $^1\text{H}$  NMR it can be clearly identified a peak at 1.04 ascribed to a  $\text{CH}_3$  moiety, assigned to 2-methylsuccinic. Other signals can also be identified in the range 5.5-7.5 ppm related to methylene moieties and in the range 3.0-3.5 ppm ascribed to proton belonging to a carbon atom bonded to carbonyl carbons. This is quite aligned with the result from  $^{13}\text{C}$  NMR, indicating the existence of carboxylic acids derivatives from CA. However, based on  $^1\text{H}$  NMR it is not possible to conclude which carboxylic acid derivatives are present more than what it has been concluded from the  $^{13}\text{C}$  NMR.

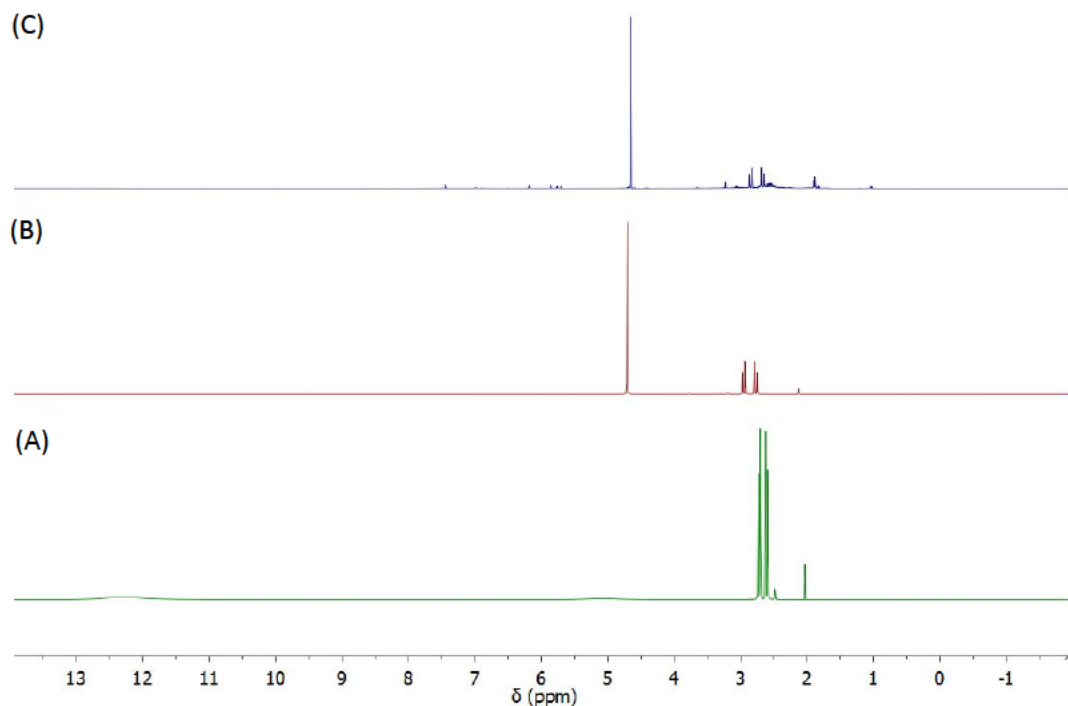


Figure 5.20 –  $^1\text{H}$  NMR spectra of (A) original CA, (B) CA after 3 hours thermal treatment at 140 °C and (C) mixture of CA with SHP, after 3 hours thermal treatment at 140 °C

The assignments done by  $^{13}\text{C}$  NMR have been partially confirmed by 2D-HMBC-NMR, shown in Figure 5.21. The formation of 5-membered ring of citric acid, as well as the citramalic acid is more clearly identified, as well as the 2-methylsuccinic acid. Furthermore, it is possible to identify ketone moieties at around 215 ppm, but it is not possible to distinguish whether this peak is due to the formation of 3-oxopentanedioic acid, 3-oxobutanoic or pyruvic acid. This indicates that apart from the dehydration derivatives from CA, still some product/products due to decarboxylation process is/are generated. Regarding the alkene compounds, it has not been possible to distinguish by the 2D-HMBC-NMR analysis the different derivatives due to their similarity in terms of structure.

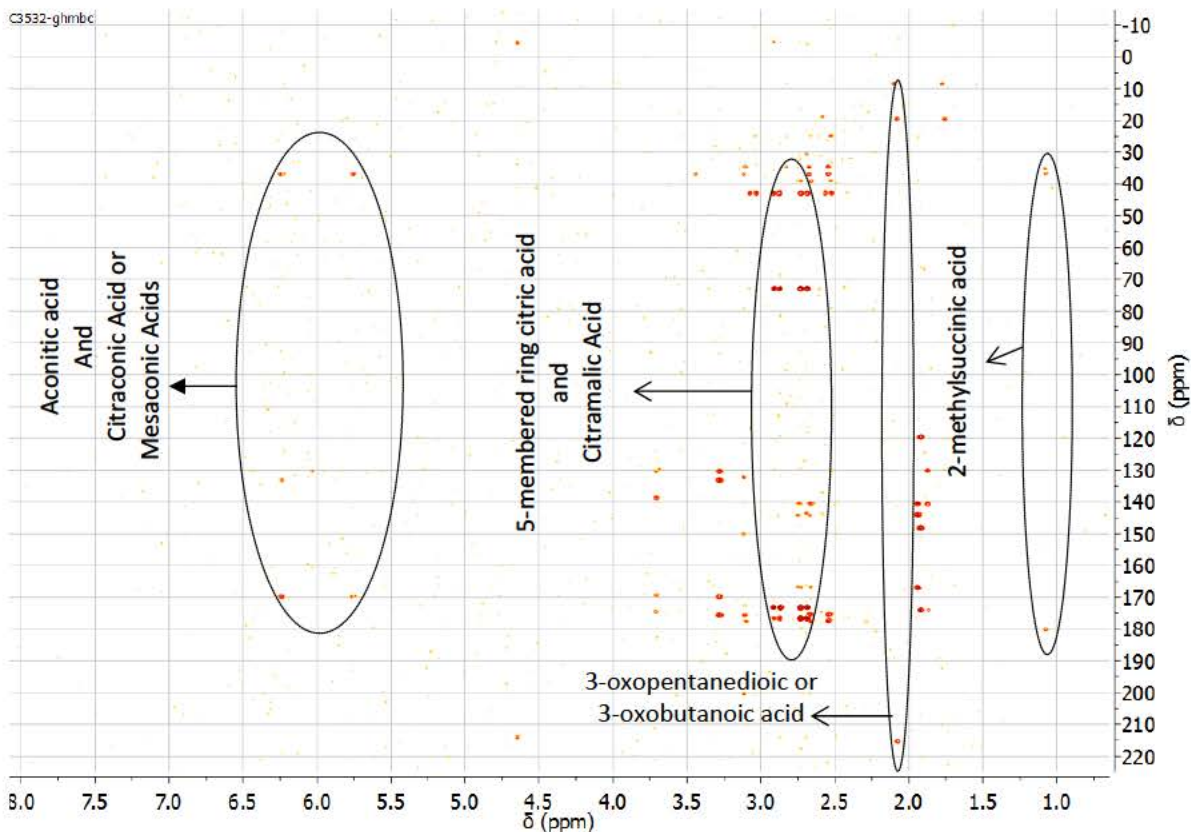


Figure 5.21 – HMBC NMR spectrum of the mixture CA with SHP after 3 hours thermal treatment at 140 °C

The thermal decomposition of CA occur by at least two different mechanisms [40], decarboxylation and dehydration, according to work reported by Y. Yang [37]. Based on the  $^{13}\text{C}$  NMR and  $^1\text{H}$  NMR analysis it is proposed that CA follows mostly the decarboxylation mechanism under thermal treatment at 140 °C when no SHP is in media, while it follows mainly the dehydration mechanism when SHP is present. The mechanism proposed for the transformation of CA when mixed with SHP is depicted in Scheme 5.4. It is particularly relevant the formation of the five membered ring compound derivative from CA, which is a more reactive compound in the esterification with MAL. Apart from this, it takes place mostly the formation of alkene carboxylic acids such as aconitic acids, citraconic acid, itaconic acid and mesaconic acid. Furthermore, due to the presence of SHP, 2-methylsuccinic acid is formed by partial reduction of mesaconic acid leads to the formation of 2-methylsuccinic acid.

Due to the formation of CA derivatives when mixed with SHP, the reactivity of the system containing MAL and CA was expected to be different when SHP is added.  $^{31}\text{P}$  NMR analysis was carried out in order to further understand the possible new interactions between MAL and CA

when SHP is in the media, like for instance the formation of acylphosphinates described in previous works [41, 42].

In Figure 5.22 is compared the  $^{31}\text{P}$  NMR spectra of SHP and the mixture of CA with SHP (C3SHP) after 3 hours thermal treatment at 140 °C. In the spectrum of SHP shows a main signal at 8.08 ppm assigned to hypophosphite while in the spectrum of the mixture C3SHP an additional signal at 3.98 ppm can be found. It is important to note that in the mixture with CA, SHP will convert partially to its acid form [15]. On the other side, it is known that hypophosphorous acid undergoes disproportionation when heated at least at 130 °C leading mostly to phosphorous acid [43, 44]. Considering this, the signal at 3.98 ppm is assigned to the phosphorous acid.

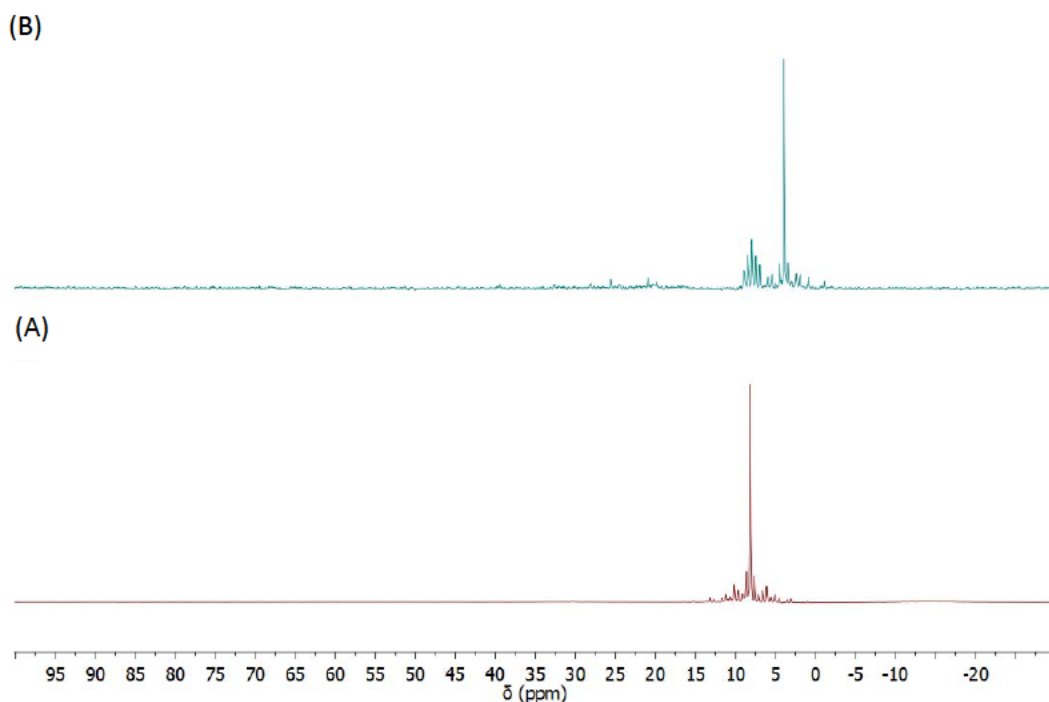


**Figure 5.22 –  $^{31}\text{P}$  NMR spectra of (A) original SHP and (B) mixture of CA with SHP after 3 hours thermal treatment at 140 °C**

Furthermore, in the spectrum of the mixture C3SHP (Figure 5.23) additional signals can be identified at 20.91, 25.97 and 28.07 ppm assigned to alkyl derivatives of hypophosphorous acid, and signals at 32.65 and 39.41 are assigned to alkyl derivatives of phosphorous acid [45]. All these signals indicate that the phosphorous compounds (i.e. hypophosphorous and phosphorous) are bonded to alkyl compounds derivatives from CA after the thermal treatment. Several reactions of phosphorous acids with organocompounds are well described in the bibliography. For instance,

phosphorous acids can react with olefins; they can also react with ketones under heating and third, they can react with tertiary alcohols [43]. These three reactions could take place between the CA derivatives and SHP upon thermal treatment leading to a mix of organophosphorus compounds. However it is not possible to distinguish each individual organophosphorus compound by NMR analysis.

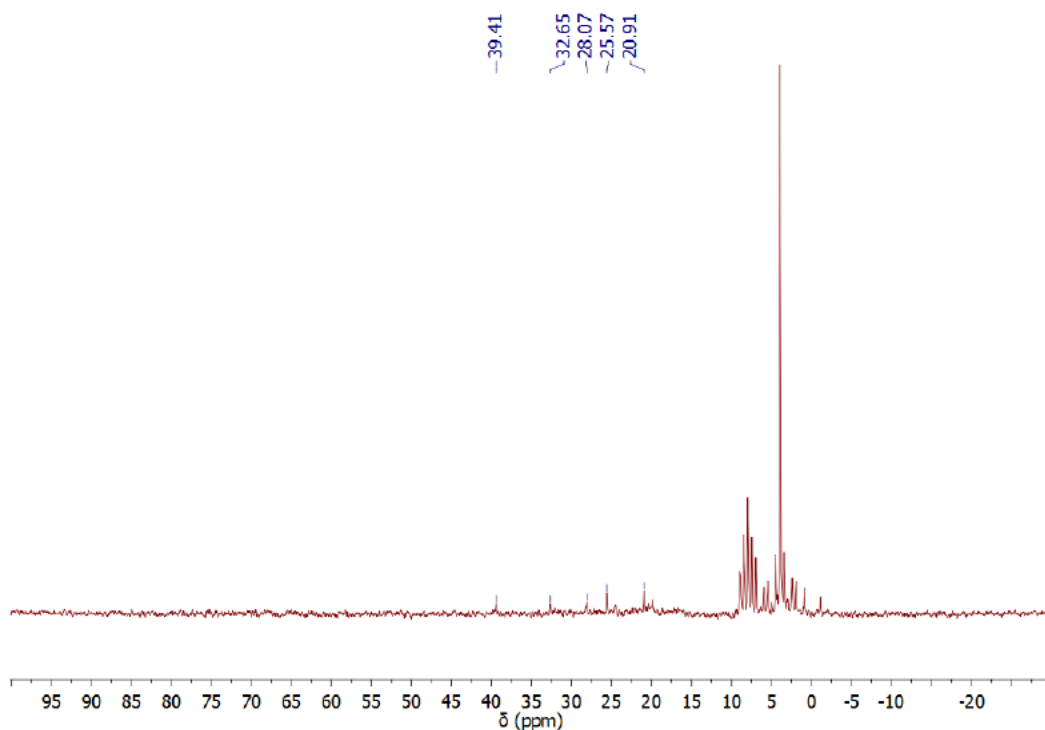


Figure 5.23 –  $^{31}\text{P}$  NMR spectra of the mixtures CA with SHP after 3 hours thermal treatment at 140 °C

In Figure 5.24 is compared the spectra of mixture C3SHP with the compositions M60C3SHP, both after 3 hours thermal treatment. First it can be observed that the signals assigned to hypophosphorus and phosphorus acids remains in the composition M60C3SHP after thermal treatment. Regarding to the signals assigned to the organophosphorus compounds, the ones at around 20 and 25 ppm still remains in the composition M60C3SHP after thermal treatment. These signals cannot be identified in the soluble part of the cured composition M60C3SHP after 4 hours (Figure 5.25). This may indicate that all possible organophosphorus compounds are part of the insoluble polymer network formed by curing treatment in the composition M60C3SHP.



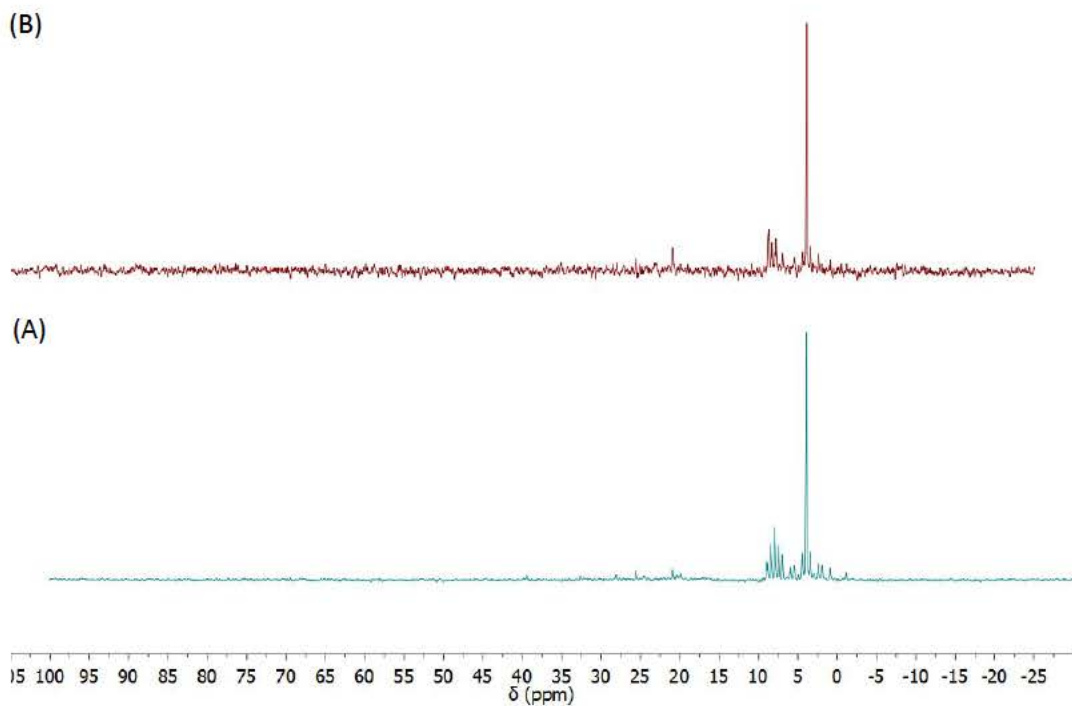


Figure 5.24 –  $^{31}\text{P}$  NMR spectra of (A) mixture of CA with SHP and (B) the composition M60C3SHP, all after 3 hours thermal treatment at 140 °C

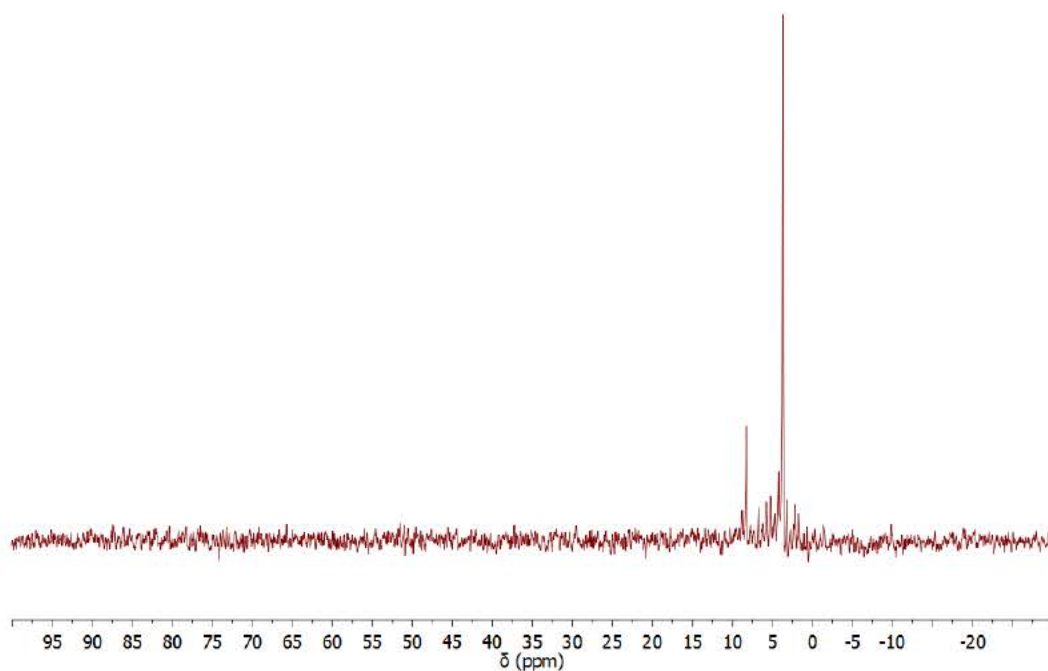
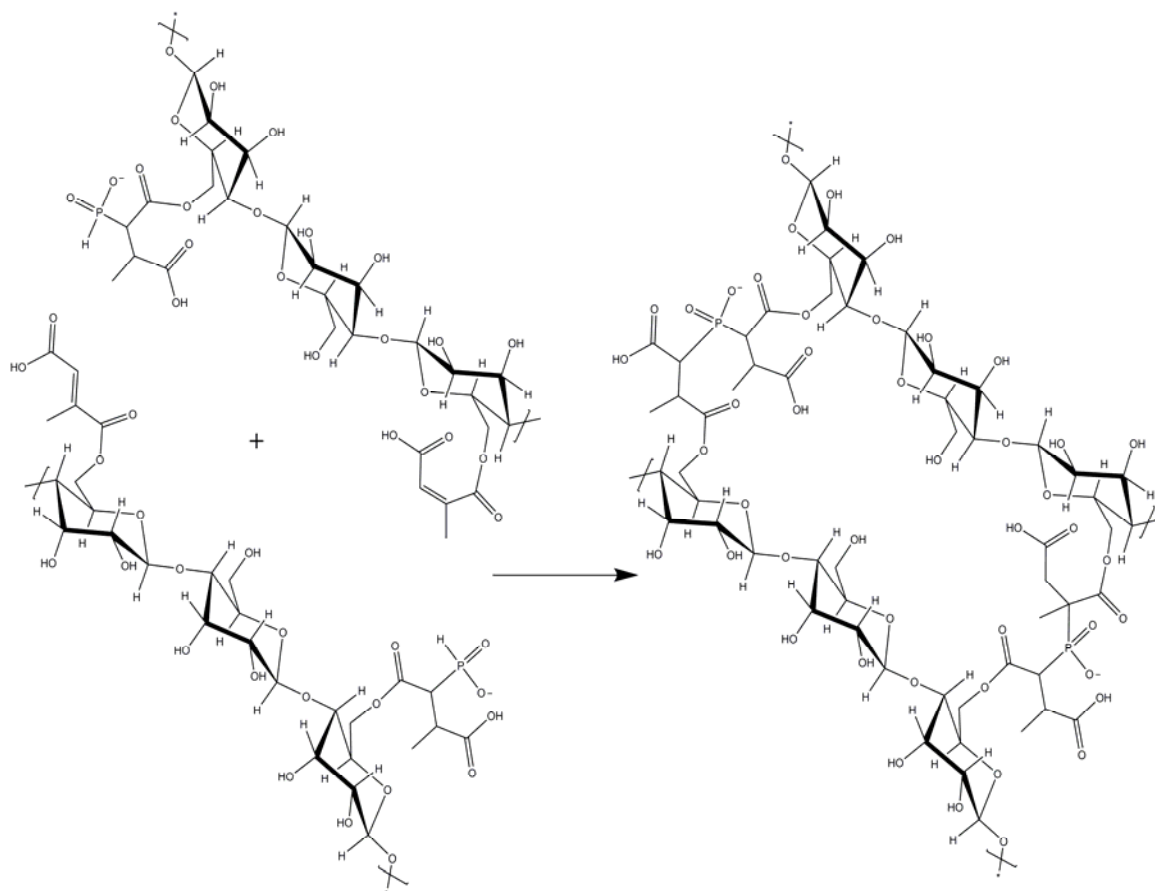


Figure 5.25 –  $^{31}\text{P}$  NMR spectra of the composition M60C3SHP after 4 hours thermal treatment at 140 °C

By  $^{31}\text{P}$ -NMR analysis it is demonstrated that apart from the dehydration mechanism of CA, which lead to different alkene polycarboxylic acids; the latter may react with the phosphorous compounds through their double bond C=C. This would enable the possibility of SHP to work as crosslinker [20, 22, 23, 42], being incorporated into the polymer network formed between MAL, CA and CA derivatives as shown in Scheme 5.5. As mentioned above, the only polycarboxylic acid partially remaining not reacted, but in the solution, after 4 hours curing is the CA; therefore, the rest of the polycarboxylic acids (i.e. CA derivatives) are part of the polymer network together with the alkyl phosphorous compounds.



**Scheme 5.5 – Polymer network including crosslinking with SHP**

The results are quite revealing because they suggest that the SHP added as catalyst in the system containing MAL and CA works in two different ways. First, it promotes the dehydration of CA over the decarboxylation. This generates more reactive species, like 5-membered ring, which accelerates the esterification reaction between MAL and CA. Second, the phosphorous compounds react with the alkene CA derivatives. As a consequence, SHP plays the role of

crosslinker, bonding different condensation products result of the esterification reaction between MAL and one carboxylic acid group of the different polycarboxylic acids (Scheme 5.5). Both mechanisms may explain the higher crosslinking rate and the better mechanical performance of the system containing MAL and CA when SHP is present.

## 5.6 CONCLUSIONS

---

The reactivity of the thermoset system comprising maltodextrin and citric acid can be improved by the addition of sodium hypophosphite, leading to a better mechanical performance of the glass fiber material.

Sodium hypophosphite accelerates the esterification reaction between maltodextrin and citric acid. This makes possible to decrease the temperature of the thermal treatment from 140 to 130 °C reaching the same degree of esterification. It also accelerates the speed of crosslinking leading to shorter gel time and reaching the maximum moduli of the crosslinked system in shorter time. In fact, the apparent activation energy is lower when sodium hypophosphite is added to the system containing maltodextrin and citric acid.

The impact of the sodium hypophosphite is also noticeable in the mechanical properties of the glass fiber material, increasing the stiffness and the endurance to weathering conditions. Therefore, the material becomes a better thermoset.

It has been demonstrated by NMR that sodium hypophosphite plays two main roles in the polycondensation reaction between maltodextrin and citric acid. The first refers to dehydration process of citric acid, which leads to more reactive species (e.g. cyclic anhydride). By the generation of the new species the esterification reaction with the hydroxyl groups of maltodextrin goes faster. This may explain as well the acceleration of the polycondensation process. The second role refers to the crosslinking activity of the sodium hypophosphite. It can react with the double bonds C=C of the citric acid derivatives (formed after dehydration of citric acid) which are linked by the carboxyl group to the maltodextrin. This would enhance the crosslinking of the system.

Based on the results obtained, it is worth to say that the system comprising maltodextrin and citric acid with sodium hypophosphite as catalyst is the most preferable system among the ones

studied in this thesis work, to be considered in industrial applications like, for instance, manufacturing of mineral wool insulation material.

## 5.7 REFERENCES

---

1. Otera J and Nishikido J. Reaction of Alcohols with Carboxylic Acids and their Derivatives. Esterification: Wiley-VCH Verlag GmbH & Co. KGaA, 2010. pp. 3-157.
2. John C. Gilbert SFM. Experimental Organic Chemistry: A Miniscale and Microscale Approach, 6th ed. Boston: Cengage Learning, 2015.
3. Chrissafis K, Paraskevopoulos KM, Papageorgiou GZ, and Bikiaris DN. Journal of Analytical and Applied Pyrolysis 2011;92(1):123-130.
4. Tsai C-J, Chang W-C, Chen C-H, Lu H-Y, and Chen M. European Polymer Journal 2008;44(7):2339-2347.
5. Umare SS, Chandure AS, and Pandey RA. Polymer Degradation and Stability 2007;92(3):464-479.
6. Olivato JB, Müller CMO, Carvalho GM, Yamashita F, and Grossmann MVE. Materials Science and Engineering: C 2014;39(0):35-39.
7. Olivato JB, Grossmann MVE, Bilck AP, and Yamashita F. Carbohydrate Polymers 2012;90(1):159-164.
8. T. Heinze TL, A. Koschella. Esterification of Polysaccharides. Germany: Springer-Verlag Berlin Heidelberg, 2006.
9. Kapuśniak J. Journal of Polymers and the Environment 2005;13(4):307-318.
10. Bai Y and Shi Y-C. Carbohydrate Polymers 2011;83(2):520-527.
11. Welch CM. Textile Research Journal 1988;58(8):480-486.
12. Yao W, Wang B, Ye T, and Yang Y. Industrial & Engineering Chemistry Research 2013;52(46):16118-16127.
13. Widsten P, Dooley N, Parr R, Capricho J, and Suckling I. Carbohydrate Polymers 2014;101:998-1004.
14. Zhao C and Sun G. Industrial & Engineering Chemistry Research 2015;54(43):10553-10559.
15. Ji B, Tang P, Yan K, and Sun G. Carbohydrate Polymers 2015;132:228-236.
16. Yang CQ and Wang X. Journal of Polymer Science Part A: Polymer Chemistry 1997;35(3):557-564.
17. Mao Z and Yang CQ. Journal of Applied Polymer Science 2001;81(9):2142-2150.
18. Yang CQ. Journal of Polymer Science Part A: Polymer Chemistry 1993;31(5):1187-1193.

19. Yang CQ. *Journal of Applied Polymer Science* 1993;50(12):2047-2053.
20. Yang CQ, Chen D, Guan J, and He Q. *Industrial & Engineering Chemistry Research* 2010;49(18):8325-8332.
21. Yang CQ, Xu Y, and Wang D. *Industrial & Engineering Chemistry Research* 1996;35(11):4037-4042.
22. Yang CQ, He Q, and Voncina B. *Industrial & Engineering Chemistry Research* 2011;50(10):5889-5897.
23. Peng H, Yang CQ, Wang X, and Wang S. *Industrial & Engineering Chemistry Research* 2012;51(35):11301-11311.
24. Halpern JM, Urbanski R, Weinstock AK, Iwig DF, Mathers RT, and von Recum HA. *Journal of Biomedical Materials Research Part A* 2014;102(5):1467-1477.
25. B. Jaffrennou DS, J. Douce. Sizing composition for mineral wool comprising a monosaccharide and/or a polysaccharide and an organic polycarboxylic acid, and insulating products obtained, US8951341B2. US: Saint-Gobain Iover, 2008.
26. Lessan F, Montazer M, and Moghadam MB. *Thermochimica Acta* 2011;520(1-2):48-54.
27. Hashemikia S and Montazer M. *Applied Catalysis A: General* 2012;417-418:200-208.
28. Tung C-YM and Dynes PJ. *Journal of Applied Polymer Science* 1982;27(2):569-574.
29. Martin JS, Laza JM, Morrás ML, Rodríguez M, and León LM. *Polymer* 2000;41(11):4203-4211.
30. Buchdahl R. *Journal of Polymer Science: Polymer Letters Edition* 1975;13(2):120-121.
31. Pan X, Sengupta P, and Webster DC. *Biomacromolecules* 2011;12(6):2416-2428.
32. Ma Q, Liu X, Zhang R, Zhu J, and Jiang Y. *Green Chemistry* 2013;15(5):1300-1310.
33. Wangsakan A, McClements DJ, Chinachoti P, and Charles Dickinson L. *Carbohydrate Research* 2004;339(6):1105-1111.
34. Kroh LW. *Food Chemistry* 1994;51(4):373-379.
35. Luna M and Aguilera J. *Food Biophysics* 2014;9(1):61-68.
36. Fischer JW, Merwin LH, and Nissan RA. *Applied Spectroscopy* 1995;49(1):120-126.
37. Ye T, Wang B, Liu J, Chen J, and Yang Y. *Carbohydr Polym* 2015;121:92-98.
38. Sharma A, Cody GD, Scott J, and Hemley RJ. Chapter 3 - Molecules to Microbes: In-Situ Studies of Organic Systems Under Hydrothermal Conditions A2 - Manaa, M. Riad. *Chemistry at Extreme Conditions*. Amsterdam: Elsevier, 2005. pp. 83-108.
39. Duddeck H. *Magnetic Resonance in Chemistry* 2002;40(3):247-247.
40. Dollimore D and O'Connell C. *Thermochimica Acta* 1998;324(1-2):33-48.
41. Coma V, Sebti I, Pardon P, Pichavant FH, and Deschamps A. *Carbohydrate Polymers* 2003;51(3):265-271.
42. Peng H, Yang CQ, and Wang S. *Carbohydrate Polymers* 2012;87(1):491-499.
43. Frank AW. *Chemical Reviews* 1961;61(4):389-424.

44. Hopkins BS. *Journal of Chemical Education* 1937;14(12):600.
45. Klein H-F. *Angewandte Chemie International Edition* 2005;44(45):7331-7331.

---

# *CHAPTER VI*

---

## *APPLICATION OF BINDER FORMULATION BASED ON MALTODEXTRIN AND CITRIC ACID IN THE MINERAL WOOL INDUSTRY*

---





## 6.1 INTRODUCTION

---

### 6.1.1 BINDER IN THE MINERAL WOOL MANUFACTURING PROCESS

---

The binder used in the mineral wool manufacturing process is a water mixture containing 5-15 % of active material. As mentioned in Chapter I, it comprises a thermoset resin and several additives and its application manufacturing process is mainly relevant in two steps; first in the fiberization and collecting step, and secondly in the curing step [1]. In the fiberization step a so-called binder ring is located just below the fiberization disk. The binder is sprayed over the fibers when these last go through the binder ring (Figure 6.1).

The fibers sprayed with binder are collected on a conveyor belt. By this step, the loose fibers join together and they lose part of the water before entering in the curing step. In the curing oven the thermoset resin sets and the loose fibers turn into a fibrous mat. The ratio of cured binder in finish product (i.e. fiber with cured binder) after curing step is 3-15 % relative to the total weight of the product, depending on the finish product requirements.



Figure 6.1 – Spraying of binder over fibers just after fiberization [2]

#### 6.1.1.1 CURING OF BINDER

---

The joint fiber mat coming from collecting step enters in a curing oven and it is moved along the curing oven in-between two metal belts. These belts compress and move the fiber mat

forward, fixing the thickness of the mat during the thermal processing (Figure 6.2). This allows to get bonded the non-woven fibers with the proper conformation to obtain the finish product. For curing, the energy in the oven is obtained by gas combustion, and the air inside the oven is strongly recirculated, passing through the mat in the direction normal to its larger surfaces. This method makes the volatiles generated by the curing reaction to be released faster and the heat exchange more efficient; therefore it accelerates the curing process. The curing oven is divided in several zones, for instances, 6 zones. In the first half of the total of zones the air goes through the product from bottom to top side, while in the second half the air goes through the product from top to bottom side.



**Figure 6.2 – Curing oven for mineral wool manufacturing [2] (left) and mineral wool mat entering in the curing oven (right)**

The temperature inside the product is lower than the set point of the curing oven as consequence of the insulation capacity of the product. For that reason, in order to control the curing process, the temperature in the product is monitored by a thermocouple connected to a data logger device. As an example, in Figure 6.3 is shown a temperature profile measured in four different points across the width of the fiber mat along the curing process. The product is remaining in the curing oven 1-4 min depending on the speed of the production line and the length of the curing oven. The speed of the production line is adjusted according to the grams of material by square meter required for a product with a given density and thickness. As a consequence, the curing oven conditions, temperature and speed of air fans, need to be adjusted to get proper curing. Normally, the higher the speed of the production line, the higher the temperature set point and the speed of the air fans needs to be set. The optimal curing profile for

a certain product would also depend on the binder curing behavior and thus, of its chemical composition.

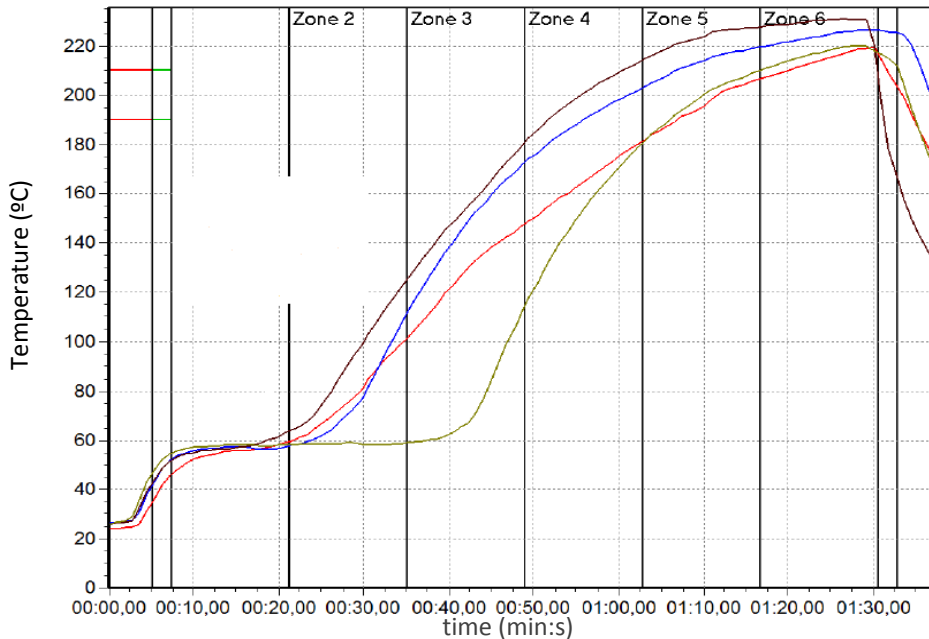


Figure 6.3 – Temperature profile in four different points across the width of the fiber mat in the curing oven

## 6.1.2 SPECIFICATIONS OF MINERAL WOOL INSULATION MATERIALS

The specifications of thermal insulation materials are different depending on their final application, either buildings, building equipment or industrial installations. Nevertheless, thermal conductivity ( $\lambda$ ) is their most important property. The thermal conductivity defines the ability of the material to conduct heat at a given temperature. Therefore it indicates the insulation capacity of the material. The higher the thermal conductivity the lower the insulation capacity of the material is.

Thermal insulation materials based on mineral wool resist heat flow due to air cavities (i.e. dead air-cells) existing in the interior of the material. This reduces (by hindering the air movement) convective heat transfer. It is the air entrapped in the insulation material which provides the major contribution to thermal resistance, not the solid part of the material. Creating small cells, when the temperature difference between both sides of insulation material is not high also reduces the thermal conductivity by radiation. The small cells make the radiation paths to be

broken within small distances, in this way the long-wave infrared radiation is absorbed and/or scattered by the insulation material. However, conduction usually increases as the cell size decreases. Therefore, the combination of the three ways of heat transfer (i.e. convection, radiation, conduction) determines the effectiveness of the insulation material. It is important to note that the air-based insulation materials, such as mineral wool, cannot go below the thermal conductivity of static dry air. However, others like plastic foam insulation which use fluorocarbon gas instead of air in their cells lead to lower thermal conductivity [3].

The most accurate way to determine thermal conductivity is to measure it according to a standard method, such as the steady-state methods, guarded hot plate and the heat flow meter hot plate [4-7]. Among these, the norm EN 12667:2008 is the most frequently used for the measurement of thermal conductivity of mineral wool insulation materials [7].

Apart from thermal conductivity, other properties are specified for mineral wool insulation materials according to the European standard norm EN 13162:2008 [8]. This document was prepared by the Technical Committee CEN/TC 88 “Thermal insulating materials and products”. It specifies the relevant product characteristics and includes also procedures for testing, evaluation of conformity, marking and labelling; but it does not specify the required level of a given property to be achieved by a product used in a particular application. This last is normally established by the mineral wool manufacturer based on the requirements of the different applications. The most common product properties and the corresponding test methods specified by the mineral wool manufacturers are quoted in Table 6.1.

**Table 6.1 – Properties and test methods according to EN 13162:2008**

<b>Property</b>	<b>Test Method</b>
<b>Thermal resistance – thermal conductivity</b>	EN 12667 [7]
<b>Length and width</b>	EN 822 [9]
<b>Thickness</b>	EN 823 [10]
<b>Tensile strength parallel to faces</b>	EN 1608 [11]
<b>Reaction to fire</b>	EN 13501-1 [12]
<b>Short term water absorption</b>	EN 1609 [13]

The length and width specification refers to the measured full-size products, either blankets or slabs of mineral wool. The measurement procedure is given by the norm EN 822 [9] sets the positions to do the measurement (Figure 6.4) and its tolerances.

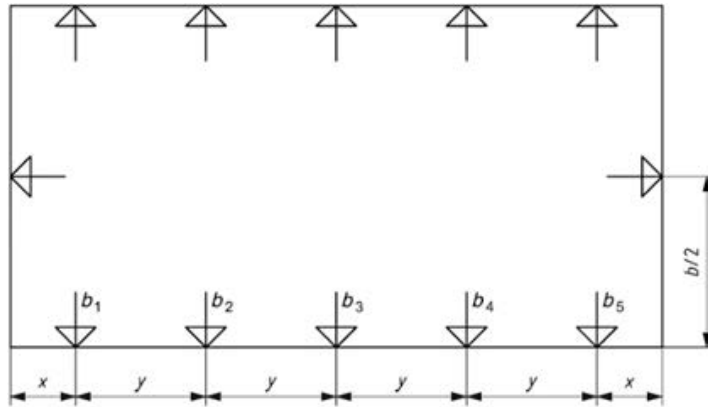


Figure 6.4– Positions to measure length and width of a product which length is  $\geq 4.5$  m and width is  $\leq 1.5$  m

The thickness specification refers also to the measured thickness of a full-size product. For the measurement it is used a device which is able to press the product surface with a given pressure in different positions (Figure 6.5) according to the norm EN 823 [10].

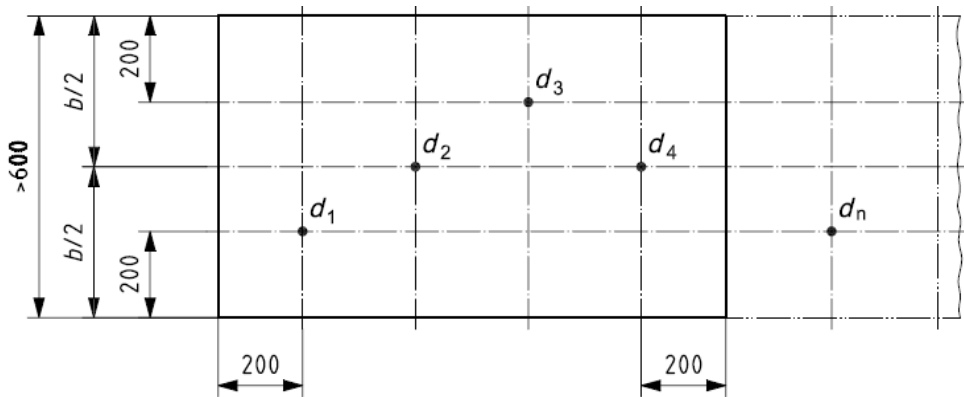
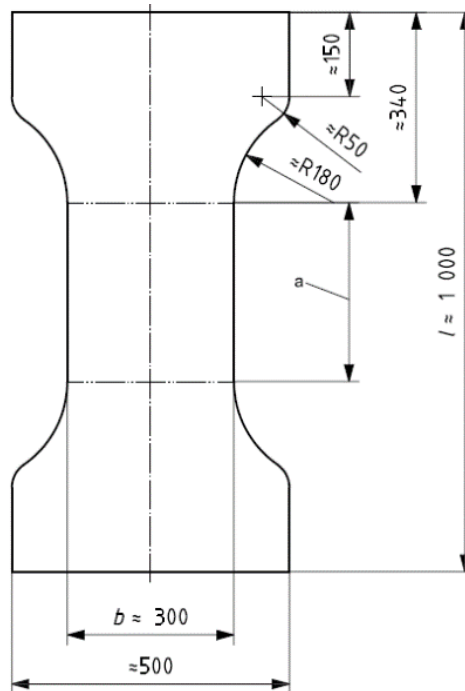


Figure 6.5 – Positions to measure thickness of a product which width is  $> 600$  mm (dimensions in mm)

The specification “tensile strength parallel to faces” refers to the measured tensile strength of the product, parallel to its faces. The aim of this specification is to determine whether the product has sufficient strength to withstand stresses during its transportation and application. For the measurement, a test specimen is attached between two clamps in a tensile testing machine; then it is pulled at a given speed until the specimen is broken. The value taken according to the specification is the maximum load achieved before the specimen is broken. In Figure 6.6 is shown an example of the specimen shape, according to the norm EN 1608 [11].



**Figure 6.6 – Shape and dimensions in mm of the specimen for the measurement of tensile strength**

The norm EN 13501-1 [12] specifies the classification of construction products according to their reaction to fire as class A1, A2, B, C, D, E or F. Where the order from less reactive to more reactive to fire is  $A1 < A2 < B < C < D < E < F$ . The classification is done based on the values of some properties such as temperature increase due to the reaction to fire, loss of weight of the material and the time that the flame remains, all according to the norm EN ISO 1182 [14]; and heat combustion of the material measured according to the norm EN ISO 1716 [15].

The specification for the short term water absorption refers to the capacity of the product to uptake water when it is partially immersed in water for 24 hours. In Figure 6.7 is shown the device to immerse the product sample according to the norm [13]

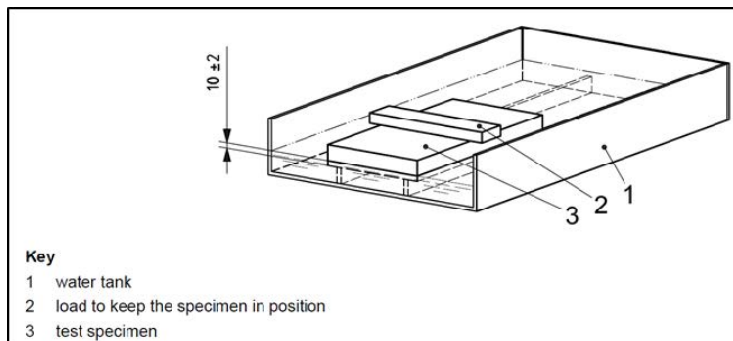


**Figure 6.7 – Example of device to immerse the product sample to test short water absorption**

Additionally to the declared properties, the mineral wool product as other construction materials is required to preserve the properties after long time installed. In order to test the behavior of the product against environmental conditions for long time, a so-called accelerated aging treatment is applied to the product. For that the product is stored in a climate chamber for certain time, at a given temperature and humidity; and after the aging treatment, the most affected properties of the product are tested again, like for instance, the tensile strength parallel to faces.

## 6.2 AIM OF THIS CHAPTER

---

The steps of the mineral wool manufacturing process where the binder is involved cannot be fully reproduced at lab scale. Therefore the behavior of the polycondensation systems studied in previous chapters cannot be fully predicted in the industrial process and finished product just by lab testing. For that reason the system comprising maltodextrin, citric acid and sodium hypophosphite has been tested at industrial scale. Several glass wool products, with different density and thickness recommended for different applications have been produced. The properties of the different products have been evaluated in order to establish whether they comply with the mineral wool specifications.

As a representative example, in this chapter is described the industrial test run in a glass wool manufacturing plant and the properties of the resulting product: a glass wool mat with thermal conductivity  $A \text{ W/m}\cdot\text{K}$ , density around  $B \text{ kg/m}^3$  and thickness  $C \text{ mm}$ , packed in rolls.

## 6.3 MATERIALS AND METHODS

---

### 6.3.1 MATERIALS

---

For the thermoset system it was used commercial powdered maltodextrin, manufactured by spray-drying of liquid maltodextrin derived from starch enzymatic hydrolysis; crystalline white powder of anhydrous citric acid (CA) and, sodium hypophosphite monohydrate. For the binder

system three additives were used: a coupling agent, a water repellent and a de-dusting agent. The products were used without additional purification.

## 6.3.2 METHODS

---

Industrial production of glass wool insulation material was carried out for a product with density B kg/m<sup>3</sup>, thickness C mm and declared thermal conductivity A W/m·k. The details about binder and the thermoset system used are described below.

### 6.3.2.1 BINDER PREPARATION

---

A thermoset system containing MAL and CA with SHP was mixed in water at the ratio shown in Table 6.2.

**Table 6.2 – Composition of the thermoset system**

Reactant	% in total dry weight
MAL	30-70
CA	30-70
SHP	0.5-5.0

For that it was prepared a batch with nearly 6 tons of mixture at 30 % dry content. MAL was dissolved in city water under mechanical stirring and then CA was added keeping the stirring until the solution was homogeneous. Finally SHP was added keeping the same stirring conditions until it was completely dissolved. The quantities of each material added in the mixture are quoted in Table 6.3.

**Table 6.3 – Quantities of different reactants added in the batch preparation of the thermoset system**

Reactant	kg
MAL	E
CA	F
SHP	G
Water	H



The mixture shown in Table 6.3 (thermoset system) was prepared and introduced in the production line together with the additives through system of pipes as depicted in Figure 6.8. The final dry content of the binder was approximately 11 % dry content, shared by the different components as indicates in Table 6.4.

Reactant	% in total dry weight
Thermoset system	J
Coupling agent	L
Water repellent	M
De-dusting oil	N

The flow of binder and each different component was adjusted accordingly to get around D % cured binder in the finished product (i.e. relative to the fiber plus cured binder).

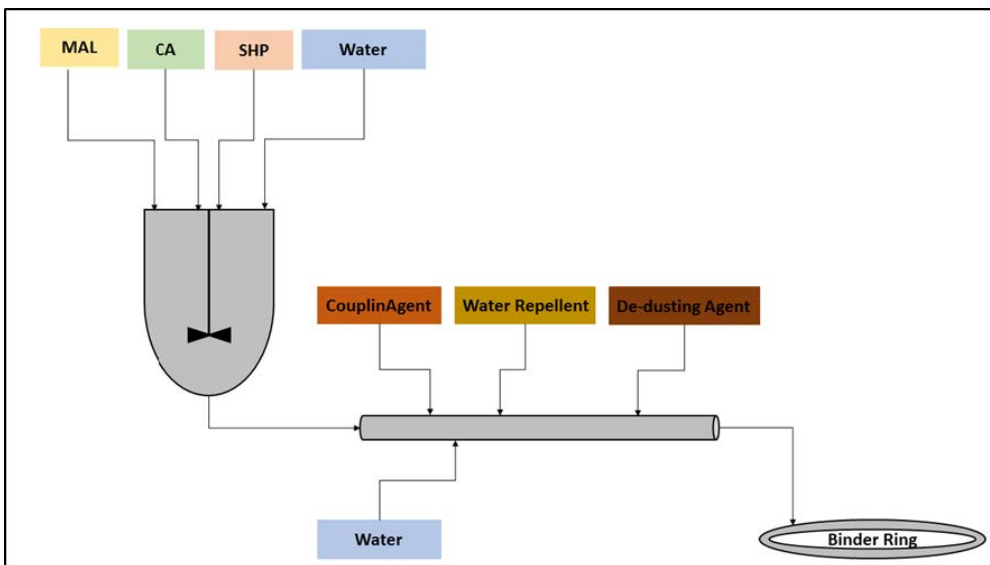


**Figure 6.8 – Flow-chart of the binder preparation**

### 6.3.2.2 CURING OVEN

The binder system was sprayed on the glass fibers and subsequently, the fibers collected into a mat. The fiber mat joint by the binder was introduced in the oven following the typical mineral wool manufacturing steps. The curing oven had O heating zones with the set points shown in Table 6.5. The product remained in the oven around 1.5 min.

**Table 6.5 – Set points for temperature, speed of fan for air recirculation and the direction of the air flow**

	<b>Zone 1</b>	<b>Zone 2</b>	<b>Zone 3</b>	<b>Zone 4</b>	<b>Zone 5</b>	<b>Zone 6</b>
<b>T (°C)</b>	P	Q	R	S	T	U
<b>Fan flow (rpm's)</b>	V	W	X	Y	Z	ZZ
<b>Air flow direction</b>	↑	↑	↑	↓	↓	↓

### **6.3.3 CONTROL OF MANUFACTURING PROCESS**

---

The process was controlled by the automatic systems installed in the production line. The process parameters controlled were the following:

- Flow of reactants and water depending on the quantity of fiber produced per hour.
- Dry content of thermoset system preparation and the binder preparation.
- Temperature and speed of fans in the curing oven.
- Density of the product as well as its distribution all over the surface of the product.
- Thickness of the product.
- Packaging parameters such as the roll diameter of the product and weight of roll.

### **6.3.4 CONTROL OF PRODUCT SPECIFICATIONS**

---

The product specifications were checked according to the norms described in the introduction of this chapter (Table 6.1) after CC weeks storing the product at room temperature. By keeping the product 9 weeks in the storage before testing we assure that the samples are representative of the product delivered to the market. Apart from the standard tests quoted in Table 6.1, other analyses in the finished product were done as explained next.

#### **6.3.4.1 AGING BEHAVIOR TEST**

---

Samples of the product obtained by the manufacturing process were kept under humidity 95 % and temperature 35 °C for 1 week in a climate chamber; this is known as aging treatment. After this treatment the most affected properties [16] of product were checked, such as, tensile

strength of product parallel to faces was tested according to the norm EN 1608 [11], as well as thickness (norm EN 823 [10]).

#### *6.3.4.2 RESISTANCE TO GROWTH OF MICROORGANISMS*

---

The product obtained from the industrial test was analyzed according to the norm EN 846, method A and B [17], in order to determine the resistance to growth of microorganisms in the mineral wool product manufactured with bio-based thermoset system comprising MAL and CA. The samples required for the analysis were prepared according to the norm.

#### *6.3.4.3 FORMALDEHYDE EMISSIONS TEST*

---

The emissions of formaldehyde were determined for the product obtained from the industrial test according to the norm EN 16000-3 [18] after 7 days keeping the sample of product in measurement chamber. It is known that after 7 days the formaldehyde emissions reach its maximum in a mineral wool product [19], therefore this measurement is considered representative of the capacity of the product to release formaldehyde.

## **6.4 RESULTS AND DISCUSSION**

---

### **6.4.1 PROCESS PARAMETERS**

---

The flow rate of the different reactants and water into system of pipes, and the flow rate of binder are quoted in Table 6.6. All these flow rates provided given by the automatic system of the production line, for FF % efficiency of the process (measured as percentage by dividing the quantity of dry binder obtained in finished product by the quantity of binder introduced in the process, taken for example 1 kg of finished product as reference), dry content of the binder sprayed GG % in relation to the weight of fibers, and the target dry binder content in finished product HH %.

**Table 6.6 – Flow of the different the reactants and water in the pipes system, and the flow of binder**

<b>Reactant</b>	<b>Flow (kg/h)</b>
<b>Thermoset system</b>	II
<b>Coupling agent</b>	JJ
<b>Water repellent</b>	KK
<b>De-dusting agent</b>	LL
<b>Water</b>	MM
<b>Binder</b>	NN

The curing oven conditions applied were the ones shown in Table 6.5 and the profile of temperature measured inside the product is shown in Figure 6.9. It can be observed that the water evaporation temperature (i.e. 100 °C) is achieved at the end of zone 1, therefore in the first zone all the energy is spent for initial warming up; neither water evaporation nor polycondensation reaction has started in this zone. Evaporation of water would start in zone 2, and also at the end of this zone the polycondensation reaction may start based on the results from previous research work (Chapter II-V). From the end of zone 2 to the middle of zone 5 the temperature in the product is continuously increasing. When the temperature is higher than approximately 170 °C, the polycondensation system may have partially decomposed. This would happen as from beginning of zone 3. In the second half of zone 5 and full zone 6, the temperature is more or less constant at 230 °C. The product remained in the oven 1.5 min in total, from which the product was 75 seconds at temperature higher than 140 °C. As a consequence of the high temperatures inside the product, the polycondensation system is able to react but it would be also partially decomposed. That is one of the reasons to have less than 100 %, and in fact FF %, efficiency of the process in terms of dry binder in the finished product. The other reason for the FF % efficiency of the process is the binder lost in the forming step of the manufacturing process. At this step the mat of joint fibers is hold down to the metal belt helped by the suction air from beneath belt. This suction hold the mat of fibers resting on the moving belt, as it is being transported downstream to the curing oven. As a negative consequence of this suction, the binder is carried by the suctioned air through the belt into the waste or process water, and thus, it does not contribute to bonding of the sprayed fibers. Nevertheless this efficiency depends on the productions line set-up mainly, as it is similar to the efficiency of phenolic resin.

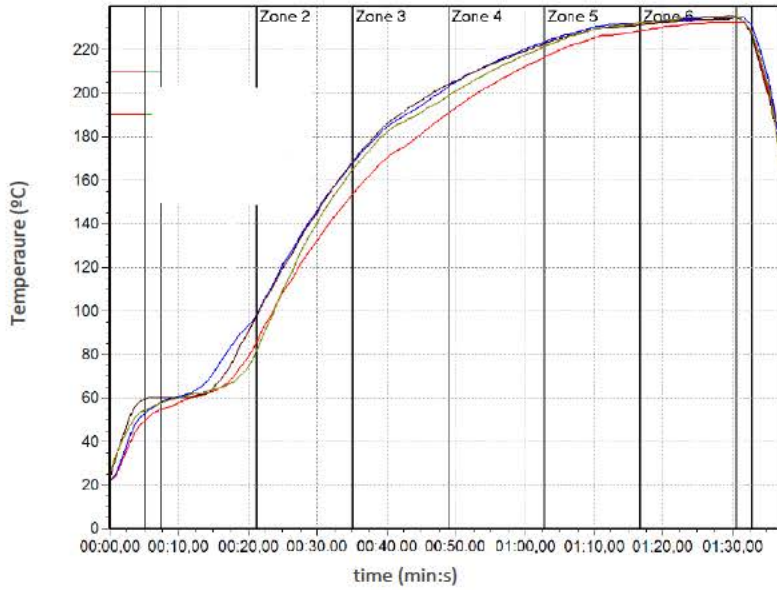


**Figure 6.9 – Temperature profile in four different points in the fiber mat inside the curing oven**

After the curing oven, the product mat is cut and roll-up, giving rolls of around 00 m long and PP m width. The resulting product after opening one roll is shown in Figure 6.10.



**Figure 6.10 – Finished product from industrial test after open the roll packaging**

## 6.4.2 PRODUCT PROPERTIES

---

### 6.4.2.1 THERMAL CONDUCTIVITY

---

Thermal conductivity at 10 °C was tested according to the norm EN 12667 [7] by the heat flow meter method, with a single sample and symmetric configuration. The temperature between plates was 20 °C, with cold plate at 0 °C and hot plate at 20 °C. It is important to note that the norm does not specify the value of thermal conductivity declared, but how to measure and calculate it. Two specimens were cut from a full-size roll of product. The average value obtained is shown in Table 6.7. The thermal conductivity value complies with the declared value. This means that the use of the thermoset system based on MAL and CA has not negative impact in the thermal conductivity of the finished product.

Table 6.7 – Thermal conductivity

	Measured value (W/m·K)	Declared value (W/m·K)
<b>Thermal Conductivity</b>	(C-0.001) ± 0.001	0.039

### 6.4.2.2 LENGTH AND WIDTH

---

According to the norm EN 822 [9] one measurement was required in one full-size product taken in the measurement points shown in Figure 6.5. In Table 6.8 are shown the measured average values for length and width compared to the specification after CC weeks storage of the product. After CC weeks the product is within specifications. This indicates that the use of thermoset system based on MAL and CA has no negative impact in the accomplishment of the mineral wool product specification.

Table 6.8 – Length and width measurements

	Measured value (mm)	Declared value (mm)	Specification
<b>Length</b>	TT+75	TT	Declared value ± 2 %
<b>Width</b>	UU+12	UU	Declared value ± 1.5 %

### 6.4.2.3 THICKNESS

The thickness was measured in two full-size rolls, as required by the norm EN 823 [10]. In Table 6.9 is shown the measured average value for thickness compared to the specification after CC weeks storage of the product and after aging treatment. According to the data obtained, the product is within the specification. This means that the product may be accepted for commercialization in terms of thickness.

Table 6.9 – Thickness measurement

Thickness	Measured value (mm)	Declared value (mm)	Specification
Before Aging Treatment	$(B+3) \pm 6$	B	Declared value - 2 % Declared value + 10 %
After Aging Treatment	$(B+5) \pm 4$		

### 6.4.2.4 TENSILE STRENGTH PARALLEL TO FACES

The tensile strength of the product has been measured although it does not need to be declared. This test helps to determine the mechanical behavior of the material after long time storage and installation. For that reason one roll of product has been tested after 4 weeks storage, before and after aging treatment. According to the norm EN 1608 [11], 12 specimens were cut from one full-size roll; 6 specimens were tested before aging treatment and 6 specimens were tested after aging treatment. The average of measured values is shown in Table 6.10. It can be observed that the tensile strength parallel to faces is higher than the required by the specification before and after aging treatment; nevertheless it decreases strongly due to the aging treatment.

Table 6.10 – Tensile strength measurements

Tensile Strength	Measured value (kPa)	Declared value	Specification (kPa)
Before Aging Treatment	$VV \pm 1.1$	Not declared	1.9
After Aging Treatment	$(VV-4) \pm 0.7$		

In Table 6.11 is shown the data obtained from the measurement of a similar product from market, which is manufactured with phenolic resin. Comparing data from Table 6.10 with the data

from Table 6.11 it can be observed that the tensile strength of the material is higher before aging treatment when using the thermoset system based on MAL and CA, however it decreases more significantly during the aging treatment. This indicates that the use of thermoset system based on MAL and CA lead to mechanical properties still good for the final product application, although it might lead to slightly lower mechanical performance, in long term, than the mineral wool manufactured with phenolic resins.

**Table 6.11 – Tensile strength measurements for product manufactured with phenolic resin**

<b>Tensile Strength</b>	<b>Measured value (kPa)</b>	<b>Declared value</b>	<b>Specification (kPa)</b>
<b>Before Aging Treatment</b>	(WW) ± 0.5	Not declared	1.9
<b>After Aging Treatment</b>	(WW) ± 0.7		

#### 6.4.2.5 REACTION TO FIRE

The reaction to fire was evaluated according to the norm EN 13501-1 [12]. For that 5 specimens were cut from a full-size roll of material to test the non-combustibility according to the norm EN 1182 [14] and 3 specimens to test the heat of combustion according to the norm EN 1716 [15]. The average of the values obtained is shown in Table 6.12. The average values are compared with the specification for reaction to fire class A1 (i.e. the class corresponding to the most resistant materials to fire), according to the norm EN 13501-1 [12]. The properties related to fire behavior of the product (i.e. calorific power, flame time, weight loss and increase of temperature) comply with the specification for class A1. Therefore the product with the thermoset system based on MAL and CA is class A1 regarding to the reaction to fire; this means it can be rated with the highest resistance to fire.

**Table 6.12 – Fire resistance properties**

<b>Property</b>	<b>Measured value</b>	<b>Declared value</b>	<b>Specification A1 Class</b>
<b>Heat of Combustion (MJ/kg)</b>	1.2 ± 0.1	< 2	< 2
<b>Flame Time (s)</b>	1.8 ± 0.8	< 5	< 5
<b>Weight Loss (%)</b>	7.5 ± 0.7	< 50	< 50
<b>Increase Temperature (°C)</b>	19.7 ± 2.1	< 30	< 30



### 6.4.2.6 WATER ABSORPTION

---

Water absorption has been tested for 4 specimens of a full-size roll of product as stated by the norm EN 1609 [13]. The average value of the measurements is shown in Table 6.13. The obtained value is higher than the specification and with strong variability; but it may be improved by adding more hydrophobic agent to accomplish the specification in case it is required by the application. Therefore, the results achieved would not be critical for the use of the thermoset system based on MAL and CA for mineral wool insulation product since they could be improved by increasing the ratio of hydrophobic agent, as it has been proved in other industrial tests.

Table 6.13 – Water absorption measurements

	Measured value (kg/m <sup>2</sup> )	Declared value
<b>Water Absorption</b>	1.5 ± 1.2	Not declared

### 6.4.2.7 RESISTANCE TO GROWTH OF MICROORGANISMS

---

According to the norm EN 846 two different methods can be applied to test the resistance of the material to growth of fungi, by method A, and to fungi-static effect, by method B [17]. The test was done for 1 specimen cut from a full-size roll of product. It was determined that there is no growth observed of fungi by any of both methods in the product manufactured with the thermoset system based on MAL and CA. Therefore, it is expected that the mineral wool product will not promote the growth of fungi inside it once it is installed.

### 6.4.2.8 FORMALDEHYDE EMISSIONS

---

The formaldehyde emissions of one specimen of the manufactured product were determined according to the norm EN 16000-3. Although the later states that the measurement must be done after 28 days in the chamber, in this case it was done after 7 days. It is known from previous studies [19] that formaldehyde emissions reach a maximum after 7 days in the chamber. The value obtained was < XX µg/m<sup>2</sup>·h, which is the lower detection limit of the method. This demonstrates that the mineral wool product manufactured with the thermoset system based on MAL and CA would not release significant amounts of formaldehyde.

## 6.5 CONCLUSIONS

---

Mineral wool insulation product has been successfully manufactured using a thermoset system based on maltodextrin and citric acid. It has been proved that the commonly used mineral wool process does not need major changes in its design in order to use this alternative thermoset system. Its preparation and introduction in the production line can be done by means of the already existing facilities. The process parameters used for the manufacturing with this thermoset system has been adjusted according to the necessities of the product quality. Despite of the short time available in a real industrial process to cure the material, it has been demonstrated that it is possible to achieve sufficient crosslinking it for the alternative thermoset system, although it can be partially decomposed due the high energy applied in the curing.

The product obtained from the industrial tests was evaluated according to the specification norm for the mineral wool insulation material for buildings. This evaluation has proved that the mineral wool insulation product manufactured with the thermoset system based on MAL and CA complies with the main properties declared by the manufacturers. In particular, the product complies with the requirements for thermal conductivity, which is the main property of any insulation material. Also the mechanical properties were successfully accomplished (i.e. length, width, thickness and tensile strength parallel to faces). Nevertheless it is worth to mention that, although the product manufactured with the alternative thermoset system is leading to better mechanical performance, in short term storage, than traditional product using phenolic resins, its performance deteriorates more pronouncedly in long the term, leading to slightly lower performance than traditional material. The behavior against fire of the mineral wool produced with the alternative thermoset complies with the specification for products with A1 class fire resistance (i.e. the maximum fire resistance) and the water absorption requirements may be passed by the addition of hydrophobic agent, depending on the final requirements of the intended product application.

Other properties, which could be affected by the use of a bio-based thermoset system, such as the growth of microorganisms, has been tested leading to the conclusion that the use of the thermoset system based on MAL and CA does not promote the growth of microorganisms. And, finally, regarding the formaldehyde emissions, it has been proved that they are below the lower

detection limit when the alternative bio-based thermoset system based on MAL and CA is used for the manufacturing of mineral wool insulation material.

## 6.6 REFERENCES

---

1. B. Sirok BB, P. Bullen. Mineral Wool, Production and Properties. England: Cambridge International Science Publishing Ltd, Woodhead Publishing Limited and CRC Press LLC, 2008.
2. Pilato L. Phenolic resins: A century of progress. New York: Springer Berlin Heidelberg, 2010.
3. Al-Homoud DMS. Building and Environment 2005;40(3):353-366.
4. Thermal Insulation – Determination of Steady-state Thermal Resistance and Related Properties – Heat Flow Meter Apparatus. In: Standardization IOF, editor. ISO 8301. Geneva, 1991.
5. Thermal Insulation – Determination of Steady-state Thermal Resistance and Related Properties – Guarded Hot Plate Apparatus. In: Standardization IOF, editor. ISO 8302. Geneva, 1991.
6. Thermal Performance of Building Materials and Products – Determination of Thermal Resistance by Means of Guarded Hot Plate and Heat Flow Meter Methods – Dry and Moist Products of Medium and Low Thermal Resistance. In: Standardization ECf, editor. EN 12664. Brussels, 2001.
7. Thermal Performance of Building Materials and Products – Determination of Thermal Resistance by Means of Guarded Hot Plate and Heat Flow Meter Methods – Products of High and Medium Thermal Resistance. In: Standardization ECf, editor. EN 12667. Brussels, 2001.
8. Thermal Insulation Products for Buildings - Factory made mineral wool (MW) products - Specification. In: Standardization ECf, editor. EN 13162. Brussels, 2008.
9. Thermal Insulating Products for Building Applications - Determination of length and width. In: Standardization IOF, editor. ISO 29465. Geneva, 2008.
10. Thermal insulating products for building applicaitons - Determination of thickness. In: Standardization IOF, editor. ISO 29466. Geneva, 2008.
11. Thermal insulating products for building applications - Determination of tensile strength parallel to faces. In: Standardization IOF, editor. ISO 29766. Geneva, 2008.
12. Fire classificaiton of construction products and building elements - Part 1: Classification using test data from reaction to fire tests. In: Standardizaiton ECf, editor. EN 13501-1. Brussels, 2002.

13. Thermal insulating products for building applications - Determination of short-term water absorption by partial immersion. In: Standardization IOF, editor. ISO 29767. Geneva, 2008.
14. Reaction to fire tests for building products - Non-combustibility test. In: Standardization IO, editor. EN ISO 1182. Geneva, 2002.
15. Reaction to fire tests for building products - Determination of the heat of combustion. In: Standardization ECf, editor. EN ISO 1716. Brussels, 2002.
16. Kim H-S and Kim H-J. Polymer Degradation and Stability 2008;93(8):1544-1553.
17. PLastics. Evaluation of the action of microorganisms. In: Standardization IOF, editor. ISO 846. Geneva, 1997.
18. Determination of formaldehyde and other carbonyl compounds - Active sampling method. In: Standardization IOF, editor. ISO 16000-3. Geneva, 2001.
19. T. Neuhaus RO, A.U. Clausen. Formaldehyde emissions from mineral wool in building constructions into indoor air. Indoor Air 2008. Copenhagen, Denmark, 2008.

---

# *FINAL CONCLUSIONS*

---



An alternative bio-based and non-toxic thermoset system has been developed for its application in composite materials, based on wood or glass fibers. The new thermoset system consists of maltodextrin, citric acid and sodium hypophosphite.

The system has been selected after studying different compositions containing maltodextrin and polycarboxylic acids, namely citric or tartaric. Citric acid is the most appropriate polycarboxylic acid due to two main reasons; first, because it is more reactive regarding to the esterification than tartaric acid, and second, because it presents better crosslinking capacity.

The combination of four techniques, IR, TGA, rheology and mechanical testing, is a very powerful methodology to study the polycondensation systems based on maltodextrin and polycarboxylic acid. The esterification reaction taking place between the different compounds can be detected and quantified. Also the crosslinking capacity of the different systems can be evaluated. Furthermore, mechanical testing provides a closer prediction to the behavior in the final application, allowing the selection of the most suitable composition.

Two alternatives were found to improve the system comprising maltodextrin and citric acid; by the addition of a metal oxide, preferably calcium oxide, and by the addition of sodium hypophosphite.

The use of calcium oxide enhances the crosslinking of the system due to the interaction of calcium ion with the citric acid and the polycondensate derivatives of maltodextrin and citric acid. However, the use of sodium hypophosphite shows a positive impact in the two key factors related to the effectiveness of the thermoset, the speed of the esterification reaction and the crosslinking.

It has been proposed a mechanism of action for the sodium hypophosphite. This mechanism follow two paths; the first one based on the enhancement of the dehydration process of the citric acid under thermal treatment and, the second one based on the reaction between the phosphorous compounds and the polycarboxylic acids derivatives from the dehydration of citric acid. This last path is the reason for the sodium hypophosphite to contribute to the crosslinking, by attaching different polycondensation chains result of the reaction between the maltodextrin and the different polycarboxylic acids derivatives from citric acid.

The thermoset system consisting of maltodextrin, citric acid and sodium hypophosphite has been successfully used in the industrial process of the mineral wool manufacturing. The mineral

wool product obtained complies with the standard specification for the European market, with no release of formaldehyde.



---

# CONCLUSIONES FINALES

---

Se ha desarrollado un sistema termoestable basado en fuentes renovables y libre de sustancias tóxicas para el ser humano en como alternativa a los sistemas derivados del petróleo, para su aplicación en materiales compuestos formados por fibras de madera o vidrio. Este sistema alternativas está compuesto por maltodextrina, ácido cítrico e hipofosfito de sodio.

El sistema ha sido seleccionado después de estudiar diferentes composiciones que contienen maltodextrina Y ácidos policarboxílicos, a saber, cítrico o tartárico. Se comprobado que el ácido cítrico es el más adecuado debido a dos razones principales; primero, porque es más reactivo con respecto a la esterificación que ácido tartárico, y segundo, porque presenta una mejor capacidad de entrecruzamiento.

La combinación de cuatro técnicas analíticas, IR, TGA, reología y ensayos mecánicos, es una metodología potente para estudiar los sistemas de policondensación a base de maltodextrina y ácido policarboxílico. La reacción de esterificación que tiene lugar entre los diferentes compuestos puede ser detectada y cuantificada. Asimismo, la capacidad de entrecruzamiento de los diferentes sistemas puede ser evaluado; y además, los ensayos de propiedades mecánicas ayudan a predecir de forma más próxima el comportamiento de las diferentes composiciones en la aplicación final. Esto permite la selección de la composición más adecuada de forma muy fiable.

Se encontraron dos formas de mejorar el sistema que comprende maltodextrina y ácido cítrico; mediante la adición de un óxido metálico, preferiblemente óxido de calcio, y también mediante la adición de hipofosfito de sodio.

El uso de óxido de calcio aumenta el entrecruzamiento del sistema debido a la interacción de los iones de calcio con el ácido cítrico y los derivados policondensados de maltodextrina y ácido cítrico. Sin embargo, el uso de hipofosfito de sodio muestra un impacto positivo en los dos factores clave relacionados con la eficacia del sistema, la velocidad de reacción de esterificación y el entrecruzamiento.

Se ha propuesto un mecanismo de acción para el hipofosfito de sodio. Este mecanismo sigue dos rutas; el primero basado en la promoción del proceso de deshidratación del ácido cítrico bajo tratamiento térmico y el segundo basado en la reacción entre los compuestos de fósforo y los ácidos policarboxílicos derivados de la deshidratación de ácido cítrico. Esta última ruta justifica parcialmente que el hipofosfito de sodio contribuya al entrecruzamiento, uniendo diferentes cadenas policondensadas resultado de la reacción entre la maltodextrina y los diferentes ácidos policarboxílicos derivados del ácido cítrico.

El sistema termoestable que consiste en maltodextrina, ácido cítrico e hipofosfito de sodio se ha utilizado con éxito en el proceso industrial de fabricación de lana mineral. El producto de lana mineral obtenido cumple con la especificación estándar para el mercado europeo, y sin liberación de formaldehído.

---

# *ANNEX 1*

---



In figure 9.1 it is shown an example of the isothermal TGA experiment at 140 °C applied to the different compositions analyzed. There it can be distinguished the Step A and Step B referring in the Chapter III.

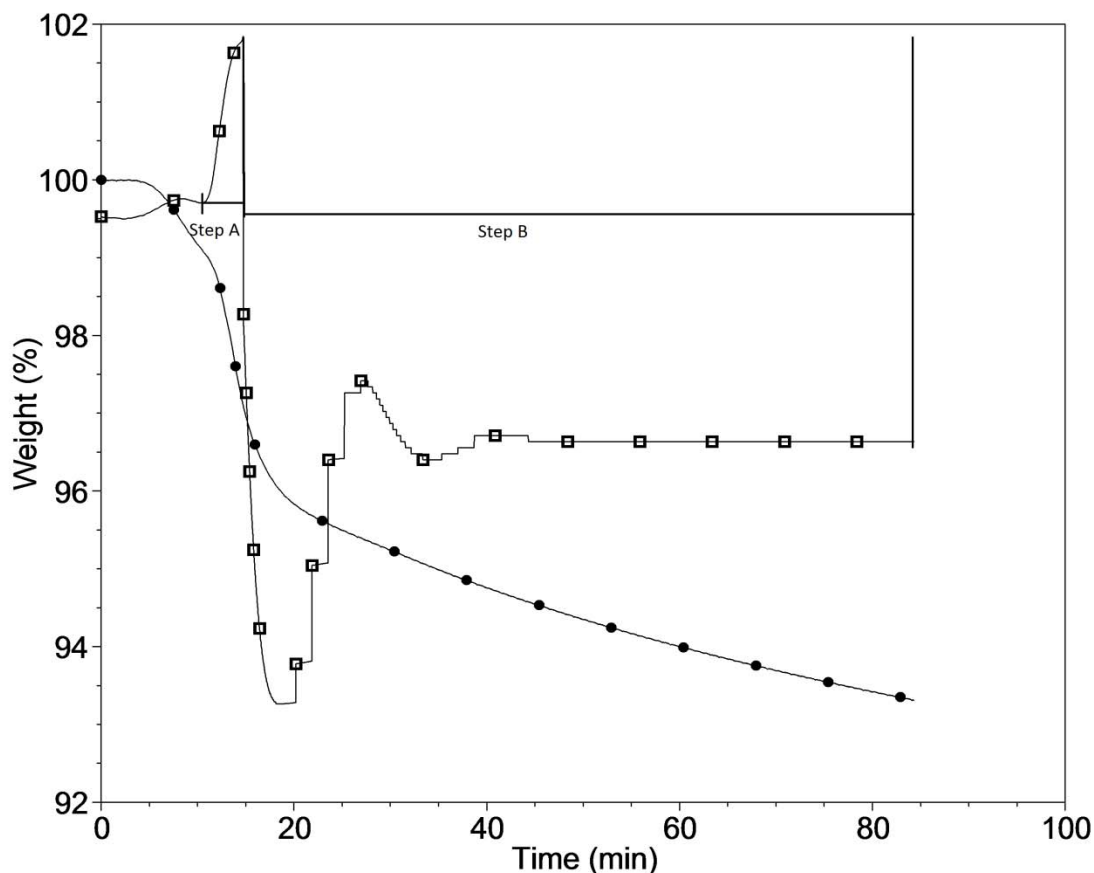


Figure 9.1 – TGA and corresponding derivative for the composition MAL60CA during isothermal experiment at 140 °C for 60 min

As described in the main manuscript different compositions were cured by heating treatment at 140 °C for different periods of time. IR spectrum was measured every hour from 1 hour to 4 hours. In Figure 9.2 and Figure 9.3 it is shown the IR spectra at different heating times for the composition MAL20CA, MAL40CA, MAL60CA and MAL80CA respectively.

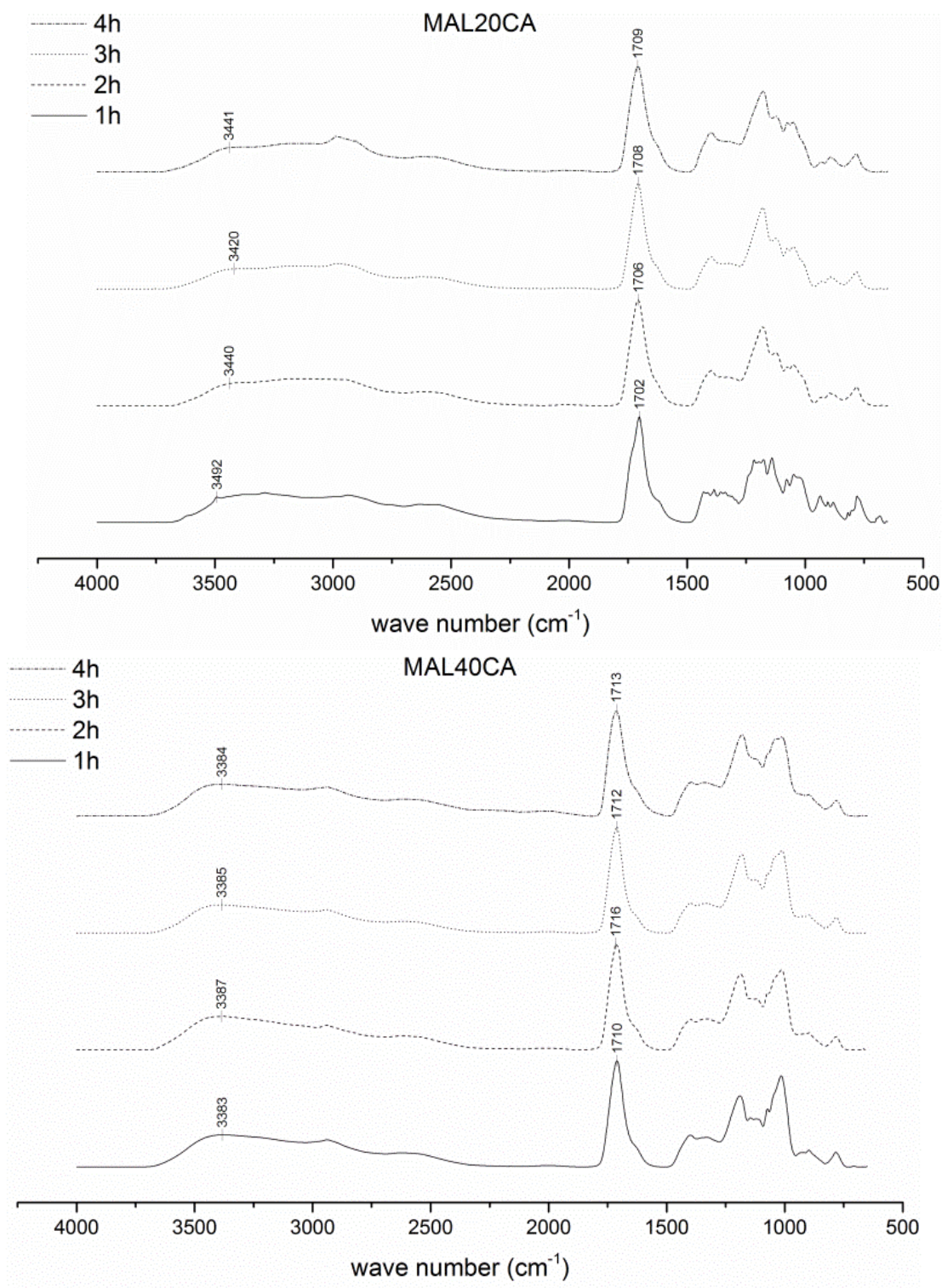


Figure 9.2 – IR spectra of composition MAL20CA and MAL40CA under heating at 140 °C at different times

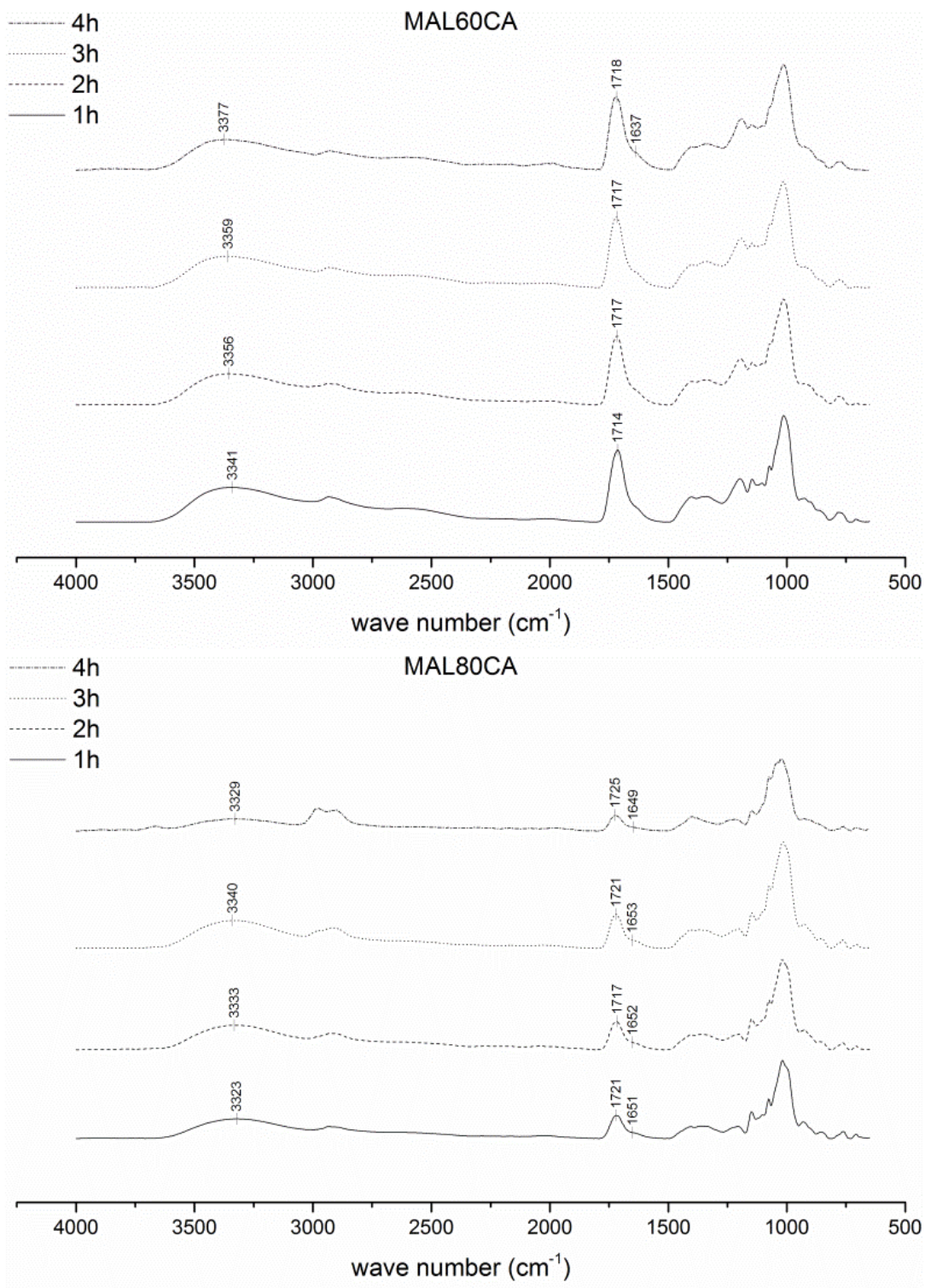


Figure 9.3- IR spectra of composition MAL60CA and MAL80CA under heating at 140 °C at different times

In Figure 9.4 and 9.5 is shown the IR spectra at different heating times for the composition MAL20TA, MAL40TA, MAL60TA and MAL80TA respectively.

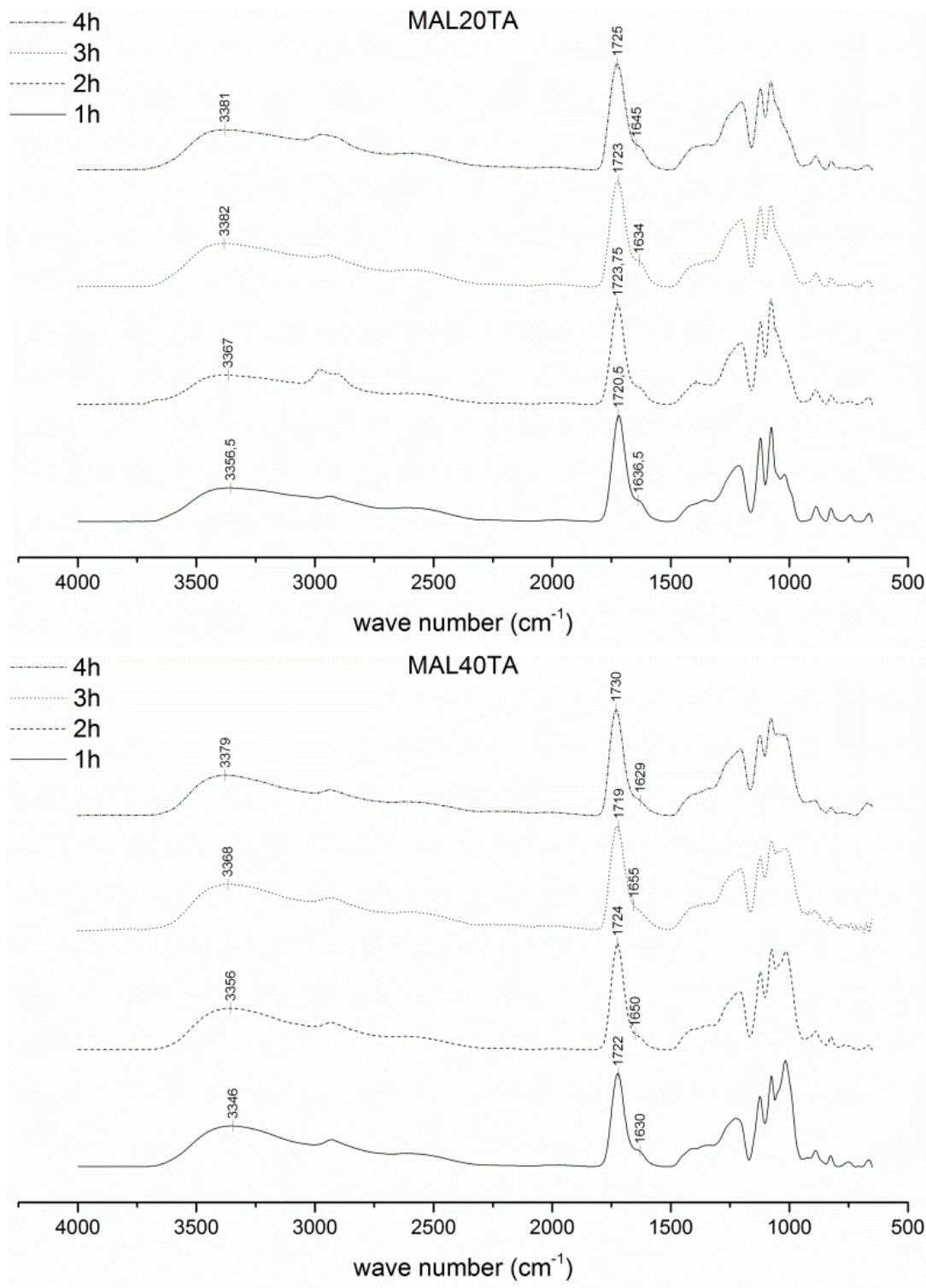


Figure 9.4 – IR spectra of composition MAL20TA and MAL40TA under heating at 140 °C at different times



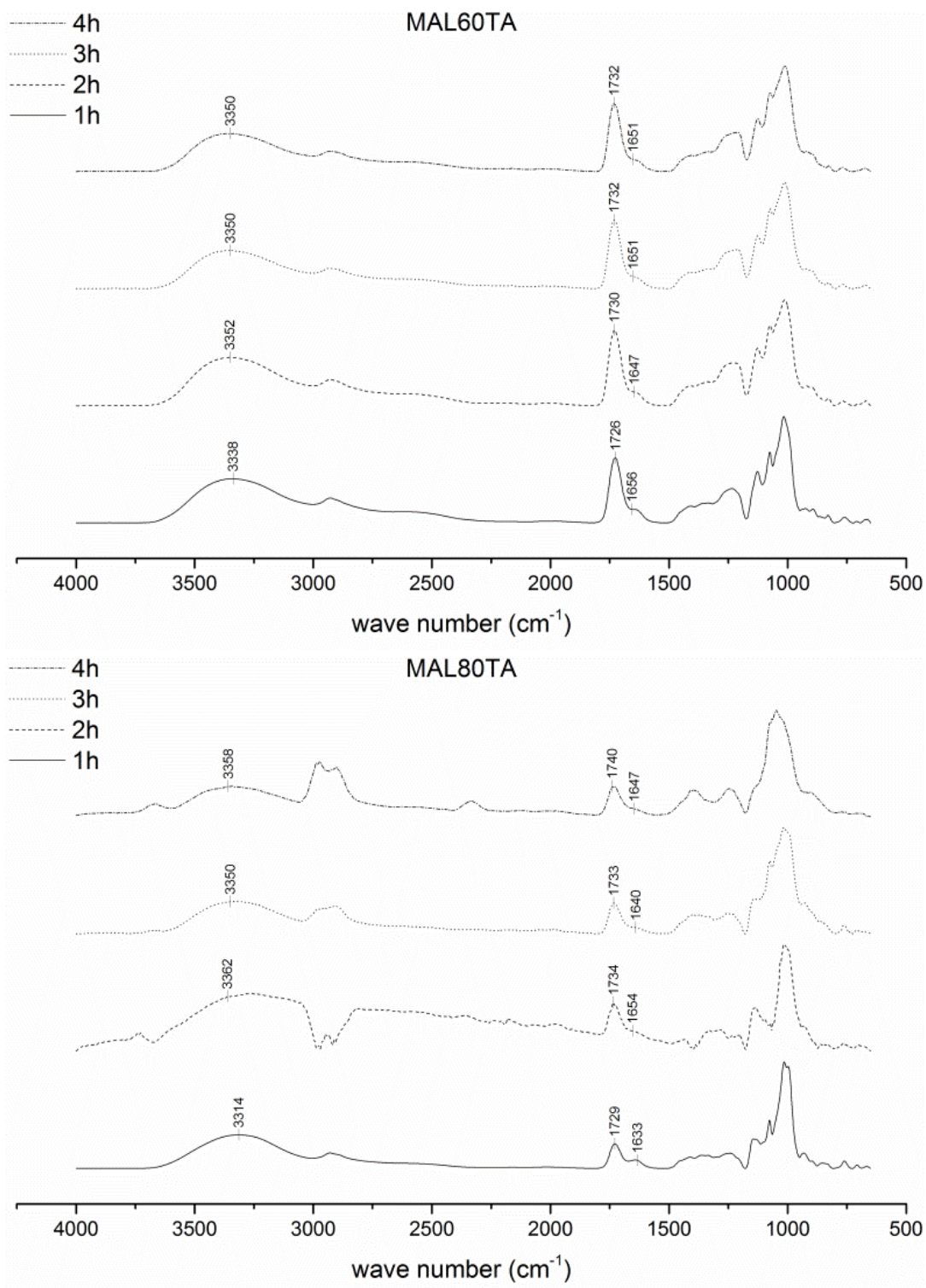


Figure 9.5 – IR spectra of composition MAL60TA and MAL80TA under heating at 140 °C at different times

In all the spectra above is specifically pointed the CO stretching band and OH band which have been considered to follow the progress of the esterification reaction, based on the ratio  $A_{\text{CO}}/A_{\text{OH}}$ .

In Figure 9.6, Figure 9.7, Figure 9.8 and Figure 9.9 are shown the rheological scans of the compositions MAL20CA, MAL40CA, MAL60CA and MAL80CA respectively.

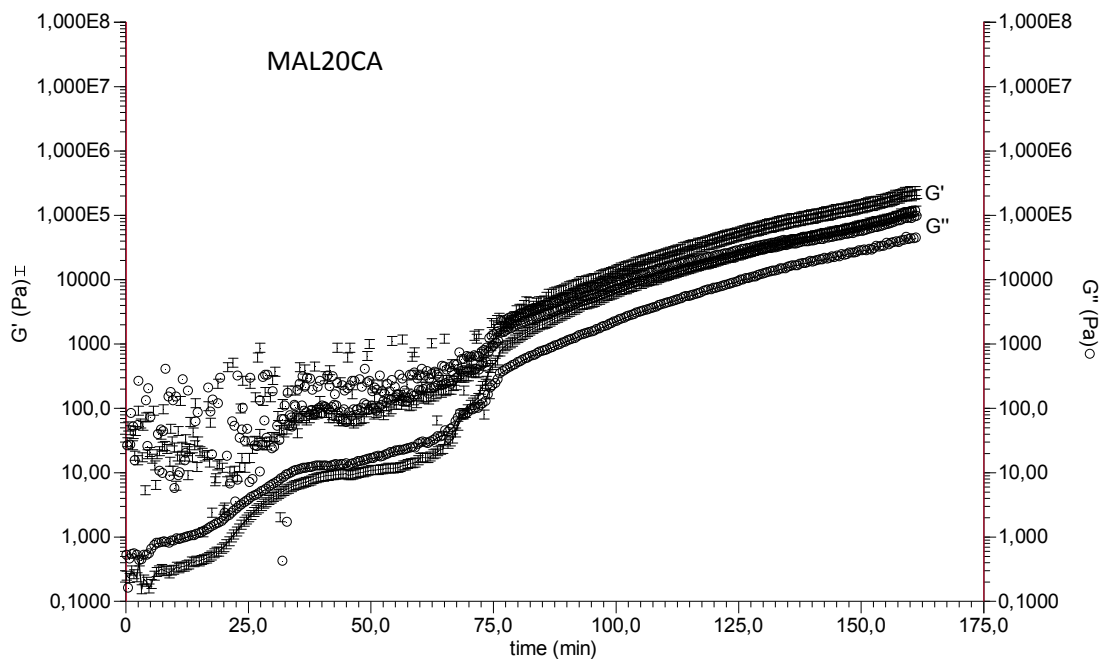


Figure 9.6 - Plot of log G' and log G'' against time of composition MAL20CA

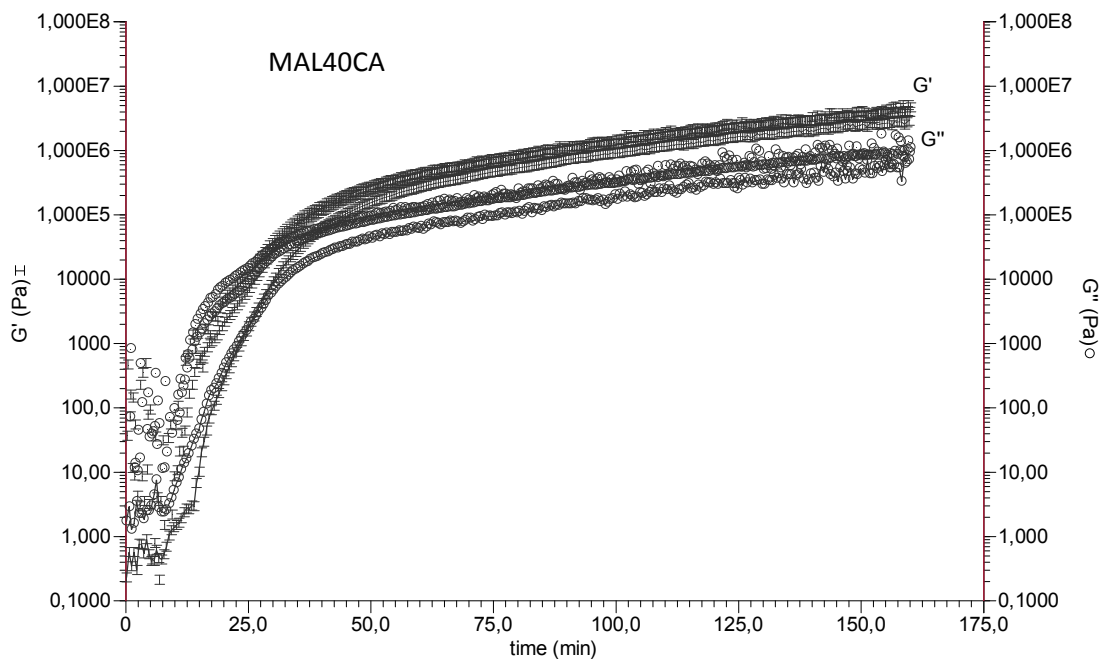


Figure 9.7 – Plot of log G' and log G'' against time of composition MAL40CA

As mentioned in the main manuscript isothermal rheological scan at 140 °C was carried for the different compositions studied. The different scans were stop when a plateau of maximum modulus was achieved and it was independent of the frequency (1, 13 and 25 Hz).

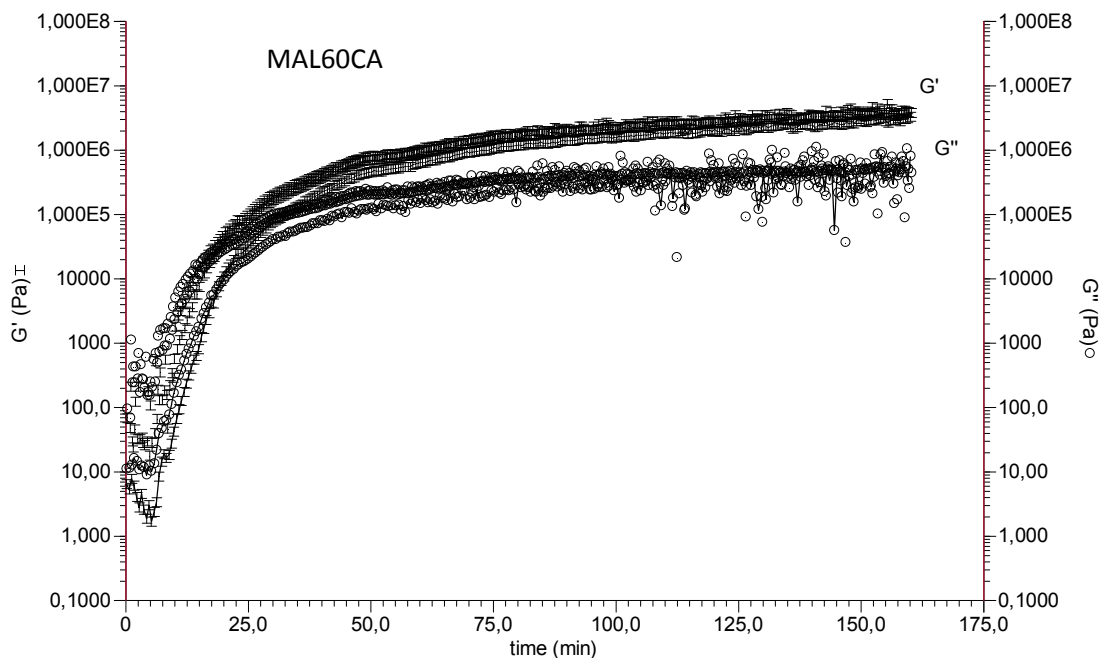


Figure 9.8 – Plot of log G' and log G'' against time of composition MAL60CA

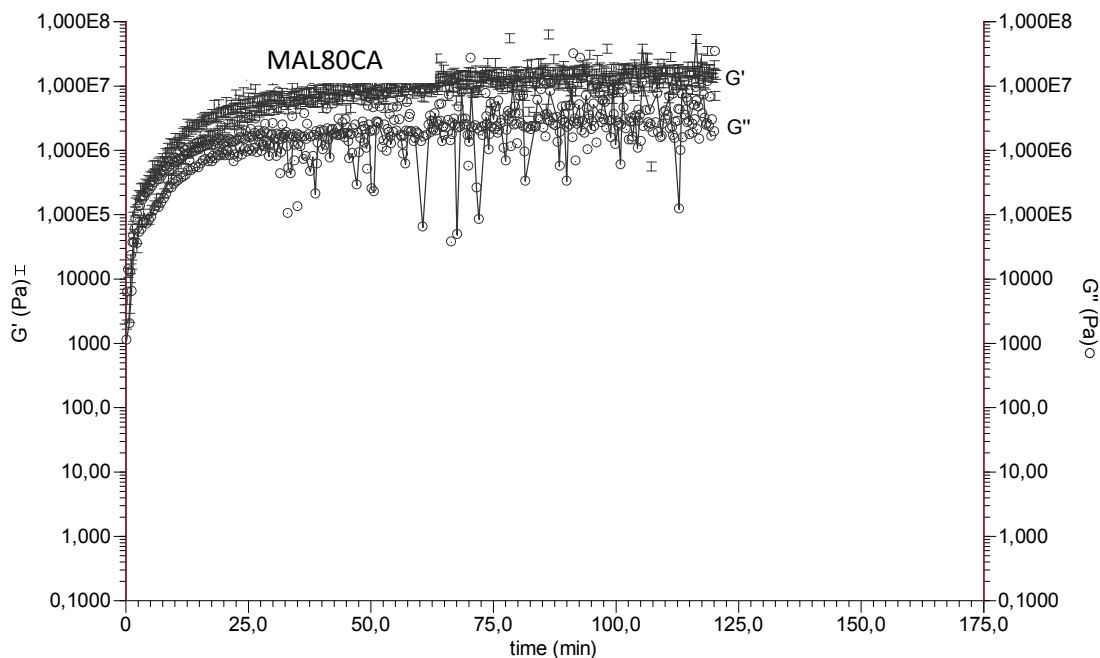


Figure 9.9 – Plot of log G' and log G'' against time of composition MAL80CA

In Figure 9.10, Figure 9.11, Figure 9.12 and Figure 9.13 are shown the rheological scans of the compositions MAL20TA, MAL40TA, MAL60TA and MAL80TA respectively.

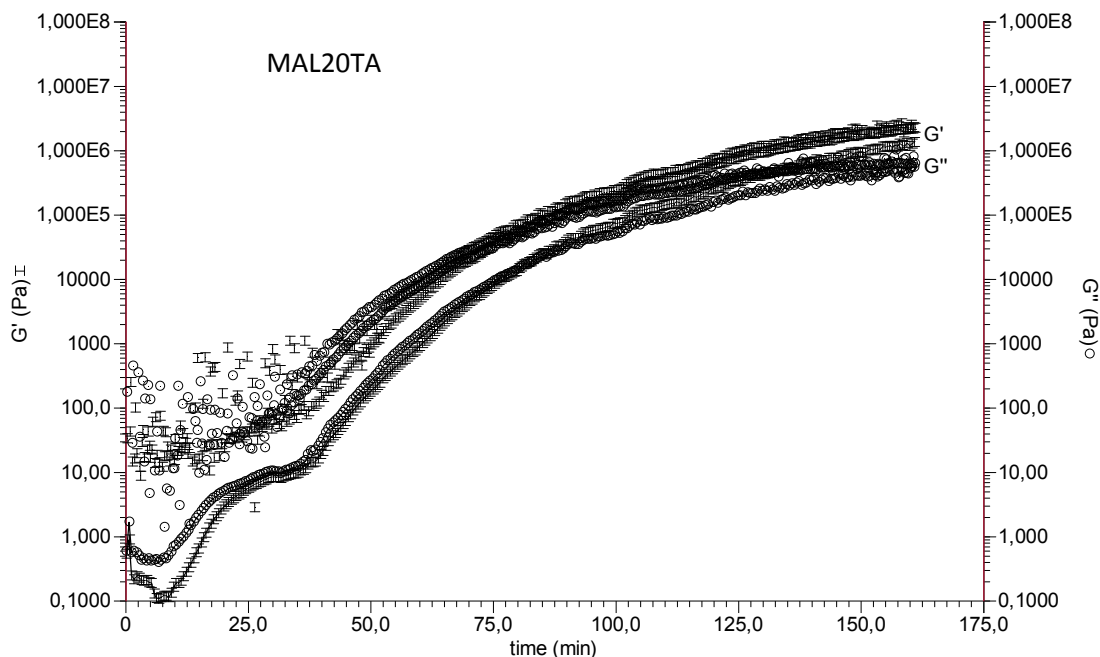


Figure 9.10 – Plot of log G' and log G'' against time of composition MAL20TA

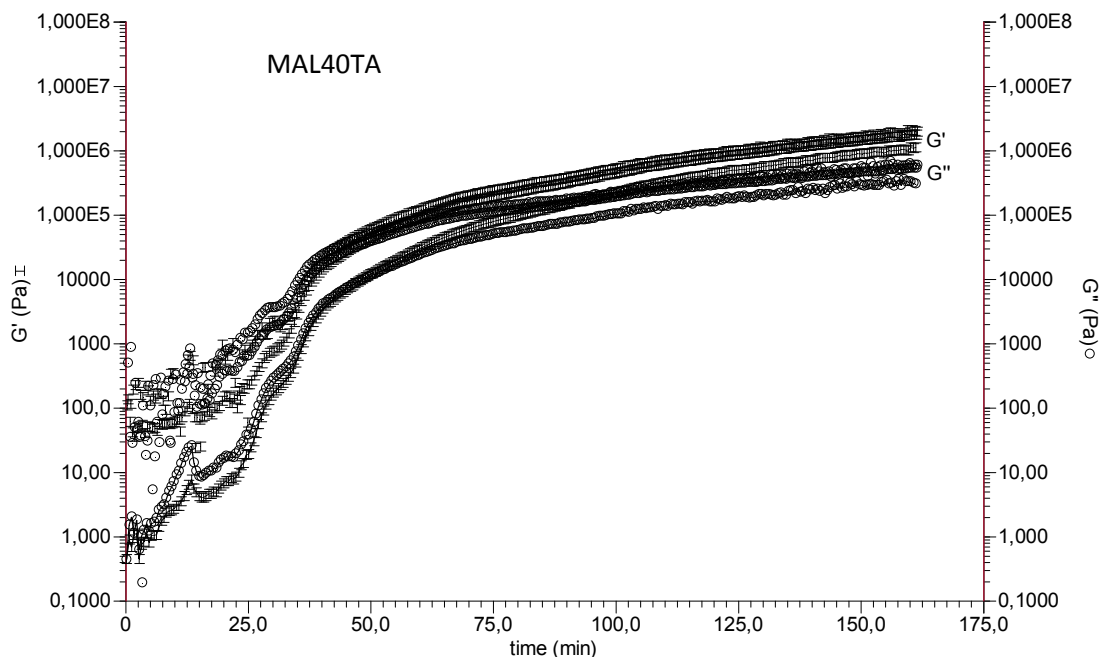


Figure 9.11 – Plot of log G' and log G'' against time of composition MAL40TA

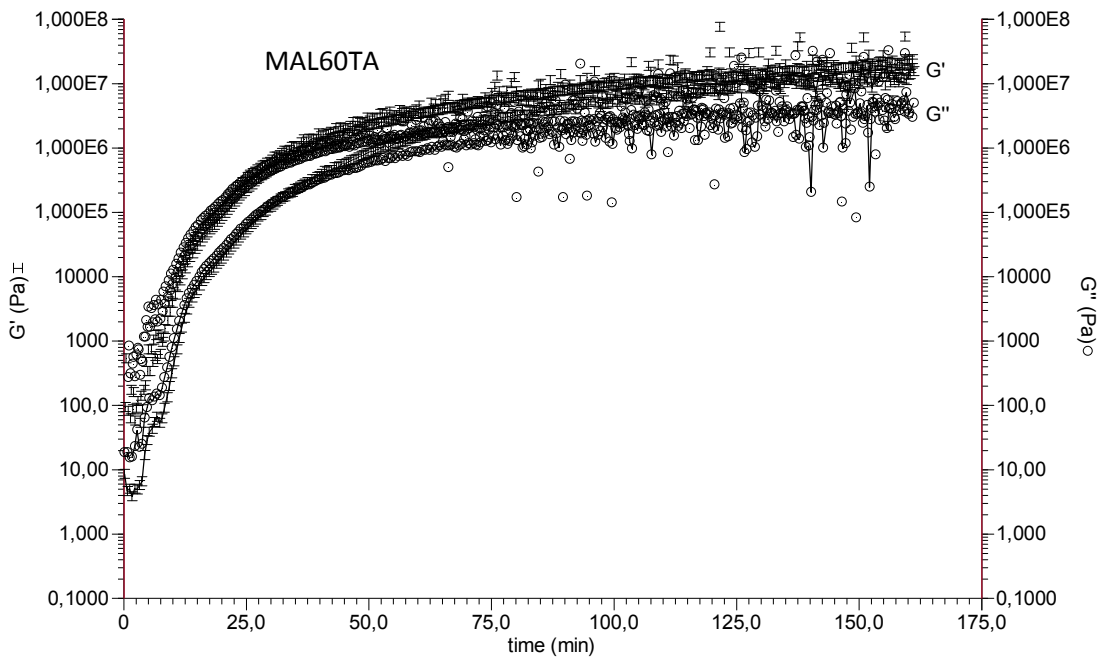


Figure 9.12 – Plot of log  $G'$  and log  $G''$  against time of composition MAL60TA

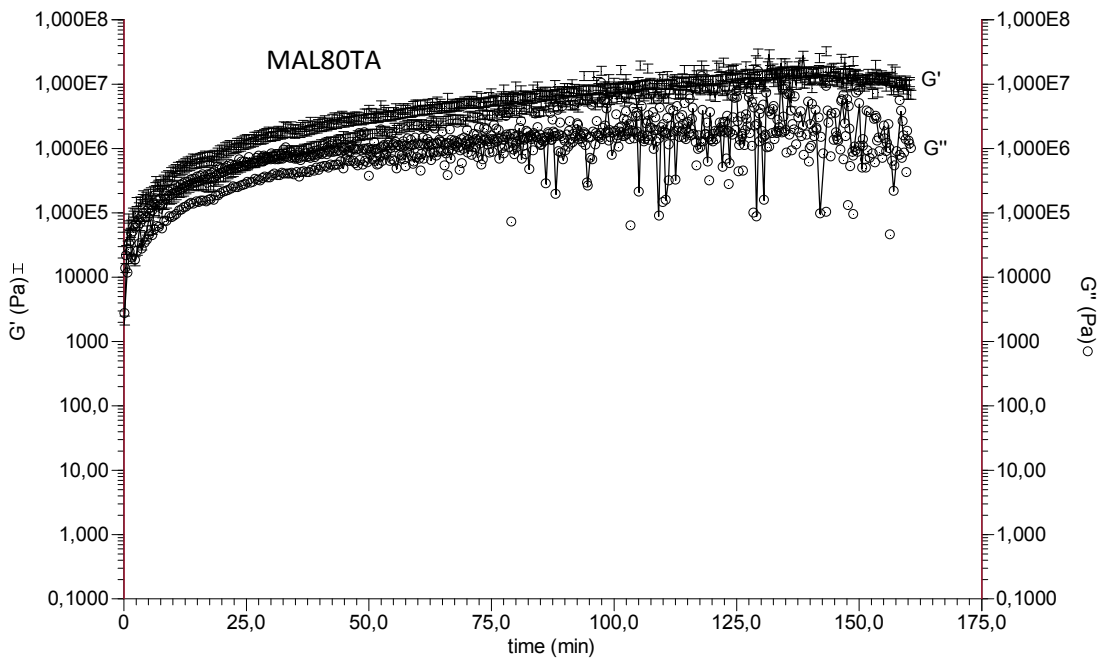
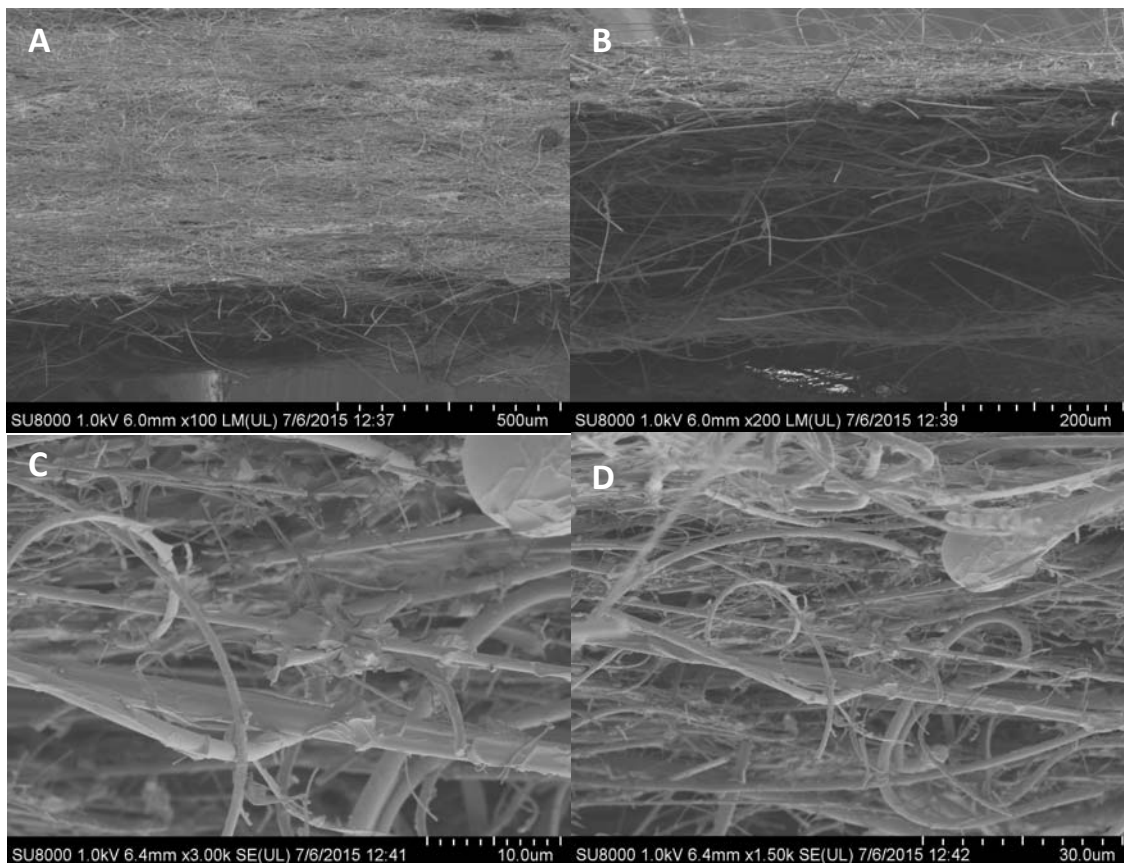


Figure 9.13 – Plot of log  $G'$  and log  $G''$  against time of composition MAL80TA

Scanning electron microscopy (SEM) micrographs of the cross-section after tensile strain test, and the surface of the glass-paper impregnated with composition MAL60TA are shown in Figure 9.14.



**Figure 9.14 - SEM micrographs of glass paper impregnated with composition MAL60CA upon thermal treatment 30 min, surface (A), cross-section (B), glass fibers in the cross-section (C and D)**

In Figure 9.15 is provided the results of tensile strain test according to the method described in the main manuscript. These results have been taken as reference for comparison of the studied systems with the non-bio-based thermoset systems currently in use in the industry (i.e. phenolic resin).

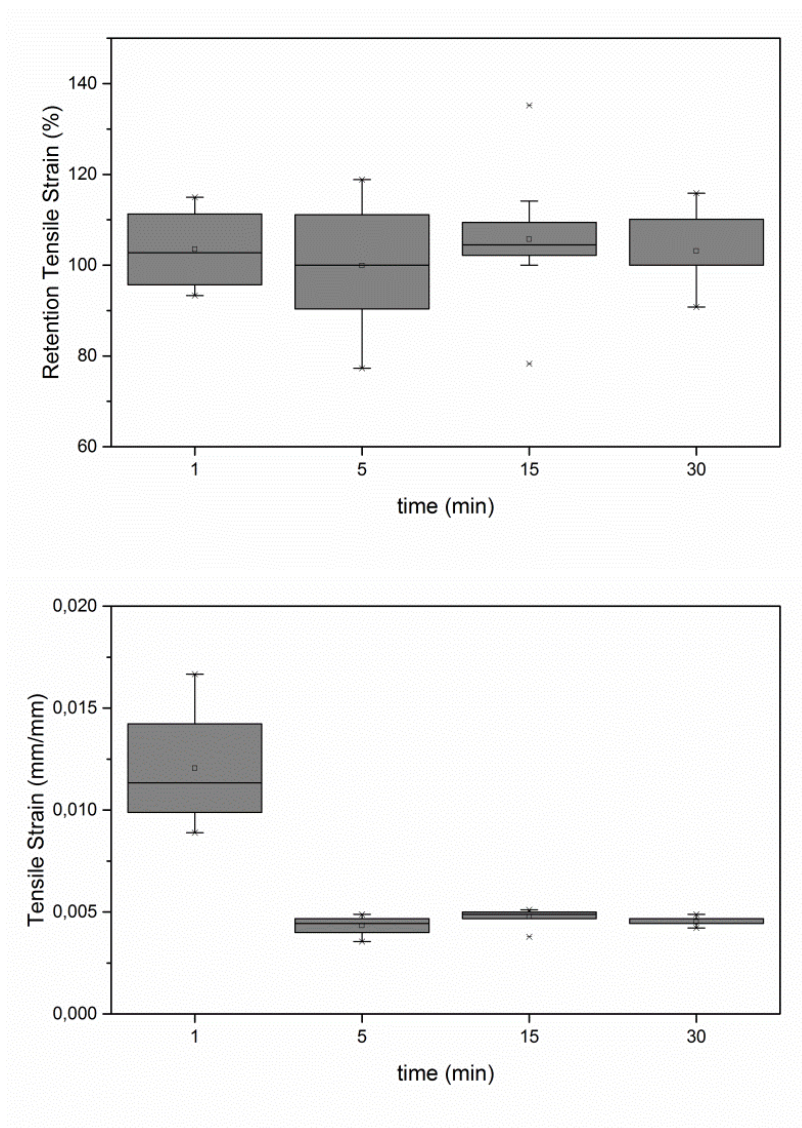


Figure 9.15 – Tensile strain against heating time for a commercial phenolic resol

